



**HAL**  
open science

# Gene regulatory network for lateral root formation in *Arabidopsis thaliana*

Duy Chi Trinh

► **To cite this version:**

Duy Chi Trinh. Gene regulatory network for lateral root formation in *Arabidopsis thaliana*. Plants genetics. Université Montpellier, 2019. English. NNT : 2019MONTG003 . tel-02304191

**HAL Id: tel-02304191**

**<https://theses.hal.science/tel-02304191>**

Submitted on 3 Oct 2019

**HAL** is a multi-disciplinary open access archive for the deposit and dissemination of scientific research documents, whether they are published or not. The documents may come from teaching and research institutions in France or abroad, or from public or private research centers.

L'archive ouverte pluridisciplinaire **HAL**, est destinée au dépôt et à la diffusion de documents scientifiques de niveau recherche, publiés ou non, émanant des établissements d'enseignement et de recherche français ou étrangers, des laboratoires publics ou privés.

# THÈSE POUR OBTENIR LE GRADE DE DOCTEUR DE L'UNIVERSITÉ DE MONTPELLIER

En Biologie du Développement

École doctorale n°584 GAIA : Biodiversité, Agriculture, Alimentation, Environnement, Terre, Eau

Unité de recherche DIADE : Diversité, Adaptation et Développement des Plantes

## Propriétés du réseau de gènes contrôlant l'organisation du primordium de racine latérale chez *Arabidopsis thaliana*

## Gene regulatory network for lateral root formation in *Arabidopsis thaliana*

Présentée par TRINH Duy Chi  
Le 22 mars 2019

Sous la direction de Dr. Laurent LAPLAZE

Devant le jury composé de

Mr Alain GOJON, Directeur de Recherche, INRA, Montpellier

Mme Sandra BENSMIHEN, Chargé de Recherche, CNRS, Toulouse

Mr Frédéric DOMERGUE, Chargé de Recherche, CNRS, Bordeaux

Mme Soazig GUYOMARC'H, Maître de conférences, Université de Montpellier

Mr Laurent LAPLAZE, Directeur de Recherche, IRD, Montpellier

Mme Valérie LEGUÉ, Professeur, Université Blaise Pascal de Clermont-Ferrand

Mr Joop VERMEER, Professeur, Université de Zurich

Président du jury

Examineur

Rapporteur

Invité

Directeur de thèse

Rapporteur

Examineur



UNIVERSITÉ  
DE MONTPELLIER

This PhD was prepared in the DIADE research unit  
**D**iversité - **A**daptation - **D**eveloppement des plantes

Centre IRD de Montpellier  
911 Avenue Agropolis  
34394 Montpellier Cedex 5  
France



## Abstract in English

Post-embryonic lateral root organogenesis plays an essential role in defining plant root system architecture, and therefore plant growth and fitness. The aim of the thesis is to elucidate the gene regulatory network regulating lateral root development and *de novo* root meristem formation during root branching in the model plant *Arabidopsis thaliana* by combining a system-biology-based analysis of lateral root primordium transcriptome dynamics with the functional characterization of genes possibly involved in regulating lateral root organogenesis.

The first part of the thesis deals with the identification the target genes of PUCHI, an AP2/EREBP transcription factor that is involved in controlling cell proliferation and differentiation during lateral root formation. We showed that loss of PUCHI function leads to defects lateral root initiation and primordium growth and organisation. We found that several genes coding for proteins of the very long chain fatty acid (VLCFA) biosynthesis machinery are transiently induced in a PUCHI-dependent manner during lateral root development. Moreover, a mutant perturbed in VLCFA biosynthesis (*kcs1-5*) displays similar lateral root development defects as does *puchi-1*. In addition, roots of *puchi-1* loss of function mutant show enhanced and continuous callus formation in auxin-rich callus induction medium, consistent with the recently reported role of VLCFAs in organizing separated callus proliferation on this inductive growing medium. Thus, our results demonstrate that PUCHI positively regulates the expression of VLCFA biosynthesis genes during lateral root development, and further support the hypothesis that lateral root and callus formation share common genetic regulatory mechanisms.

A second part of the thesis specifically addresses the issue of identifying key regulators of root meristem organization in the developing lateral root primordium. Material enabling the tracking of meristem cell identity establishment in developing primordia with live confocal microscopy was generated. A gene network inference was run to predict potential regulatory relationships between genes of interest during the time course of lateral root development. It identified potential regulators of quiescent center formation, a key step in functional organization of the lateral root primordia into a new root apical meristem. The characterization of some of these candidate genes was initiated.

Altogether, this work participated in deciphering the genetic regulation of lateral root formation in *Arabidopsis thaliana*.

**Key words:** gene regulatory network, lateral root, stem cell niche, meristem formation, very long chain fatty acids (VLCFAs), PUCHI

## Abstract in French

L'organogenèse post-embryonnaire des racines latérales joue un rôle essentiel dans l'établissement de l'architecture du système racinaire des plantes, et donc dans leur croissance et leur performance. L'objectif de cette thèse est de caractériser le réseau de gènes régulant le développement des racines latérales et en particulier, l'organisation fonctionnelle du primordium de racine latérale, formant un nouveau méristème racinaire, chez la plante modèle *Arabidopsis thaliana* en combinant des études de biologie des systèmes appliquées à la dynamique du transcriptome lors de la formation des racines latérales avec la caractérisation fonctionnelle de gènes candidats pour la régulation de ce phénomène d'organogenèse.

La première partie de la thèse concerne l'identification des cibles de PUCHI, un facteur de transcription de type AP2/EREBP impliqué dans le contrôle de la prolifération et de la différenciation cellulaire dans le primordium de racine latérale. Le phénotype liés à la perte de fonction de PUCHI a été caractérisé en détail et a mis en évidence un rôle de ce facteur de transcription dans l'initiation des racines latérales et le développement et l'organisation des primordia. Par l'analyse de profils spatiaux et temporels d'expression de gènes, nous avons pu mettre en évidence que l'expression de gènes codant des protéines impliquées dans la biosynthèse des acides gras à très longues chaînes (VLCFA) est transitoirement activée durant la formation de la racine latérale et que cette dynamique est dépendante de PUCHI. De plus, le mutant *kcs1-5*, perturbé dans la biosynthèse de VLCFAs, présente un phénotype de développement des racines latérales similaire à celui de *puchi-1*. Par ailleurs, la perte de fonction *puchi-1* augmente fortement la formation de calcs continus dans des racines cultivées sur milieu inducteur riche en auxine, ce qui est cohérent avec le rôle récemment décrit des VLCFA racinaires dans la formation et l'organisation de calcs distincts lorsque la racine est cultivé sur milieu inducteur de calcs. L'ensemble de nos résultats démontre que PUCHI régule positivement l'expression de gènes de biosynthèse de VLCFAs lors de la formation de racines latérales et la callogenèse. Nos résultats confortent également l'hypothèse selon laquelle la formation des racines latérales et celle de calcs racinaires partagent des mécanismes de régulation communs.

La seconde partie de la thèse s'intéresse à l'identification de facteurs régulateurs clés dans l'organisation fonctionnelle du primordium de racine latérale et particulièrement, l'organisation d'un nouveau méristème racinaire. J'ai contribué à produire de nouvelles lignées de plantes permettant de suivre en temps réel par microscopie confocale la mise en place des identités cellulaires caractéristiques d'un méristème racinaire dans le primordium de racine latérale en développement. En utilisant un algorithme d'inférence de réseau de gènes, j'ai produit puis analysé les relations prédites de régulation entre gènes d'intérêt, afin d'identifier des gènes candidats potentiellement impliqués dans la formation du centre quiescent, un élément clé dans l'organisation du primordium et la mise en place du nouveau méristème racinaire. La caractérisation fonctionnelle de certains de ces gènes candidats a été initiée.

Ces travaux de thèse ont donc contribué à mieux comprendre les mécanismes de régulation de la formation des racines latérales chez *Arabidopsis thaliana*.

**Mots clés:** réseau de régulation du gène, racines latérales, niche de cellules souches, formation de méristème, acides gras à très longue chaîne (VLCFAs), PUCHI

## ACKNOWLEDGEMENTS

First of all, I express my greatest gratitude to my PhD supervisors, Dr. Laurent Laplaze and Dr. Soazig Guyomarc'h. I feel truly privileged to be your student. You two have guided me through this journey with kindness, encouragement and great patience. Thank you very much Dr. Laurent for spending your valuable time discussing via video and answering all my requests with incredible efficiency. Thank you very much Dr. Soazig for finding the time between the university and the lab to be there for enthusiastic discussions, as well as for all the help with my everyday life. I and my little family, especially my daughter, deeply appreciate your generous support during our stay.

I thank Dr. Sandra Bensmihen, Dr Frédéric Domergue, Dr. Alain Gojon, Dr. Valérie Legué, and Dr. Joop Vermeer for participating in my PhD defense jury.

I am deeply grateful to all members of my PhD committee to my study. Thank you all very much, Dr. Thierry Joet, Dr. Patrick Lemaire, Dr. Philippe Nacry, Dr. François Parcy and Dr. Benjamin Peret, for spending many hours with me to discuss my work and to encourage me one every year.

I am grateful to the team leader Professor Pascal Gantet who introduced me to this PhD program and helped me get this study opportunity. I also thank all other members of the Cereal Root Systems team for their help during my thesis: Dr. Mikaël Lucas for network analysis using Pythonis, Dr. Antony Champion for molecular work, Daniel Moukouanga for everyday lab tasks, Dr. Alexandre Grondin, Mathieu Gonin, Jérémy Lavarenne, Nguyen Trang Hieu, Luong Ai My, Branly Wilfried Effa Effa, Marilyne DEBIEU, Carla De La Fuente Cantó and Kwanho Jeong for accompanying me through the journey with a lot of discussions and help, both in the lab and outside the lab.

I thank Prof. Malcolm Bennett (Nottingham, UK) for his valuable comments on my work. I thank Dr. Stéphane Dussert and Virginie Vaissayre (IRD, Montpellier), Frédérique Tellier and Prof. Jean-Denis Faure (Paris), and Dr. Yohann Boutté (Bordeaux) for all the hard work on fatty acids analyses. I appreciate the help of Dr. Tatsuaki Goh and Dr. Hidehiro Fukaki with research materials and helpful discussions.

I thank Myriam Collin (IRD), Carine Alcon and Alexandre Martinière (SupAgro Montpellier) for all the help with microscopy.

I acknowledge the essential help of Dr. Alain Ghesquiere, Bruno Barthelemy, Virginie Champion, Manuelle Rival (IRD) and Cendrine Jay-Allemand (GAIA) for processing all the paperwork necessary for my study.

My special thank goes to Dr. Luu Doan Trung (SupAgro Montpellier) for your kindness. Not only did you prepare me for the PhD, you also provided me and my family a lot of valuable help during the period.

I thank University of Science and Technology of Hanoi (USTH), Vietnam International Education Cooperation Department (VIED), French Embassy in Vietnam and Campus France for providing all financial and administrative support during the three years.

Last but not least, my special appreciation and gratitude go to my big and little family. This PhD would not be possible without your generous support and encouragement.

---

**TABLE OF CONTENTS**

ABSTRACT IN ENGLISH.....	2
ABSTRACT IN FRENCH.....	3
ACKNOWLEDGEMENTS .....	4
TABLE OF CONTENTS .....	6
LIST OF FIGURES.....	9
FREQUENTLY USED ABBREVIATIONS .....	10
GENERAL INTRODUCTION .....	11
CHAPTER I .....	15
<b>Lateral root formation: building a meristem <i>de novo</i></b>	
I. INTRODUCTION .....	17
II. TISSUE CONTEXT AND EARLY EVENTS OF LATERAL ROOT PRIMORDIUM	
ORGANOGENESIS .....	20
2.1. Competence of pericycle cells for root organogenesis.....	20
2.2. Oscillatory LR priming by endogenous cues .....	23
2.3. Lateral root founder cell specification.....	25
2.4. Lateral root primordia initiation .....	27
2.5. Control of lateral root spacing/density .....	29
III. BUILDING A NEW ORGAN: A COHERENT PROGRAM OF COORDINATED CELL	
DIVISIONS, WITH NEWLY SET AXIS OF GROWTH AND BOUNDARIES .....	30
3.1. Control and sequence of cell division and division planes.....	30
3.2. LRP cellular organization and anatomical patterning .....	33
3.3. Lateral root primordia boundary .....	35
3.4. LRP shape progression through surrounding tissues and LRP emergence .....	36
3.5. Connectivity between developing lateral root primordia and the primary root.....	37
IV. MERISTEM FORMATION AND ACTIVATION DURING LATERAL ROOT FORMATION .....	38
4.1. Common molecular mechanisms controlling embryonic root apical meristem and LRP meristem	
formation .....	38
4.2. Lateral root meristem activation.....	41
V. LRP ORGANOGENESIS AS A COMMON BASIS FOR ORGAN REGENERATION FROM	
CALLUS .....	43
VI. GENERAL CONCLUSIONS .....	47

CHAPTER II .....	49
<b>PUCHI regulates LRP initiation, positioning, patterning and emergence</b>	
I. INTRODUCTION .....	50
II. RESULTS .....	51
2.1. PUCHI expression pattern.....	51
2.2. PUCHI negatively regulates LRP initiation, positioning and development .....	53
2.3. Cell division pattern is disturbed in <i>puchi-1</i> LRPs.....	58
2.4. PUCHI is required for correct LRP meristem organization .....	61
2.5. <i>puchi-1</i> roots generally have normal auxin response .....	62
2.6. <i>puchi-1</i> pericycle is more sensitive to auxin treatment .....	64
2.7. Cytokinin signalling is altered in <i>puchi-1</i> LRPs.....	65
III. DISCUSSIONS .....	66
3.1. PUCHI controls LRP initiation and spacing .....	66
3.2. Loss of PUCHI function leads to LRP development defects .....	68
3.3. PUCHI regulates cell divisions and stem cell niche establishment, possibly through hormonal signalling .....	69
IV. CONCLUSION AND PERSPECTIVES .....	72
 CHAPTER III.....	 73
<b>PUCHI regulates VLCFA biosynthesis genes during LRP and callus formation</b>	
I. INTRODUCTION .....	74
II. RESULTS .....	79
2.1. More on VLCFA biosynthesis genes in relevant datasets.....	79
2.2. PUCHI regulates the spatio-temporal expression patterns of VLCFA biosynthesis genes during LRP formation .....	83
2.3. VLCFA mutants and <i>puchi-1</i> display similar defects in lateral root development .....	89
2.5. PUCHI is required for root but not shoot regeneration from callus .....	93
2.6. PUCHI regulates expression of <i>KCSI</i> during callus formation .....	94
2.7. Mutation in PUCHI alters VLCFA composition in root calli .....	95
2.8. Probing suberin content in WT and <i>puchi-1</i> roots.....	99
III. DISCUSSION AND PERSPECTIVES.....	101
3.1. VLCFA biosynthesis genes are expressed in LRPs and the endodermis .....	101
3.2. VLCFA biosynthesis genes are involved in LRP development and callus formation and are regulated by PUCHI.....	102
3.3. How do VLCFAs contribute to LRP development?.....	105
3.4. The PUCHI network regulating LRP development and callus formation.....	108
IV. CONCLUSIONS.....	109

---

CHAPTER IV .....	115
<b>Potential genes regulating stem cell niche formation</b>	
I. INTRODUCTION .....	116
II. RESULTS .....	117
2.1. Identify potential regulators of root stem cell niche establishment in developing LRPs based on a proxy.....	117
2.2. Identify potential regulators of LRP stem cell niche by whole network analysis .....	125
III. DISCUSSION AND PERSPECTIVES.....	133
SUPPLEMENTAL FIGURES .....	136
CHAPTER V .....	143
<b>General discussions and perspectives</b>	
I. PUCHI controls multiple aspects of plant development partially via regulating VLCFA biosynthesis	144
II. TDCor as a hypothesis-generating tool to identify potential genes regulating stem cell niche establishment.....	147
III. Final conclusion .....	148
CHAPTER VI .....	149
<b>Materials and methods</b>	
FRENCH SUMMARY.....	158
REFERENCES.....	183
APPENDIXES .....	204
APPENDIX 1 .....	205
APPENDIX 2 .....	210
APPENDIX 3 .....	213
PUBLICATIONS, COMMUNICATIONS AND TRAINING .....	215
LIST OF PUBLICATIONS.....	216
SCIENTIFIC COMMUNICATION.....	216
TRAINING/FORMATION.....	217

## LIST OF FIGURES

<b>Figure 1.1.</b> Arabidopsis primary root and lateral root meristems. ....	18
<b>Figure 1.2.</b> Key events during lateral root primordium initiation and their regulators .....	21
<b>Figure 1.3.</b> Schematic presentation of LRP organogenesis and embryonic root organogenesis. ....	31
<b>Figure 1.4.</b> Distribution patterns of some key regulators in different developmental contexts. ....	39
<b>Figure 2.1.</b> Prediction of the gene regulatory network during LRP development .....	51
<b>Figure 2.2.</b> Expression of <i>GFP-PUCHI</i> in LRPs and the primary root. ....	52
<b>Figure 2.3.</b> <i>puchi-1</i> mutant produces more LRPs and is delayed in LRP development. ....	54
<b>Figure 2.4.</b> Kinetics of LRP development in WT and <i>puchi-1</i> . ....	56
<b>Figure 2.5.</b> Distribution of developmental stages of un-emerged LRPs in the marked regions in WT and <i>puchi-1</i> roots. ....	57
<b>Figure 2.6.</b> <i>puchi-1</i> LRPs are defective in cell division pattern. ....	59
<b>Figure 2.7.</b> Cellular organization in the presumptive LR meristem is disturbed in <i>puchi-1</i> LR. ....	60
<b>Figure 2.8.</b> Expression of the QC-specific marker <i>QC25::CFP</i> is altered in <i>puchi-1</i> mutant. ....	62
<b>Figure 2.9.</b> Auxin gradient as revealed by <i>DR5::GFP</i> reporter in WT and <i>puchi-1</i> LRPs and LR. ....	63
<b>Figure 2.10.</b> <i>puchi-1</i> roots produce more LRPs when treated with auxin NAA. ....	65
<b>Figure 2.11.</b> Expression pattern of the cytokinin signaling reporter construct in WT and <i>puchi-1</i> LRPs. ....	66
<b>Figure 2.12.</b> Summary of PUCHI roles during LRP development .....	72
<b>Figure 3.1.</b> Enrichment analysis using BinGO on 217 genes .....	75
<b>Figure 3.2.</b> Schematic representation of the VLCFA elongation cycle. ....	76
<b>Figure 3.3.</b> The PUCHI network inferred by TDCor .....	77
<b>Figure 3.4.</b> Measurement of key VLCFA biosynthetic gene expression by RT-qPCR .....	78
<b>Figure 3.6.</b> Expression of VLCFA biosynthesis genes in the developing LRP .....	82
<b>Figure 3.7.</b> VLCFA genes are expressed in LRPs and their expression patterns are dependent on PUCHI .....	85
<b>Figure 3.8.</b> <i>KCS</i> genes are expressed in LRPs and their expression patterns are dependent on PUCHI. ....	87
<b>Figure 3.9.</b> <i>puchi-1</i> and <i>kcs1-5</i> mutant produce more LRPs and are delayed in LRP development. ....	90
<b>Figure 3.10.</b> Callus formation was enhanced in <i>puchi-1</i> and <i>kcs1-5</i> roots. ....	92
<b>Figure 3.11.</b> <i>puchi-1</i> roots have weaker root, but not shoot, regeneration capacity. ....	94
<b>Figure 3.12.</b> <i>KCSI</i> is expressed in calli and its expression pattern is dependent on PUCHI. ....	95
<b>Figure 3.13.</b> An analysis of VLCFA classes .....	96
<b>Figure 3.14.</b> Global FA analysis revealed that mutation of PUCHI altered VLCFA composition in roots treated with CIM. ....	99
<b>Figure 3.15.</b> Suberin staining of roots with Fluorol yellow. ....	100
<b>Figure 3.16.</b> Possible PUCHI network regulating pericycle cell division and LRP formation and development. ...	109
<b>Figure S3.1.</b> Expression pattern of <i>pKCSI::GUS</i> and <i>pECR::GUS</i> in the root. ....	110
<b>Figure S3.2.</b> Expression of <i>pKCR1::GUS</i> in endodermal cells .....	111
<b>Figure S3.3.</b> <i>cer10-2</i> roots produced more lateral organs than did WT roots. ....	112
<b>Figure S3.4.</b> Total fatty acid profile from Arabidopsis thaliana roots. ....	112
<b>Figure S3.5.</b> An analysis of VLCFA classes .....	113
<b>Figure S3.6.</b> A subnetwork predicted by TDCor with the addition of suberin-related genes .....	114
<b>Figure 4.1.</b> First downstream neighbors of <i>LBD16</i> .....	117
<b>Figure 4.2.</b> Expression profile of <i>PISTILLATA</i> during LRP development .....	118
<b>Figure 4.3.</b> Expression of <i>PI::GFP</i> in the WT background. ....	119
<b>Figure 4.6.</b> Whole network analyses reveal modules in gene network controlling LRP development. ....	126
<b>Figure 4.7.</b> Expression profiles extracted from the LR dataset of the genes in the three modules .....	128
<b>Figure 4.8.</b> Lateral root phenotype of some mutants of genes in the 3 <sup>rd</sup> module. ....	132
<b>Figure S4.1.</b> Expression profiles in the LR dataset of some predicted regulators of <i>PISTILLATA</i> .....	136
<b>Figure S4.2.</b> Expression profiles in the LR dataset of some predicted targets of <i>PISTILLATA</i> .....	137
<b>Figure S4.3.</b> Expression profiles of genes in the third module in the LR dataset. ....	138
<b>Figure 5.1.</b> Illustration of the gravistimulation assay. ....	153
<b>Figure 5.2.</b> Outline of organ regeneration assays .....	154

### FREQUENTLY USED ABBREVIATIONS

ARF	AUXIN RESPONSE FACTOR
Aux/IAA	AUXIN/INDOLE-3-ACETIC ACID
CIM	callus-inducing medium
Dex	dexamethasone
DMSO	dimethylsulfoxide
ECR	enoyl-CoA reductase
FA	fatty acid
FC	founder cell
GFP	GREEN FLUORESCENT PROTEIN
GR	glucocorticoid receptor
GUS	$\beta$ -glucuronidase
HACD	hydroxyl-acyl-CoA dehydratase
hpg	hour post gravistimulation
IAA	indole-3-acetic acid
KCR	$\beta$ -Ketoacyl-CoA reductase
KCS	3-keto-acyl-CoA synthase
LR	lateral root
LRIS	lateral root inducible system
LRP	lateral root primordium
MS	Murashige and Skoog
NAA	naphthalene-1-acetic acid
NPA	1-naphthylphthalamic acid
PAS	<i>PASTICCINO</i> genes
PCR	polymerase chain reaction
PI	PISTILLATA
QC	quiescent center
qRT-PCR	quantitative real-time PCR
RAM	Root apical meristem
TDCor	Time Delay Correlation
TF	transcription factor
VLCFA	very long chain fatty acid
WT	wild type

# **GENERAL INTRODUCTION**

Plant root system architecture (RSA) is the three-dimensional configuration of a whole root system in its living environment (Morris et al., 2017). RSA is considered a major determinant of plant viability and crop yield, and is a target for breeding to improve crop performance especially under various stresses (Smith and De Smet, 2012; Zhan et al., 2015). Root branching is of particular importance because it largely determines soil exploration of a root system and this can affect dramatically its water and nutrient acquisition (Lynch, 2013; Morris et al., 2017). Accordingly, the molecular mechanisms of root branching have been extensively studied in the model plant *Arabidopsis thaliana* (Arabidopsis) whose mature root system is largely derived from lateral roots (LRs) formed after germination. LRs originate from a small group of xylem-pole pericycle cells of the primary root that are primed by auxin to acquire founder cell identity (Möller et al., 2017). These founder cells undergo a succession of anticlinal and periclinal cell divisions that eventually results in the formation of a dome-shaped lateral root primordium (LRP; Malamy & Benfey, 1997; Lucas et al., 2013; Goh et al., 2016; Von Wangenheim et al., 2016). The LRP emerges through overlaying parental root tissues to become a functional LR (Swarup et al., 2008; Stoeckle et al., 2018).

Lateral root development is an excellent experimental system to study post-embryonic organogenesis. Interestingly, lateral root formation includes the *de novo* organization of a root apical meristem whose stem cell niche will subsequently sustain the continuous growth of the new LR (Laskowski et al., 1995; Malamy and Benfey, 1997). Moreover, recent studies have showed that lateral root formation shares common mechanisms with organ regeneration in tissue culture, especially the first step of callus formation (Perianez-Rodriguez et al., 2014; Fan et al., 2012; Sugimoto et al., 2010; Atta et al., 2009). Understanding these mechanisms is particularly relevant for many biotechnology applications in the field of plant regeneration and multiplication.

While many genes involved in lateral root development have been identified, little is known about the mechanisms that progressively organize the LRP into a root meristem (Trinh et al., 2018). LRP formation is not dependent on a stereotypical cell division pattern and therefore on cell lineage (Lucas et al., 2013; Von Wangenheim et al., 2016). LRP organization is a dynamic process dependent on complex gene regulatory networks and on cell-cell interactions including biomechanical interactions (Du and Scheres, 2017a; Stoeckle et al., 2018; Lucas et al., 2013). Interestingly, inference of the gene regulatory network involved in LR formation suggested an early patterning mechanism defining the central region and flanks of the LRP and identified genes involved in this process (Lavenus et al., 2015). The central region of a developing LRP self-organizes into a structure similar to that at the primary root apical meristem (RAM) (Laskowski et al., 1995; Malamy and Benfey, 1997). Some of the central cells express quiescent center (QC)-

specific markers such as *WOX5::GFP* and *QC25::CFP* (Tian et al., 2014a; Goh et al., 2016; Du and Scheres, 2017b), and in the primary RAM these QC marker-positive cells are important in regulating stem cell identity and root meristem maintenance (Xu et al., 2006). Several important transcription factors (TF) controlling meristem formation during LRP development have been described, such as *SHORTROOT-SCARECROW*, and *PLETHORAs* (Goh et al., 2016; Du and Scheres, 2017b). However, there may exist many other important factors regulating meristem formation during LRP development. In LRP flanks, *PUCHI* encoding a AP2/EREBP-family TF was previously showed to control cell division and proliferation during LRP formation (Hirota et al., 2007). *puchi-1* loss-of-function mutant produces LRPs exhibiting additional anticlinal and periclinal cell divisions from early stages and their LR have abnormally enlarged flank cells (Hirota et al., 2007). Yet, the molecular targets regulated by *PUCHI* during LR development are not known.

In the frame of the research unit "Plant Diversity, Adaptation and Development" (IRD/ University of Montpellier), the research team I worked with is interested in deciphering the regulation mechanisms that control lateral root formation in various plant models, including *A. thaliana*. To have a systematic view on genes possibly involved in LRP formation and development, the team developed an algorithm called Time Delay Correlation (TDCor) (Lavenus et al., 2015) to infer genetic interaction from a time-course transcriptomic dataset profiling every stage of LRP organogenesis (Voß et al., 2015). This algorithm is based on similarity (Pearson correlation) between time-shifted expression profiles of genes in the LR dataset to suggest their possible regulator-to-target relationships (positive or negative regulation). This approach was validated experimentally using the targets of *ARF7*, a key player in LRP formation (Lavenus et al., 2015).

The team has exploited this inference strategy to explore the potential targets of *PUCHI* during LR development and looked for the molecular processes that may be influenced by *PUCHI* in the root. Interestingly, a number of genes coding for factors involved in the biosynthesis of very-long-chain fatty acids (VLCFAs) were found to have similar expression profiles but shifted in time to that of *PUCHI*. qRT-PCR further showed that expression of key VLCFA biosynthesis genes at the first stage of LRP formation was dependent on *PUCHI*. *PUCHI* was therefore hypothesized to regulate the expression of genes involved in the biosynthesis of very long chain fatty acids (VLCFA) during LR development.

My 3-year thesis initiated in that context in May 2016, with the aim to explore further and characterize experimentally the hypothesis that *PUCHI* acts as a master regulator of the VLCFA biosynthesis pathway during LR formation. In addition, I started a new and complementary

research axis using the inference algorithm TDCor to identify upstream regulators controlling meristem establishment in the developing LRP. This PhD thesis is organized in five chapters:

**Chapter I** reviews recent advances on understanding LRP formation and development, with a link to plant regeneration from callus.

**Chapter II** describes the roles of PUCHI during LRP development through a detailed phenotyping of the loss-of-function mutant of *PUCHI*.

**Chapter III** demonstrates that PUCHI regulates the expression of VLCFA biosynthesis genes during LRP formation, and that this regulation is important for LRP formation and callus formation.

**Chapter IV** explores genes potentially involved in stem cell niche formation during LRP development and proposes further experiments to be done.

**Chapter V** provides a general discussion and perspectives resulting from this work.

**Chapter VI** describes the materials and methods used in the work.

# CHAPTER I

**Lateral root formation: building a meristem *de novo***

### Abstract

The complex and adaptable architecture of the plant root system in soil is of paramount importance for crop growth and performance. Root growth depends on the activity of the root apical meristem, an organized population of proliferating progenitor cells continuously replenished from a stem cell niche. Root branching, which greatly contributes to root system architecture in most dicot species, consists in *de novo* formation of new root meristems in existing root tissues. This phenomenon illustrates the ability of plants to repeatedly generate new tissues specialized in post-embryonic continuous growth and greatly impacts the elaboration of the root system architecture and its adaptation to environmental constraints. Here, we review the recent findings and models related to lateral root organogenesis in the dicot species *Arabidopsis thaliana*, with emphasis on the mechanisms controlling *de novo* root meristem formation. Experimental evidence suggests that critical regulatory modules are common between embryonic and post-embryonic root meristem organogenesis, and that the lateral root formation molecular pathway is in part common with organ regeneration from callus.

**Keywords:** lateral root, root branching, root meristem formation, *Arabidopsis*, auxin, organogenesis, stem cell niche

Note: this is the adapted from the review on Annual Plant Reviews online

Trinh, C.D., Laplaze, L. & Guyomarc'h, S. (2018) Lateral Root Formation: Building a Meristem *de novo*. In Annual Plant Reviews online. John Wiley & Sons, Ltd, Chichester, UK, pp. 1–44.

## I. INTRODUCTION

The root system fulfils multiple essential roles for the plant, including soil exploration and water and nutrient uptake, interactions with surrounding biotic and abiotic environments, plant anchorage to the substrate, and in some instances, vegetative reproduction or storage of photosynthates (Beeckman, 2009). In doing so, it greatly influences crop performance and yield (Rogers and Benfey, 2015). For example, changes in root system and water uptake explain a large part of the continuous increase in maize yield in the U.S. over the past 70 years (Hammer et al., 2009). Root system architecture (RSA), which refers to the spatial configuration of the whole root system of a plant in soil, is a potent parameter influencing root system function and crop growth (Lynch, 1995; de Dorlodot et al., 2007; Lynch, 2007; Rogers and Benfey, 2015). RSA traits have been frequently overlooked in past breeding programs due to the difficulty to access and quantify them. However, recent advances in phenotyping technologies and physiological modelling open the way for smart crop breeding programs targeting root traits and especially RSA (Smith and De Smet, 2012; Kuijken et al., 2015). These new breeding strategies offer a valuable approach to meet the demand in crop production in the current challenging context of increasing global human population and intensifying adversary soil and climatic conditions (Godfray et al., 2010; Tai et al., 2014; Smith and De Smet, 2012).

Plant RSA is modulated by 1) root growth, *i.e.* increase in root length, 2) root angle and 3) root branching, *i.e.* the formation of new roots such as lateral roots (LRs, originating from existing roots including lateral roots) and adventitious roots (emerging from shoot tissues, such as stem bases; Osmont et al., 2007; Bellini et al., 2014). Root growth relies on the activity of specialized tissues called root apical meristems that are organized populations of dividing cells including a self-maintained stem cell niche (Aichinger et al., 2012; Choe & Lee, 2017; Figure 1.1). Secondary root formation consists of *de novo* organogenesis of new root meristems from seemingly differentiated tissues. Contribution of post-embryonic root organogenesis to the elaboration of the plant RSA varies greatly depending on species. While the primary root and LRs emerging from it contribute to a significant extent to RSA development in dicot species, adventitious roots are predominant in RSA of most monocot species (Bellini et al., 2014). Root growth and branching are influenced by endogenous physiological cues as well as by environmental factors, such as soil texture, nutrient and water availability, and microbial interactions (Malamy, 2005; Tian et al., 2014b; Bao et al., 2014; Morris et al., 2017). This plasticity in RSA is of paramount importance for plant adaptation to environmental constraints.

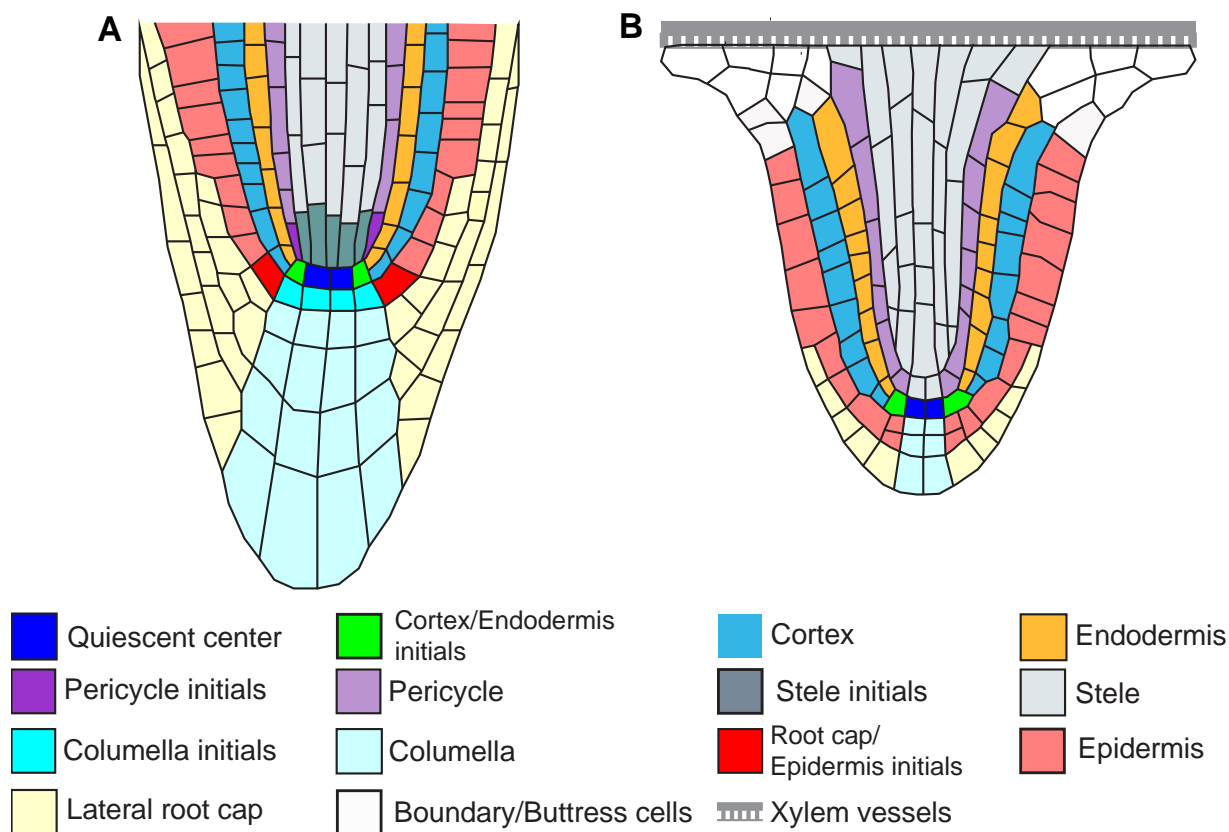


**Figure 1.1.** Arabidopsis primary root and lateral root meristems. Schematic organization of the apical meristem of Arabidopsis primary root (A) and emerged lateral root (B). Cell types of primary root apical meristem and presumptive cell types of lateral root apical meristems are indicated in the colour legend. In root apical meristems, the stem cells are called “initials” and the organizing centre is termed “quiescent centre” (QC).

Meristems are complex tissues gathering cells with little differentiation and retaining mitotic activity (Stahl and Simon, 2005). Division and differentiation of these cells are tightly regulated through a network of genetic factors and cell-to-cell communications providing plants with the ability to continuously generate new tissues and organs after germination. As a result, meristematic cells express repertoires of cell cycle-related genes but also specific factors influencing cell fate, such as chromatin modifiers and hormone and peptide signalling pathways (reviewed in Lee et al., 2013; Chiatante et al., 2018). Regulators of the structural properties of the tissue such as cytoskeleton organization, cell membrane dynamics, as well as primary cell wall formation are also of great importance for meristematic activity (Sassi and Traas, 2015). Importantly, emergent properties in this intricate regulation network generate long-lasting dynamic organization at the tissue scale, and especially, the maintenance of a central stem cell niche. Stem cells are undifferentiated cells able to divide with no apparent limit, renewing the stem cell pool as well as producing progenitor cells that will participate in the production of one or more

differentiated cell types (Laux, 2003; Spradling et al., 2001). In plant meristems these stem cells are prevented from differentiating by signalling from a group of other cells, the meristem organizing centre (Doerner, 1998). Specifically in root apical meristems, the stem cells are called “initials” and the organizing centre is termed “quiescent centre” (QC; Choe & Lee, 2017). As in animal stem cell niches (Ivanova, 2003; Zipori, 2004), the transcriptomic signature of plant stem cells remains elusive, although association of some specific transcription factors has been shown to be important (de Luis Balaguer et al., 2017; Galinha et al., 2007; Sarkar et al., 2007; Scheres, 2007). However, hormonal, epigenetic, and transcriptional regulators have been identified that play a critical role in stem cell niche establishment, organization, and maintenance (Choe and Lee, 2017). Not surprisingly, some factors, such as cell cycle effectors, are important for both shoot and root meristems. In addition, common schemes involving related molecules participate in both shoot and root meristem organization. For example, the ratio between auxin and cytokinin hormonal signalling greatly influences the balance between cell division and differentiation, although with seemingly different outputs in shoot and root contexts (Galinha et al., 2009; Vanstraelen and Benková, 2012). Additionally, in both shoot and root meristems transcription factors specifically expressed in the organizing centre inhibit the differentiation of neighbouring stem cells and are targets of a negative feedback mediated by non-cell autonomous peptides and membrane-located receptors (Stahl et al., 2013). Nevertheless, other aspects of meristem regulation, and especially hormonal and peptide signal transduction and its impact on cell differentiation, are specific to root or shoot development (Galinha et al., 2007).

The root apical meristem activity continuously generates new cells that participate to root growth as well as to renewal of the root cap, an important interface of the root meristem with the environment (Petricka et al., 2012; Perilli et al., 2012; Sozzani and Iyer-Pascuzzi, 2014). Still, only one or few root apical meristems are generated during plant embryogenesis. A significant proportion of the root system of a growing plant thus originates from post-embryonic root formation through a tightly regulated sequence of cell division and differentiation. This organogenesis process implies precise changes in cell cycle activities as well as modifications in cell gene expression programs (Birnbaum, 2016).

This review focuses on lateral root (LR) development, *i.e.* root organogenesis from existing root tissues, with emphasis on the processes generating a new functional root meristem. To that purpose, we will predominantly consider the model plant *Arabidopsis thaliana*, in which LR formation has been extensively studied. *Arabidopsis* is a dicot plant whose RSA consists of a primary root, LRs of multiple orders, *e.g.* tertiary roots, and few adventitious roots (Gutierrez et al., 2012; Smith and De Smet, 2012). *Arabidopsis* primary roots and LRs have a relatively simple

anatomy, making them a valuable model for developmental biology studies (Lavenus et al., 2013b). The young *Arabidopsis* root is made of one layer of each tissue namely from the outside to the inside, the epidermis, the cortex, the endodermis and the pericycle enclosing the vascular tissues, which includes two xylem and two phloem poles (Dolan et al., 1993; Figure 1.1). In addition, *Arabidopsis* is amenable to LR induction protocols, live imaging techniques, and genetic reporter and mutant strategies (Jansen et al., 2013; Koornneef and Meinke, 2010). A wealth of information has been gathered on the processes regulating embryonic root meristem establishment, primary root meristem maintenance and plasticity, as well as on the cellular and molecular events underlying post-embryogenesis LR formation. Here, we synthesize recent published data highlighting observed properties of post-embryonic root meristem formation and aim to identify remaining gaps in our understanding of this biological process that greatly contributes to plant development and crop production.

## **II. TISSUE CONTEXT AND EARLY EVENTS OF LATERAL ROOT PRIMORDIUM ORGANOGENESIS**

### **2.1. Competence of pericycle cells for root organogenesis**

LR formation in *Arabidopsis* originates exclusively from pericycle cells (Figure 1.2). The pericycle is a single layer of cells representing the outermost cells of the vascular cylinder (Beeckman and De Smet, 2014). Pericycle cells are produced by inner initials of the primary root meristem. Due to this anatomical position, some pericycle cells neighbour either xylem pole or phloem pole cells. Interestingly this relative positioning is of functional importance, since lateral root primordia (LRPs) originate exclusively from xylem-pole pericycle (XPP) cells in many plants such as *Arabidopsis* (Dubrovsky, 2000; Parizot et al., 2007), and only from phloem pole pericycle cells in others such as maize (Jansen et al., 2012).

What makes those pericycle cells competent for LRP initiation is not clearly understood. However, a transcriptomic analysis in maize showed that compared to non-pericycle cells, pericycle cells preferentially express a subset of genes related to protein synthesis, transcription, and signal transduction, which could explain their competence for cell division (Dembinsky et al., 2007). In addition, analyses of the expression pattern of cell cycle regulators in roots suggested that stele tissues, including pericycle, retained S-phase related gene expression longer than other root tissues (Beeckman et al., 2001). Consistent with this hypothesis, a recent analysis of mitosis distribution in *Arabidopsis* root tips showed that, together with endodermis and vascular cells, pericycle cells retained mitotic activity longer than cortex cells or epidermis cells (Lavrekha et al., 2017). The pericycle actually consists of a heterogeneous population of cells: *Arabidopsis* XPP

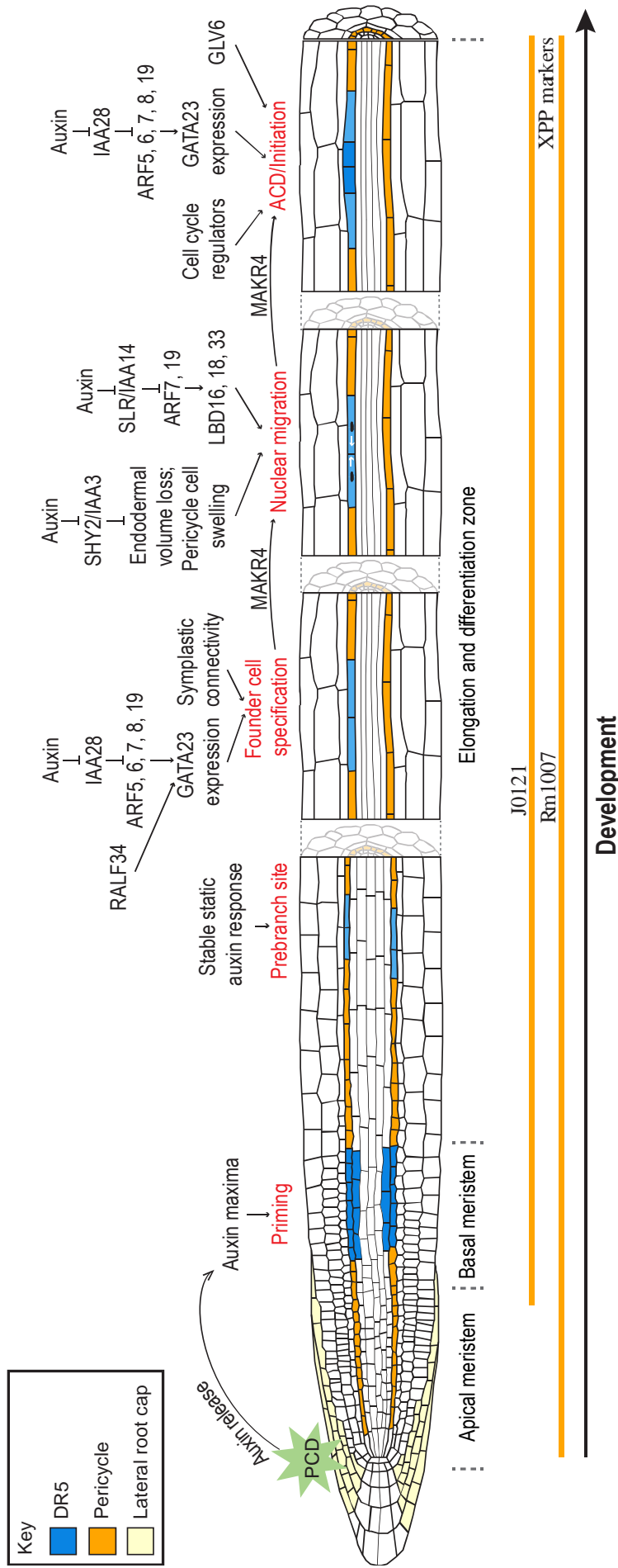


**Figure 1.2.** Key events during lateral root primordium initiation and their regulators (modified from Lavenus et al., 2013). Pericycle cells are primed partly through auxin released from programmed cell death (PCD) in the lateral root cap. Subsets of primed cells at opposite xylem poles that retain stable static auxin response are called prebranch sites, but usually only one will develop into founder cells. Founder cells then swell and their nuclei migrate to the common cell wall (white arrows). An asymmetric cell division (ACD) then occurs marking the initiation of the lateral root organogenesis program. Expression patterns of xylem-pole pericycle (XPP) cell markers (J0121 and Rm1007) and developmental zones along the primary root are indicated.

cells in the mature root retain some meristematic cell-specific features such as fragmented vacuoles, large nuclei and dense cytoplasm, and expression of S-phase related cell cycle regulators in contrast to “differentiated” pericycle cells (Casimiro et al., 2003; Beeckman et al., 2001; Parizot et al., 2007). De Almeida Engler et al. (2009) identified 16 cell cycle genes displaying preferential expression in the Arabidopsis XPP cell file. The D-type Cyclin *CYCD4;1* is expressed in XPP cells in the root meristem, and its loss of function causes a premature elongation of these cells associated with a reduced LR density (Nieuwland et al., 2009). Conversely, phloem pole pericycle cells were shown to differentiate and become quiescent significantly earlier than other pericycle cells, including XPP cells (Lavrekha et al., 2017). Longer cell cycle activity in XPP cells exiting the root meristem is dependent on the activity of *ABERRANT LATERAL ROOT FORMATION 4* (*ALF4*) as in the *alf4* mutant XPP cells only weakly express the G2-to-M transition transgene *CYCB1;1::GUS* (DiDonato et al., 2004; Celenza et al., 1995). *ALF4* is widely expressed in plant tissues and encodes a plant-specific regulator modulating the activity of SCF complexes required for the signalling of the plant hormones auxin and gibberellin (Bagchi et al., 2018). Consistent with this longer cell cycle activity of pericycle cells being instrumental for LR formation, the *alf4* mutant plants display a strong reduction in root branching, even in presence of the root-formation promoting hormone auxin (DiDonato et al., 2004; Bagchi et al., 2018).

Importantly, XPP cells express specific repertoires of genes as exemplified by the J0121 enhancer trap line that displays robust *GFP* expression in XPP cell files from the elongation zone of the meristem onwards, as well as, interestingly, in related shoot tissues competent for root formation (Casimiro et al., 2001; Laplace et al., 2005; Sugimoto et al., 2010). Another enhancer trap line, Rm1007, showed *GFP* expression specifically in XPP cells and in the corresponding initials, adjacent to the root meristem quiescent centre, including in young embryos, indicating that the genomic region highlighted by the Rm1007 insertion drives very early XPP cell fate-specific expression (Parizot et al., 2007).

The close relationship between vascular pole differentiation and pericycle cell competence for LR formation suggests a robust crosstalk between these two cell populations in the primary root meristem. For example, Arabidopsis *lonesome highway* (*lhw*) mutant, that has only one xylem and one phloem pole, specifically produces LRPs along that single xylem strand (Parizot et al., 2007). Conversely, roots of the *wooden leg* (*wol*) mutant lack phloem specification and the J0121 marker is present throughout the pericycle. Interestingly, despite this characteristic, LR formation is severely affected in the *wol* mutant background, suggesting that both xylem and phloem specification in the primary root is required for functional LR formation (Parizot et al., 2007). Patterning of xylem and phloem vascular identities in the central domain of the root meristem is

regulated through a complex network of transcriptional signalling and hormonal crosstalk (reviewed in Vaughan-Hirsch et al., 2018). A combination of experimental and modelling approaches suggested that mutual inhibition between auxin and cytokinin signalling patterned the alternating of xylem and phloem poles in *Arabidopsis* root meristem (Bishopp et al., 2011a). Signalling between vasculature identity and competence of pericycle cells for LR formation could involve auxin maxima in the xylem axis and phloem axis, in *Arabidopsis* and in maize, respectively (el-Showk et al., 2015; Jansen et al., 2012). Indeed, treatments by exogenous auxins or auxin transport inhibition alter the anatomical distinction between XPP and non XPP cells in *Arabidopsis* (Parizot et al., 2007). However, neither auxin nor cytokinin short term treatments modify the expression pattern of J0121 and Rm1007 transgenes, indicating a robust patterning mechanism of XPP cell identity in the root meristem (Parizot et al., 2007).

## **2.2. Oscillatory LR priming by endogenous cues**

In *Arabidopsis* LRs originate only from XPP cells, but not every XPP cell develops into a LRP. Indeed in the basal meristem of the parental root tip, oscillating mechanisms periodically select subsets of XPP cells and prepare them to enter LR formation, a phenomenon called “priming” (Möller et al., 2017). This selection process has a major impact on RSA by defining the potential sites for root branching. The molecular processes underlying this priming event are still not fully understood, but are associated with changes in auxin signalling (De Smet et al., 2007). Monitoring expression of the synthetic auxin-responsive *DR5 (DIRECT REPEAT5)* promoter revealed regular pulses of auxin signalling activity in the two protoxylem strands in the basal meristem. Transcriptomic analyses showed that the expression levels of hundreds of genes were also oscillating in that segment of the root, according to the same period as auxin signal oscillations (Moreno-Risueno et al., 2010). While cells exit the basal meristem, those temporal fluctuations progressively cease and high signal stabilizes into local auxin maxima correlating with future sites of LR formation (Xuan et al., 2015; De Smet et al., 2007). The specification of these sites with high and stable *DR5* signal, termed prebranch sites, is dependent on auxin signal transduction and probably on a complex network of transcription factors (Moreno-Risueno et al., 2010). The root cap plays a crucial role in creating these auxin pulses. First, a defect in auxin synthesis in the root cap impairs the amplitude of auxin signalling oscillations in the basal meristem, suggesting that auxin molecules that signal XPP priming may originate from the root cap (Xuan et al., 2015). Second, periodic programmed cell death occurs in lateral root cap cells creating rhythmic influxes of auxin into inner cells of the elongation zone of the meristem, which tightly correlate with prebranch site formation (Xuan et al., 2016). Pulsating fluxes of auxin from the root cap to the

meristem might participate in generating peaks in auxin signalling activity in the protoxylem cell files, contributing to prebranch site specification.

Basipetal (from the root tip shootward) auxin fluxes from the columella through the lateral root cap and the root epidermis have been extensively studied in *A. thaliana* in particular in relation to gravitropism (Band et al., 2012; Wisniewska et al., 2006; Rashotte et al., 2000). Consistent with the model of root cap-derived auxin priming XPP cells, parental root waving, mechanical bending, or gravistimulation modulate LR formation, possibly because of gravity-modulated auxin fluxes or changes in auxin routes due to tissue bending that affects shootward auxin distribution (Lucas et al., 2008; Ditengou et al., 2008; Laskowski et al., 2008; Scheres and Laskowski, 2016). However, even agar-constrained roots, growing with only little deviation from gravity, display oscillation in auxin signalling and regularly spaced prebranched sites (Moreno-Risueno et al., 2010). This suggests that an endogenous clock mechanism produces uniformly spaced pre-branch sites to recruit pericycle cells and make them competent for *de novo* organogenesis.

Recently, Laskowski & ten Tusscher (2017) analysed the properties of the priming process in order to elucidate the molecular steps controlling auxin signalling oscillations and subsequent stabilization of auxin signal maximum. Both could rely on emergent properties (i.e. properties that arise from the collaborative functioning of a system, but do not belong to any one part of that system) of the global genetic system controlling auxin distribution, auxin signal transduction, and cell fate specification in the meristem (Alon, 2007). Feedback mechanisms can generate oscillating gene expression patterns that result in locally fluctuating transcriptomes (De Caluwé et al., 2016) or, when combined with cell-to-cell communication, create spatial patterning of distinct cell identities (reviewed in Green and Sharpe, 2015). Other network motifs, *i.e.* specific association of gene regulatory interactions, can instead buffer variations in gene expression (*e.g.* Vernoux et al., 2011). Particularly interesting in a developmental perspective are regulatory network properties that make the system “choose” between two potential dynamic trends, causing bifurcation in system state trajectories, distinct cell fates and potentially symmetry breaking at a tissue scale (Bishopp et al., 2011a). Such critical properties are described in various aspects of plant developmental regulation by auxin, including in root tissues. Feedback of cell parameters on auxin transporter expression and polarization can create and enhance non-uniform auxin distribution across tissues in a robust manner. As a result, asymmetric auxin distribution, locally transduced by cell specific signalling mechanisms, can create shifts in cell identity among neighbours. Van Norman et al. (2013) propose that the priming process, caused by auxin signal pulses, could enhance cell sensitivity to later auxin accumulation and its competence to translate it into the onset of a new organogenesis program. Bistable properties of auxin signalling modules could explain

the “memorization” of that auxin signal in the prebranch sites only. Such a toggle-switch behaviour of an auxin-signalling motif has been described (Lau et al., 2011).

### **2.3. Lateral root founder cell specification**

Within some prebranch sites, a subset of pericycle cells is later specified to become lateral root founder cells. Founder cells (FCs) refer to pre-existing cells that initiate the formation of a new organ through cell division (Laskowski et al., 1995); thus FC specification corresponds to the last apparent transition in cell identity before the onset of organogenesis. FC specification again involves a local increase in auxin signalling (De Rybel et al., 2010; Goh et al., 2012a; De Smet et al., 2007; Moreno-Risueno et al., 2010). Selective stimulation of auxin production in one or several pericycle cells is sufficient to transform them into FCs and trigger LR organogenesis (Dubrovsky et al., 2008). Conversely, in normal conditions, emergent properties of the auxin transport and signalling network may explain why, while XPP cell specification, priming and prebranch site definition may occur symmetrically on both xylem poles of the Arabidopsis vascular cylinder (De Smet et al., 2007; Goh et al., 2012a), effective initiation of LR development only occurs on one of those two sides (Goh et al., 2012a; el-Showk et al., 2015).

Auxin transcriptomic signalling is known to involve degradation of Aux/IAA proteins and activation of associated AUXIN RESPONSE FACTOR (ARF)-family transcription factors (reviewed in Weijers and Wagner, 2016). Interestingly, an auxin signalling pathway involving IAA28 and several ARFs it interacts with is required for FC specification (De Rybel et al., 2010). This auxin signalling module induces the expression of the transcription factor *GATA23* in pericycle cells that will develop into a LRP before any sign of LR initiation (Figure 1.2). Artificially inducing *GATA23* expression in the pericycle greatly increases LRP density, indicating that it positively regulates LR formation (De Rybel et al., 2010). *GATA23* is therefore considered a marker for LR FCs, but its targets relevant for LR formation remain unknown. Interestingly, *GATA23* expression is also positively controlled by RAPID ALKALINIZATION FACTOR 34 (RALFL34), a small signalling peptide that could participate in auxin-mediated regulation of FC specification (Murphy et al., 2016).

Chromatin remodelling factors, for example Polycomb group (PcG) proteins, are known to regulate developmental transitions in both plants and animals by modulating the expression of key developmental genes (Schuettengruber et al., 2017). PcG proteins can form two multiprotein complexes: Polycomb repressive complex 1 (PRC1) and PRC2 which modify histone marks on chromatin to repress gene expression (Derkacheva and Hennig, 2014). Arabidopsis mutants impaired in subunits of the PRC2 complex CURLY LEAF (CLF) and EMBRYONIC FLOWER 2 (EMF2) displayed increased density of LR FCs and emerged LRs, suggesting that the PRC2

complex might inhibit LR FC specification (Gu et al., 2014). *CURLY LEAF* is expressed in the basal meristem and in presumptive FCs, and directly represses the expression of the auxin efflux carrier-encoding gene *PIN-FORMED 1 (PIN1)* via histone modification (Gu et al., 2014). *PIN-FORMED 1* participates to auxin signal concentration in the root tip and in LRPs (Benková et al., 2003; Blilou et al., 2005). Accordingly, an increase in the auxin-sensitive *DR5* promoter activity was reported in root apical meristems and in FCs of a loss-of-function *clf* mutant (Gu et al., 2014). Other chromatin remodelling processes were shown to participate in the regulation of cell fate transition during LR founder cell specification, such as histone deacetylation (Singh et al., 2012), ATP-dependent chromatin remodelling (Fukaki et al., 2006; Ho et al., 2013), or histone variant deposition (Manzano et al., 2012). The precise hierarchy of these regulatory levels in combination with the auxin signalling network remains to be elucidated.

Plasma membrane-located signalling processes during FC specification are suggested by the impaired conversion of prebranch sites into LRPs in a mutant defective in the *MEMBRANE-ASSOCIATED KINASE REGULATOR4 (MAKR4)* gene (Xuan et al., 2015). The *MAKR4* protein belongs to the same protein family as *MAKR5* (Kang and Hardtke, 2016) and *BRI1 KINASE INHIBITOR 1 (BKI1)* (Wang & Chory, 2006; Jiang et al., 2015), that are regulators of receptor kinases-associated signalling pathways. Expression of *MAKR4*, which is induced by auxin, is strongly enhanced in pericycle cells before cell division occurs and displays oscillations similar to that of *DR5::LUC* reporter expression. Importantly, the *makr4* mutant has a normal number of prebranch sites but produces fewer LRPs, and overexpression of *MAKR4* promotes LRP formation. The data indicates that *MAKR4* participates in the transition of a prebranch site into a LRP (Xuan et al., 2015).

Proper cell-to-cell communication via plasmodesmata is also necessary for correct LR FC specification (Benitez-Alfonso et al., 2013). In *plasmodesmal-localized b-1,3-glucanase 1 (pdbg1)*, *pdbg2* single and double mutants whose increased callose deposition in the stele and LRPs block plasmodesmata, LR are formed at higher density, sometimes even fused to each other (Benitez-Alfonso et al., 2013). Closer inspection revealed expanded domains of *GATA23* expression and auxin signalling activity (as reported by *DR5* promoter-based transgene expression) around FCs, indicating that the correct function of these plasmodesmata-located proteins is necessary to restrict FC specification to a subset of selected cells. How exactly symplastic communication keeps LR formation in check is currently not understood, but possibly through the movement of non-cell autonomous factors, such as transcription factors, peptides, metabolites or hormones (Benitez-Alfonso, 2014; Van Norman et al., 2011; Bishopp et al., 2011b; Yue and Beeckman, 2014; Benitez-Alfonso et al., 2013).

## 2.4. Lateral root primordia initiation

In *Arabidopsis*, LRP initiation is first visually recognized by the swell of LR FCs, together with the shrink in volume of overlaying endodermal cells (Vermeer et al., 2014). Subsequently, nuclei of two longitudinally adjacent FCs, in each row, migrate to the common cell wall (De Rybel et al., 2010). Then these two cells undergo an anticlinal and asymmetric division yielding two shorter daughter cells next to each other (Casimiro et al., 2001; De Rybel et al., 2010). This typical cell division occurs in 4 to 6 abutting pericycle cell files concomitantly (Goh et al., 2016; Von Wangenheim et al., 2016). Because this asymmetric cell division produces two daughter cells with distinct shape and fate, it is a formative rather than a proliferative cell division (Gunning et al., 1978; Smolarkiewicz and Dhonukshe, 2013). Occurring independently of an established stem cell niche context and in a seemingly differentiated tissue, it is a landmark of the initiation of a new developmental program (De Smet and Beeckman, 2011). This first round of pericycle cell division produces the so-called stage I LRP (Malamy and Benfey, 1997). LRP initiation can also occur in a less common way from files of single pericycle cells (Dubrovsky et al., 2001; De Smet et al., 2006).

The swelling of FCs prior the first asymmetric cell division is assisted by volume loss of endodermal cells induced by auxin perception (Vermeer et al., 2014). Indeed, when endodermal cells expressed the stabilized form of SHY2, an Aux/IAA auxin signalling inhibitor, they were unable to lose their volume, hence maintained their turgidity. In those conditions underlying pericycle cells could not swell nor initiate asymmetric cell division, indicating that this space accommodation interaction between pericycle and endodermis is necessary for LR initiation (Vermeer et al., 2014). Moreover, ablation of an overlying endodermal cell triggers pericycle cell division, although in a periclinal manner, unless auxin was added (Marhavý et al., 2016).

An early characteristic feature of LR initiation is the change of cell polarity revealed by nuclear migration in pericycle cells preceding the asymmetric cell division. This is controlled by auxin-triggered expression of the *LATERAL ORGAN BOUNDARIES DOMAIN (LBD)* family transcription factors *LBD16*, *LBD18* and *LBD33* in pericycle cells (Goh et al., 2012a). The expression of *LBD16* in XPP and FCs is dependent on the SLR/IAA14-ARF7-ARF19 auxin signalling pathway (Goh et al., 2012a). Interestingly, artificially converting *LBD16* into a transcriptional repressor does not affect auxin signal in LR FCs but blocks the polar nuclear migration and subsequent anticlinal division of these cells, suggesting that the SLR/IAA14-ARF7-ARF19-LBD16 signalling cascade transduces auxin signalling into changes in pericycle cell polarity (Goh et al., 2012a). The transcription factor bZIP59 physically interacts with LBDs, including *LBD16*, *LBD17* and *LBD29* to control LRP initiation (Xu et al., 2018b).

Transcriptomic analysis of auxin-induced LR initiation shed light on the early molecular events leading to pericycle cell division (Vanneste et al., 2005; De Smet et al., 2008; De Almeida Engler et al., 2009). Cell cycle progression is tightly regulated by an intricate and dynamic network involving transcription regulators (such as E2F and RBR) and cyclin-dependent kinases whose activity is post-transcriptionally regulated by phosphorylation, protein-protein interaction, as well as APC/C-mediated ubiquitination and degradation (Genschik et al., 2014; Breuer et al., 2014; Komaki and Sugimoto, 2012). One G1-to-S phase specific gene (*CYCD3;2*), one S-specific gene (*CYCA2;4*) and two G2-to-M related genes (*CYCB2;5* and *CDKB2;1*) are upregulated in roots submitted to auxin-induced LR formation (Vanneste et al., 2005). Conversely, some genes encoding cell cycle inhibitors such as *KRP2*, *KRP4*, *KRP7* and *WEE1* are downregulated in the pericycle upon auxin treatment (De Almeida Engler et al., 2009). In normal conditions, the *CYCB1;1* gene, encoding a G2-to-M transition specific cyclin, is strongly expressed in XPP cells undergoing the first division (Himanen, 2002; Beeckman et al., 2001).

In addition to the change in LR FC cell polarity, SLR/IAA14-dependent auxin signalling is essential for their first divisions. Either *slr* gain of function mutation or loss of function mutation of its two ARF partners ARF7 and ARF19 prevents LR formation because the first anticlinal and subsequent periclinal divisions of pericycle cells are blocked (Fukaki et al., 2002). The implication of SLR/IAA14 in priming and FC specification can be excluded because it is not expressed in basal meristem (Fukaki et al., 2002) and competence for LR FC specification of *slr* pericycle cells is still maintained (De Smet et al., 2007; De Rybel et al., 2010). The transcriptomic analysis by Vanneste et al. (2005), demonstrated that specific G1-to-S, S, and G2-to-M cell cycle regulators act downstream of IAA14-ARF7-ARF19 mediated auxin signalling. In addition, active ARF7 and ARF19 transcription factors stimulate the expression of *LBD18* and *LBD33* which in turn stimulate the expression of E2Fa, a potent activator of S-phase promoting gene expression (Berckmans et al., 2011). Another pathway for auxin-mediated cell cycle reactivation in XPP cells could consist in the downregulation of *KRP2*, an inhibitor of *CYCD2;1*-CDKA complex activity which could stimulate G1-to-S transition (Sanz et al., 2011).

The first asymmetric cell division in LRP formation is also regulated by a peptide belonging to the GOLVEN/root growth factor/CLE-like (GLV/RGF/CLEL) family, *GLV6* (Fernandez et al., 2015). *GLV6* is expressed in FCs preceding the migration of nuclei, and *GLV6* silencing or overexpressing lines display decreased or increased FC division, respectively. In addition, overexpression of *GLV6* or treatment of roots with *GLV6* peptides disrupts the migration of FC nuclei to the common cell wall without disturbing cell cycle progression, converting the asymmetric cell division into a symmetric division (Fernandez et al., 2015). Thus cell-to-cell

communication mediated by GLV6 and possibly other GLV/RGF/CLEL family peptides is probably involved in the correct coordination of the asymmetric LR FC division (Fernandez et al., 2015).

The double mutant impaired in AURORA kinases (*aur1 aur2*) shows a strong defect in division plane orientation during LR formation, as early as the first asymmetric cell division. Although LR initiation density and polar localization of FC nuclei are unaffected, the positioning of the new cell wall is uncontrolled (Van Damme et al., 2011). Interestingly, while this results in a reduced proportion of emerged LRPs, this does not totally preclude LR formation, indicating the robustness of this organogenesis program (Van Damme et al., 2011).

## 2.5. Control of lateral root spacing/density

Mechanisms controlling LR FC specification and LRP initiation along the primary root deeply impact the overall root branch production, *i.e.* LRP density (number of LRPs divided by the length of the parent root). In addition, other factors are required for efficient LRP spacing. The gene encoding the membrane localized receptor-like kinase *ARABIDOPSIS CRINKLY4 (ACR4)* is expressed specifically in the short daughter cells after the first asymmetric cell division. The *acr4* mutant produces LRPs at higher densities and these LRPs usually stretch, sometimes even fuse together, indicating that ACR4, and possibly related kinases, control cell proliferation and spacing of newly initiated LRPs (De Smet et al., 2008). ACR4 was proposed to be the receptor of GLV6 and other related peptides (Fernandez et al., 2013), and possibly to transduce perceived signals inside the cell through a phosphorylation cascade involving the PROTEIN PHOSPHATASE 2A (PP2A; Yue et al., 2016). Cytokinin synthesized at the flanks of existing LRPs was found to act as an inhibitor of LRP initiation, thereby preventing closely formed LRPs (Chang et al., 2015). Interestingly, expression of *ACR4* and *GLVs* were significantly reduced in mutants defective in cytokinin biosynthesis, but ACR4 and cytokinin seem to act in partially separate pathways (Chang et al., 2015). Another peptide, C-TERMINALLY ENCODED PEPTIDE 5 (*CEP5*), is also involved in the regulation of LRP initiation and positioning (Roberts et al., 2016). Overexpression of the *CEP5* gene and exogenous treatment by the *CEP5* peptide reduce LRP initiation events and induce the formation of closely positioned LR, while *CEP5 RNAi* lines display an increase in LRP stage I and II density. Remarkably, *CEP5* is expressed specifically in phloem pole pericycle cells and adjacent phloem cells, indicating an unknown crosstalk between different pericycle populations (Roberts et al., 2016). Similarly, the PLETHORA (PLT) transcription factors PLT3, PLT5, PLT7 act redundantly downstream of the ARF7- and ARF19-mediated auxin signalling pathway to regulate LRP spacing (Hofhuis et al., 2013).

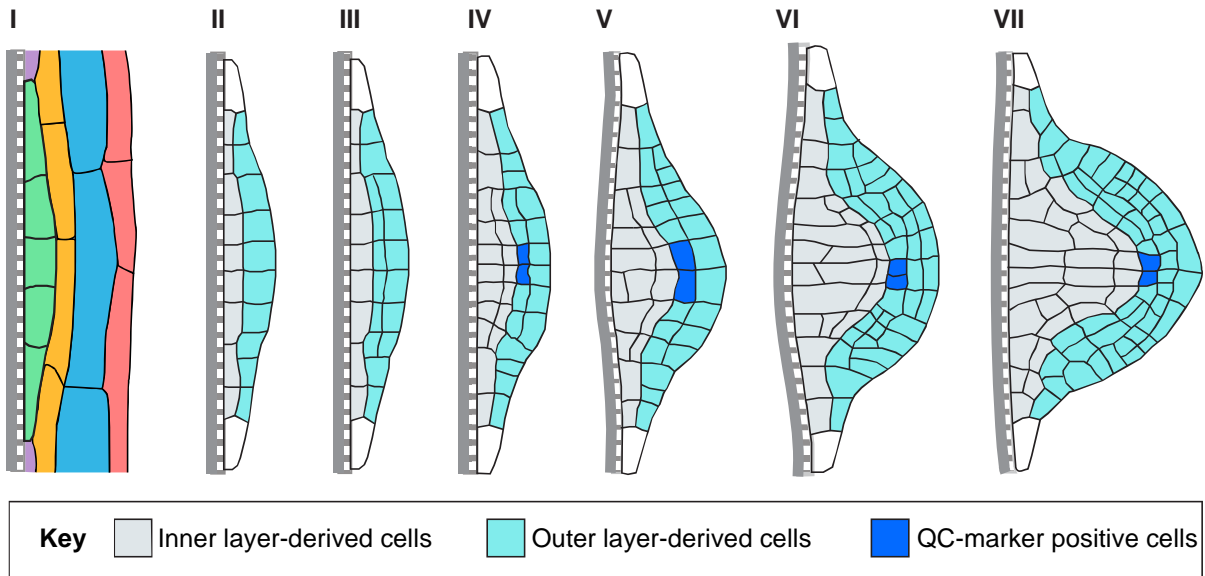
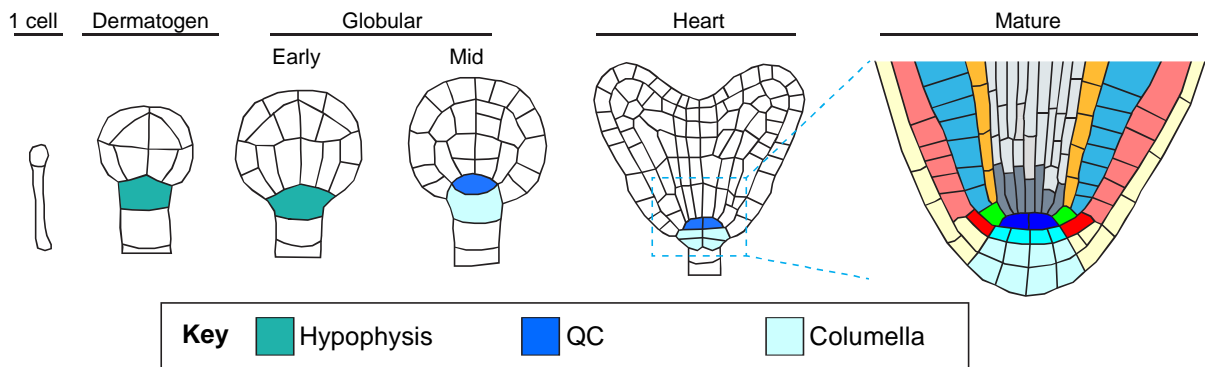
In summary, cells competent for LR formation are pericycle cells that have been progressively selected through a series of regulatory events: competence acquisition (or conservation) in the root meristem along with vascular strands patterning; priming of subsets of these cells through an endogenous clock mechanism followed by memorization of the prebranch site status, and eventually initiation of the LR organogenesis program revealed by anticlinal asymmetric cell division of so-called LR FCs. At each of these steps, local auxin signalling is involved in cell selection and state transition. Regular LR patterning along the root results from a robust emergent behaviour of the endogenous regulatory system (Figure 1.2). Still, this system allows the integration of environmental inputs, which translate into changes in auxin distribution, thus allowing adaptive responses of LR initiation to environmental constraints (Yu et al., 2015, 2016).

### **III. BUILDING A NEW ORGAN: A COHERENT PROGRAM OF COORDINATED CELL DIVISIONS, WITH NEWLY SET AXIS OF GROWTH AND BOUNDARIES**

After initiation, LRPs evolve in terms of tissue organization and morphology, developing in a direction perpendicular to the main root axis. LRP development is categorized into stages characterized by structural and positional features (Malamy & Benfey, 1997; Figure 1.3). Briefly, LRPs of stage I, II, III and IV are one, two, three and four cell layers thick, respectively, thanks to successive periclinal divisions. Stage V LRPs penetrate the endodermis and are characterized by two cuboidal cells of the second outermost layer. At stage VI, LRPs have the typical dome shape reminiscent of the primary root tip, and its outermost layer has around 12 cells. LRPs of stage VII are more complex structurally and touching the epidermis, ready for emergence (Malamy and Benfey, 1997). From founder cells to an emerged LR, LRP organogenesis relies on a series of cell divisions in different planes that need to be well coordinated to ensure proper organization and development of the new organ.

#### **3.1. Control and sequence of cell division and division planes**

As mentioned above, cell division is instrumental in LRP organogenesis, and in *Arabidopsis* conserved landmarks define important steps in the process of new LR formation. However, in contrast to embryo organogenesis which follows a highly regular cell lineage (Palovaara et al., 2016), cell division in developing LRPs do not follow a fully stereotypic sequence, leading to significant differences in cell numbers between LRPs of the same stage

**A - Lateral root organogenesis****B - Embryonic root organogenesis**

**Figure 1.3.** Schematic presentation of LRP organogenesis and embryonic root organogenesis. (A) LRP organogenesis is usually described as different stages (I-VII and finally emergence). The stage I LRP (4 green cells) divides periclinally to form stage II LRP having two cell layers. The inner layer of stage II LRP will eventually develop into ground tissues and pericycle (grey), while the outer layer develops into the endodermis, cortex, epidermis and root cap (light blue). From stage IV onwards, some central cells start expressing QC markers. For simplicity, the pericycle, endodermis, cortex and epidermis tissues of the parent root that are shown at stage I LRP are not shown in stage II-VII LRPs. (B) After fertilization, the embryo develops from the zygote through different stages. At dermatogen stage, a hypophysis is established which will divide asymmetrically to form a lens-shape cell and a basal cell (mid globular stage), and eventually develop into the root apical meristem (from heart stage onwards). Colour legend for figure A-I (except the stage I LRP) and B-Mature is as of Figure 1.1.

(Lucas et al., 2013; Von Wangenheim et al., 2016). Nevertheless, modelling and experimental observation revealed that division of LRP cells may follow a small set of rules: (i) cells tend to follow the “shortest wall” principle, meaning that the positioning and geometry of newly formed

cell wall frequently minimize the surface contact between the two daughter cells, (ii) cells often alternate their division plane (*i.e.* periclinal and anticlinal) between two consecutive divisions, and (iii) the outer layer predominantly divides periclinally prior to the inner layer (Von Wangenheim et al., 2016). Remarkably, despite variation in cell number, LRP shapes at a particular stage appear to be consistent (Lucas et al., 2013), indicating some higher levels of regulation contributing to the dome shape formation. Differential contribution of each pericycle founder cell to the LRP organogenesis participates in this dome shape development. In live time course analysis, ~60% of the LRP cell population derived from two or five founder cells (Von Wangenheim et al., 2016). Importantly, mutants of AURORA kinases, that are impaired in the control of cell division planes, can still form LRPs having typical domed-shape but lacking layered organization (Lucas et al., 2013; Van Damme et al., 2011). All the data points to a great conservation in shape formation of developing LRPs.

Changes in cell division planes guide major transitions during the LRP morphogenesis, namely, the establishment of a new axis of growth, perpendicular to the main axis of the parental root, and the transition from bilateral to radial development. The first transition corresponds to the first periclinal divisions of stage I primordium cells, creating two cell layers characteristic of the stage II primordium. What controls this perpendicular shift in cell division plane orientation is currently not clearly understood. A long-standing model for cell division plane orientation in plants, which can be formulated as the “shortest wall” rule, proposes that the new cell wall follows one of the possible configurations that minimize the interface area between the two daughter cells. This model fits observed cell division planes in many cases, especially in embryos, shoot meristems, and LR development (Louveaux et al., 2016; Yoshida et al., 2014; Von Wangenheim et al., 2016). However even in those contexts in some instances, this model could not predict division plane orientation. Monitoring of the first periclinal division in the developing LRPs using light sheet microscopy showed that only 50% of the dividing cells followed the “shortest wall” rule (Von Wangenheim et al., 2016). More recently, a mechanical, tension-based rule for cell division plane orientation was proposed (Louveaux et al., 2016). This rule could explain cell division plane orientation better than the “shortest wall” principle in tissues submitted to anisotropic forces, which could be the case for the swelling pericycle cells constrained between the underlying XPP cells, the overlaying endodermis, and the neighbouring pericycle cells. Interestingly, endodermis cell ablation, which modifies mechanical constraints in the surrounding tissues, provokes the periclinal cell division of the underlying pericycle cell (Marhavý et al., 2016). Alternatively, high auxin concentration was proposed to instruct dividing cells to escape the default “shortest wall” rule during embryo development (Yoshida et al., 2014). Dividing pericycle cells are known to be

sites of high auxin signalling, dependent from convergent auxin transport from neighbouring pericycle cells as well as overlaying endodermal cells (Marhavý et al., 2013; Benková et al., 2003). Strikingly, auxin supplementation after endodermis cell ablation causes ectopic pericycle cell division plane to shift from periclinal to anticlinal (Marhavý et al., 2016). Altogether, this data supports the hypothesis that auxin distribution across the tissue and/or mechanical constraints influence formative periclinal cell plane orientation and the onset of the LRP growth axis.

Interestingly, by meticulously documenting the orientation of cell division in 3D of hundreds LRPs from stage I to VI, Lucas et al. (2013) found that cells on the flanks of LRPs undergo either tangential or radial division. As a consequence, these cells form a ring surrounding the mass of daughter cells originated from the central cell files, contributing to the transition from the bilateral structure of the newly initiated LRP to its radial structure at later stages (Lucas et al., 2013). Because of the particular position of these cells at the flanks of the developing primordium, their specific division geometry could also be influenced by local mechanical or hormonal cues.

### **3.2. LRP cellular organization and anatomical patterning**

During regular Arabidopsis LR development, the sequence of cell divisions, although not fully stereotyped, produce conserved anatomical landmarks in the elaboration of the LRP cellular patterning (Malamy and Benfey, 1997). Notably, important transitions are (i) the first round of periclinal cell divisions at the stage I to II transition, (ii) the organisation of a small group of subapical cells reminiscent of a meristem-organizing centre at the stage IV to V transition, concomitant with LRP breaking through the endodermis, acquiring dome shape and radial symmetry (Goh et al., 2016), and (iii) the elongation of basal cells during LRP emergence (Malamy & Benfey, 1997; Figure 1.3). These transitions highlight changes in the identity and behaviour of some LRP cells and contribute to the LRP functional patterning. For instance, specific gene expression profiles distinguish the outer layer from the inner layer cells in stage II LRPs. The expression of *SCARECROW (SCR)* is first detected specifically in the outer layer of stage II LRPs, while *SHORT-ROOT (SHR)* expression is detected weakly from stage I and in both inner and outer layers of stage II LRPs (Tian et al., 2014a; Malamy and Benfey, 1997; Goh et al., 2016). Gene expression patterns become more and more complex as the LRP grows and organizes into a new root apical meristem. The molecular events controlling *de novo* meristem patterning will be addressed in the next section. First, we will consider major regulators of overall LRP morphogenesis and patterning.

Analysis of auxin signalling (as reported by *DR5*-based reporter expression) in developing primordia shows that while being strongly and homogeneously enhanced in stage I LRPs as compared to surrounding tissues, auxin activity is gradually confined to the central cells in outer

cell layers of developing LRPs, and to the tip of emerged LRs (Benková et al., 2003). In various tissues, gradients of auxin distribution are known to be predominantly controlled by the polar localization of PIN-FORMED family auxin carriers, although other auxin transporters, or auxin biosynthesis or degradation, can participate (Zhao, 2010; Petrasek and Friml, 2009; Tang et al., 2017). Several members of the *PIN* family are expressed in developing primordia, including *PIN1* and *PIN3*, although for some genes experimental results differ depending on the reporter constructs used (Guyomarc'h et al., 2012; Benková et al., 2003). Notably the *pPIN1::PIN1:GFP* reporter construct (rescuing the *pin1* mutant phenotype) is expressed early during LRP development and the recombinant protein displays a polar distribution in the cell membrane pointed to the primordium tip, consistent with *DR5*-reported auxin signalling gradients. LRPs produced in a context of impaired auxin transport, either through genetic mutations or chemical treatments, display dramatic alterations in shape and organization and eventually often fail to emerge (Geldner et al., 2003; Moriwaki et al., 2011; Benková et al., 2003). Conversely, artificially inducing pericycle cell division, either by cyclin transgenic expression or by endodermal cell ablation, provokes the accumulation of cells without any sign of primordium patterning unless auxin is added (Marhavý et al., 2016; Vanneste et al., 2005). This data collectively demonstrates that non-uniform auxin distribution in the primordium is instructive for its cellular organization.

The distribution pattern of PIN proteins is regulated by the *PLT* genes, a family of AINTEGUMENTA-like transcription factors which have multiple roles in auxin-regulated root development (Du and Scheres, 2017b; Scheres and Krizek, 2018; Blilou et al., 2005; Galinha et al., 2007). While *PLT3*, *PLT5* and *PLT7* are expressed in some pericycle cells prior to the first asymmetric cell division of LRPs, *PLT1*, *PLT2* and *PLT4* are expressed in LRPs of later stages (Hofhuis et al., 2013). The expression of *PLT3*, *PLT5* and *PLT7* is required for the expression of *PLT1*, *PLT2* and *PLT4*, so that the triple mutant *plt3 plt5 plt7* is actually a PLT null mutant in the context of LRP development (Du and Scheres, 2017b). A majority of LRPs in the triple mutant *plt3 plt5 plt7* lack periclinal cell division in early stages and show abnormal cell division planes at later stages, resulting in abnormally shaped LRPs. These LRPs have very low expression of *PINs* including *PIN1* and *PIN3*. Few LRPs of this mutant are able to emerge (Du and Scheres, 2017b), again pointing to the role of polar auxin distribution in LRP development.

Some transcription factors were shown to play a critical role during the first step of LRP cellular organization. The GRAS family transcription factor *SHORTROOT (SHR)* gene is expressed in primary meristem stele, including the pericycle and stage I developing LRPs, and the SHR protein is also detected in the overlying endodermis layer (Goh et al., 2016). As early as stage II, the cytoplasmic SHR protein is confined to the inner layer of the developing LRPs, while

nuclear SHR proteins are detected in the outer cell layer (Goh et al., 2016). Concomitantly expression of an SHR target, the related transcription factor *SCR* gene, is initiated in the outer layer of stage II primordia, and later is restricted to the second outermost layer, contacting the *SHR*-expression domain (Goh et al., 2016).. Importantly, analysis of loss-of-function mutants showed that SHR function is required for proper lateral LRP organization (Lucas et al., 2011; Goh et al., 2016). In addition, SCR controls specifically the cell division in the outer layer of stage II primordia. In *scr-3* mutant primordia, this division is blocked whereas cell division in the inner layer continues with little modifications compared to the wild type. As a consequence, the *scr-3* LRP patterning is severely affected from stage II onwards (Goh et al., 2016).

### 3.3. Lateral root primordia boundary

To describe the organization of a LRP, the concepts of boundary (or flank/periphery) and centre domains are frequently used. LRP boundary and centre domains can be delimited by the ring of cells originated from tangential and radial cell division described above. These cells seem to act as a structure to support the rapidly developing LRP apex and are termed “buttress cells” (Lucas et al., 2013; Figure 1.1). Their cell division pattern could be distinctively controlled since several cell cycle genes are preferentially expressed in the boundary (De Almeida Engler et al., 2009).

A few genes involved in the regulation of LRP boundary have been reported. The auxin transporter *PIN6* gene is expressed specifically in the boundary of developing LRPs and is involved in auxin homeostasis during plant development. LRPs of seedlings overexpressing *PIN6* undergo more rounds of anticlinal cell division, resulting in misshaped LRPs (Cazonelli et al., 2013). *PUCHI* encodes a transcription factor of the AP2/EREBP family involved in the control of LRP morphogenesis. Its expression is detected in the whole LRP of early stages and gradually confines to the flank domain of LRPs of later stages. Periphery cells of LRPs of *puchi-1* mutant have extra anticlinal cell divisions, and some of those cells may be enlarged, suggesting that *PUCHI* regulates cell division pattern and cell differentiation during LRP development (Hirota et al., 2007). *PUCHI* functions downstream of auxin signalling and is proposed to co-act with LBD16/18 to control LRP development (Kang et al., 2013; Hirota et al., 2007). Its targets are currently unknown.

Loss of function of *ARABIDOPSIS HOMOLOG of TRITHORAX1 (ATX1/SDG27)*, a chromatin remodelling factor, impacts the coordination of cell division and cell differentiation in both primary root meristems and developing LRPs. Developing LRPs lacking ATX1 function are delayed, disorganized, and frequently exhibit enlarged flanking cells (Napsucialy-Mendivil et al., 2014). Still, the auxin signalling pattern in *atx1* (as reported by *DR5::GFP*) looked similar to

normal LRPs suggesting that *ATXI* controls LRP patterning and cell proliferation independently of auxin response (Napsucialy-Mendivil et al., 2014).

Similarly, loss of function of the transcription factor *MYB36* causes misspecification of the LRP boundary (Fernández-Marcos et al., 2017). In the primary root meristem *MYB36* is a target of *SCR* and a master regulator of endodermis cell differentiation (Lieberman et al., 2015). In LRPs, *MYB36* is expressed specifically in boundary cells and regulates genes involved in reactive oxygen species homeostasis. It is hence proposed that *MYB36* regulates cell proliferation of LRP boundary domain by controlling their redox status (Fernández-Marcos et al., 2017).

### **3.4. LRP shape progression through surrounding tissues and LRP emergence**

As LRP cells divide, the LRP grows in contact with overlaying tissues, the first one being the endodermis. While the LRP develops from stage I to stage IV, the overlying endodermis, which contains lignified and suberized cell walls (Naseer et al., 2012; Vishwanath et al., 2015), is subjected to important cell wall modifications (Vermeer et al., 2014). LRPs of mutants having increased deposition of suberin or lignin in the endodermis (*i.e.* more physical constraints) or plants in which the auxin-mediated response of endodermis has been impaired, are flatter compared to those of WT, leading to a delay in LRP emergence (Lucas et al., 2013). By tracking the height of LRPs during their development, Goh et al. (2016) showed that LRP heights increase gradually from stage I to IV, but display a dramatic increase in LRP height during stage V when LRPs cross the endodermis. That sudden change can be explained by cell expansion rather than cell division (Goh et al., 2016). The shape of LRPs also changed from flat-topped to dome-shaped after breaking through the endodermis (Lucas et al., 2013; Goh et al., 2016).

The Casparian strips surrounding endodermis cells and linking them together form a supracellular network that is sturdy and resistant to pectinases (Geldner, 2013a), meaning that it is difficult for endodermal cells to separate to accommodate LRP penetration. Overlaying endodermal cells lose their cell volumes instead and become flatter. Plasma membranes of these cells are sometimes even fused together, but their integrity largely remains intact (Vermeer et al., 2014). Consequently, endodermal cells are separated at small breaking points just enough for the penetration of a LRP (Vermeer et al., 2014).

Although the volume loss mechanism of endodermal cells minimizes the impact of LRPs on Casparian strip integrity, it still can be compromised. A layer of suberin is deposited at the site of LRP penetration, covering both the endodermal cells and LRP surface (Li et al., 2017). This layer of suberin is thought to compensate to the damage of the Casparian strip, ensuring the function as an apoplastic barrier of the endodermis (von Wangenheim et al., 2017).

Although the cortex and epidermis pose less physical constraints to a developing LRP, they are also important for LRP development and participate actively to the process (reviewed in Stoeckle et al., 2018). Epidermal cells of two adjacent cell files are separated from one another to facilitate the progression of a LRP (Swarup et al., 2008). This separation is regulated by activity of cell-wall remodelling enzymes in cells directly overlaying a developing primordium. Expression of these enzymes is regulated by a ARF7-LBD29-LAX3-LBD18 cascade (Porco et al., 2016; Lee and Kim, 2013; Swarup et al., 2008) and other players such as *BRS1* (Deng et al., 2017).

Water movement between cells is partially controlled by water channels called aquaporins integrated in cell membranes (Li et al., 2014). A combination of experimental analysis of root tissue permeability to water and plasma membrane intrinsic aquaporins (PIPs) gene expression suggested that a complex spatio-temporal regulation of water fluxes across the root tissues, at least partially mediated by auxin, was critical for LRP emergence (Péret et al., 2012). A modelling approach proposed that for optimal LRP emergence, auxin-mediated fine tuning of water transport could participate in increasing cell turgor in the LRP while decreasing it in the overlaying cortical and epidermal cells (Péret et al., 2012). Moreover, during LRP development, tonoplast intrinsic aquaporin (TIP) protein levels are also regulated spatio-temporally, and defects in TIPs led to defects in LRP emergence. It was proposed that TIPs finely control the movement of water from surrounding tissues into cells at the base of LRPs, allowing these cells to expand rapidly, thereby facilitating the emergence of LRPs (Reinhardt et al., 2016). This model is consistent with the observation that the emergence of LRPs through overlying tissues is largely due to the rapid expansion of these basal cells (Malamy and Benfey, 1997; Goh et al., 2016). A recent study showed that during LRP formation, the circadian clock is re-phased, and this modulation regulates auxin-related genes and is required for LR emergence (Voß et al., 2015). One possible explanation is that the re-phased circadian clock helps differentially control hydraulic properties of cells within LRPs and in surrounding layers, thereby facilitating LRP emergence (Voß et al., 2015).

### **3.5. Connectivity between developing lateral root primordia and the primary root**

The LR vasculature needs to connect to that of the primary root for proper functioning. Stele connection happens only when the LR already emerges as revealed by phloem unloading and stele marker expression studies (Oparka et al., 1995; Malamy and Benfey, 1997). In LRPs, the connection with the primary root stele relies on symplastic connectivity, *i.e.* plasmodesmata. Using the symplastic reporter *pSUC2-GFP*, it was shown that symplastic connection is present at early stages of LRP development, but is completely blocked at later stages until a functional stele is formed in emerged LRs (Guyomarc'h et al., 2012; Benitez-Alfonso et al., 2013). This change is correlated with the progressive deposition of callose at plasmodesmata, a process regulated by

callose-degrading enzymes encoded by *PLASMODESMAL-LOCALIZED B-1,3-GLUCANASE (PdBG)* genes (Benitez-Alfonso et al., 2013).

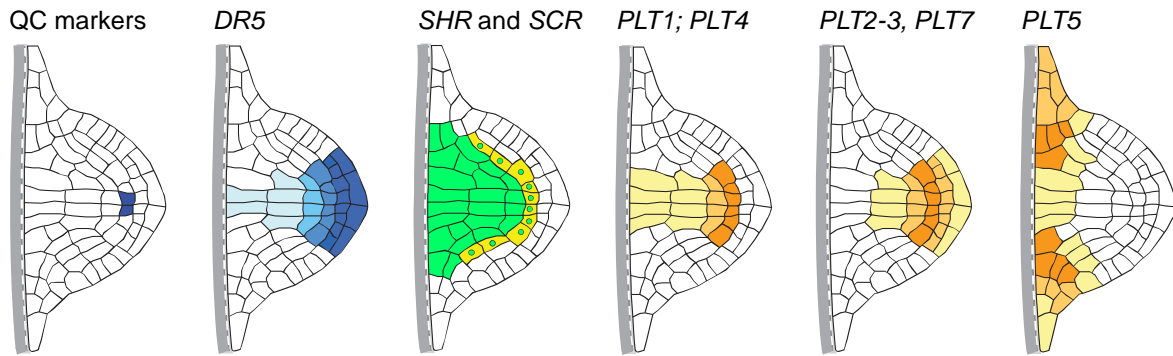
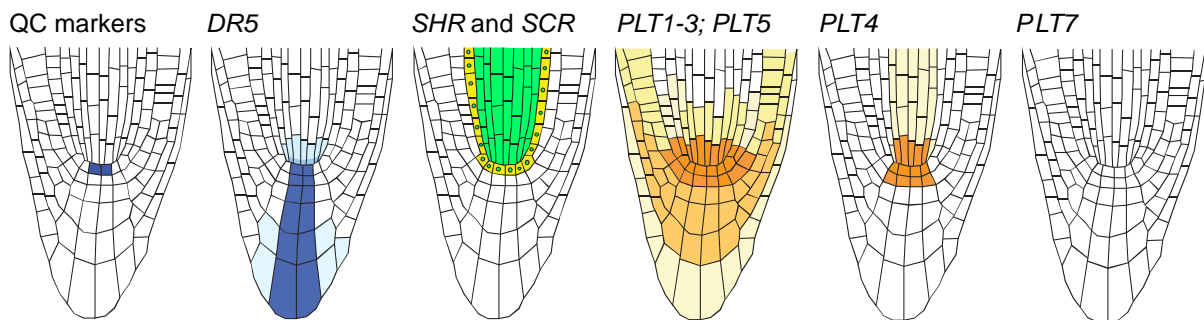
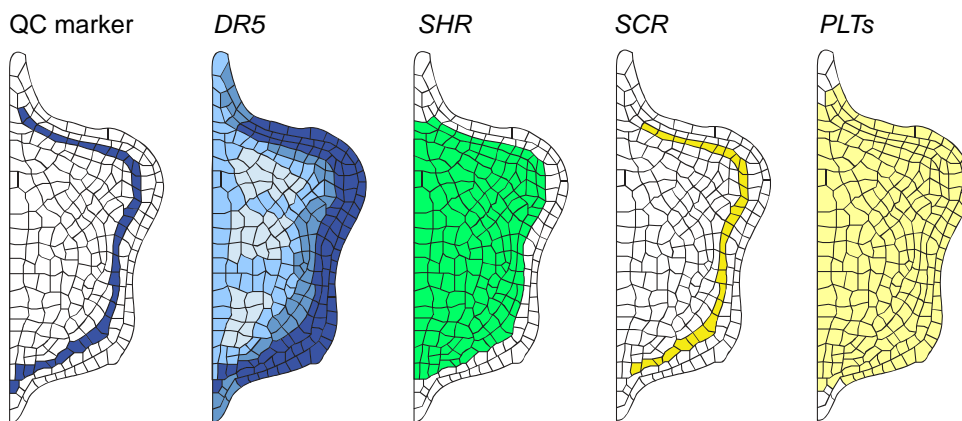
#### **IV. MERISTEM FORMATION AND ACTIVATION DURING LATERAL ROOT FORMATION**

The root apical meristem is a specialized tissue ensuring root elongation and root cap regeneration through tightly regulated cell division and differentiation. In *Arabidopsis*, primary root apical meristem formation during embryogenesis and its post-embryonic maintenance have been thoroughly studied (reviewed in ten Hove et al., 2015; Figure 1.3B). *Arabidopsis* root apical meristem displays a simple and stereotyped cellular organization with a central stem cell niche surrounding the organizing centre, called quiescent centre (QC), and providing new progenitors for all the cell types of the root and the root cap (Figure 1.1). Stem cells, called initials, can be recognized from their location, close to the QC, and from their ability to produce progenitor cells through asymmetric cell division. Progenitor cells, or transit amplifying cells, can be recognized by the expression of cell fate specific marker genes as well as by proliferative cell divisions tending to conserve clonally related cell file structures. Key players during the embryonic root apical meristem formation and maintenance include auxin and its regulators, and transcription factors such as *WUSCHEL RELATED HOMEODOMAINS (WOXs)*, *PLTs* and *SHR-SCR* (Figure 1.4B).

##### **4.1. Common molecular mechanisms controlling embryonic root apical meristem and LRP meristem formation**

Recent studies have pointed to a parallel in the regulation of meristem formation and maintenance during embryogenesis and LRP development.

*WUSCHEL RELATED HOMEODOMAINS 5 (WOX5)*, a marker for the primary root quiescent centre (Haecker et al., 2004), is also expressed during lateral root formation. *WOX5* function in columella stem cell maintenance appears to be conserved between primary root, lateral roots, and adventitious roots (Hu and Xu, 2016; Sarkar et al., 2007; Tian et al., 2014a). *WOX5* is expressed at least from the stage IV-stage V transition onwards, in the 2 or 4 central cells presumptive of the QC anatomical organisation (Rosspopoff et al., 2017; Goh et al., 2016), although its expression

**A - Stage VII lateral root primordia****B - Primary root apical meristem****C - Callus in callus induction medium**

**Figure 1.4.** Distribution patterns of some key regulators in different developmental contexts. Auxin gradient revealed by DR5 promoter, and expression patterns of QC markers, SHR, SCR and PLTs in stage VII lateral root primordia (A), primary root apical meristem (B) and callus in callus induction medium (C). SHR protein (green) is produced in stele and moves into the adjacent cell layer to activate the expression of SCR (yellow). Note the similarity in expression patterns of these regulators in these different contexts.

may start even earlier, as suggested by other reporter constructs (Du and Scheres, 2017b; Tian et al., 2014a; Ditengou et al., 2008). The importance of the stage IV-V transition for presumptive QC establishment is further supported by the onset of the QC-specific enhancer trap QC25 expression in the subapical cells of the developing primordium (Goh et al., 2016)..

Expression of *WOX5* during embryonic root formation is dependent on the SHR-SCR module (Sarkar et al., 2007). In the embryo, *SHR* is transcribed in the root stele (vascular tissues and pericycle), and SHR controls *SCR* expression in the endodermis and QC in a non-cell autonomous fashion (Nakajima et al., 2001; Cui et al., 2007; Fisher and Sozzani, 2016). Similarly, during LRP development, SHR is found in presumptive stele tissues, whereas *SCR* expression is confined to the endodermis precursor layer (Lucas et al., 2011; Goh et al., 2016). Expression of *SHR* in the inner layer but not in the outer layer is an early patterning event in stage II LRPs. Moreover, *SCR* expression seems to be activated by SHR, and is required for proper QC specification in the developing LRPs (Sabatini et al., 2003; Goh et al., 2016). SHR is also required for LRP initiation and development and for asymmetric divisions of cortex/endodermis initials in LRs (Lucas et al., 2011).

*PLTs*, key players in embryonic root development, are also important for LRP formation. *PLT1*, *PLT2* and *PLT3* redundantly control embryonic root meristem establishment, since the triple mutant *plt1plt2plt3* produces rootless seedlings and the *plt1plt2* double mutant embryos only produce abnormal root meristems with no expression of QC marker genes (Aida et al., 2004). *PLT3*, *PLT5* and *PLT7* are expressed as early as in stage I primordia where they control the asymmetric periclinal divisions giving rise to the stage II primordium. The activity of *PLT3*, *PLT5* and *PLT7* is necessary to switch on the differential expression of *SHR* and *SCR* in the two layers of the stage II primordium, as well as to induce expression of other *PLTs* including *PLT1*, *PLT2* and *PLT4* (Du and Scheres, 2017b). Interestingly, as the LRP progresses *PLT5* expression is progressively confined to the base of the LRP, while the others are predominantly expressed in the central region comparable to the situation in the primary root meristem (Du and Scheres, 2017b). In addition, the expression of *PLTs* is necessary to restrict auxin signalling maximum at the tip of the developing primordia by controlling expression of auxin transporter *PIN* genes, again similar to the situation in the primary root apical meristem (Du and Scheres, 2017b; Galinha et al., 2007). As a result, in the *plt3 plt5 plt7* mutant background LRPs are usually severely disorganized and contain enlarged cells. Very few of these LRPs emerge, indicating that LRPs of the *plt3 plt5 plt7* mutant could not form a functional meristem (Du and Scheres, 2017b; Hofhuis et al., 2013). Instead the double mutant *plt1 plt2* can produce lateral roots but the meristem of these roots are disorganized and differentiate shortly after LR emergence, similar to the phenotype of the primary root apical meristem (Aida et al., 2004). Together the data reveal a master role of *PLT3*, *PLT5*, and *PLT7* genes in initiating the regulatory cascade that controls the functional patterning of the LRP centre.

ARF5/MONOPTEROS (MP) is critical for embryonic root formation, since loss-of-function *mp* alleles, or dominant gain-of-function alleles of its inhibitor IAA12/BODENLOS, result in rootless seedlings (ten Hove et al., 2015). MP exerts its functions by positively controlling expression of multiple auxin transporter genes, including *PIN1*, *PIN4*, *PIN7*, *AUX1* and *LAX2*, to trigger polar auxin accumulation necessary for embryonic root specification (Weijers et al., 2006; ten Hove et al., 2015). Recently, using a mutant background which allows studying the roles of MP post-embryonically, Krogan et al. (2016) demonstrated that MP directly binds to promoters of *PIN1*, *PIN3*, and *PIN7* to regulate their expression levels and auxin distribution in developing LRPs. Polar distribution of PIN1:GFP proteins in LRPs of the mutant also diminishes, coincident with the defects in LRP development. These mutant LRPs are disorganized and unable to develop after emergence, suggesting that a functional meristem is not established or maintained (Krogan et al., 2016).

Experimental evidences described above point to a similarity in molecular mechanisms governing primary and lateral root development, although differences possibly linked to the distinct tissue context, can be noted. Especially, it is interesting to stress the contrasting roles of *PLT3,5,7* members and *PLT1,2,4* members in lateral root development, the former being required for the onset of expression of the latter, by the stage when *WOX5* expression in the presumptive QC starts. In addition, specific regulatory network properties might be involved to organise the developing lateral root primordia and define its boundaries as well as its central domain, in which the root meristem can be patterned (Lavenus et al., 2015).

#### **4.2. Lateral root meristem activation**

A first approach to determine the formation of a new root apical meristem in the developing LRP relies on the identification of a cellular pattern reminiscent of the primary root meristem cellular anatomy. Cytological analyses of developing LRP by Malamy and Benfey (1997) highlighted conserved features in longitudinal sections of developing primordia. Especially, while a first sequence of anticlinal and periclinal cell divisions generated a regular four-layered primordium, subsequent cell division created a group of 2 square-shaped cells in the subapical position, which corresponds to the position of the future QC. This landmark cell division corresponds to stage V primordia. Subsequent cell divisions maintain this cellular organisation, and position of presumptive initials can soon be recognized, while the developing LRP grows through the cortex and epidermis cell layers (Malamy and Benfey, 1997).

However, analysing cellular organization is not enough to determine if a meristem-like structure indeed functions like a meristem. In general, an active root meristem is recognized as a group of dividing and differentiating cells that is continuously replenished thanks to the

maintenance of a stem cell niche. Therefore, applying this criterion to developing LRPs with the aim to identify a functional meristem requires either to analyse the expression of meristem cell fate markers and/or to precisely monitor dynamics in cell division and differentiation in developing LRPs.

Investigating cell division in developing primordia has long been difficult, but recent progresses in live imaging are now contributing to overcome this technical challenge (Du and Scheres, 2017b; Goh et al., 2016; Von Wangenheim et al., 2016). In their detailed analysis of Arabidopsis LRP development, Malamy and Benfey (1997) described conserved cell divisions creating the cellular organization similar to that of the primary root meristem around stage VI, but subsequent cell divisions were difficult to track. During LRP emergence, primordium apical cell number remains almost constant while basal cells quickly expand, thus supporting the model of cell elongation-driven LR emergence and post-emergence lateral root meristem activation (Malamy and Benfey, 1997).

As reported earlier, analyses of marker gene expression in developing primordia support the hypothesis of QC being set as early as from stage V onwards, although *WOX5* might already be expressed at earlier stages (Du and Scheres, 2017b; Goh et al., 2016). Whether these cells do actually behave like a stem cell niche organizing centre remains to be elucidated, since *WOX5* stem-cell promoting activity was only shown in the primary and lateral root columella stem cells (Pi et al., 2015; Tian et al., 2014a). Conversely, tracking initial stem cell fate remains difficult because no cell marker is available to clearly identify root “stem cell-ness” quality. However, *SHR* is expressed in inner cells abutting the *WOX5*-expressing cells in a comparable manner as in root meristem vascular initials (Figure 1.4A; Goh et al., 2016). Comparably, *SCR* is expressed in cells flanking the presumptive QC, the characteristic position of cortex/endodermis initials (Du and Scheres, 2017b; Goh et al., 2016). NAC domain transcription factors *FEZ* and *SOMBRERO* (*SMB*) are expressed in the primary root cap where they control the division of root cap stem cells (Willemsen et al., 2008). *FEZ* is also expressed in as early as stage VI LRPs, at the very tip of the dome and in cells in contact with the presumptive QC, similar to the situation in mature root meristems (Du and Scheres, 2017b). Expression of *SMB* is detected in stage VI LRPs, in the outermost layer of the primordium tip, consistent with its described role in specifying root cap progenitor cells (Du and Scheres, 2017b). Last, expression of the MYB related transcription factor *WEREWOLF* involved in epidermis specification (Lee and Schiefelbein, 1999) is also detected in the presumptive epidermis layer of emerging LRPs (Du and Scheres, 2017b). Thus, many markers for root stem cell identity are already expressed in developing LRPs before emergence, supporting the hypothesis that a complete root meristem stem cell niche is organized before LRP emergence.

As a functional test to identify meristematic activity, the ability of LRPs of different stages to develop independently of exogenous auxin supply was assayed using excision protocols (Laskowski et al., 1995). LRPs with no less than 3 to 5 cell layers (which corresponds approximately to LRPs of stages III to V) are able to develop after excision from the parental root (Laskowski et al., 1995; Malamy and Benfey, 1997), in accordance with the report that LRPs at these stages are able to synthesize auxin IAA on their own (Ljung, 2005). Detailed analysis of LRP development by Goh et al. (2016) supports the model that LRP development is a biphasic process, comprising an early morphogenesis phase and a later meristem formation phase. Importantly the transition happens at around stage V, coincident with the shift from bilateral symmetry to radial symmetry of LRPs (Lucas et al., 2013; Goh et al., 2016), and with the onset of expression of both *WOX5* and *QC25*, typical markers of root QC, in the central cells of the second outermost layer (Goh et al., 2016; Rosspopoff et al., 2017). In the root apical meristem, a QC is specified at the overlap between *SHR-SCR* and *PLTs*, which are activated by local auxin signaling maximum (Sablowski, 2007; Aida et al., 2004). If this criterion is applied to lateral roots, then the *WOX5*- and *QC25*-positive cells in stage IV-V LRPs can be considered a QC (Du and Scheres, 2017b; Goh et al., 2016). Rosspopoff et al. (2017) suggested that these QC marker positive-cells constitute a functional stem cell niche that is required for the direct conversion of a LRP into a shoot meristem during the artificial cytokinin-induced shoot regeneration process.

Taken together, the data suggests the progressive establishment of a stem cell niche organization from the stage II, with *SCR/SHR*-dependent outer layer specification, to lateral root emergence, with the induction of epidermis and root cap identities. A critical step in this *de novo* root meristem organogenesis process occurs at the stage IV-V transition, when the primordium breaks through the overlying endodermis layer, develops a radial symmetry centred on a QC-specific marker expressing niche, and acquires autonomy relative to the auxin fluxes from the parent root. Interestingly, this newly established root stem cell niche may only be active after LR emergence (Malamy and Benfey, 1997). The characterization of the *aberrant lateral root formation 3 (alf3)* mutant, that is unable to sustain LR growth after emergence unless exogenous auxin is supplied (Celenza et al., 1995), also supports the hypothesis that a major transition in LRP meristem activity takes place at LR emergence.

## **V. LRP ORGANOGENESIS AS A COMMON BASIS FOR ORGAN REGENERATION FROM CALLUS**

Organ regeneration is a process of *de novo* organogenesis of shoots or roots from wounded or detached plant tissues. It is widely used in plant tissue culture to multiply plants quickly. Tissue culture usually goes through two steps: first callus formation, and then root or shoot organogenesis

induction using different combinations of phytohormones. More and more evidence indicate that the process of organ regeneration employs similar regulatory mechanisms to that of LRP formation, especially at the first step of callus formation (Figure 1.4).

First of all, callus and LR formation share a similar cellular origin. When cultivated in auxin-rich medium, callus develops from pericycle cells in root explants and from cells surrounding vasculature bundles in other aerial organs (Sugimoto et al., 2010). The *alf4-1* mutant is defective in pericycle cell divisions, consequently unable to produce any LRs. Consistent with this, callus formation from *alf4-1* root explants is blocked when cultivated in multiple combinations of auxin and cytokinin concentrations (Sugimoto et al., 2010). Interestingly, callus formation from aerial organs, including cotyledons and petals, is also inhibited in the *alf4-1* mutant. Close inspection of the pericycle marker line J0121 showed *GFP* expression in cells surrounding the midvein of the cotyledons and the petals. This expression gradually diminishes when callus formation progresses, similar to what happens in root pericycle cells during LRP and callus formation in roots (Che et al., 2007; Sugimoto et al., 2010; Laplace et al., 2005). These pericycle-like cells are also present in leaves and are involved in hormone-free root regeneration (Liu et al., 2014; Bustillo-Avenidaño et al., 2018). This data indicates that pericycle and pericycle-like cells are essential for both LRP formation and callus formation from explants of various origins.

Contrary to the previous perception that callus is an unorganized mass of undifferentiated cells, callus is actually an organized structure resembling a LRP. Both callus and LRP originate from pericycle or pericycle-like cells, and then develop into structures of multiple cell layers (Atta et al., 2009; Sugimoto et al., 2010). Cell identity markers in the root apical meristem and LRP are also expressed in callus in comparable domains (Figure 1.4). For example, *pSCR::GFP*, a marker for endodermal and QC cells in the primary root meristem, is expressed in a single cell layer under the epidermis, while *pSHR::SHR::GFP*, the marker for stele, endodermal and QC cells, is expressed in multiple subepidermal cell layers comparable to the stele (Sugimoto et al., 2010). The outer layer of the callus expresses the epidermis-specific markers *MERISTEM LAYER 1* and *GLABRA2*, and even displays root cap functional characteristics, such as the presence of statoliths (Atta et al., 2009; Sugimoto et al., 2010). Moreover, the QC marker *WOX5* whose expression is activated during LRP development (Tian et al., 2014a; Goh et al., 2016; Rosspopoff et al., 2017) is also expressed in a single subepidermal cell layer in the callus, although its expression range is expanded probably because of the disturbed auxin gradient provided by the callus induction medium (Sugimoto et al., 2010). These analyses indicate that callus shares important characteristics with the root apical meristem and the LRP. Indeed, transcriptomic analyses showed that callus forming from various organs is enriched in root tip-expressed genes. In addition, there

is a large overlap in genes upregulated in root, cotyledon and petal explants during callus formation, indicating that this process shares common mechanisms in these different contexts. However, the number of genes upregulated in aerial explants are much higher than those in root explants, suggesting that callus formation from aerial organs requires intermediate steps (Sugimoto et al., 2010).

Callus formation also depends on the auxin signalling module comprising *ARF7*, *ARF19* and their *LBD* targets (*LBD16*, *LBD17*, *LBD19*, *LBD29*) which plays critical roles in controlling LRP initiation, development and emergence (Okushima et al., 2007; Lee et al., 2009a; Goh et al., 2012a). *LBD* genes (*LBD16*, *LBD17*, *LBD18*, *LBD29*) are also strongly induced in both shoot and root explants cultivated in callus induction medium (Fan et al., 2012). These LBDs physically interact with the transcription factor AtbZIP59 to control callus formation (Xu et al., 2018b). Overexpression of these genes is sufficient to induce spontaneous callus formation at various degrees and positions in the seedlings (Fan et al., 2012; Xu et al., 2018b). Conversely, suppression of LBD function reduces LR formation from primary roots and almost abolishes callus formation capability of root explants (Fan et al., 2012). Like in LRP development, *LBD* genes also act downstream of auxin via *ARF9* and *ARF19* in the context of callus formation (Lee et al., 2017; Fan et al., 2012).

Interestingly, the formation of callus-like structures in leaf vascular tissues induced by root-knot nematodes also depends on *LBD16* (Olmo et al., 2017). Another *LBD* gene, *LBD29*, which regulates LR initiation through maintaining cell division competence of pericycle cells (Feng et al., 2012), also controls callus formation on callus induction medium (Xu et al., 2017). During callus formation, *LBD29* activates genes of different functional categories such as transcriptional regulation, ROS and lipid metabolism, and cell wall hydrolysis. Overexpression of some putative targets induces spontaneous callus formation at various degrees, similar to the phenotype of *LBD29*-overexpressing plants (Xu et al., 2017).

Callus formation is an important intermediate step for *de novo* organ regeneration by hormonal treatment. In this procedure, explants are first incubated in auxin-rich callus induction medium to induce the formation of calli that acquire pluripotency for subsequent shoot regeneration. When transferred to a shoot induction medium that has high cytokinin-to-auxin ratio, some callus cells transform into shoot progenitors that will eventually develop into shoots (Kareem et al., 2015). *PLTs*, key regulators in LRP and root apical meristem formation (Du and Scheres, 2017b; Galinha et al., 2007), also play pivotal roles in hormone-induced organ-regeneration. Like in a developing LRP, expression of *PLT3*, *PLT5* and *PLT7* genes is up-regulated during callus formation and shoot regeneration (Du and Scheres, 2017b; Kareem et al., 2015). Single mutants

in these genes are able to regenerate shoots in shoot induction medium, but the regeneration capability is completely lost in the triple mutant. Moreover, overexpression of *PLT5* or *PLT7* is enough to induce shoot regeneration in the *plt3 plt5 plt7* mutant background in hormone-free medium. This data indicates that *PLT5* and *PLT7* transcription factors are necessary and sufficient for shoot regeneration from callus. Expression of key root stem cell maintenance regulators, including *SCR*, *PLT1* and *PLT2* is upregulated in callus originated from wild type shoot and root explants, but not detected in *plt3 plt5 plt7* calli (Kareem et al., 2015). *PLT3*, *PLT5* and *PLT7* factors also positively regulate the expression of the auxin efflux carrier *PIN1* gene during callus formation. Altogether, the data points to a common regulatory pathway involving *PLT* genes in LRP formation and *de novo* organ regeneration: in both processes (i) *PLT* genes are required, and (ii) *PLT3*, *PLT5* and *PLT7* regulate *PLT1* and *PLT2* and also *PIN1* expression in a similar manner (Du and Scheres, 2017b; Kareem et al., 2015).

As described for LR FC specification and LRP formation, chromatin-remodelling factors also play critical roles in callus formation. ARABIDOPSIS TRITHORAX-RELATED 2 (*ATXR2*), a trithorax group protein as *ATX1* mentioned above, modifies target gene expression by deposition of positive histone marks. *ATXR2* binds to the promoter of *LBD16* and *LBD29* with the help of *ARF7* and *ARF19* transcription factors to induce permissive chromatin conformation on these loci. Consistent with the critical roles of LBDs in callus formation, the ability of leaf explants to form calli is significantly reduced in the *atxr2* mutant background and enhanced in an *ATXR2* overexpressing line (Lee et al., 2017). Although it is not clear if this regulation of *ATXR2* on *LBDs* is also true in LRP formation, lateral root production in the *atxr2* mutant is significantly reduced compared to the wild type (Lee et al., 2018a). Finally, subunits of the Polycomb repressive complex 2 (*PRC2*), which negatively regulates LR FC specification, were shown to inhibit callus formation given that single or combined mutants of these subunits produce callus spontaneously in tissue culture (Chanvivattana, 2004; Bouyer et al., 2011).

Interestingly, although not exactly in the context of LRP development, callus formation and adventitious root formation from leaf explants are demonstrated to share a common genetic pathway. In CIM, leaf explants produce callus through two steps: founder cell specification and callus formation (Yu et al., 2017). In the first step, pericycle-like (procambium) cells highly express *WOX11*, a *WOX5*-related transcription factor that acts redundantly with *WOX12* to convert competent cells into callus founder cells. *WOX11* and *WOX12* then activate the expression of *LBD16* and *WOX5* to induce founder cell division to form a callus (Liu et al., 2018; Hu & Xu, 2016; Sheng et al., 2017). This two-step mechanism is conserved in both monocot and dicot plants (Hu et al., 2017). The genetic pathway comprising of *WOX11*, *WOX12* and *WOX5*,

along with other important genetic factors such as *PLT1*, *PLT2* and *SHR*, is also involved in adventitious root founder cell specification and hormone-free root regeneration from leaf explants (Liu et al., 2014; Hu & Xu, 2016; Bustillo-Avendaño et al., 2018; Sheng et al., 2017). This newly unravelled molecular mechanisms for callus formation can help bridge the gaps between LR and adventitious root formation.

## VI. GENERAL CONCLUSIONS

Root system architecture greatly impacts plant growth and crop yield, and root branching contributes to a major extent to root system development. Root branching consists in a strikingly robust event of post-embryonic organogenesis that progressively generates, thanks to coordinated proliferation of pericycle-derived founder cells, a new functional root meristem including a stem cell niche. Major regulators of cell fate and cell behaviour, especially cell cycle, are involved in triggering and then controlling this organogenesis process. Specific transcription factors, chromatin modifiers, and signalling pathways impact gene expression in a precise time and space dependent manner, although we are still far from having elucidated all their interactions and understanding the properties of the entire network. Importantly non-cell autonomous signals, such as mobile peptides, directional fluxes of the plant hormone auxin, and transcription factors able to move through plasmodesmata, mediate cell-to-cell coordination across tissues and the emergence of developmental patterns. Moreover, *de novo* root meristem formation associated to root branching shares common regulatory mechanisms together with root meristem specification in the embryo and plant regeneration from calli, raising interesting evo-devo as well as biotechnological perspectives. However, many questions are still open regarding key developmental events during LRP organogenesis. How pericycle cell competency for root organogenesis is precisely regulated remains unclear. In addition, the precise molecular mechanisms underlying pericycle cell priming, prebranch site formation and founder cell specification are unknown. Last, the regulatory network properties controlling the organisation of a new root apical meristem are not understood. Hopefully, the comparison of root formation from embryonic, post-embryonic, and calli tissues will help to unravel the fundamental properties of this organogenesis program.



# **CHAPTER II**

**PUCHI regulates LRP initiation, positioning, patterning and emergence**

## I. INTRODUCTION

In Chapter I, we have seen that there are many factors, mostly transcriptional ones, involved in the regulation of LR formation. However, our understanding is still fragmented because classical approaches only focus on a limited aspect at a time, hence we lack a systematic view of how these components interact to form a network that successfully controls the organization of a new functional meristem.

To have a global view of the LRP formation process, our team used a systems biology approach to identify the gene regulatory network (GRN) governing LR formation in the model plant *A. thaliana* and study its dynamical behaviour (Lavenus et al., 2015). This approach combines a time course transcriptomic dataset specific for lateral root formation (Voß et al., 2015) and an in-house algorithm called TDCor to predict putative gene-to-gene regulatory relationships and to infer the predicted topology of the operating gene regulatory network (Lavenus et al., 2015). The inferred topology displays two subnetworks that may represent two major waves of gene expression during LRP formation. The first wave led by ARF7-ARF19 would trigger LRP initiation and early morphogenesis. The second wave led by ARF5 is thought to activate genes involved in meristem formation. The mutual inhibition of the two-subnetworks could also produce the bifurcation and spatial distinction between flank and meristem cell identities in the developing primordium (Lavenus et al., 2015; Figure 2.1). This prediction may functionally underlie a major step of LRP morphogenesis, namely the distinction of a central zone where a new root meristem is organized, and of a flank/peripheral zone which may acts as a buttress to support the central zone.

Here, we further studied the ARF7-regulated AP2/ERF transcription factor PUCHI, a major node in the sub-network controlling LRP formation and early morphogenesis as proposed by the inferred topology. The roles of PUCHI in controlling LRP cell division and (flank) morphology have been originally described in (Hirota et al., 2007). Generally, two phenotypes were reported for the loss-of-function mutant *puchi-1*, including (i) more anticlinal cell division resulting in wider LRPs and also flatter LRPs (lack the prominent domed-shape) than those in the wide-type (WT), and (ii) swollen LRP flank cells. *puchi* mutant had been shown to have higher LRP density than did the WT (Kang et al., 2013). Recently it was demonstrated that PUCHI expression in the cells adjacent to the LR founder cells may inhibit the formation of nearby LRPs right from the founder cell specification step (Toyokura et al., 2018). PUCHI expression is induced by the peptide TARGET OF LBD SIXTEEN 2 (TOLS2) and its receptor RECEPTOR-LIKE KINASE7 (RLK7,) and the cascade is downstream of the transcription factor LBD16 (Toyokura et al., 2018).

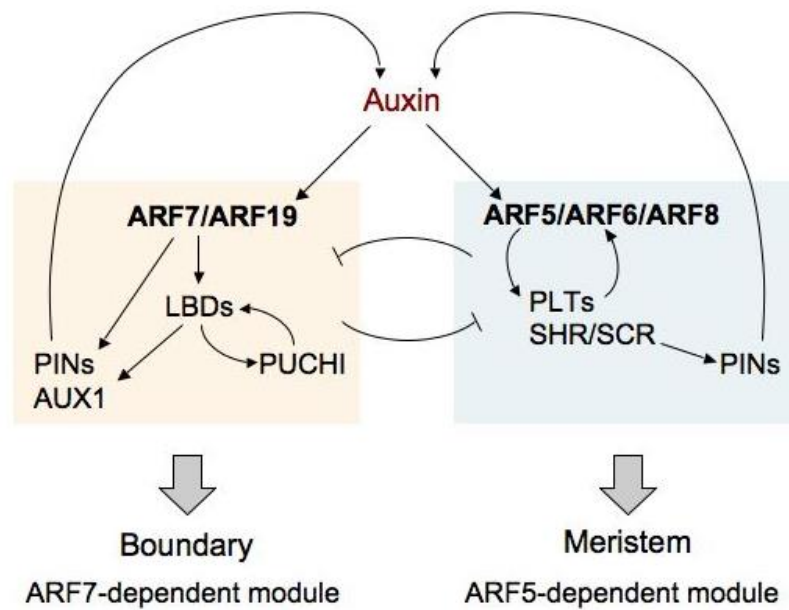


**Figure 2.1.** Prediction of the gene regulatory network during LRP development organized into two subnetworks by TDCor (Ph.D. thesis of Julien Lavenus, 2014).

To understand better the roles of PUCHI in LRP formation, a detailed phenotyping of the loss-of-function mutant *puchi-1* was performed with a focus on LRP formation and related events. The response of the *puchi-1* mutant to auxin and cytokinin, key hormones regulating LRP formation, and the expression pattern of several important markers for LRP formation in the mutant background were also examined.

## II. RESULTS

### 2.1. PUCHI expression pattern

PUCHI expression pattern has been described in the original paper of (Hirota et al., 2007). Using the *pPUCHI:GFP-PUCHI* construct that rescues the defective LRP morphology in *puchi-1* background, the authors reported that *PUCHI* is specifically expressed in nuclei of LRPs from stage I onwards. The expression is detected in all cells of LRPs of earlier stages, but gradually confined to the cells in the base and flanks of the primordium. The presence of GFP signal in other tissues were not described (Hirota et al., 2007).

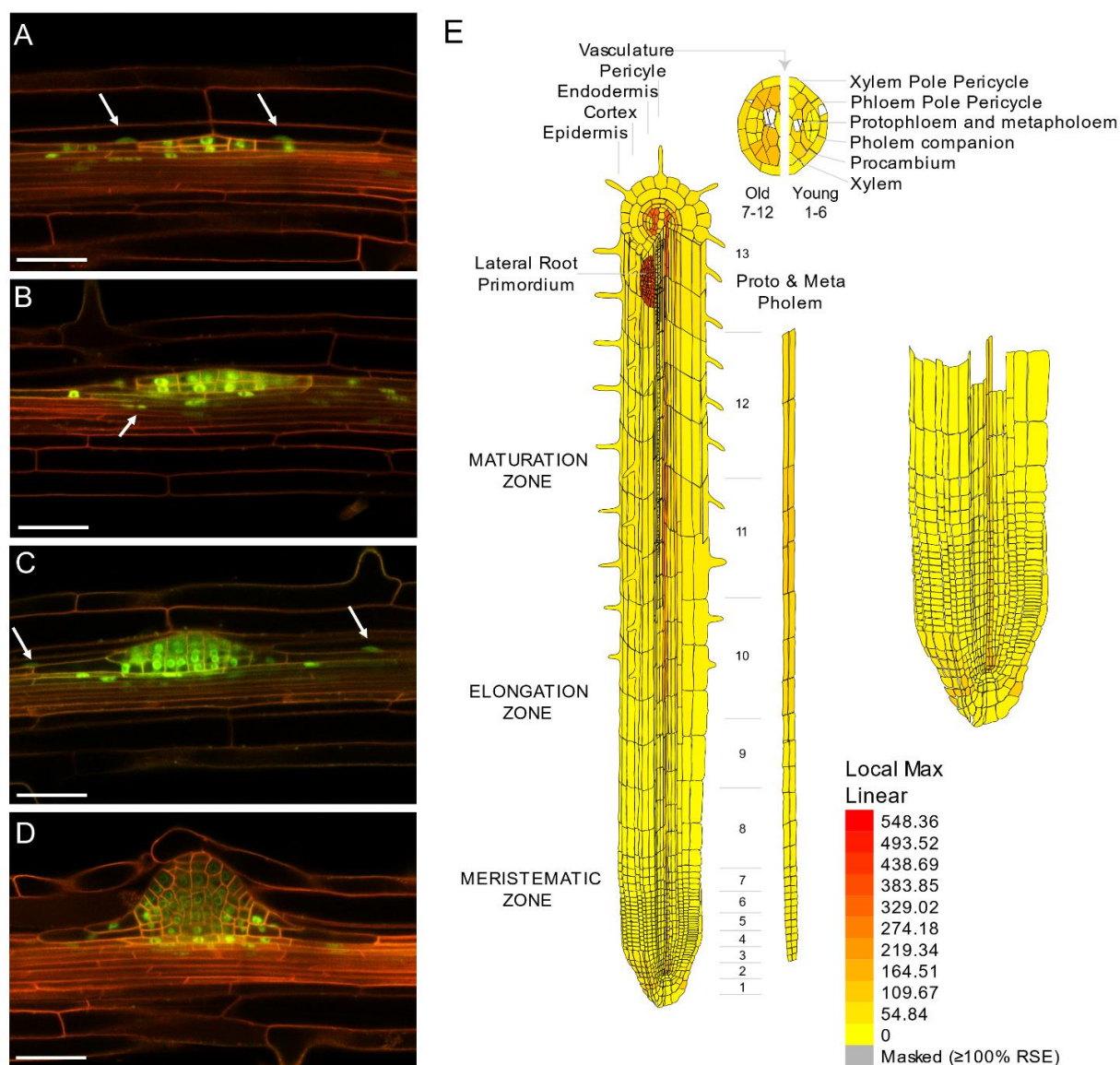


**Figure 2.2.** Expression of *GFP-PUCHI* in LRPs and the primary root. (A) *GFP-PUCHI* expression could be detected in endodermal cells surrounding the developing LRP (arrow). (B) Expression of *GFP-PUCHI* in a stage II LRPs and in the stele. (C) and (D) The expression is gradually restricted to the base and flanks. Cell membrane (orange) is visualized using WAVE131Y. (E) Expression pattern of *PUCHI* obtained from the ePlant webservice <http://bar.utoronto.ca/eplant/>. Expression levels in different root tissues are color-coded from low (yellow) to high (red) according to a linear scale. High expression of *PUCHI* is reported in the LRP and in vascular tissues (Brady et al., 2007).

A more detailed analysis on the expression pattern of *pPUCHI:GFP-PUCHI* in our growing conditions was performed. In general, we confirmed the original description of *PUCHI* expression pattern during LRP development (Hirota et al., 2007; Figure 2.2A-C). Its expression was also found in pericycle cells flanking the developing LRP (Figure 2.2C, arrows). Besides LRPs, the presence of the GFP signal was also frequently detected in endodermal cells overlaying

young LRPs that are still below the endodermis (Fig 2.2A, arrow) and frequently in the stele (Figure 2.2B, example arrow). The expression of *PUCHI* in the endodermis seemed to strictly associate with LRPs, while its presence in the stele could be detected far from a LRP (not shown). The presence of *GFP-PUCHI* in primary meristematic zone where LRP priming happens was not detectable. This finding was checked against the dataset published by (Brady et al., 2007) that provides a comprehensive expression profiles of all root cell types. Consistent with our observation, the data suggests that besides LRPs, *PUCHI* may be expressed in the stele and the lateral root cap of the primary root (Figure 2.2E).

## 2.2. PUCHI negatively regulates LRP initiation, positioning and development

To better characterize the role of PUCHI during LR development, the LR development phenotype of the *puchi-1* mutant was analysed in detail. For this, the number of emerged LR and developing LRPs produced in 9-day old WT and *puchi-1* seedlings were quantified. To facilitate the phenotype description, we adopted the convention proposed by Dubrovsky and Forde (2012) in dividing the Arabidopsis primary root into three zones, namely, the root branching zone where LRPs have emerged, the LR formation zone where LRPs are initiated and developing, and the root tip. The root branching zone is the one shootwards of the most recently emerged LR, while the LR formation zone is between the most recently emerged LR to the newly initiated LRP near the root tip (Figure 2.3A).

At 9-d, WT and *puchi-1* seedlings had similar primary root lengths (Figure 2.3A). We confirmed the morphological phenotypes of *puchi-1* mutant LRPs and LR described in (Hirota et al., 2007), namely the presence of additional anticlinal cell layers and abnormally large flank cells (Figure 2.3B). Regarding LRP formation, in the LR formation zone we observed an increase in LRP number in *puchi-1* mutant, leading to ~ 3 times higher LRP density in the mutant (Figure 2.3C). In the root branching zone of the WT, we observed several emerged LR and occasionally un-emerged LRPs which may correspond to arrested or delayed LRPs (Celenza et al., 1995; Nacry et al., 2005; Dubrovsky et al., 2006). However, in *puchi-1* mutant, while the density of emerged LR was similar to that of WT, there was a strikingly high number of un-emerged LRPs (Figure 2.3C). These un-emerged LRPs constituted up to ~20% of total *puchi-1* LR organs (or total LRPs = LRPs in the LR formation zone + emerged LR and un-emerged LRPs in the branching zone). It is consistent with the higher LRP initiation in the LR formation zone and a normal density of emerged LR in the branching zone (Figure 2.3C). As a whole, *puchi-1* mutant produces more LR

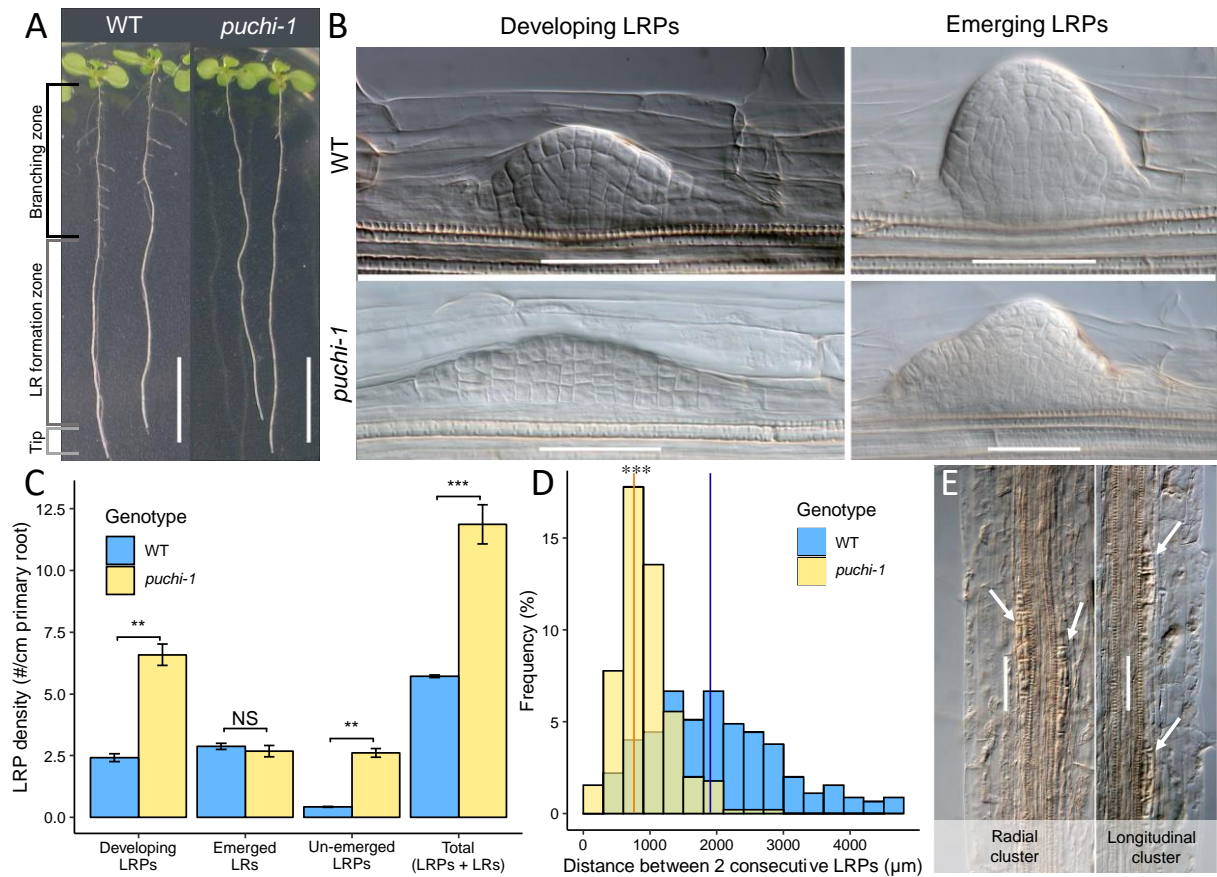


**Figure 2.3.** *puchi-1* mutant produces more LRPs and is delayed in LRP development.

(A) Three zones of *Arabidopsis* primary root regarding lateral root formation and development as suggested in (Dubrovsky and Forde, 2012). Scale bars = 1cm. (B) Morphology of *puchi-1* LRPs. Note the increase in peripheral cell layers and thus the width of the *puchi-1* developing LRP, as well as the defects in the flanks of the emerging one. Scale bars = 50  $\mu$ m. (C) Density of developing LRPs, emerged LR, un-emerged LRPs, and total LR initiations (LRPs + LR) in 9-day old WT and *puchi-1* seedlings. Developing LRPs are those in the LR formation zone. Un-emerged LRPs are those located in the branching zone of the primary root but have not crossed the epidermis. Data are represented as Mean  $\pm$  SEM (standard error of the means) of three biological replicates; number of seedlings = 20-30 in each repeat. (D) Frequency distribution of distances between two consecutive LRPs in WT and *puchi-1* roots. Each bin of the histogram represents a range of 300  $\mu$ m. Number of LRPs = 222 and 228 for WT and *puchi-1*, respectively. The orange and dark blue bar indicates the mean LRP distance in *puchi-1* and WT, respectively. The star in the histogram for *puchi-1* indicate the significant difference between its mean distance and that of WT. (E) Examples of longitudinal and radial clusters of LRPs in *puchi-1* roots. Arrowheads indicate LRPs. Scale bars = 50 $\mu$ m. Significance was determined by Student's t-test. \*\*  $p < 0.01$ , \*\*\*  $p < 0.001$ .

organs along the primary root, resulted in ~ 2-fold increase in the total LRP density (Figure 2.3C). The result is in general consistent with the study of (Kang et al., 2013; Toyokura et al., 2018) and suggests that PUCHI is a negative regulator of LR initiation.

Consistent with the increase in total LRP density and no significant changes in primary root lengths, measuring the distances between two consecutive LR organs revealed that these organs were formed at much shorter intervals in *puchi-1* than in WT (Figure 2.3D). In the mutant LRPs that are formed closely together were frequently observed. The distance between two adjacent LR organs in WT has been reported to be usually greater than 300 $\mu$ m (Dubrovsky et al., 2006). However, *puchi-1* roots produced many clusters of LRPs within 300 $\mu$ m of one another (Figure 2.3D, the first bin of the histogram for *puchi-1*). These *puchi-1* LRP clusters could either be longitudinal (*i.e.* along a protoxylem pole) or radial (*i.e.* along opposite protoxylem poles; Figure 2.3E). The absolute numbers of LRP clusters in ~ 220 LRPs of each genotype are given in Table 2.1, showing a striking abundance of closely-positioned LRPs in the mutant compared to the WT. Since some authors also used 400 $\mu$ m as the distance to define a LRP cluster (Murphy et al., 2016), we add the number of LRPs formed within 300-400  $\mu$ m of one another to the table. Thus, our data revealed that *PUCHI* functions as a negative regulator of LRP initiation in the pericycle and also controls the spacing between LRPs.

**Table 2.1.** Numbers of LRP clusters in ~ 200 LRPs in WT and *puchi-1*. Numbers in brackets in *puchi-1* total LRP clusters show the fold change compared to the WT.

Genotype	Distance between two consecutive LRPs					
	0-100 $\mu$ M	100-200 $\mu$ M	200-300 $\mu$ M	300-400 $\mu$ M	Total (0-300 $\mu$ M)	Total (0-400 $\mu$ M)
WT (222 LRPs)	0	0	2	5	2	7
<i>puchi-1</i> (228 LRPs)	10	33	66	12	109 (54.5x)	121 (17.3x)

The presence of many un-emerged LRPs in *puchi-1* branching zone suggests that in addition to LRP initiation density, loss of *PUCHI* function would also impact LRP development. To test this hypothesis, we used a gravistimulation-based LR induction system (Lucas et al., 2008; Péret et al., 2012) to analyze the kinetics of LRP development in *puchi-1* compared to the WT. In this system, WT and *puchi-1* seedlings were first grown vertically for 5 days in squared plates, then the plates were turned by 90°. LRPs are formed at the primary root bending regions, and their stages were categorized as described in (Malamy and Benfey, 1997) at five time points (18, 22,

30, 36 and 48 hours post gravistimulation (hpg)). This system allows us to track the development of LRPs over time. Gravistimulation induced the initiation of LRP in 100% of the *puchi-1* and WT seedlings. However, a delay in *puchi-1* LRP development was already observed at 18 hpg since more LRPs in the WT reached stage II than in *puchi-1* background (Figure 2.4A). The difference in LRP developmental progression between the two genotypes became more obvious over time. At 48 hours, when a majority of WT LRPs had emerged, most *puchi-1* LRPs had only reached developmental stages IV, V or VI (Figure 2.4A). To see how long *puchi-1* LRPs need to emerge, we did the gravistimulation assay for 2.5, 3 and 4 days and found that a majority of the mutant LRPs started to emerge at 2.5 days post gravistimulation (dpg). Moreover, while 100% WT seedlings had produced LR from 2.5 dpg onwards, the figure for *puchi-1* only reached 70% when the assay was extended for 6 days (Figure 2.4B). The data indicate that correct expression of *PUCHI* is required for normal developmental progression and emergence of LRPs.

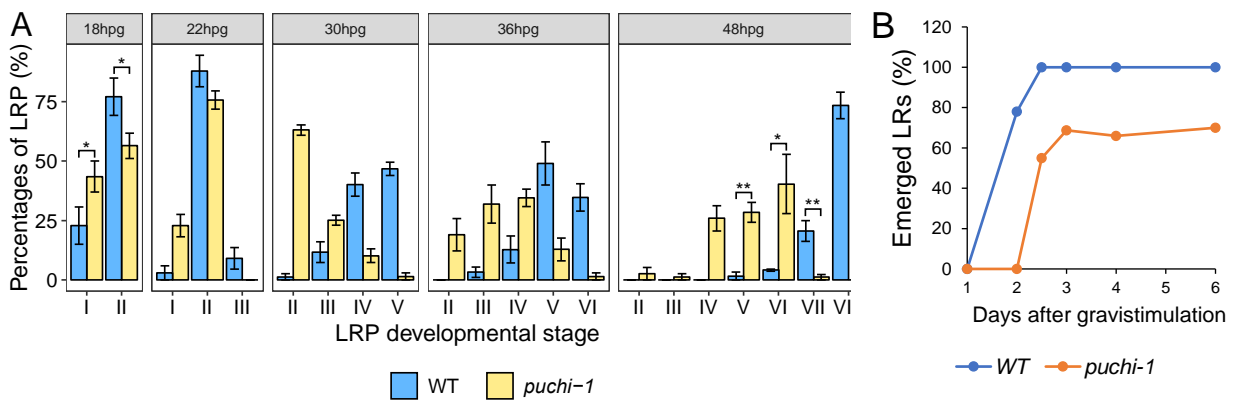


**Figure 2.4.** Kinetics of LRP development in WT and *puchi-1*. (A) Distribution of developmental stages as described by Malamy and Benfey (1997) achieved by gravistimulation-induced LRP formation in WT and *puchi-1* roots at 18, 22, 30, 36 and 48 hours post gravistimulation (hpg). Stage VIII corresponds to newly emerged LR. Data are represented as Mean  $\pm$  SEM (standard error of the means) of three biological replicates, with number of seedlings = 20-30 in each repeat. Significance was determined by Student's t-test. \*  $p < 0.05$ , \*\*  $p < 0.01$ . For simplicity, statistical significance was only given for the two time points 18 and 48 hpg. (B) Kinetics of LRP emergence in WT and *puchi-1* after gravistimulation. A different set of WT and *puchi-1* seedlings were used for each time point. In each set,  $n = 20$  for WT and 30-50 for *puchi-1*.

Given that un-emerged LRPs represents up to one fifth of total LRPs in *puchi-1* background, and that *puchi-1* LRPs progress much slowly than those of WT, the question was whether these un-emerged LRPs are in fact delayed (growing slowly) or arrested (stop growing altogether). For this, a tracking assay was performed in which primary roots were observed under a binocular and the newly emerged LR in each seedling was marked. Lateral roots shootward of the newly emerged

LRs in each seedling were counted. Then the seedlings were put back to the growing chamber in normal growing conditions. After 4 day and 9 day, the number of LRs shootward of the marks were counted again to see if any additional lateral roots appeared in that region during this period. The same root zone was also observed under a microscope to assess the developmental stages of un-emerged LRPs at those two time points.

**Table 2.2.** Tracking the numbers of emerged LRs in the branching zone after 4 and 9 days of further growth (2 separate experiments)

Time points	No. of emerged LRs at T0 (9d old plants)	No. of emerged LRs at T0 + 4d	% increase	No. of emerged LRs at T0 (9d old plants)	No. of emerged LRs at T0 + 9d	% increase
WT	234	235	0.4	90	91	1.1%
<i>puchi-1</i>	139	141	1.4%	76	79	3.9%

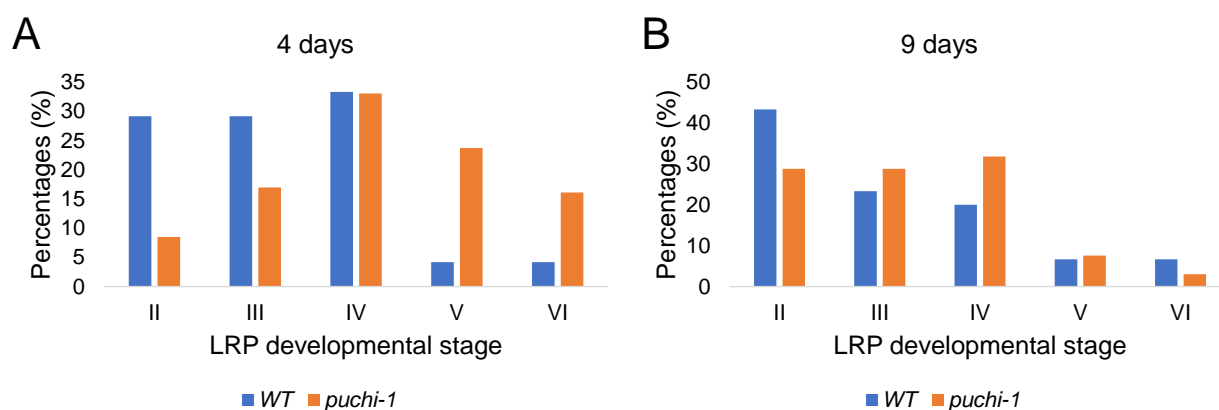


**Figure 2.5.** Distribution of developmental stages of un-emerged LRPs in the marked regions in WT and *puchi-1* roots. Root branching zones of 9-day old seedlings were marked, and the seedlings were returned to the normal growth condition for 4 and 9 additional days. After that, un-emerged LRPs in the zone were counted and staged. In (A), number of LRPs = 78 and 118 for WT and *puchi-1*, respectively. In (B), number of LRPs = 100 and 66 for WT and *puchi-1*, respectively.

At 4 and 9 day after marking, we saw only one new LR appeared in WT roots in the marked zone (Table 2.2). This is most probably the result of the emergence of a slowly developing LRP. In *puchi-1* roots, we detected the appearance of more additional LRPs in the marked regions than in the WT during the time frame of this experiment (Table 2.2). *puchi-1* roots produce a high number of delayed LRPs in the branching zone, and it is possible that a small percentage of these

delayed LRPs are still functional and will eventually emerge. Microscopic observation revealed that at 4d, un-emerged LRPs in WT were mostly at stage II-IV (91.7%) while those in *puchi-1* covered diverse stages (Figure 2.5A). Around 15% of these delayed LRPs are at stage VI; some of them have normal morphology, suggesting that they are capable of developing further. Consistent with that, at 9d, we could see more newly emerged LR in the marked zone in *puchi-1* seedlings, and at this point the distribution of developmental stages of *puchi-1* LRPs look more similar to that of the WT (Figure 2.5B). Percentages of stage II-IV LRPs in WT and *puchi-1* were 86.7 and 89.4%, respectively. Altogether, the data again emphasizes the very slow development of some LRPs and strongly suggest that most of the un-emerged LRPs in *puchi-1* are arrested, *i.e.* not be able to develop and eventually emerge into a LR.

### 2.3. Cell division pattern is disturbed in *puchi-1* LRPs

One of the phenotype of *puchi-1* LRPs reported in the original papers is that they have additional anticlinal cell divisions, leading to wider and flatter LRPs (Hirota et al., 2007; Kang et al., 2013) which was clearly observed in our experimental condition (Figure 2.3B).

The process of LRP formation and the definition of different developmental stages have been described in detail in WT Arabidopsis, revealing certain cell division sequences particularly in the early stages (Malamy and Benfey, 1997; Von Wangenheim et al., 2016). First, in WT, anticlinal divisions of pericycle LR founder cells produce a single-layered stage I LRP. Then, periclinal divisions produce a stage II LRP has two cell layers: one inner layer (IL) and one outer layer (OL). The OL then divide periclinally again to form a 3-layered LRP (IL, OL1 and OL2). The IL of this stage III LRP in turn performs a periclinal division to form a stage IV LRP having four cell layers (IL1, IL2, OL1 and OL2; Malamy & Benfey, 1997; Goh et al., 2016; Von Wangenheim et al., 2016; our observation; Figure 2.6A). In *puchi-1*, however, simultaneous periclinal divisions in the IL and OL, creating a stage IV LRP with ongoing cell division in both cell layers, were occasionally observed (6/30 stage IV *puchi-1* LRPs) (Figure 2.6B). This pattern of division was not detected to WT LRPs under our observation (0/30 stage IV WT LRPs). Therefore, in addition to controlling the frequency of periclinal cell divisions in young LRPs, *PUCHI* seems to also regulate periclinal cell division in LRPs which possibly results in a disorganization of LRP cell anatomy (Figure 2.6C).

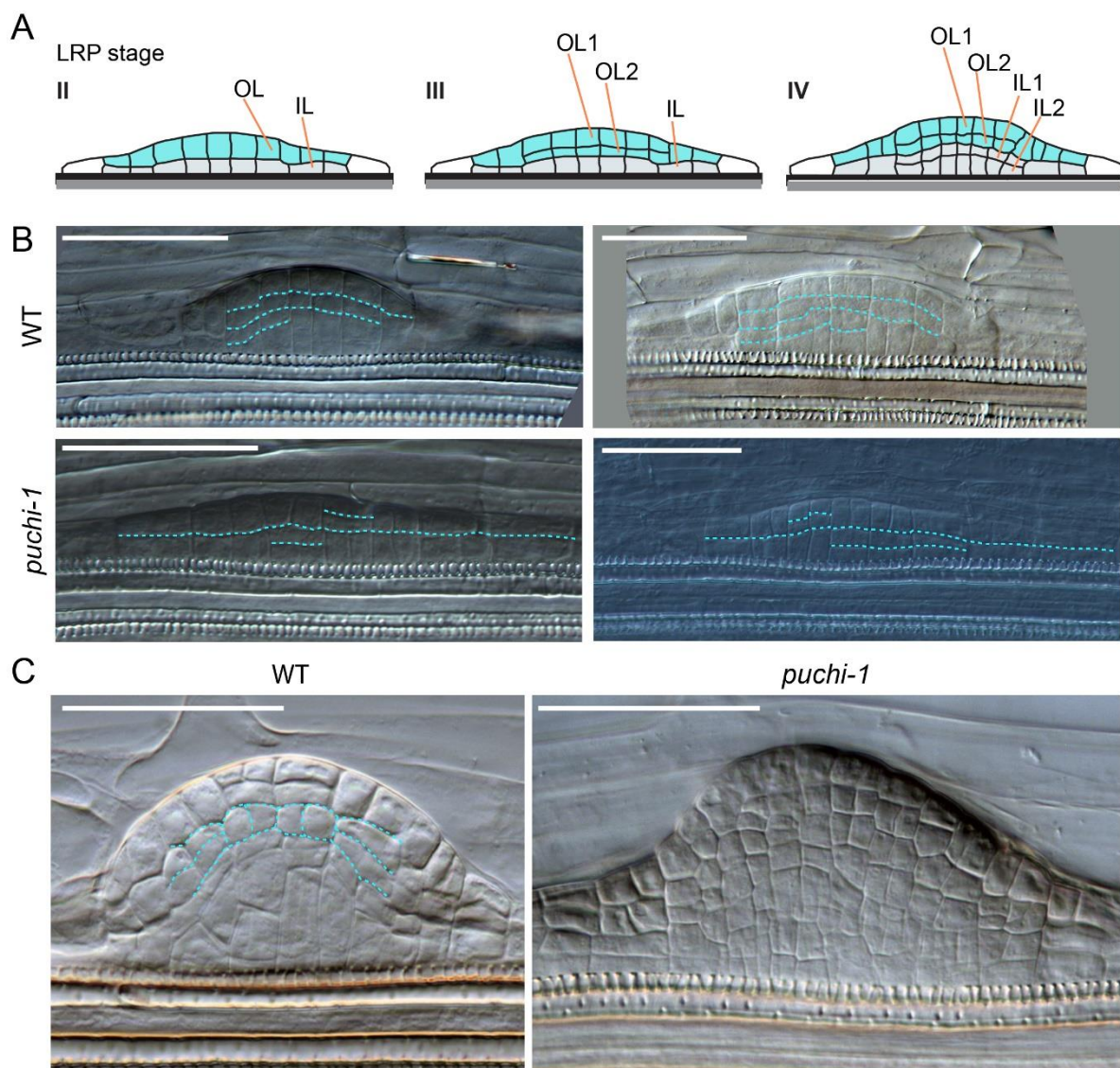


**Figure 2.6.** *puchi-1* LRPs are defective in cell division pattern. (A) Common cell division sequence in WT LRPs where the periclinal cell division happens in the outer layer (OL) first, then in the inner layer (IL) of the stage II LRP (Malamy and Benfey, 1997; Goh et al., 2016; Von Wangenheim et al., 2016). (B) *puchi-1* LRPs are longer and flatter than WT counterparts. Some of them display unusual cell division pattern where the OL and IL divide simultaneously. The dashed cyan lines indicate periclinal cell division planes. (C) In WT LRPs of stage V and beyond, the putative quiescent center is clearly visible in WT developing LRPs (two cells at the center) but not so in *puchi-1* LRPs. The cyan line outlines the putative QC and meristem. Scale bars = 50  $\mu$ m.

*puchi-1* LRPs of more advanced stages also displayed changes in cellular pattern beside the flanks. For example, as showed in Figure 2.6C, it is difficult to say which cells correspond to the would-be quiescent center (QC) as described in (Malamy and Benfey, 1997; Goh et al., 2016), while that feature is easily recognized in the WT LRP. However, since this difference may not be described easily, we focused on the tip of emerging LRPs whose cellular pattern is less variable

than that of developing LRPs. We used the expression of *SHR* through expression of *pSHR:SHR-GFP* (Nakajima et al., 2001) as a delimitator of the stem cell niche in the emerging LRs because *SHR* is transcribed in the stele and the pericycle, and the protein moves to the nucleus of the QC and endodermal cells (Nakajima et al., 2001). In WT LRs, *SHR-GFP* protein was observed in the stele (whole cell, diffuse signal), and in the endodermis and QC (with a nucleus-specific signal), similar to the pattern in the primary root (Nakajima et al., 2001). The asymmetric cell division

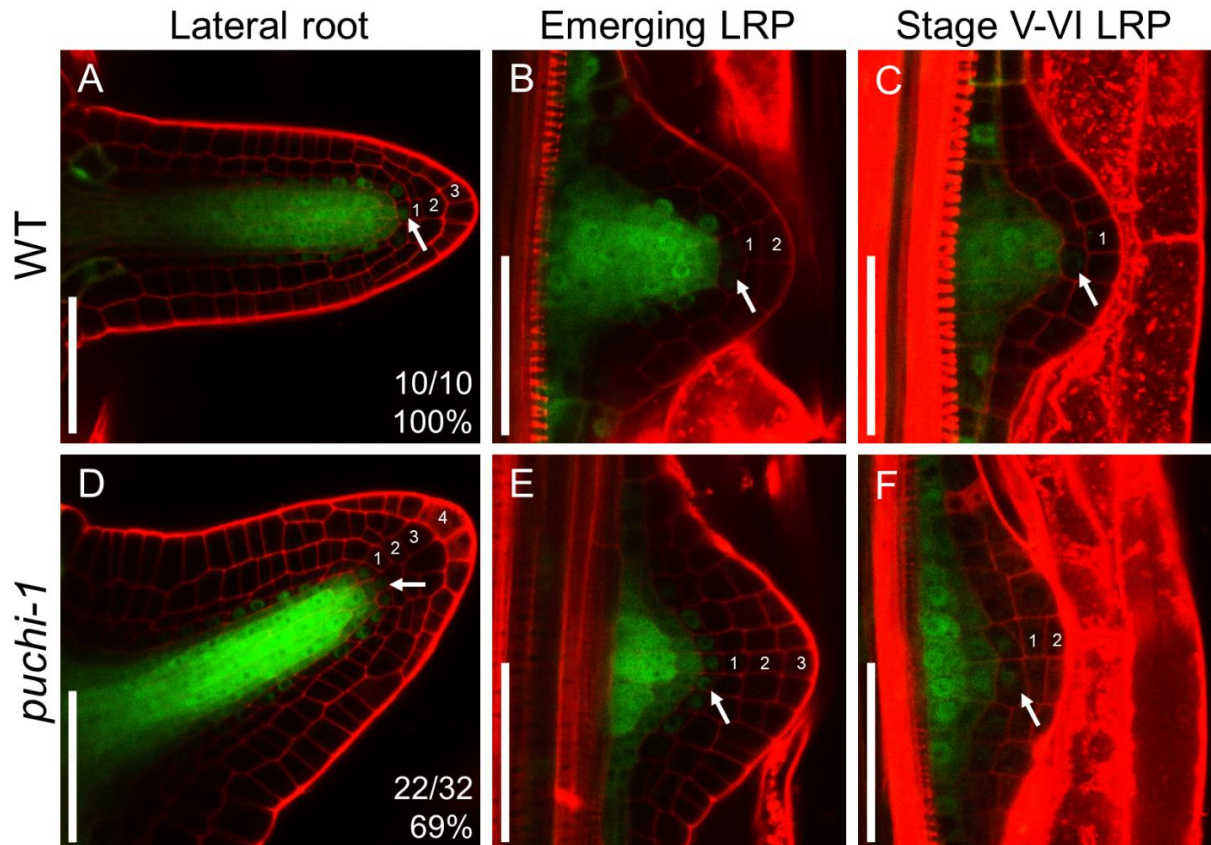


**Figure 2.7.** Cellular organization in the presumptive LR meristem is disturbed in *puchi-1* LR. GFP signal is from *pSHR::SHR-GFP* expression. Cell membrane is visualized using Propidium iodide (red). White arrows indicate the cell layer where nuclear localized *SHR-GFP* signal is visible. The numbers of cell layers from the tip of LRPs/LRs to the layer displaying nuclear-localized *SHR-GFP* signal were indicated.

creating the endodermis and the cortex was also clearly visible. The endodermis and QC-specific nuclear-localized signal of *SHR-GFP* could be seen three cell layers away from the tip (10/10 observed LR) (Figure 2.7A). A similar pattern could also be observed in *puchi-1* LR with the putative QC, the endodermis and the stele showing *SHR-GFP* signal. However, in the mutant LR the nuclear-localized GFP signal was seen four instead of three cell layers away from the tip (22/32 observed LR) (Figure 2.7D). A similar shift in the relative position of *pSHR:SHR-GFP* expression

compared to the LRP outermost layer was also observed in developing and emerging LRPs, although a statistics was not performed yet (Fig 2.7B, C, E, F).

The data suggest that PUCHI is also involved in the patterning of the LR central domain, not just of the flanks. Because *pPUCHI:GFP-PUCHI* is not expressed in the tip of emerging LRPs (Hirota et al., 2007, our observation), the change in the expression domain of SHR protein relative to the root tip was probably maintained from the defects in cellular patterning of central area of early stages.

In summary, our observation reveals that *PUCHI* regulates both anticlinal and periclinal cell division in developing LRPs, and this regulation ensures the proper cellular pattern at the lateral root tip as well as the correct morphogenesis of the LRP flanks.

#### **2.4. PUCHI is required for correct LRP meristem organization**

Since cellular division and patterning are disturbed in *puchi-1* LRPs which are also defective in development, we wondered if meristem organization occurs normally. Previous results with *pSHR: SHR-GFP* suggest that mutation of *PUCHI* may perturb the expression pattern of factors controlling meristem establishment. It was previously shown that expression of QC-specific marker genes was detected in the central cells of the developing LRP before emergence (Goh et al., 2016; Du and Scheres, 2017b). Therefore, one of these commonly used markers, *QC25::CFP* was introduced into the *puchi-1* background to analyse the effects of PUCHI loss-of-function on its expression pattern. During LRP development in the WT, *QC25::CFP* activation is first detected in central cells of the second outer most layer at the transition from stage IV to V, co-incident with the transition from bilateral symmetry to radial symmetry of the LRP (Goh et al., 2016).

Similar to what has been described, we only observed the expression of *QC25::CFP* in WT LRPs of stage V onwards. In LRPs younger than stage VII, the signal was confined to some central cells of the second outer most layer (Figure 2.8A-C). However, in *puchi-1* we observed several unusual features. First, *QC25::CFP* expression could be detected in younger LRPs, as early as in those of stage II (Figure 2.8D). Second, the signal was not as well restricted to some central cells as in the WT and was usually seen in inner cells as well (Figure 2.8E-F). Third, in *puchi-1* LRPs, cells expressing *QC25::CFP* most prominently was dislocated by one layer compared to the WT, which is consistent with the *pSHR:GFP-SHR* expression pattern in the mutant LRPs. Altogether, our observation shows that QC activation and establishment, as revealed by the QC marker *QC25::CFP*, in time and space is disturbed in *puchi-1* LRPs.

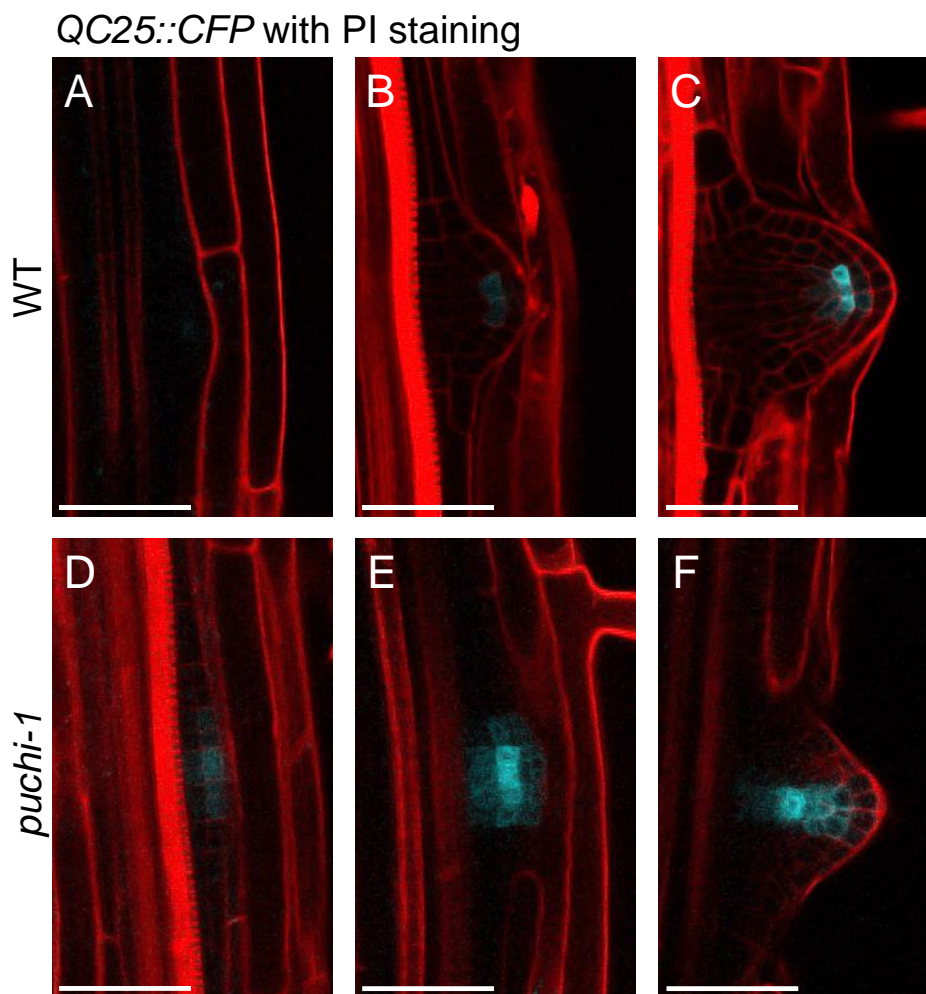


**Figure 2.8.** Expression of the QC-specific marker *QC25::CFP* is altered in *puchi-1* mutant. (A) to (C) In WT LRPs, *QC25::CFP* expression could only be detected from stage V onwards, and was confined to several central cells. (D) to (E) In *puchi-1*, *QC25::CFP* expression could be observed from stage II onwards, and could be expanded and displaced. Cell membrane is visualized using Propidium iodide (red). Defective expression of *QC25::CFP* (early onset or expanded domain) was observed in 15/15 tested plants.

### 2.5. *puchi-1* roots generally have normal auxin response

Given the essential roles of auxin in LRP formation and development (Lavenus et al., 2013a), we investigated the auxin response in *puchi-1* roots to see if auxin signalling may correlate with *puchi-1* LRP phenotypes.

*puchi-1* LRPs are defective in morphology, and their development/emergence is greatly delayed (Figure 2.4). It was reported that (i) an auxin gradient is gradually established in developing LRPs (Benková et al., 2003) and (ii) auxin regulates the expression of cell wall remodeling enzymes in LRP overlaying tissues to assist LRP emergence (Swarup et al., 2008; Péret et al., 2013).

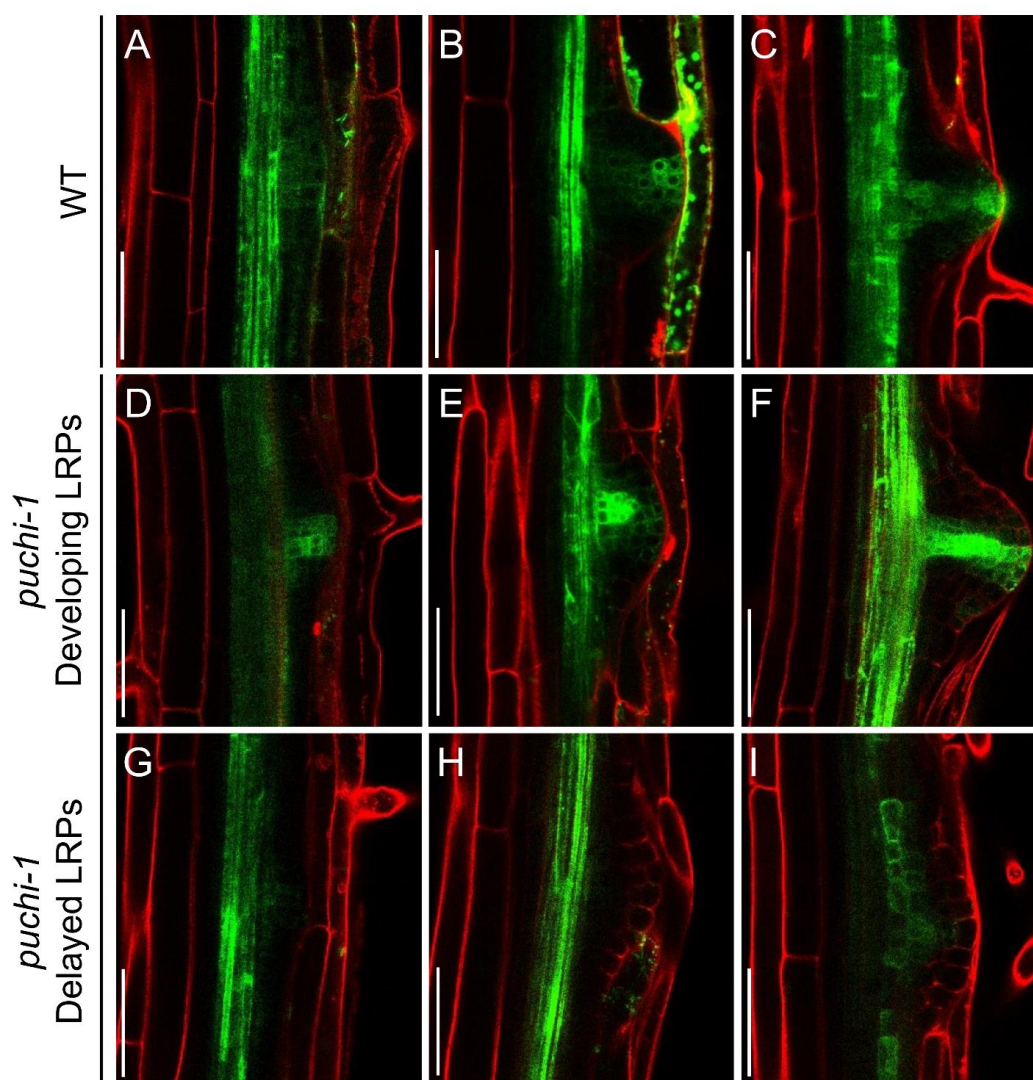


**Figure 2.9.** Auxin gradient as revealed by *DR5::GFP* reporter in WT and *puchi-1* LRPs and LRs. (A) to (C) In WT, a clear auxin signaling gradient was gradually established during LRP development. Auxin response also happened (particularly prominent in B) in cells overlying developing LRPs to assist their emergence. (D) to (F) The gradient similar to that of WT was also observed in developing LRPs in *puchi-1*. However, note the skew in auxin signal in the LRP in D and lesser auxin response in LRP overlying cells. (G) to (I) In delayed LRPs, auxin response was usually very weak or did not form an auxin maximum. Auxin response in cells overlaying these LRPs was usually hard to detect. The white lines are added to assist with the visualization of LRP contours. Scale bars = 50  $\mu$ m.

We therefore observed the auxin responses in LRPs and their overlaying tissues in *puchi-1* LRPs using the *DR5::GFP* synthetic auxin response reporter (Friml et al., 2003). The DR5 promoter consists of tandem direct repeats of 11 bp that includes the auxin-responsive TGTCTC element commonly found in auxin-inducible genes (Ulmasov et al., 1997). *DR5::GFP* is an established reporter to visualize auxin signaling response at a cellular level during LRP development

(Dubrovsky et al., 2008). In WT LRPs, a clear *DR5::GFP* gradient was present in developing LRPs and LRs (Fig. 2.9A-C). A similar auxin signaling gradient was also observed in most developing LRPs in *puchi-1* (Fig. 2.9D-F). However, sometimes the auxin maximum was located more deeper inside the LRP, and not located at the middle of the LRP, which is in agreement with a skewed shape of *puchi-1* LRPs (Fig. 2.9D, E). In contrast, in a majority of delayed (probably arrested) LRPs in *puchi-1* background, the auxin signaling gradient was not visible (Fig. 2.9G-I). This probably means that there is no more auxin signaling in those delayed LRPs to promote their development, and is in agreement with our previous results showing that those primordia were arrested.

In the WT, a *DR5::GFP* signal was observed in cells overlaying LRPs where cell wall remodeling activities are supposed to happen (for example, Fig. 2.9B). Cells overlaying developing LRPs in *puchi-1* showed a similar DR5 signal, even though the GFP intensity may be weaker, suggesting that auxin response may be lower compared to those in the WT (Fig. 2.9D, E). This may contribute to the delay in LRP emergence in *puchi-1* roots. GFP signal in cells overlaying un-emerged LRPs in *puchi-1* branching zone is usually very weak or undetectable (Fig. 2.9G-I).

In conclusion, here we showed that in general, a clear auxin signaling gradient is established during LRP formation in both WT and *puchi-1* background, in agreement with the ability of *puchi-1* roots to make LRs. However, in some *puchi-1* LRPs, a proper auxin gradient was either not in the center of the LRP or not established at all, especially in the delayed LRPs. It suggests that loss of PUCHI function might interfere with the regulated distribution of auxin signal during root branching. Further experiments will be required to confirm this hypothesis, and to explore its functional relevance for the defects of *puchi-1* LRPs in developmental progression and emergence.

## **2.6. *puchi-1* pericycle is more sensitive to auxin treatment**

Considering LR initiation as a response of pericycle cells to an auxin signal (de Smet, 2012; Xuan et al., 2016; Möller et al., 2017), the increase in LRP number, hence density, along *puchi-1* primary roots suggests that the mutant pericycle cells either experience higher auxin concentrations compared to WT or respond more to similar auxin levels, resulting in more frequent LRP priming and initiation. I therefore tested the effects of auxin treatment to LRP initiation in the mutant. For this, we grew WT and *puchi-1* seedlings on MS medium supplemented with NAA at different concentrations for 9 days, and the number of developing LRPs and total LRPs (LRPs + LRs) were counted.

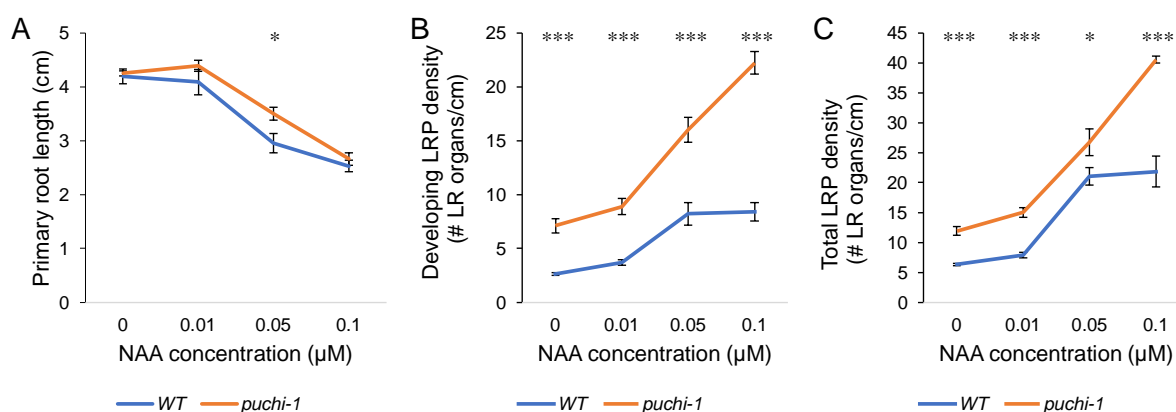


**Figure 2.10.** *puchi-1* roots produce more LRPs when treated with auxin NAA. WT and *puchi-1* seeds were sown on MS medium supplemented with NAA at different concentrations and the seedlings grew for 9 days. Primary root lengths, LRP density in the LR formation zone (developing LRP density) and total LRP density were measured. Data are represented as Mean  $\pm$  SEM. Two replicates were done showing similar results;  $n = 10$  seedlings in each repeat. Figures are from one repeat. Significance was determined by Student's t-test. \*  $p < 0.05$ , \*\*  $p < 0.01$ , \*\*\*  $p < 0.001$ .

First, we observed that WT and *puchi-1* primary roots responded similarly to auxin treatment in terms of root growth inhibition. Primary root lengths of the two genotypes decreased by  $\sim 40\%$  at  $0.1 \mu\text{M}$  NAA (Figure 2.10A). This demonstrates that *puchi-1* is not impaired in general auxin response. In contrast, LRP density increased sharply with auxin concentration. This increase was due mostly to the over-production of LRPs instead of the decrease in primary root lengths because at  $0.1 \mu\text{M}$  NAA root lengths reduced by  $\sim 40\%$  while total LRP density increased by  $\sim 3.5$  times compared to the control condition (Figure 2.10B,C). However, while developing LRP density and total LRP density (LRP + LRs) seems to reach a plateau at  $0.05$  and  $0.1 \mu\text{M}$  NAA in WT, they still increased in *puchi-1*. These data suggest that pericycle cells are more sensitive to auxin in *puchi-1* and this may explain the increase in LRP formation observed in this mutant.

## 2.7. Cytokinin signalling is altered in *puchi-1* LRPs

Besides auxin, cytokinins also regulate LRP initiation and development (Laplaze et al., 2007; Chang et al., 2015). To see if *puchi-1* LRP defects are correlated with perturbations in cytokinin signaling, the *TWO COMPONENT SIGNALING SENSOR NEW (TCSN)::GREEN FLUORESCENT PROTEIN (GFP)* reporter was introduced into the *puchi-1* mutant background and its expression in the WT and *puchi-1* was compared. The *TCSn::GFP* construct contains consensus sequence from the promoters of well-documented direct cytokinin target genes, and is widely used to analyze cytokinin signaling in Arabidopsis (Zurcher et al., 2013).

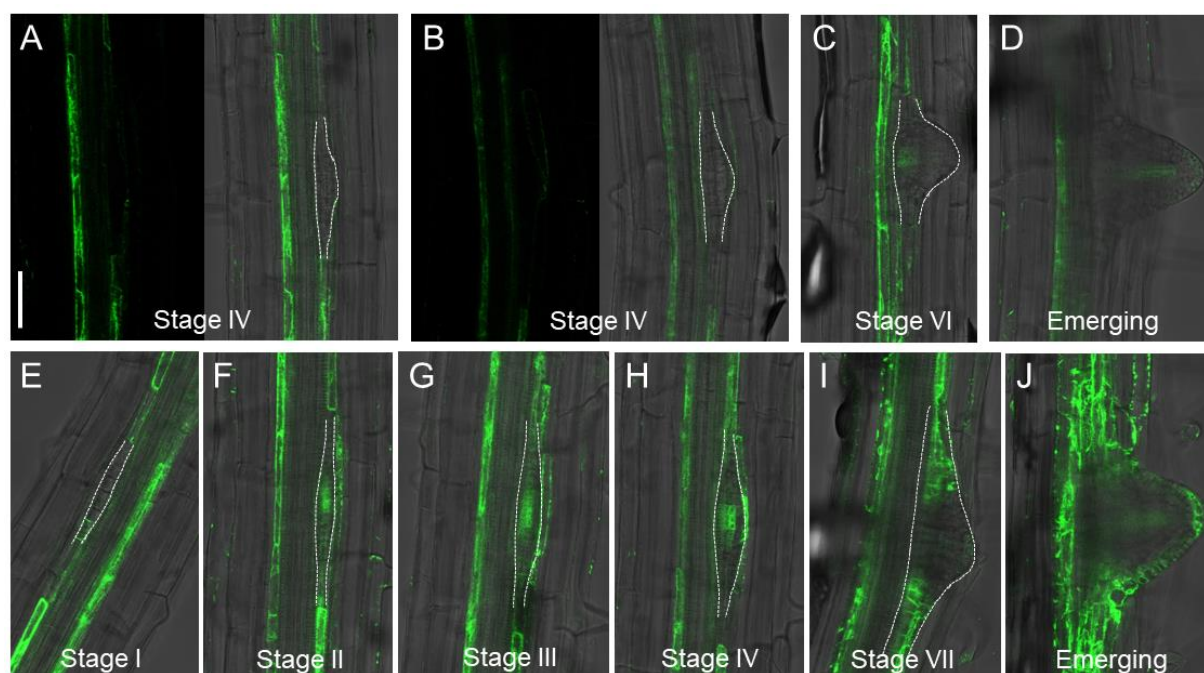


**Figure 2.11.** Expression pattern of the cytokinin signaling reporter construct *TCSn::GFP* reporter in WT and *puchi-1* LRPs. (A) to (D): In WT, *TCSn::GFP* reporter expression was not observed in LRPs until stage VI onwards. From then, the signal was observed in the presumptive stele of the LRP but not in its flanks. (E) to (J): In *puchi-1*, cytokinin signaling was observed inside LRPs of various stages, including stage II and III, and also strongly in flanks of more advanced LRPs. The white lines are added to assist with the visualization of LRP contours. Scale bar = 50  $\mu$ m. Defective *TCSn::GFP* expression (early appearance and in LRP flanks) were observed in 5/5 *puchi-1* seedlings. n = 5 seedlings for the WT.

In WT, *TCSn::GFP* was not observed in LRPs younger than stage VI, and from stage VI onwards the expression was restricted to pro-vasculature cells (Figure 2.11A-D). Pericycle cells adjacent to a LRP showed *TCSn::GFP* expression, but the LRP flank cells did not (Figure 2.11B,C). These features are consistent with previous studies (Bielach et al., 2012; Chang et al., 2015). However, in *puchi-1* background, *TCSn::GFP* was observed in developing LRPs of all stages, and the signal was usually stronger in central cells in inner layers. In more advanced LRPs, cytokinin signaling was clearly observed in the flanks.

### III. DISCUSSIONS

#### 3.1. PUCHI controls LRP initiation and spacing

PUCHI has been previously reported to be an important regulator of the first, morphogenetic, phase of LR development and a regulator of cell division in LRP (Hirota et al., 2007; Lavenus et al., 2015). It also regulates bract formation in flowers (Hirota et al., 2007; Karim

et al., 2009). Here we characterized the mutant phenotype in our experimental settings and found that PUCHI also regulates LRP initiation and spacing.

Our data show that the *puchi-1* loss-of-function mutation enhanced LRP initiation in normal and auxin-treated conditions, which is in agreement with the recent report that *PUCHI* is expressed in cells adjacent to LR founder cells to inhibit nearby pericycle cells from becoming founder cells (Toyokura et al., 2018). However, what happens downstream of PUCHI, or how PUCHI exerts its inhibitory function, is still unknown. The lateral inhibition of LRP initiation has been proposed for other factors, for example, the membrane localized receptor-like kinase ARABIDOPSIS CRINKLY4 (*ACR4*; De Smet et al., 2008), cytokinin homeostasis genes (Chang et al., 2015) or the RAPID ALKALINIZATION FACTOR- LIKE 34 (*RALFL34*) peptide (Murphy et al., 2016). High LRP initiation in these mutants may due to different causes. Elevated endogenous auxin IAA levels in the roots may increase LRP initiation as suggested in the *shy2-101/iaa3* mutation (Goh et al., 2012b). In certain conditions pericycle cells are more sensitive to auxin, hence they are more responsive to auxin-induced priming and LRP initiation. One example is plants overexpressing cell cycle regulators such as *CYCD3;1* (De Smet et al., 2010).

Increased LRP density usually comes hand in hand with aberrant LRP positioning, which is the formation of closely-positioned LRPs (LRP clusters). Double and triple mutants of *PLT3*, *5*, *7* produce up to ~40% more total LRPs (Hofhuis et al., 2013), and the triple mutant produces ~ 30 times more LRP clusters (within 300  $\mu\text{m}$  of each other). Total LRP density in *ralfl34-1* mutant increases by ~ 25%, and number of LRP clusters (LRPs being closer to each other than 400  $\mu\text{m}$ ) increased by ~ 3 times (Murphy et al., 2016). *RALFL34* expression is found not only in LRPs but also in flanking pericycle cells (Murphy et al., 2016). This flanking expression of *RALFL34* is therefore thought to be involved in the regulation of LRP positioning. The *acr4* mutant has ~ 19% increase in total LRP density but produces ~ 18 times more aberrantly positioned LRPs (opposite or adjacent to each other). Since *ACR4* expression is observed only in LRPs, it may act non-cell autonomously to regulate LRP initiation (De Smet et al., 2008). Mutants impaired in symplastic connectivity (due to enhanced callose accumulation in the stele, for example) showed ~ 2 fold increase in LRP density and frequent LRP clusters (Benitez-Alfonso et al., 2013).

Beside increased LRP density, *puchi-1* roots also produced a strikingly high number of LRP clusters. These LRP clusters could be occasionally seen in the WT. The number of LRP clusters in ~ 220 LRPs in *puchi-1* was ~ 54.5 times higher than in WT (Table 2.2). Since the total LRP density in *puchi-1* was ~2 times higher than in the WT, the 54.5 time increase in LRP clusters could not be explained by the increased LRP density. This suggests that beside LRP initiation PUCHI also plays a role in LRP spacing. PUCHI somehow regulates the interval and position of

LRP initiation so that LRPs of the same or opposite protoxylem poles do not form closely. However, we did not observe the expression of *pPUCHI:GFP-PUCHI* in the basal meristem the zone important for LRP initiation (De Smet et al., 2007; Moreno-Risueno et al., 2010; Xuan et al., 2016). We did find *PUCHI* expression in pericycle cells flanking developing LRPs, suggesting that *PUCHI* in those cells may play a role in inhibiting cell division of nearby pericycle cells. This observation is consistent with a recent report (Toyokura et al., 2018) on *PUCHI* expression in pericycle cells adjacent to LR founder cells. In addition, we observed the expression of *PUCHI* in the stele. Interestingly, intercellular (symplastic) connectivity between the stele and other tissues has been demonstrated to be important for LRP initiation and spacing (Benitez-Alfonso et al., 2013). This symplastic connectivity may influence the transport of mobile factors that play a role in LRP initiation, for example, auxin and other peptides.

Altogether, our observations support that *PUCHI* negatively controls cell division in both LRPs and the pericycle, and the latter is consistent with work of (Toyokura et al., 2018) showing that cascade LBD16- TOLS2/PIPL3-RLK7-*PUCHI* negatively regulates LR initiation.

### 3.2. Loss of *PUCHI* function leads to LRP development defects

Using gravistimulation assay we demonstrated that *puchi-1* LRPs develop at a much slower rate compared to WT ones (Figure 2.3). *puchi-1* LRPs are flatter than those in WT, and a slow development/emergence is expected for LRPs lacking a prominent domed-shape (Péret et al., 2012; Lucas et al., 2013; Fernández-Marcos et al., 2017). The delay in LRP emergence maybe due to different mechanisms such as reduced LRP cell turgor (Péret et al., 2012), increased physical constraints in overlaying cells (Péret et al., 2012; Lucas et al., 2013), or additional cell divisions in LRP boundary (Fernández-Marcos et al., 2017). In *puchi-1* LRPs, defects in anticlinal cell division are the most evident cause of the delayed emergence phenotype. It is likely that because *puchi-1* LRPs are wider/flatter, the pressure they make when contacting overlaying cells is less focused or less substantial. These overlaying cells in turn response less to the weak pressure, making it more difficult for *puchi-1* LRPs to penetrate them. Interestingly, preliminary studies of *DR5::GFP* expression in the root tissues suggested that a weaker auxin signal was detected in overlying endodermis and cortex layers. This auxin signalling activity was previously associated with the spatial accommodation of endodermal and cortical cells during LRP progression (Vermeer et al., 2014).

The high LRP density and slow LRP development are consistent with high number of un-emerged LRPs in the branching zone which may be arrested. LRPs are initiated strictly acropetal, meaning that no *de novo* LRP initiation takes place between two already existed LRPs (Dubrovsky et al., 2006). This suggests that delayed LRPs in WT and *puchi-1* are those that grow slowly or

stop growing altogether instead of newly formed. Using tracking assay, we showed that even after 4 or 9 days of tracking only few LRPs in WT and *puchi-1* eventually emerged, indicating that most of un-emerged LRPs in the branching zone in both genotypes are in fact arrested (Table 2.2). This conclusion is supported by the lack of *DR5::GFP* accumulation in and auxin response over these delayed LRPs.

In *puchi-1* roots, while total LRP density increased by ~2 times, delayed LRP density increased by ~ 6 times compared to the WT, indicating that the increase in delayed LRPs in the branching zone is not simply proportional to the increase in overall LRP formation. Moreover, increased LRP formation in *puchi-1* did not result in a higher number of emerged LR. Regarding these features, *puchi-1* is reminiscent of the *shy2-101/iaa3* mutation which produces more LRPs but very few or none of them emerge into LR. This rises the hypothesis that higher LR initiation rate may be a secondary response to low emergence rate, or *vice versa* (Lucas et al., 2008). Because LRP priming and LRP development share the same source of auxin root, more auxin consumed during priming, *i.e.* more LRP initiation, would lead to less auxin available for promoting LRP growth. In contrast, if somehow *puchi-1* LRPs consume less auxin, which may lead to slow growth and more arrested LRPs, there would be more auxin available for LRP priming (Lucas et al., 2008). In addition, the fact that LRP initiation does not always lead to LRP growth supports the notion of bi-phasic LRP development which differentiates the early morphogenesis phase and the late meristem formation phase (Goh et al., 2016). The transition between two phases happens between stage IV to V when a LRP crosses the endodermis and is concomitant with the activation of QC-specific markers such as *QC25::CFP* (Goh et al., 2016). From our analyses, most of arrested LRPs in WT and *puchi-1* are at stage I-IV and only few of them at stage V or VI, indicating that they failed the critical transition. The failure maybe due to (i) insufficient co-ordination between LRP development and assistance of overlaying cells, notably the endodermis, meaning that endodermal cell wall remodelling is not effective enough to assist the penetration of a LRP, and (ii) mis-activation of meristematic genes/functions as suggested by the defects in the expression pattern of the QC-specific maker *QC25::CFP* (Figure 2.8).

### **3.3. PUCHI regulates cell divisions and stem cell niche establishment, possibly through hormonal signalling**

Hirota et al., (2007) showed that *PUCHI* is required for correct anticlinal cell division. In more advanced LRPs, *PUCHI* expression is restricted to the base and flanks, and *puchi-1* mutant shows cell over-proliferation and abnormal cell sizes at the flanks, hence correct flank morphogenesis requires *PUCHI*. It was also noted that there was a subtle defect in meristematic region around the QC in *puchi-1* emerging LR, which is the expansion of *SCRpro::GFP*

expression to the cell layer directly overlaying the QC. In WT, *SCRpro:GFP* expression is restricted to the QC layer (Hirota et al., 2007).

Here we showed that PUCHI is also required for periclinal cell division in developing LRPs. Our conclusion is based on observing cell division pattern in stage IV LRPs (Malamy and Benfey, 1997; Von Wangenheim et al., 2016). In WT, the periclinal division completes in the outer layer first, then happens to the inner layer of a stage II LRP. However, in *puchi-1* the periclinal division can happen to the inner and outer cell layer of a stage II LRP at the same time (Figure 2.6). Although our observation was made on early developing LRPs, these defects may also occur in LRPs of later stages. This suggests that PUCHI does not necessarily control specifically the anticlinal cell division but controls the cell division plane in general.

Because we have not yet performed a tracking observation for *puchi-1* LRPs, it is difficult to say if anomalies in anticlinal cell divisions result in any function defects in LRPs. However, similar to (Hirota et al., 2007), we observed an alteration in cell organization around the QC. Using *pSHR:GFP* signal as a delimitation of the meristem region, we found that there was an additional cell layer at *puchi-1* LR tip (Figure 2.7). Consistent with that, *QC25::CFP* expression was misplaced in *puchi-1* by one cell layer (Figure 2.6). It is possible that this additional cell layer corresponds to the layer that displaying unusual *SCRpro:GFP* signal reported in (Hirota et al., 2007), and that this layer is a result of periclinal cell division defects in *puchi-1*. Since PUCHI is not expressed in the meristematic domain of advanced LRPs, these defects likely happen to young LRPs and maintain themselves. How these changes in cell division and tissue organization affect overall LRP development and outgrowth remains to be studied.

A striking observation is that in the *puchi-1* mutant, cytokinin signalling as revealed by *TCSn::GFP* appeared much early during LRP formation, and was strong in flank cells of more advanced LRPs (Figure 2.11). These features were not observed in the WT. It has been demonstrated that cytokinin treatment induces cell division in LRPs; for example, LRPs of cytokinin-treated roots have more anticlinal cell layers than those in the control (Laplaze et al., 2007). In the primary root, cytokinin induces cell division of the QC (Zhang et al., 2013). Cytokinin also activates cell division in other contexts including whole plants and tissue cultures (Riou-Khamlichi et al., 1999). Therefore, it is possible that ectopic cytokinin signalling in *puchi-1* LRPs promotes cell division, creating LRPs with more cell layers as described. Specific expression of the cytokinin biosynthesis gene *ISOPENTENYL TRANSFERASE (IPT)* in LRPs using different trans-activation promoters generally induced a delay in LRP emergence (Bielach et al., 2012). Unfortunately, LRP morphology was not reported. Moreover, in axillary leaves, cytokinin activates the expression of the transcription factor *WUSCHEL (WUS)* that controls

shoot stem cell niche establishment (which comprises the QC) (Wang et al., 2017). Here we found that the expression of the QC-specific marker *QC25::CFP* and cytokinin signalling appeared earlier in *puchi-1* than in WT LRPs. Whether the early cytokinin signalling leads to the early activation of the QC marker, enhanced cell division and delayed LRP emergence of *puchi-1* LRPs is worth investigating.

*puchi-1* LRPs seemed to have a clear auxin gradient, at least in those develop well and emerge eventually. Nevertheless, we noticed that auxin maximum in *puchi-1* LRPs seemed to be in deeper cells. In addition, the clear gradient was not observed in delayed LRPs which constitute ~ 20% of total LRPs in the mutant. Moreover, *puchi-1* pericycle has higher competence for cell division in normal and auxin-treated conditions. Therefore, LR developmental defects in *puchi-1* roots may also be linked to auxin signalling.

To summarize the discussion, possible connections between *puchi-1* LRP developmental defects are depicted in the Figure 2.12. First, PUCHI inhibits LRP initiation, which has been demonstrated to be at LR founder cell specification step, and also inhibits the response of pericycle cells to auxin treatment to form LRPs. The latter effect is probably the result of the former. Second, *puchi-1* LRPs are defectives in both anticlinal and periclinal cell division, which result in abnormal LRP morphology, *e.g.*, flatter LRPs, which in turn leads to delayed LRP emergence and possibly LRP development arrest. Third, PUCHI is also important for auxin and especially cytokinin signalling, and defective hormonal signalling may lead to enhanced LRP cell division, uncontrolled stem cell niche establishment, and general LRP development. The delayed LRP emergence and enhanced LRP initiation may be link together because the two developmental processes share the same budget of root auxin.

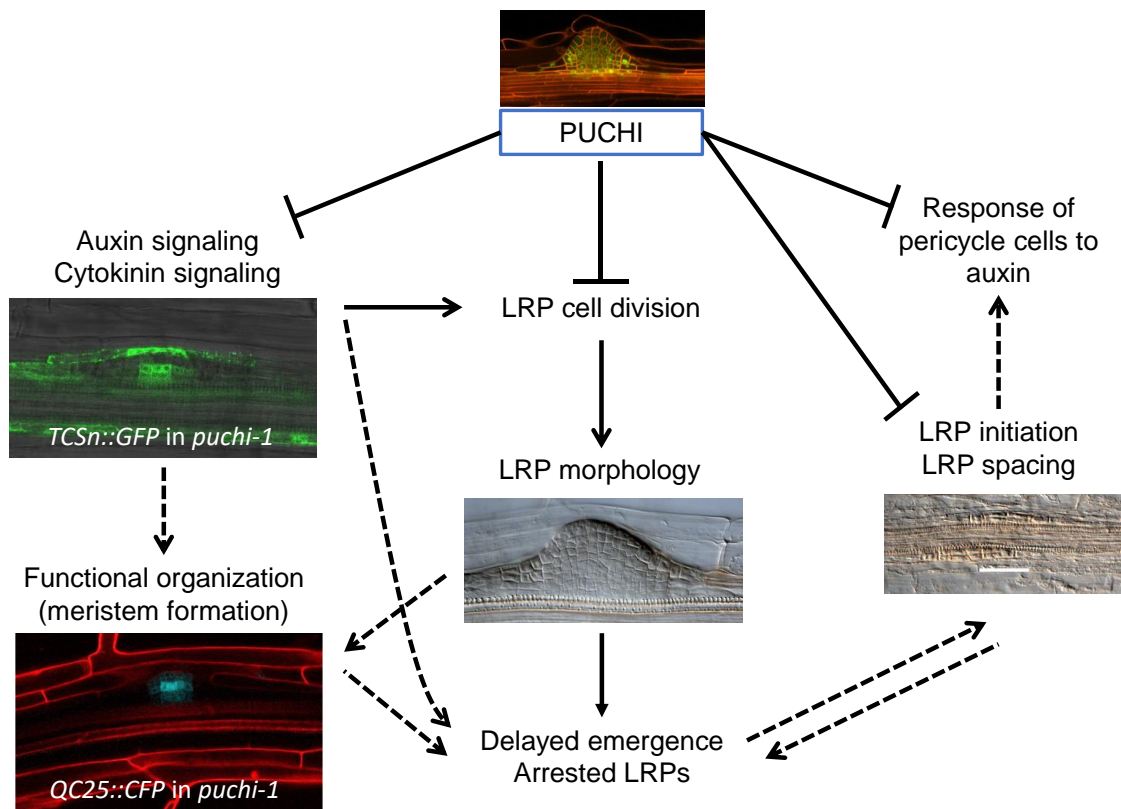


**Figure 2.12.** Summary of PUCHI roles during LRP development and possible links between the observed phenotypes of *puchi-1* LRPs.

#### IV. CONCLUSION AND PERSPECTIVES

*De novo* organogenesis processes such as LRP formation are complex and require the coordination of multiple factors. The transcription factor PUCHI was demonstrated to be required for proper LRP morphogenesis and LRP initiation (Hirota et al., 2007; Kang et al., 2013). Here, we confirmed these observations and revealed new roles and features of PUCHI. We showed that PUCHI regulates LRP initiation possibly through restrain the responsivity/sensitivity of pericycle cells to auxin. It also co-ordinates LRP positioning so that LRPs do not form closely to each other. PUCHI regulates both anticlinal and periclinal cell division during LRP formation, and lack of *PUCHI* leads to morphological and patterning defects in LR flanks and meristematic zone. Defective (extra) division in LRP cells and mis-activation of the QC are possibly the major reasons for the slow development (and early arrest) of *puchi-1* LRPs. All these phenotypes of the mutant emphasize PUCHI as a negative regulator of cell division during LRP formation and development, and are consistent with the prediction that puts it as a major player of the first sub-network. However, the genetic pathways that PUCHI modulates during LRP development were not known at the beginning of my thesis. Since PUCHI regulates multiple aspects of LRP development, it is of great interest to look for its targets during this context.

# **CHAPTER III**

**PUCHI regulates VLCFA biosynthesis genes during LRP  
and callus formation**

## I. INTRODUCTION

In Chapter II, I showed that PUCHI regulates multiple aspects of LRP formation and development. Because it is difficult to identify the precise mode of action of PUCHI from these pleiotropic phenotypic alterations, we took advantage of an unbiased transcriptomics approach to look for the direct and indirect targets of this transcription factor (TF). Here, I looked for the potential targets of PUCHI and attempted to demonstrate the regulation of PUCHI on these targets. To identify potential targets of PUCHI during LR development, our team took advantage of the time-course transcriptomic dataset profiling every stage of LRP organogenesis (Voß et al., 2015). Dr. Julien Lavenus, while being a PhD student in the team, employed the TDCor algorithm which he developed (Lavenus et al., 2015) to search in the LR dataset for genes exhibiting an expression profile highly similar to that of *PUCHI* (Pearson's correlation coefficient > 0.80) when shifted back in time by 3 hours (*i.e.* delayed by one time point in the dataset relative to *PUCHI* expression profile). This *in silico* analysis retrieved 217 potential target genes whose expression profiles are correlated with that of *PUCHI* (Appendix 1). A Gene Ontology (GO) enrichment analysis using BiNGO (Maere et al., 2005) revealed that 41 GO biological processes (of all levels) were significantly overrepresented in this group of putative downstream genes (Figure 3.1). Among them, the “VLCFA biosynthesis” category stood out as one of the most strongly overrepresented biological processes ( $p$ -value = 0.006).

VLCFAs are fatty acids with 20 or more carbons that are essential for yeast, animal and plant growth and development, although their precise functions are not fully elucidated (Bach and Faure, 2010; Haslam and Kunst, 2013). The importance of VLCFAs in LR development has been suggested since *pas1* and *KCRI* RNAi mutants produced few and severely defective LR (Beaudoin et al., 2009; Roudier et al., 2010). Moreover, VLCFAs were recently showed to negatively regulates the expression of *ABERRANT LATERAL ROOT FORMATION 4 (ALF4)*, a gene required for LRP initiation (DiDonato et al., 2004; Shang et al., 2016), and this regulation is thought to modulate the competence of root pericycle cells to produce callus in callus-inducing medium. Despite these interesting data, little is known about VLCFA biosynthesis and its regulation in the context of LRP development.

VLCFAs are synthesized in the endoplasmic reticulum membrane from long chain-fatty acyl-CoAs (16 or 18 carbons) by the fatty acid elongase complex (Figure 3.2). VLCFAs can be latter subjected to additional modifications such as hydroxylation and incorporated into various classes of membrane, storage and extracellular lipids such as phospholipids and sphingolipids, triacylglycerols, suberin and waxes (Li-Beisson et al., 2013). The composition of VLCFAs in a

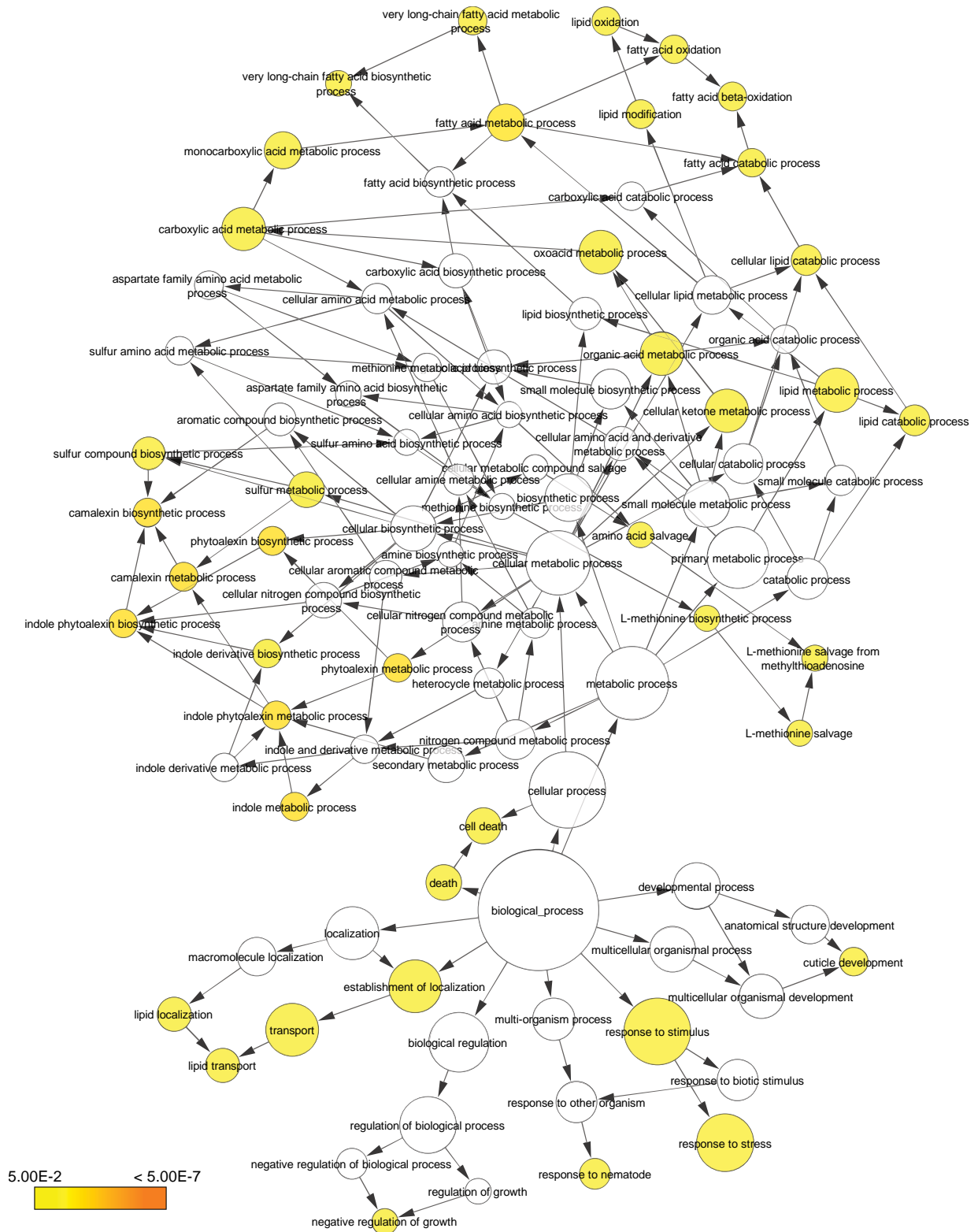


**Figure 3.1.** Enrichment analysis using BinGO on 217 genes having correlated expression profiles with that of *PUCHI*, when shifted back in time by 3 hours. Yellow nodes are biological processes that are overrepresented. “VLCFA biosynthesis process” is located at the top left. This analysis was performed initially by Dr. Julien Lavenus (Lavenus, 2013). The color gradient bar represents  $p$ -values in the statistical test done by BinGO.

tissue can be determined by direct transesterification followed by analysis by GC or GC-MS (Gas chromatography–mass spectrometry) (Li-Beisson et al., 2013; Wattelet-Boyer et al., 2016).

The fatty acid elongase (FAE) complex consists of enzymes catalyzing rounds of 2-carbon elongation in a 4-step mechanism, involving a 3-ketoacyl-CoA synthase (KCS), a 3-ketoacyl-CoA reductase (KCR), a 3-hydroxyacyl-CoA dehydratase (HACD), and a trans-2,3-enoyl-CoA reductase (ECR). Multiple KCS enzymes with various expression patterns have been described that catalyze the first step of fatty acid elongation, and their substrate affinity is thought to be responsible for the final VLCFA chain length (Joubès et al., 2008; Millar and Kunst, 1997; Kim et al., 2013). In contrast, only a limited number of genes that encode functional enzymes catalyzing each of the subsequent steps of the elongation cycle has been identified in Arabidopsis.

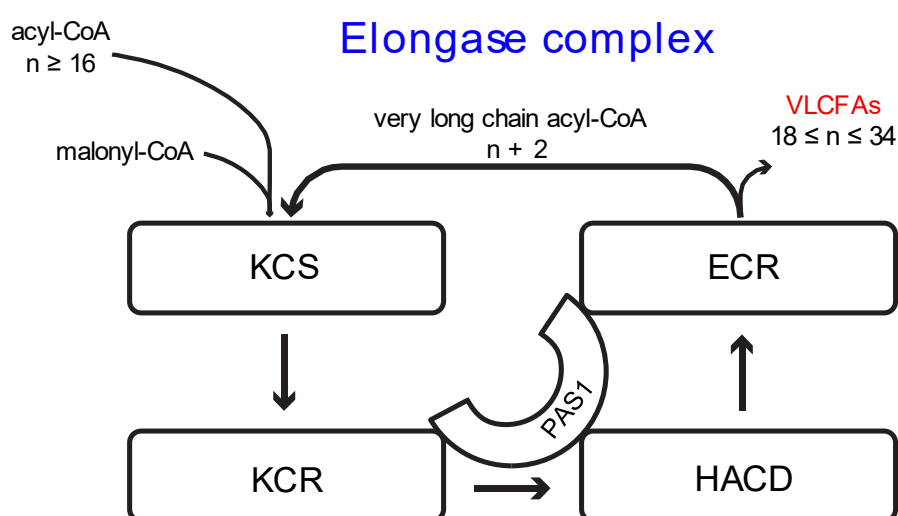


**Figure 3.2.** Schematic representation of the VLCFA elongation cycle. VLCFAs are synthesized from malonyl-CoA and acyl-CoA (number of carbon atoms in the chain  $n \geq 16$ ) by the fatty acid elongase complex comprised of KCS, KCR, HACD (PAS2 and PTPLA) and ECR enzymes. PAS1 acts as a scaffold for the complex.

*KETOACYL REDUCTASE 1 (KCR1)* encodes an Arabidopsis KCR enzyme and is expressed in the root endodermis (Beaudoin et al., 2009; Morineau et al., 2016) while *PASTICCINO 2 (PAS2)* (Bach et al., 2008) and *PROTEIN TYROSIN PHOSPHATASE-like (PTPLA)* encode two HACD enzymes and are expressed in the endodermis and the pericycle/vascular tissues of the root, respectively (Morineau et al., 2016). Last, the product of the *ENOYL CO-A REDUCTASE/ECERIFERUM 10 (ECR/CER10)* gene has ECR activity (Zheng, 2005). These enzymes are physically linked together in the fatty acid elongase complex by PASTICCINO 1 (PAS1; Figure 3.2; Roudier et al., 2010).

TDCor was then used to infer the relative position of PUCHI and VLCFA biosynthesis genes in the gene network controlling LRP formation. VLCFA biosynthesis genes (including *LACS2*, *KCS1*, *KCS2*, *KCR1*, *PAS1*, *PAS2* and *ECR*) were added to the gene list previously used by (Lavenus et al., 2015) to run the TDCor inference program. TDCor proposed a LR subnetwork topology represented in Figure 3.3. VLCFA biosynthesis genes were positioned as indirect targets of PUCHI through other transcription factors like PLT7. PUCHI was predicted to be directly regulated by LBD16, which has been experimentally demonstrated (Tatsuaki Goh, personal communication). MYB41 was proposed to play an important role directly regulating VLCFA biosynthesis genes. This prediction is also supported by the observation that in the leaf, over-expression of *MYB41* induces the expression of several VLCFA genes involved in suberin and cuticle biosynthesis, including *KCS2* and *KCS6* (Kosma et al., 2014).

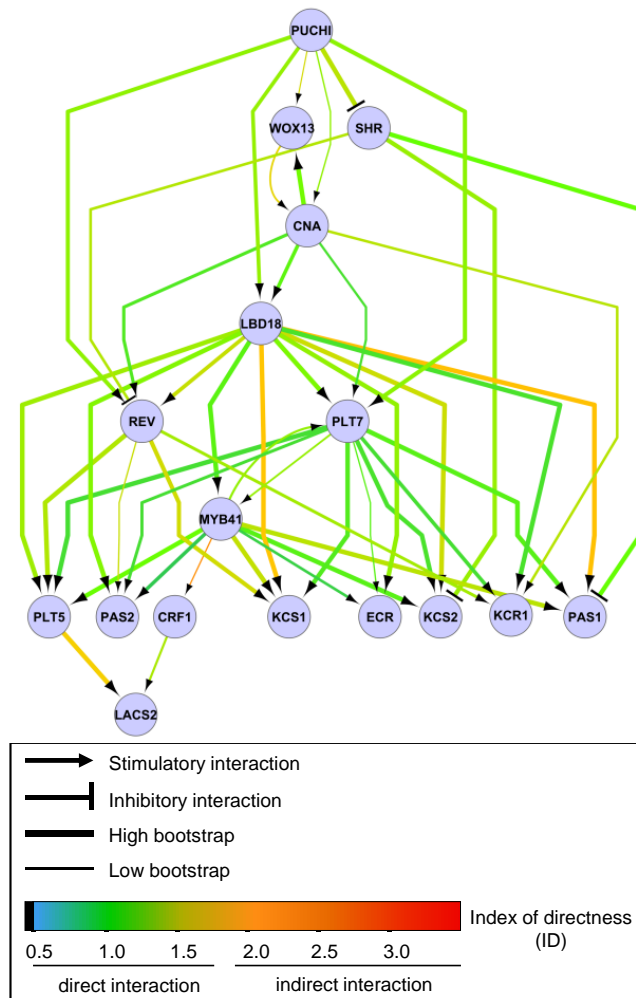


**Figure 3.3.** The PUCHI network inferred by TDCor suggests that PUCHI may regulates VLCFA biosynthesis genes indirectly via other transcription factors (from the thesis of Dr. Julien Lavenus, 2013).

Based on that experiment, Dr. J. Lavenus hypothesized that PUCHI regulates the expression of genes involved in the biosynthesis of very long chain fatty acids (VLCFA) during LR development. In order to test the hypothesis that expression dynamics of those VLCFA biosynthesis genes during LR formation is indeed dependent on PUCHI, he quantified levels of transcripts encoding VLCFA biosynthesis enzymes in wild type (WT) and *puchi-1* loss-of-function mutant roots during LR formation by RT-qPCR. An auxin-dependent LR induction system (LRIS, modified from Himanen et al. (2004)) was used to synchronously induce lateral root (LR) formation along the whole primary root. In the wild type, transcript levels of *KCS1*, *KCS2*, *KCS20*, *KCR1*, *PAS2* and *ECR/CER10* increased upon LR induction, but this response was

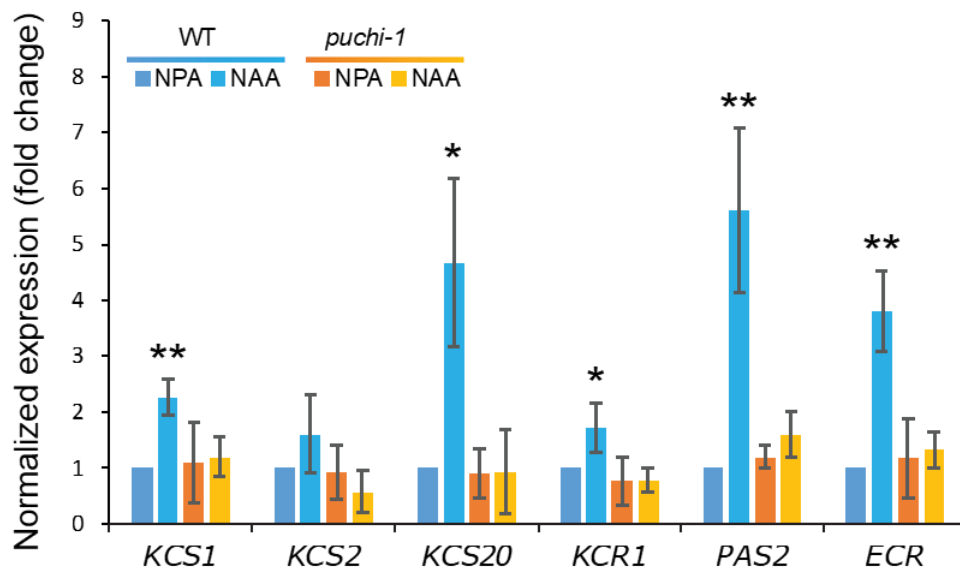


**Figure 3.4.** Measurement of key VLCFA biosynthetic gene expression by RT-qPCR in WT (blue) and *puchi-1* roots (orange). Lateral root formation is inhibited in control plants treated with the polar auxin transport inhibitor 1-N-Naphthylphthalamic acid (NPA, darker shade), while on the auxin naphthaleneacetic acid (NAA, brighter shade) lateral root initiation is induced synchronously along the primary root in both WT and *puchi-1*. Roots were harvested after 24h treatment on 5  $\mu$ M NPA or 10  $\mu$ M NAA. Normalization was achieved with the *CYCLIN-DEPENDENT KINASE A;1* (*CDKA;1*) gene. The calibrator cDNA for relative quantification of the effect of each treatment is WT under NPA treatment. Data are represented as Mean  $\pm$  SEM (standard error of the means) of three biological replicates. Significance was determined by Student's t test. \*  $p < 0.05$ , \*\*  $p < 0.01$ . This experiment was performed by Dr. Julien Lavenus (Lavenus, 2013).

disrupted in the *puchi-1* loss-of-function mutant background (Figure 3.4). Hence, expression of genes encoding key components of the elongase complex responsible for VLCFA biosynthesis is

induced during auxin-induced LRP development, and this induction is dependent on the PUCHI transcription factor.

In summary, the work of Dr. Julien Lavenus suggested that PUCHI regulates the expression of VLCFA biosynthesis genes during LRP development and demonstrated that expression levels of key genes, *KCS1*, *KCS20*, *KCR1*, *PAS2* and *ECR*, are indeed dependent on PUCHI in the auxin-induced LRP formation context. During my PhD, I confirmed these results and performed extra experiments to demonstrate that PUCHI also regulates the expression pattern of VLCFA biosynthesis genes during LRP development, and that VLCFA biosynthesis plays a significant role in LR development. VLCFAs were previously found to regulate the competence of pericycle cells to generate calli on an auxin-rich callus-inducing medium (CIM) (Shang et al., 2016). Here, I show that PUCHI is also expressed and regulates VLCFA biosynthesis genes during CIM-induced callus formation, and that the *puchi-1* and VLCFA biosynthesis mutants show similar callus phenotype and fatty acid profiles on CIM medium. Altogether, the data indicate that the regulation of VLCFA biosynthesis genes by PUCHI is part of a conserved pathway controlling cell proliferation and organization during LR and callus formation.

## II. RESULTS

### 2.1. More on VLCFA biosynthesis genes in relevant datasets

Among 217 potential targets of PUCHI identified by the method described above, the BinGO analysis listed three genes in the “VLCFA biosynthesis process” including *AT1G01120* (*KCS1*), *AT3G54010* (*PAS1*) and *AT1G67730* (*KCR1*). However, when I curated the common names and functions of those 217 genes, I also found *AT1G04220* (*KCS2*) and *AT5G10480* (*PAS2*), two functional genes involved in VLCFA biosynthesis. This is most likely because the “VLCFA biosynthesis process” term was not yet associated with *KCS2* and *PAS2* in the Arabidopsis GO database. Thus, VLCFA genes are highly overrepresented in the list of PUCHI potential targets.

Names and functions of all reported VLCFA biosynthesis genes (based on function and sequence homology analyses) are provided in Appendix 2. The availability of these genes in the LR dataset is also indicated. The presence of these genes in the LR dataset is dependent on (i) their presence of the ATH1 affymetrix chip, and (ii) the detection of significant expression level changes during the time course of LR development (Voß et al., 2015). Among 27 reported VLCFA biosynthesis genes, there are 21 *KCS*-like genes, 2 *KCR*-like, 1 *PAS2*-like, 1 *ECR*-like, 1 *PAS1*-like and 1 *PTPLA*-like genes. However, only 10 *KCS*s (*KCS1*, *KCS2*, *KCS5*, *KCS6*, *KCS9*, *KCS10*, *KCS13*, *KCS17*, *KCS18* and *KCS20*), *KCR1*, *PAS2*, *PAS1* and *PTPLA* were previously reported as being functional thanks to experiments in yeast and/or *in planta*. Eight of the 27 genes are not in the LR dataset, including *KCS7*, *KCS13*, *KCS14*, *KCS15*, *KCS18*, *KCS19*, *KSC21* and *KCR2*, not

because they are not in the Affymetrix ATH1 microarray chip used to generate the transcriptomic data but because they did not show differential expression during the time course (Voß et al., 2015).

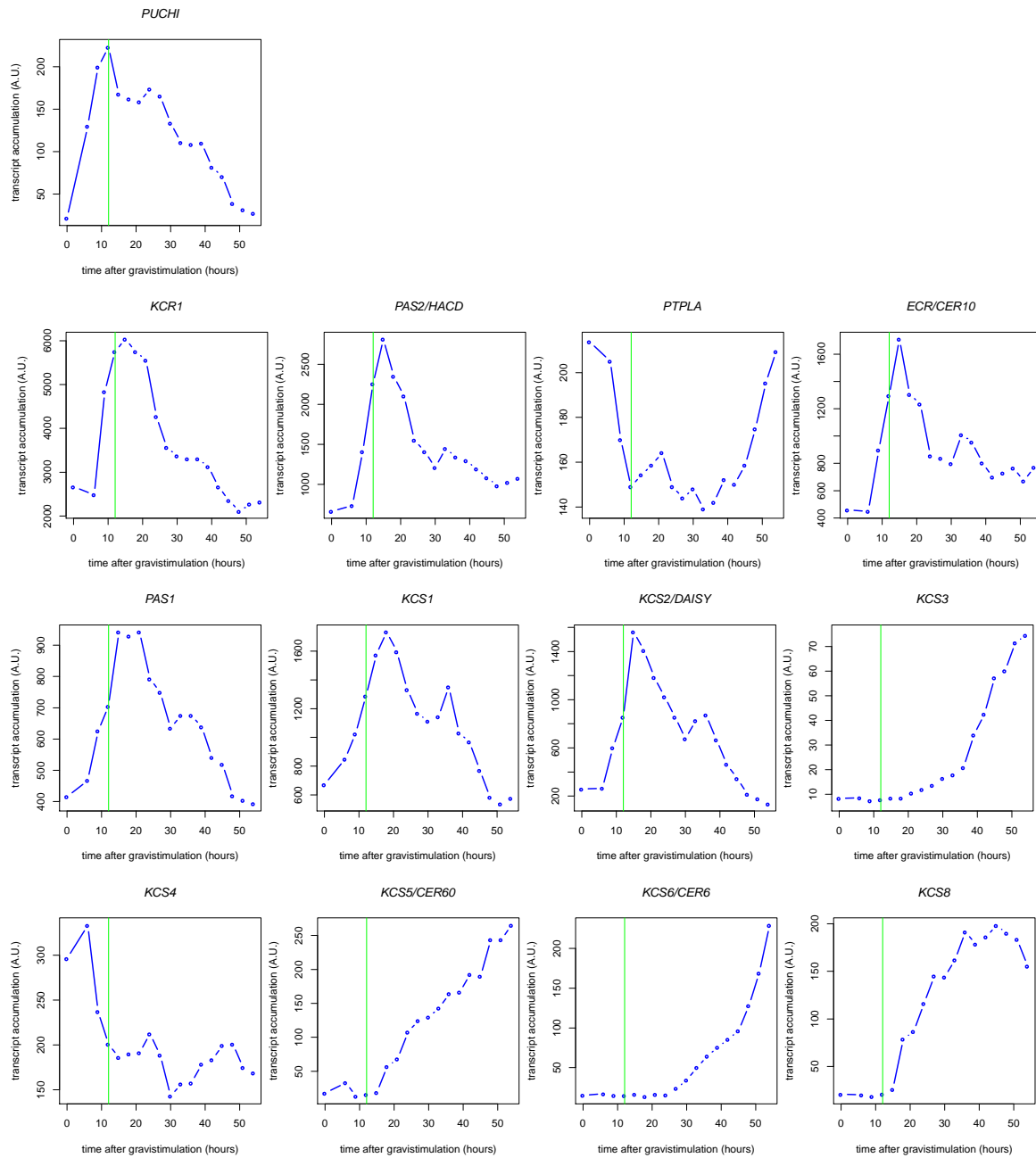


**Figure 3.5.** Expression profiles of *PUCHI* and all known genes encoding for enzymes in the fatty acid elongase complex retrieved from the transcriptomic dataset (Voß et al., 2015). Among 27 genes listed in the Appendix 2, 19 genes were retrieved, while the others did not show a differential expression in the LR dataset. Transcripts accumulation levels are expressed in arbitrary units (A.U.). The vertical green line indicates the time point when *PUCHI* expression reaches a maximum in the LR transcriptomic dataset.

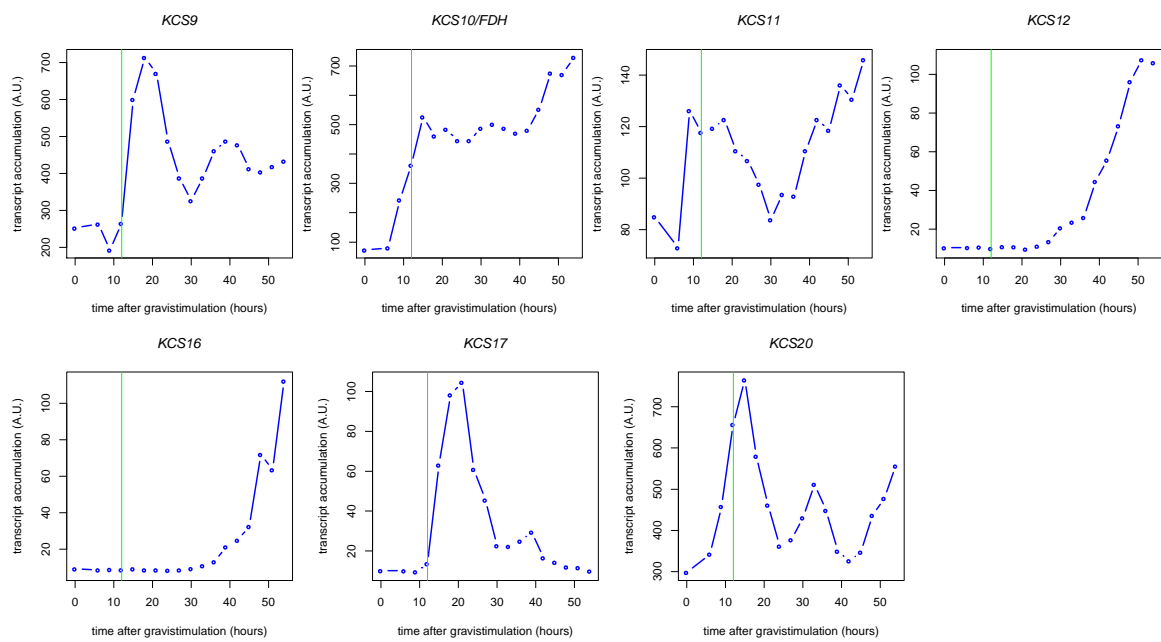


**Figure 3.5 (cont).** Expression profiles of *PUCHI* and all known genes encoding for enzymes in the fatty acid elongase complex retrieved from the transcriptomic dataset (Voß et al., 2015).

Next, the expression profiles of *PUCHI* and VLCFA biosynthesis genes in the LR dataset was compared. *PUCHI* transcript abundance rapidly rises after LR induction and peaks at around 12 hours after gravistimulation, which corresponds to the time when LR development initiates, *i.e.* when the first round of anticlinal cell division is observed (Figure 3.5 top, green line). *PUCHI* transcript levels then gradually decrease over time. Expression profiles of several VLCFA biosynthesis genes encoding key enzymes for each step of the VLCFA elongation cycle displayed similar dynamics as *PUCHI* expression. These included *KCS1*, *KCS2*, *KCS9*, *KCS17* and *KCS20* genes, all encoding members of the KCS enzyme family catalyzing the first step of VLCFA elongation, *KCR1*, *PAS2* and *ECR/CER10*, which encode enzymes catalyzing the second, third, and fourth steps of VLCFA elongation, respectively, as well as *PAS1* which encodes for the elongase complex chaperone (Figure 3.5). Other VLCFA biosynthesis genes, such as *KCS6*, also displayed dynamic changes in expression during the time course of lateral root formation, although not clearly correlated to that of *PUCHI* in the time frame of the experiment (Figure 3.5). Hence, transcriptomic data suggested that expression of a set of genes encoding for the entire VLCFA biosynthetic pathway was stimulated in a *PUCHI*-like manner during LR formation.

Figure 3.5 shows that 19 VLCFA biosynthesis genes display differential expression during the course of LRP formation. However, the root materials that were used to generate the dataset comprised not only developing LRPs but also surrounding tissues. To quickly test if VLCFA genes may be expressed specifically in developing LRPs, I search for their expression in the cell type-

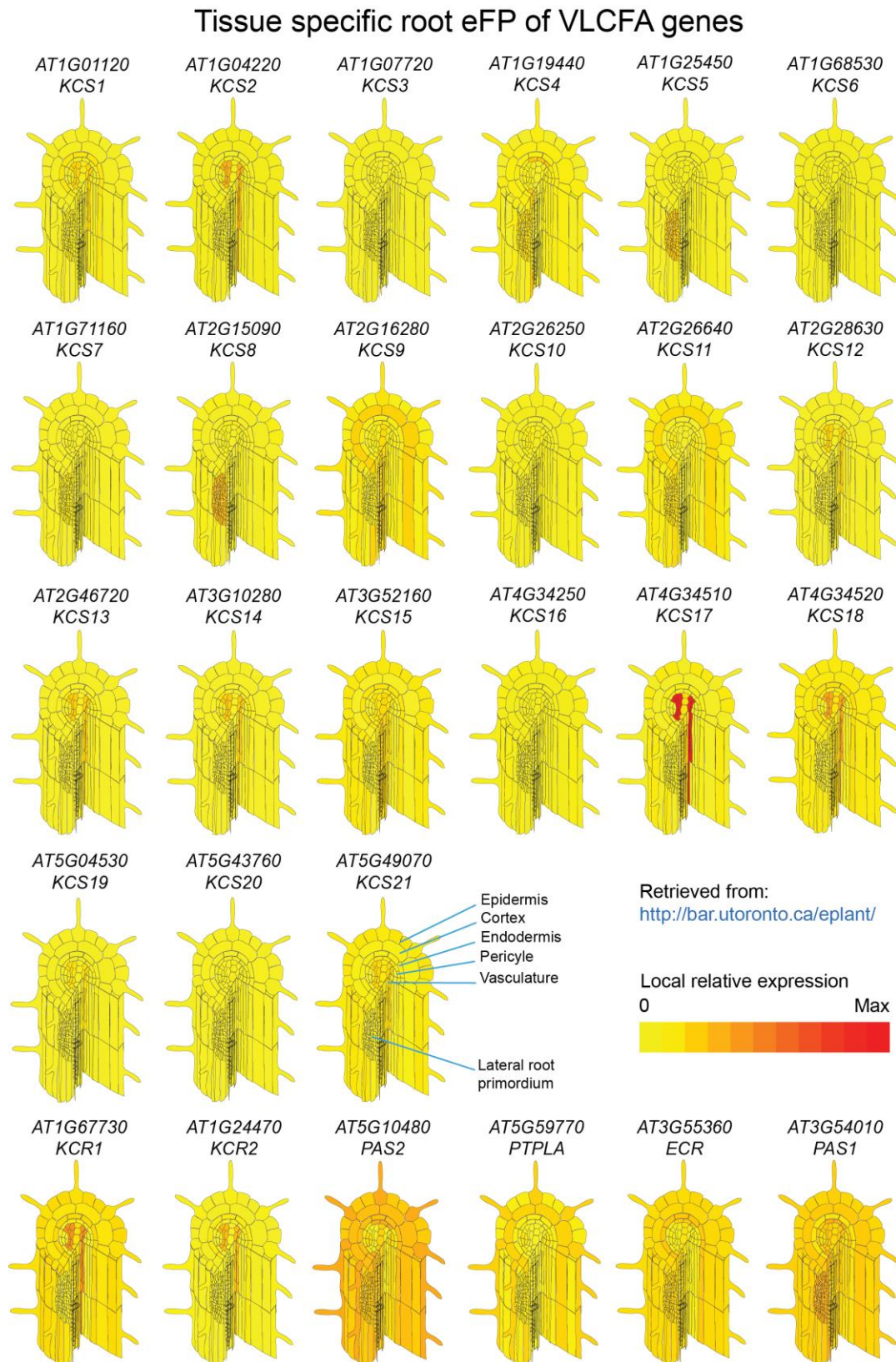


**Figure 3.6.** Expression of VLCFA biosynthesis genes in the developing LRP and surrounding tissues reported by (Brady et al., 2007) and visualized by the ePlant service (Winter et al., 2007; Waese et al., 2017). Relative expression levels are color coded and root tissues are shown.

specific microarray dataset generated by (Brady et al., 2007) and is visually displayed at the ePlant webservice (<http://bar.utoronto.ca/eplant/>; Winter et al., 2007; Waese et al., 2017). Data from the ePlant database generally showed that VLCFA genes are expressed in various root tissues, notably the stele and the endodermis. Many key genes showed high expression levels in the developing LRP such as *KCS1*, *KCS4*, *KCS5*, *KCS8*, *KCS11*, *KCR1*, *PAS2*, *ECR* and *PAS1*. Even though this dataset does not reflect temporal dynamics of gene expression, the detection of high expression of VLCFA biosynthesis genes in the developing LRP dataset suggests that some of them may be involved in LRP development and be regulated by PUCHI.

The fact that some VLCFA biosynthesis genes display a similar, but delayed, expression profile compared to that of *PUCHI* in the LR transcriptomic dataset, and that many of them are reported to be expressed in the LRP, suggest that PUCHI may positively regulate, directly or indirectly, the expression of those genes in the developing LRP. To explore further this hypothesis, we retrieved the promoter sequences (2 to 3kb upstream of the initiation codon) of 15 functional VLCFA genes in order to analyze whether PUCHI can possibly bind to these promoters. These sequences were then submitted to the binding site prediction tool of the PlantRegMap suite ([http://plantregmap.cbi.pku.edu.cn/binding\\_site\\_prediction.php](http://plantregmap.cbi.pku.edu.cn/binding_site_prediction.php)) (Jin et al., 2017) to find all transcription factors that can bind to these sequences. PUCHI was predicted to bind to 30 sites on 9 promoters out of 15 tested (Appendix 3).

In summary, bioinformatics analyses showed that many VLCFA biosynthesis genes are differently expressed and have similar profiles to that of PUCHI during LRP development and suggest that some of them may be expressed in LRPs and be regulated by PUCHI.

## **2.2. PUCHI regulates the spatio-temporal expression patterns of VLCFA biosynthesis genes during LRP formation**

Next, available reporter lines of VLCFA biosynthesis genes were collected from different sources for expression pattern study *in planta*. Transcriptional reporter lines (*promoter::GUS*) have been previously generated and described for *KCS1*, *KCS3*, *KCS5*, *KCS6*, *KCS8*, *KCS10*, *KCS12* and *ECR* (Joubès et al., 2008), for *KCR1* (Beaudoin et al., 2009), *KCS2* and *KCS20* (Lee et al., 2009b), for *PAS1* (Roudier et al., 2010), and for *PAS2* and *PTPLA* (Morineau et al., 2016). Because *KCS* gene family is large and some of them are functionally redundant, we collected *pKCS1::GUS*, *pKCS6::GUS* and *pKCS20::GUS* as representative members. The roles of these *KCS* in VLCFA biosynthesis and related processes have been described *in planta* (Appendix 2), and *KCS1* and *KCS20* have expression profiles similar to that of *PUCHI* while *KCS6* show a strong induction during LRP formation (Figure 3.5). For other key, non-redundant VLCFA biosynthesis genes, we collected reporter lines for *pKCR1::GUS*, *pPAS2::GUS*, *pECR::GUS* and *pPAS1::GUS*.

Expression pattern of VLCFA biosynthesis genes during LRP formation has been little studied, except for *PASI* (Roudier et al., 2010) and *KCSI* (Shang et al., 2016). These reporters were introduced into the *puchi-1* mutant background to see the effects of *PUCHI* loss-of-function on their expression patterns. GUS assays were performed for the collected reporter lines and their expression patterns were observed in developing LRPs and emerging LRs.

First, we confirmed that all these promoters drive a strong GUS expression in the differentiation zone of WT primary roots, consistent with their expression in the LR dataset and in the eFP browser. The general features of VLCFA biosynthesis gene promoter activity in the WT were that (i) they predominantly drive reporter gene expression in the root endodermis in the maturation zone, and the onset of this expression in this zone was highly associated with LRP initiation, and (ii) they drive GUS expression in developing LRPs and emerged LRs at different degrees. In addition, some of these constructs showed activity in the primary and lateral root tip.

*KCRI* is the only known gene for the second step (reduction) in the VLCFA synthesis pathway (Bach and Faure, 2010) and was previously shown to be involved in LR formation (Beaudoin et al., 2009). A detailed analysis of the lateral root formation zone, *i.e.* the region from the youngest initiated LRP to the newly emerged LR (Dubrovsky and Forde, 2012), of 9-day old *pKCR1::GUS* seedlings showed that *pKCR1::GUS* was expressed in the endodermis and in developing LRPs (Figure 3.7B). The earliest GUS staining appeared in a patchy manner near the differentiation zone and was specifically associated with newly initiated LRP (Stage I). In older parts, the staining was found also in epidermal cells and in LRPs. No clear difference in ground tissue staining could be detected between *puchi-1* and WT genotypes in this root area. In order to address the putative impact of *puchi-1* mutation on *pKCR1::GUS* expression in developing LRPs, GUS staining was scored in LRPs located above (shootwards) the youngest primordium that has crossed the endodermis and below (rootwards) the youngest emerged lateral root. This way of counting was necessary because the strong GUS signal in the endodermis obscured with the possible GUS staining in young LRPs that are still under the endodermis. This counting technique for developing LRPs was applied for all other GUS analyses. The effects of *PUCHI* loss of function on GUS pattern in newly emerged LRs were also recorded. For that, expression pattern of *PUCHI* during LRP development is provided for reference (Figure 3.7A and Figure 3.8A). In the WT background, the *pKCR1::GUS* transgene was strongly expressed in almost all of these developing LRPs (96%; n = 40 seedlings, Figure 3.7B), especially at the centre and at the tip, whereas only a small proportion of them lacked the GUS staining (4%; n = 40 seedlings). In *puchi-1* seedlings, however, a significantly higher number of these LRP showed no or little GUS expression (96%, n = 40 seedlings; Figure 3.7B). Curiously, these LRPs usually showed GUS

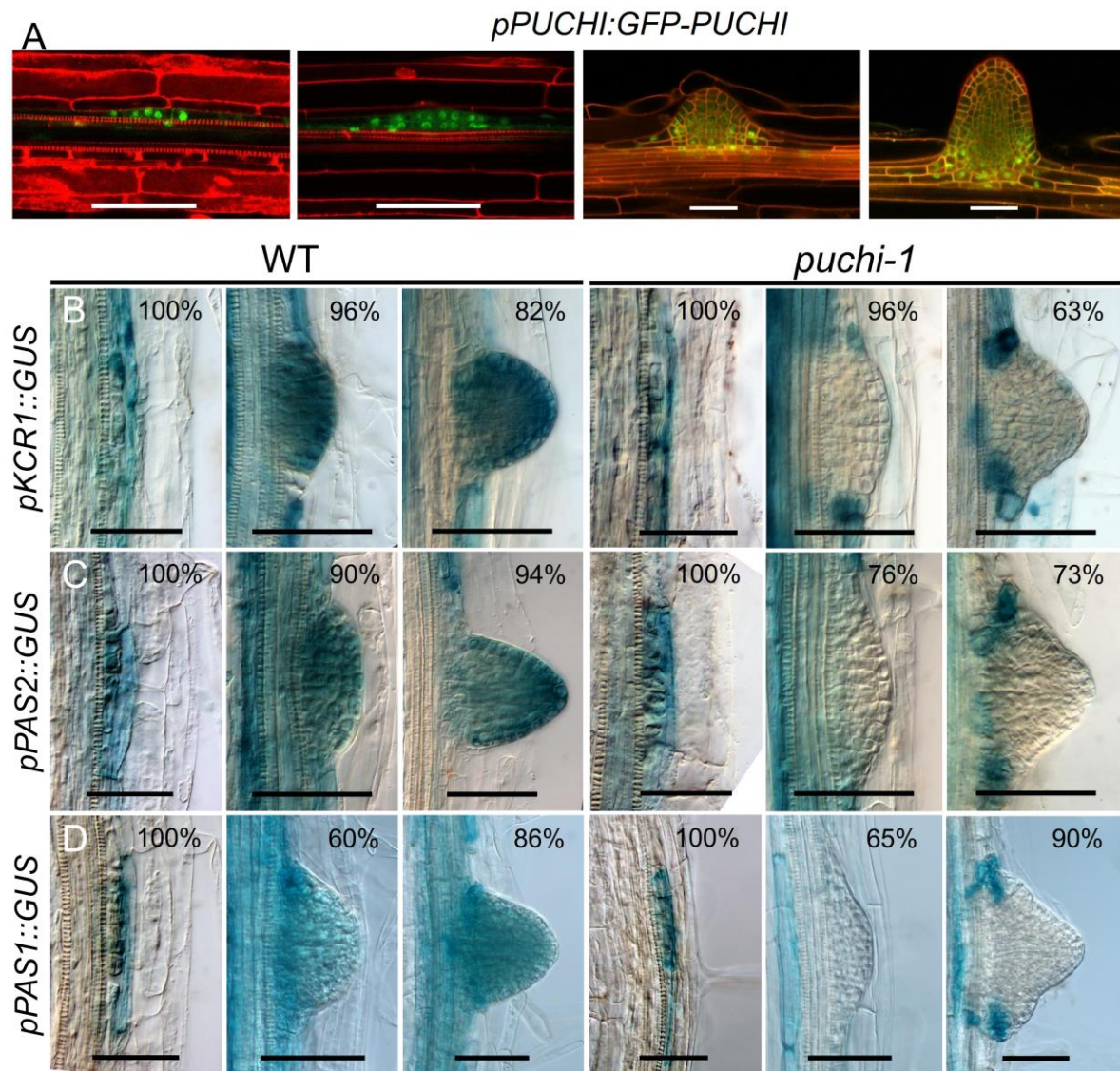


**Figure 3.7.** VLCFA biosynthesis genes are expressed in developing LRPs and their expression patterns are dependent on PUCHI, as reported by *promoter::GUS* transcriptional constructs. (A) Expression pattern of *pPUCHI::GFP-PUCHI* that restores wild-type root development in a *puchi-1* background is gradually confined to the base and flanks of LRP (described in detail in Chapter II). (B) to (D) Expression patterns of three GUS reporter constructs of VLCFA biosynthesis genes in typical WT (left) and *puchi-1* (right) LRP and newly emerged LR. A clear loss of GUS staining is observed for *pKCR1::GUS*, *pPAS2::GUS*, and *pPAS1::GUS* in developing *puchi-1* LRP. Scale bars = 50 $\mu$ m. Numbers indicate the percentage of LRP or LR displaying the corresponding expression pattern. n = 30-40 seedlings for each GUS assay.

signal in some flank cells. Additionally, *pKCR1::GUS* was strongly and symmetrically (based on our longitudinal-view imaging technique) expressed in the tip of newly-emerged lateral roots in WT (82%, n = 40 seedlings). Conversely, in a majority of *puchi-1* lateral roots, the reporter

construct was mostly expressed in some basal and distant flank cells but not in the tip (63%, n = 40 seedlings; Figure 3.7B).

*PAS2* is the only known gene for the third step (dehydration) in the VLCFA synthesis pathway (Bach and Faure, 2010) and was previously reported to be expressed in emerged lateral roots in *Arabidopsis* seedlings (Morineau et al., 2016). In general, *pPAS2::GUS* transgene displayed a similar expression pattern to *pKCR1::GUS*, *i.e.* it was expressed in a majority of examined LRPs and LR, and, while it was strongly expressed in the parental root endodermis in some mature parts of the parental root branching zone, its expression was predominantly associated to newly initiated LRP in the young LRP-developing zone of the parental root (Figure 3.7C). In *puchi-1* background, however, most of the mutant LPRs and LR did not have a strong GUS staining. Similar to *pKCR1::GUS*, in emerged *puchi-1* LR *pPAS2::GUS* expression was found only the basal and distant flank cells.

The role of the *PAS1* protein is to link VLCFA biosynthesis enzymes together to form the elongase complex, and the expression of *pPAS1::GUS* in LRPs has been briefly described (Roudier et al., 2010). Here we confirmed that *pPAS1::GUS* was expressed in developing LRPs (60%, n = 40 seedlings) and LR (86%, n = 40 seedlings) in a similar manner compared to *pKCR1::GUS* and *pPAS2::GUS*. The similarity was further observed regarding the loss of expression of *pPAS1::GUS* in the *puchi-1* background (Figure 7D).

The picture provided by *KCS* reporter lines is more complex. *KCS1* is a member of *KCS* enzyme family which is responsible for the VLCFA chain length and *KCS1* expression in developing LRPs has been reported recently (Shang et al., 2016). However, we observed that *pKCS1::GUS* obtained from (Joubès et al., 2008) did not show a tissue-specific expression pattern as other VLCFA reporters, and we detected GUS signal only in ~ 11% and ~ 14% of analyzed LRPs and LR, respectively (Figure S3.1). This *pKCS1::GUS* construct therefore might not be a good reporter line for *KCS1* expression. We then collected the translational reporter *pKCS1:KCS1-GFP* from (Shang et al., 2016) for expression pattern analyses in the WT and *puchi-1* background. This translational construct rescues the phenotype of the *KCS1* loss-of-function mutant *kcs1-5* thus indicating that the corresponding promoter contains necessary elements for its function. Using this line, we confirmed the expression of *KCS1* in 100% counted LRPs and newly emerged LR (20 seedlings). *KCS1* expression could be detected from stage II LRPs onwards, and only in the outermost layers. In *puchi-1* background, most of LRPs and LR did not show a strong GFP signal and the signal, if any, was confined to some distant flank cells (Figure 3.8B). Expression pattern of *PUCHI* during LRP development is provided again for reference (Figure 3.8A).

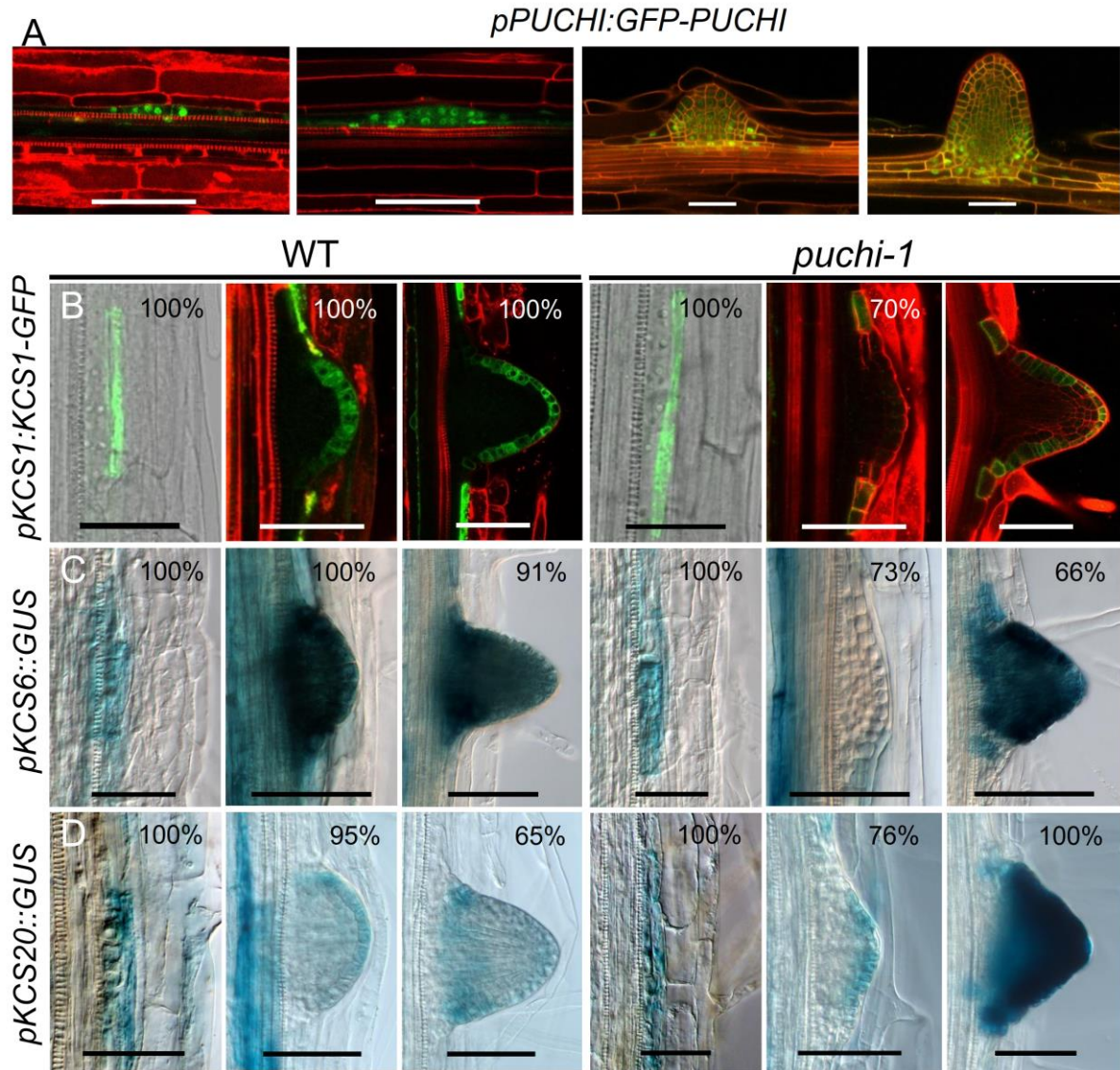


**Figure 3.8.** *KCS* genes are expressed in developing LRPs and their expression patterns are dependent on PUCHI. (A) Expression pattern of *pPUCHI:GFP-PUCHI* in *puchi-1* background is gradually confined to the base and flanks of LRP. (B) to (D) Expression patterns of three reporter constructs of VLCFA biosynthesis genes in typical WT (left) and *puchi-1* (right) LRP and newly emerged LR. A clear loss of reporter signal is observed for *pKCS1:KCS1-GFP* and *pKCS6::GUS* in developing *puchi-1* LRP. Scale bars = 50 μm. Numbers indicate the percentage of LRP or LR displaying the corresponding expression pattern. n = 20 seedlings for *pKCS1:KCS1-GFP* in WT and in *puchi-1*; n = 30-40 seedlings for each GUS assay.

*KCS6* (or *CER6*) was shown to be weakly expressed in roots compared to other *KCS* genes (Joubès et al., 2008). Our analysis of the LR transcriptomic dataset showed that *KCS6* expression kept raising during the experiment time course up to the last time point at 54 hpg. Consistent with that, expression of a *pKCS6::GUS* reporter construct was detected in the endodermis of the LRP formation zone of WT primary roots. The earliest GUS staining near the differentiation zone

behaved similarly to *pKCR1::GUS* (Figure 8C). All developing LRP in 9-day old WT seedlings displayed GUS staining (n = 40 seedlings). However, in *puchi-1* background around 73% of the corresponding LRP did not show GUS staining (n = 40 seedlings, Figure 8C). Strikingly, the expression pattern of *pKCS6::GUS* in newly emerged lateral roots was also altered, but in a contrasted manner compared to these constructs described above. While *pKCS6::GUS* was mostly expressed symmetrically, stronger at the base/flanks, and gradually reduced toward the root tips in WT lateral roots (91%, n = 40 seedlings), it was mostly expressed in the meristematic region, but not the base, in *puchi-1* lateral roots (66%, n = 40 seedlings; Figure 8C).

We observed *pKCS20::GUS* expression in the root endodermis and this was consistent with previously reported expression of *KCS20* in that tissue (Lee et al., 2009b). In addition, in the WT we also detected the expression of *pKCS20::GUS* in outer cell layers of the developing LRPs (95%, n = 40 seedlings) and in the tip and flanks of the newly emerged LRs (65%, n = 40 seedlings). In the *puchi-1* background, a lesser percentage of developing LRPs (76%, n = 40 seedlings) showed a similar expression pattern to those in the WT. However, all newly emerged LRs of the mutant displayed an intense GUS signal in the outer cell layers instead (Figure 3.8D).

ECR (CER10) is the only known reductase of the elongation cycle, and *ECR* expression in the primary and lateral root tips has been reported thanks to the *pECR::GUS* reporter construct (Joubès et al., 2008). We observed a strong GUS signal in the basal meristem and the stele of the primary root for a majority (25/35 = ~72%) of seedlings, while the others (~28%) displayed a much weaker signal in the root cap and root hairs instead (Figure S3.1). *pECR::GUS* expression could also be observed in the tip of elongated lateral roots, but not in newly emerged ones. The signal was not detected in developing LRPs in both WT and *puchi-1* background, although GUS staining could sometimes be seen in endodermal cells overlying newly initiated LRPs like other VLCFA reporter lines. However, because this reporter line did not show a consistent expression pattern within a seedling population, we think that it did not faithfully reflect the expression pattern of *ECR in planta*, similar to the case of *pKCS1::GUS*. In the eFP browser, *ECR* is expressed in developing LRPs, and stronger in the endodermis (Figure 3.6).

As mentioned above, in the WT, VLCFA biosynthesis genes were expressed in the endodermis, starting from the position where initiation of LRP development took place. The expression was patchy at this zone and then became continuous. The GUS signal of VLCFA biosynthesis genes therefore overlaid young LRPs who have not yet crossed the endodermis. In *puchi-1* background, however, we noticed that the GUS staining from some VLCFA reporter lines might not form a continuous file in the endodermis. The lack of GUS staining, interestingly,

happened to be at the cells directly overlaying a developing LRP. This phenomenon could be seen in the case of *pKCR1::GUS* (Figure S3.2).

In summary, our analyses on the expression pattern of VLCFA reporter lines in the WT and *puchi-1* mutant background demonstrate that PUCHI is required for the correct spatiotemporal expression of genes encoding enzymes involved in VLCFA biosynthesis in developing LRPs.

### 2.3. VLCFA mutants and *puchi-1* display similar defects in lateral root development

I showed in Chapter II that *puchi-1* seedlings have several defects in LRP development, including increased LRP initiation (density), which leads to shorter LRP spacing distances, and delayed LRP development. I performed similar phenotyping of VLCFA mutant seedlings to see if they may display similar LR defects as *puchi-1*.

We focused on mutants in *KCS* genes expressed downstream of PUCHI during lateral root development (*kcs1-5*, *kcs9*, *kcs2 kcs20*), and *ECR/CER10* genes because (i) mutants in *KCR1*, *PAS1* and *PAS2* display severe and pleiotropic developmental phenotypes (Bach et al., 2008; Beaudoin et al., 2009), (ii) loss-of-function phenotype for those *KCS* and *ECR* genes have been described (Shang et al., 2016; Kim et al., 2013; Lee et al., 2009b; Roudier et al., 2010; Zheng, 2005), and (iii) functional redundancy and substrate specificity of *KCS* enzymes have been studied (Kosma et al., 2014; Kim et al., 2013).

We did not observe any significant differences in LRP formation and development between *kcs9* single mutants nor *kcs2 kcs20* double mutant and WT seedlings (not shown). However, *kcs1-5* mutant, a null allele for the *KCS1* gene (Shang et al., 2016), displayed a *puchi-1* like root phenotype including an increase in LRP production, a higher number of delayed LRPs along the primary root (Figure 3.9B), a significant decrease in the distance between LRPs (Figure 3.9C) and increase in LRP clusters, and a delay in LRP development as revealed by gravistimulation assay (Figure 3.9E). Mutants in *ECR* (*cer10-2*) produced similar but weaker phenotype with more lateral organs and an increased number of delayed LRPs as compared to WT (Figure S3.3). Hence, loss-of-function of selected VLCFA biosynthesis genes resulted in similar defects in LRP development as in *puchi-1*. In both cases, the defects were weaker than those observed in *puchi-1*, possibly due to the fact that PUCHI may simultaneously regulate the expression of multiple VLCFA genes and possibly other pathways, and that VLCFA enzymes may act redundantly.

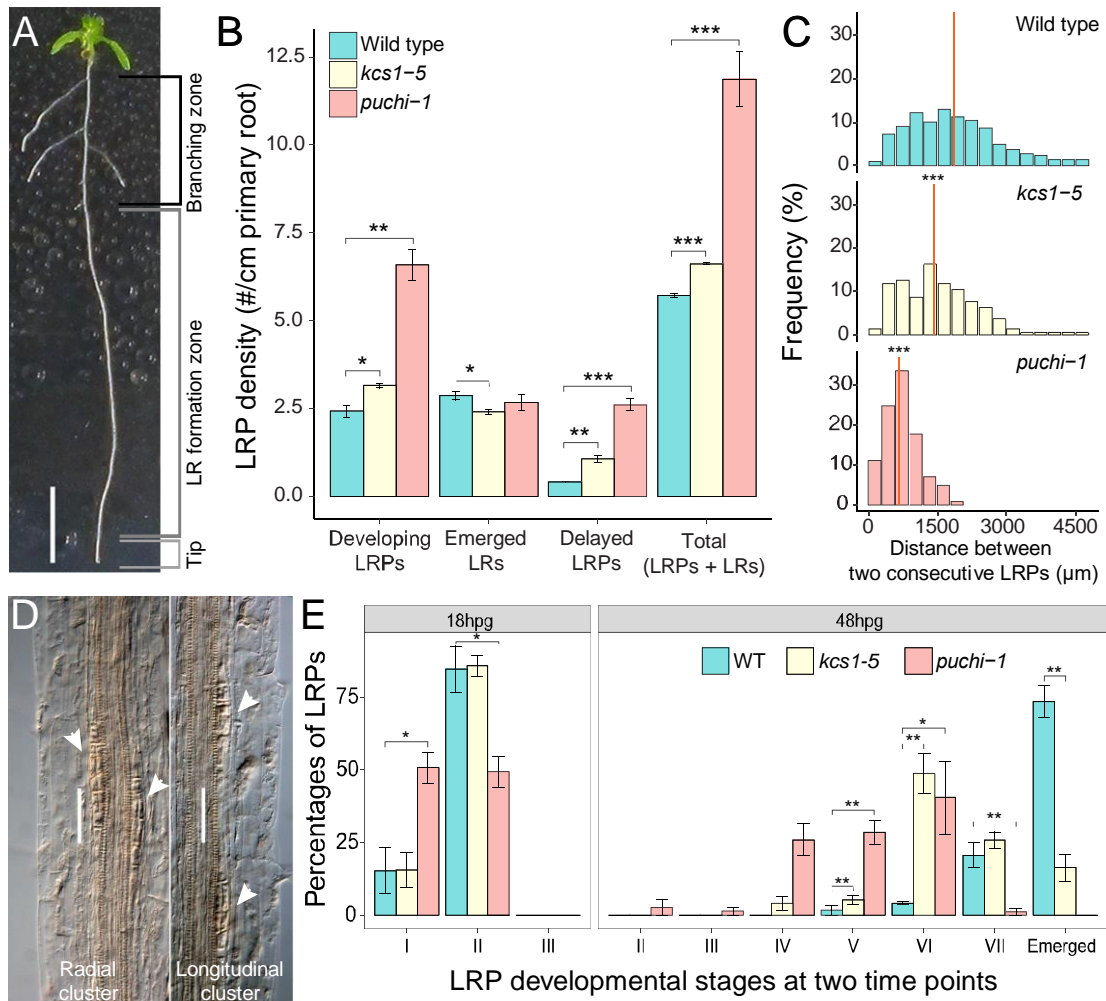


**Figure 3.9.** *puchi-1* and *kcs1-5* mutant produce more LRPs and are delayed in LRP development. (A) Three zones of Arabidopsis primary root regarding lateral root formation and development as suggested in (Dubrovsky and Forde, 2012). (B) Density of developing LRPs, emerged LRPs, delayed LRPs, and total LRPs (LRPs + LRs) in 9-day old WT, *puchi-1* and *kcs1-5* seedlings. Developing LRPs are LRPs scored in the LR formation zone. Delayed LRPs are defined as those located in the branching zone of the primary root but have not crossed the epidermis. (C) Frequency distribution of distances between two consecutive LRPs in WT, *kcs1-5* and *puchi-1* roots. Each bin of the histogram represents a range of 300  $\mu\text{m}$ . Number of LRPs = 222, 208 and 228 for WT, *kcs1-5* and *puchi-1*, respectively. The orange bar in each histogram indicates the mean LRP distance in each genotype. The stars in the histograms for *kcs1-5* and *puchi-1* indicate the significant difference between these mean distances compared to that of WT. (D) Examples of longitudinal and radial clusters of LRPs in *puchi-1* roots. Arrowheads indicate LRPs. Scale bars = 50  $\mu\text{m}$ . (E) Distribution of developmental stages as described by Malamy and Benfey (1997) achieved by gravistimulation-induced LRP formation in WT, *kcs1-5* and *puchi-1* roots at 18 and 48 hours after the gravistimulation. Data are represented as Mean  $\pm$  SEM of three biological replicates, with number of seedlings  $\geq$  20 in each repeat. Significance was determined by Student's t test. \*  $p < 0.05$ , \*\*  $p < 0.01$ , \*\*\*  $p < 0.001$ .

## 2.4. PUCHI and VLCFAs control pericycle cell proliferation on callus inducing medium

VLCFAs were recently showed to control the ability of pericycle cells to form calli in *Arabidopsis* roots grown on an auxin and cytokinin-rich callus inducing medium (CIM; Shang et al., 2016). When grown on CIM, WT roots formed calli at regular intervals, but roots of VLCFA mutants exhibited a continuous callus layer (Shang et al., 2016). This indicates that VLCFAs control pericycle cell division during callus formation, a process that shares similar features with early steps of LRP formation (Perianez-Rodriguez et al., 2014; Trinh et al., 2018). This finding prompted us to investigate the callus formation phenotype of *puchi-1* on CIM.

First, *PUCHI* expression in calli during CIM-induced callus formation was tested. Seven-day old *pPUCHI:GFP-PUCHI* seedlings were incubated on CIM for 4 days. *pPUCHI:PUCHI-GFP* was expressed in all cells of developing calli (Figure 3.10A), consistently with *PUCHI* expression being induced by auxin (Hirota et al., 2007). We next tested the phenotype of the *puchi-1* mutant in response to CIM, with *kcs1-5* being a positive control. Before being transferred to CIM, WT, *kcs1-5* and *puchi-1* roots displayed comparable anatomy (Figure 3.10B, upper panels). After 4 days of growth on CIM, all roots responded to the hormonal treatment with pericycle cell proliferation (Figure 3.10B, lower panels). However, whereas WT roots produced numerous distinct dome-shaped calli, the *puchi-1* mutant generated a continuous layer of dividing cells along its entire primary root. This phenotype was even much stronger than the fused-calli phenotype displayed by the VLCFA biosynthesis deficient mutant *kcs1-5* (Figure 3.10B; Shang et al., 2016). In our condition, the fused-calli phenotype of the *kcs1-5* mutant could be observed, but only in more mature root parts, not along the entire primary root as in *puchi-1* roots. Callus formation in the young parts of *kcs1-5* roots was similar to that of WT. To concretely compare the callus formation capacity of WT, *kcs1-5* and *puchi-1*, we measured the callus area in 1-cm-long root segment from the collar rootward, and found that callus area was significantly higher in *puchi-1* and *kcs1-5* than in WT (Figure 3.10C). Our data suggest that *PUCHI* and VLCFA are negative regulators of pericycle cell proliferation during hormone-stimulated callus formation.

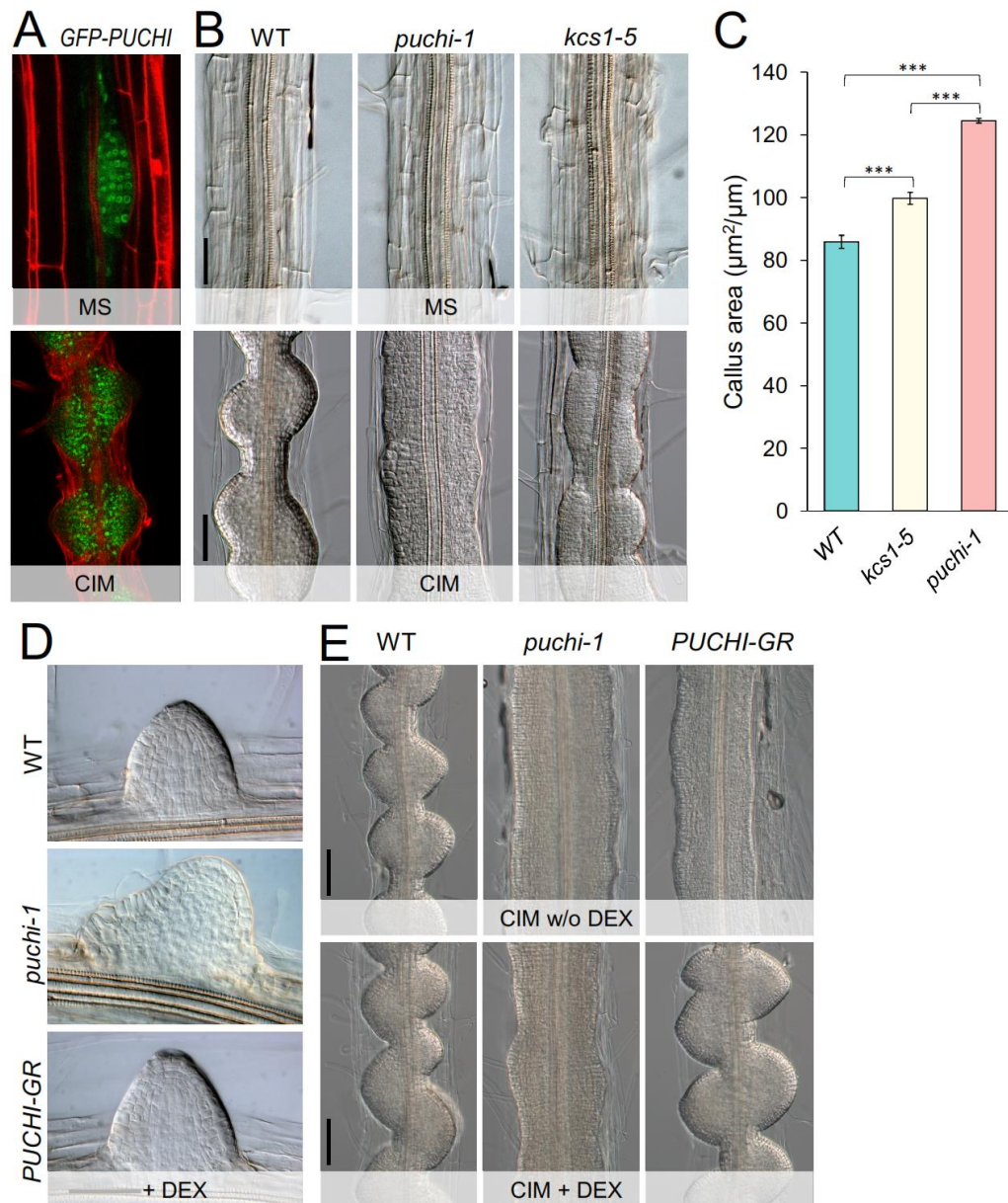


**Figure 3.10.** Callus formation was enhanced in *puchi-1* and *kcs1-5* roots. (A) *pPUCHI:GFP-PUCHI* (*GFP-PUCHI* for short) was expressed in callus induced by callus inducing medium (CIM). (B) While WT, *kcs1-5* and *puchi-1* roots of 7-day-old seedlings displayed similar radial organization when grown on half-strength MS medium (top), 4 more days of growth on CIM induced the formation of dome-shaped individual calli in WT, but of a continuous layer of proliferating cells in the *puchi-1* and *kcs1-5* background (bottom) Scale bars = 100  $\mu\text{m}$ . (C) Callus area quantification of 7-day-old WT, *kcs1-5* and *puchi-1* roots on CIM for 4 days.  $n = 20$  for each genotype. Significance was determined by Student's t-test. \*\*\*  $p < 0.001$ . (D) *pPUCHI:PUCHI-GR/puchi-1* (*PUCHI-GR* for short) plus dexamethasone (DEX) rescued the morphology defect of *puchi-1* LR. Scale bar = 50  $\mu\text{m}$ . (E) *PUCHI-GR* plus dexamethasone (DEX) rescued the callus formation defect in *puchi-1* background. Scale bars = 100  $\mu\text{m}$ .

To confirm that the callus formation phenotype of *puchi-1* roots on CIM was indeed caused by loss-of-function of *PUCHI*, we employed a functional *PUCHI* transgene fused to the glucocorticoid steroid hormone binding domain (GR) in the *puchi-1* background (*pPUCHI:PUCHI-GR/puchi-1*; material obtained from Dr. Tatsuaki Goh, Japan). Treatment of *pPUCHI:PUCHI-GR* seedlings by dexamethasone (DEX) allows the recombinant transcription factor to be targeted to the nucleus (Schena et al., 1991; Aoyama and Chua, 1997). DEX treatment rescued the morphological phenotype of *pPUCHI:PUCHI-GR/puchi-1* LRP roots on normal medium (Figure 3.10D). DEX treatment did not interfere with callus formation of WT and *puchi-1* roots. On CIM, without DEX, *pPUCHI:PUCHI-GR/puchi-1* roots formed a continuous callus (Figure 3.10E; upper panels). However, application of DEX led to the formation of distinct dome-shaped calli along the primary root that phenocopied those formed on WT roots (Figure 3.10E; lower panels). This confirmed that *PUCHI* loss-of-function was the cause of the callus proliferation phenotype observed in the *puchi-1* mutant.

## 2.5. PUCHI is required for root but not shoot regeneration from callus

Since *PUCHI* is involved in regulating callus formation from the root, I started to investigate further its role in organ regeneration (shoot and root) from callus. For this, 7-day old WT, *puchi-1* and *kcs1-5* seedlings growing on MS/2 were transferred to CIM for 4 days, then their roots were excised and transferred to shoot- and root-inducing medium (SIM and RIM). The density of roots and the number of shoots emerged from these calli-bearing root segments were tracked over time.

In WT, adventitious roots appeared first at the ends of a calli-bearing root segment, then these adventitious roots were produced along the whole segment (Figure 3.11). In *puchi-1*, however, in the time frame of the assay, very few adventitious roots were regenerated from *puchi-1* calli. In contrast, *kcs1-5* calli-bearing root segments produced as many adventitious roots as did the WT ones, although it was noticed that the older parts (with fused calli) of *kcs1-5* roots produced fewer adventitious roots. Regarding adventitious shoots, in our preliminary study WT and *puchi-1* roots were able to regenerate shoots after > 10 days on SIM (Figure 3.11).

Overall, our preliminary regeneration assays suggest that the uncontrolled callus formation in *puchi-1* led to a weaker capacity to regenerate adventitious roots, but not shoots, from the calli.

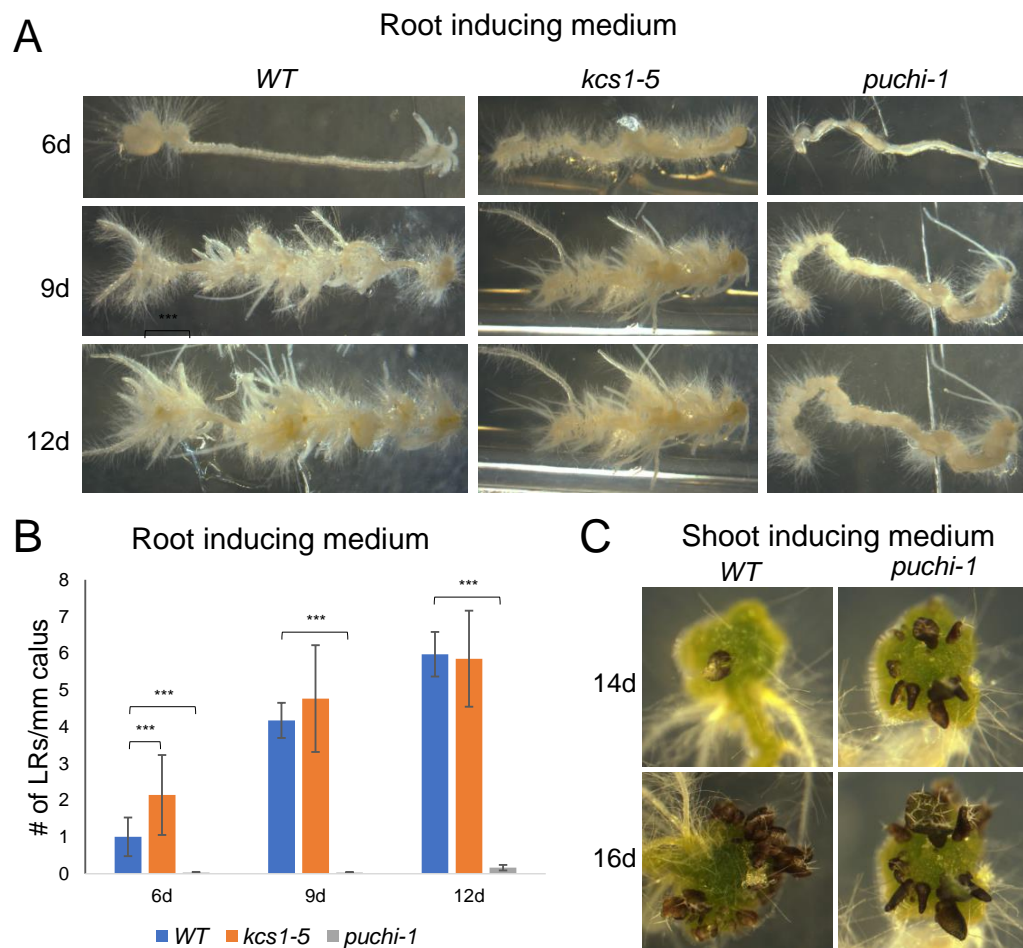


**Figure 3.11.** *puchi-1* roots have weaker root, but not shoot, regeneration capacity. (A) Adventitious roots appeared from callus root segments after being incubated on the root induction medium. (B) Quantification of the adventitious root regeneration capacity. Three biological replicates,  $n = 20, 10, 20$  for WT, *kcs1-5* and *puchi-1* each repeat, respectively. Data are represented as Mean  $\pm$  SEM. Significance was determined by Student's t test; \*\*\*  $p < 0.001$ ) (C) WT and *puchi-1* callus root segments produced adventitious roots after being incubated on the shoot induction medium.

## 2.6. PUCHI regulates expression of *KCSI* during callus formation

*puchi-1* and *kcs1-5* mutants showed similar enhanced callus formation on CIM. I therefore tested if PUCHI also regulates VLCFA biosynthesis genes in that context. WT and *puchi-1* seedlings bearing the *pKCSI:KCSI-GFP* construct were grown on CIM for 4 days, and *KCSI-GFP* expression was visualized. Basically, we observed *KCSI* expression in the outermost layer of the calli, similar to its expression in developing LRPs. Importantly, *KCSI* expression in calli was lost in *puchi-1* roots (Figure 3.11). The data demonstrates that *PUCHI* also regulates the expression pattern of *KCSI* in the callus formation context.

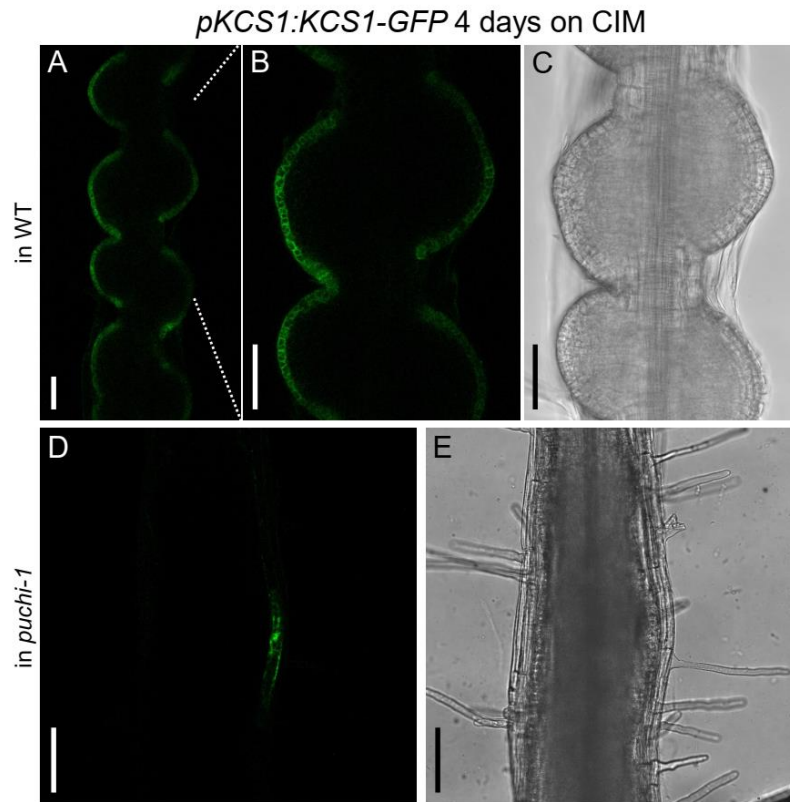


**Figure 3.12.** *KCS1* is expressed in calli and its expression pattern is dependent on PUCHI. (A) to (C) *pKCS1:KCS1-GFP* is expressed in the outer layer of the calli. A part of (A) is magnified in (B) and (C) shows the bright field image of (B). (D) to (E) The expression of *pKCS1:KCS1-GFP* is not observed in *puchi-1* callus. (E) Bright field image of (D). This root segment was chosen for presentation because it shows GFP signal in the endodermis layer while other observed root segments did not show any GFP signal. Scale bars = 50µm. n = 5 seedlings for WT and *puchi-1*.

## 2.7. Mutation in PUCHI alters VLCFA composition in root calli

Because PUCHI regulates VLCFA synthesis genes, one would expect to see a reduction in VLCFA content or an alteration in VLCFA composition in *puchi-1* roots.

In the first attempt, root materials were prepared and sent to the Cell differentiation and polarity laboratory (Lab of Prof. Jean Denis Faure, INRA Versailles) to quantify VLCFA classes in WT and the *puchi-1* mutant. The lyophilized materials were from LR-formation zone of roots of WT and *puchi-1* 9 days-old seedlings grown on normal MS medium. Fatty acids in root samples were methylated to produce fatty acid methyl esters (FAMES) and FAMES were quantified by GC-MS as described in (Morineau et al., 2016). No differences in VLCFA composition of *puchi-1* and WT roots were detected (Figure S3.4).

We hypothesized that the small proportion of *PUCHI* expressing tissues in the root materials and the low content of VLCFAs in the total fatty acids might hamper detection of small differences. Thus, we sent the same materials (roots on normal MS/2 medium) to the Laboratoire de Biogenèse Membranaire (Lab of Dr. Yohann Boutté, Bordeaux) for a deeper and more sensitive analysis of the FA pools. This team routinely performs high precision lipidomics profiling from plant tissues, including the separation of distinct classes of fatty acids such as phosphoglycerolipids and  $\alpha$ -hydroxylated FAs (components of cell membrane), and  $\alpha,\omega$ -dicarboxylic acids,  $\omega$ -hydroxylated FAs and fatty alcohols (components of suberin; Wattelet-Boyer et al., 2016). The analysis produced the FA profiles in distinct VLCFA classes including those are components of cell membrane and suberin. Again, we did not see any differences in fatty acid composition between the two root materials (Figure S3.5).

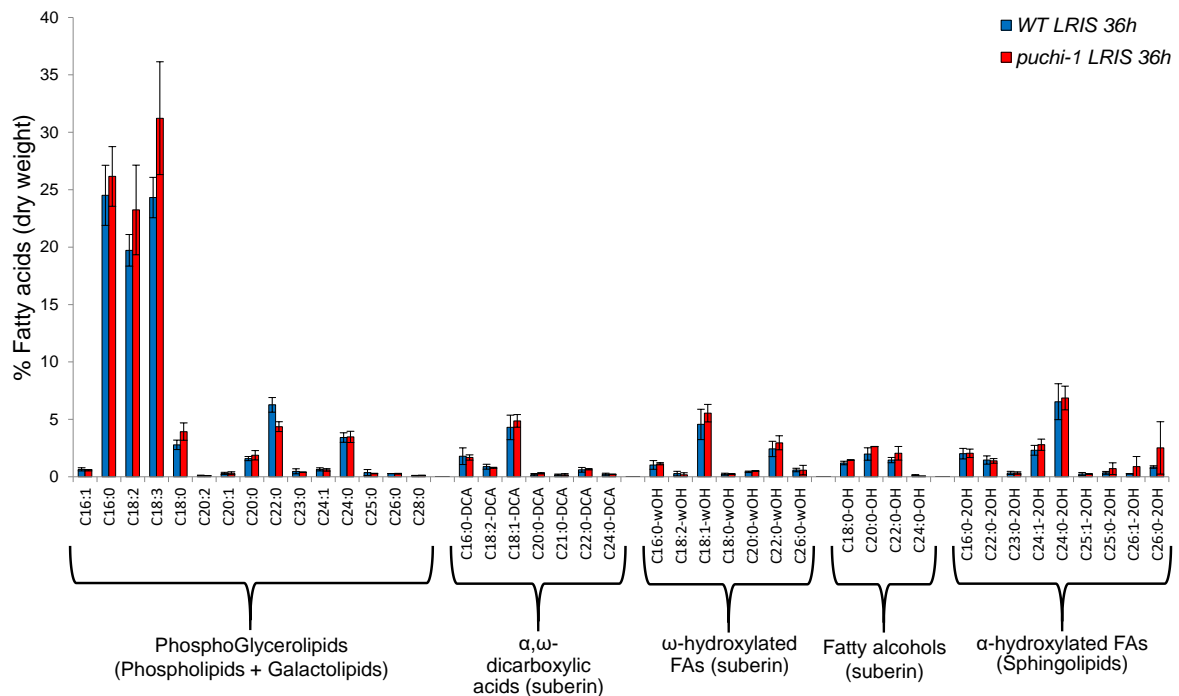


**Figure 3.13.** An analysis of VLCFA classes (in % dry weight = nmol of FA/dry weight of analysed material) of root materials of 7 days-old WT and *puchi-1* seedlings additionally grown on lateral root induction medium (LRIS) for 36 hours. Quantity of VLCFAs in different lipid classes are given.

We reasoned that it might be difficult to reveal any modifications in VLCFA content and composition between WT and *puchi-1* roots because *PUCHI* is expressed in the LRP and LRP constitute only a small fraction of the whole root. To address this issue, we produced new root materials using the lateral root induction system (LRIS) developed by Himanen (Himanen et al., 2004) which was used to confirm *PUCHI* targets by qPCR (See the Introduction of this chapter). In this experiment, WT and *puchi-1* seeds were first germinated and grown on NPA-containing

medium and no lateral roots were formed. The lateral root-less seedlings were then transferred to NAA-containing medium for 36 hours to synchronously induce LRP formation. However, no significant difference in VLCFA profile was detected between WT and *puchi-1* roots (Figure 3.13). Even though, a small but not significant reduction in C22:0 content, as well as a slight increase in C18 species in *puchi-1* roots could be noticed as compared to WT roots (Figure 3.13).

I therefore prepared the materials using the CIM condition, reasoning that in CIM-induced calli PUCHI-expressing cells make up a majority of whole root mass (see Figure 3.10A). Seven-day old WT, *puchi-1* and *kcs1-5* seedlings growing on MS medium were transferred to CIM for 4 days, and global fatty acids of these materials were analyzed. In this condition, in *puchi-1* calli we observed a significant increase in C16:0 and C18:0 and a decrease in C20:0, C22:0 and C24:0 in the phosphoglycerolipid pools. A similar decrease was also observed in VLCFAs in other fatty acid pools including  $\omega$ -hydroxylated FAs (C18:2-, C18:1- and C22:0), fatty alcohols (C20:0- and C22:0) and  $\alpha$ -hydroxylated FAs (C16:0-, C22:0- and C24:0; Figure 3.14). A similar alteration in FA composition was also observed in *kcs1-5* calli materials, although the difference in phosphoglycerolipid pools was more pronounced in *kcs1-5* than in *puchi-1* (Figure 3.14B). Globally, compared to WT calli, in *puchi-1* and *kcs1-5* calli the portion of FAs < 20 atoms of carbon increased while FAs  $\geq$  20 atoms of carbon decreased (Figure 3.14C).

In summary, fatty acids analyses demonstrated that in *puchi-1* mutant the root calli accumulates more FAs < 20 and less FAs  $\geq$  20 atoms of carbon, which is similar to the phenotype of the mutant of *KCSI*, a target of *PUCHI*. This confirms the regulatory role of PUCHI for VLCFA biosynthesis. A significant alteration in VLCFA composition was not detected in roots growing in normal MS and in LR induction medium, most probably because the difference is too subtle and localized to be detected.

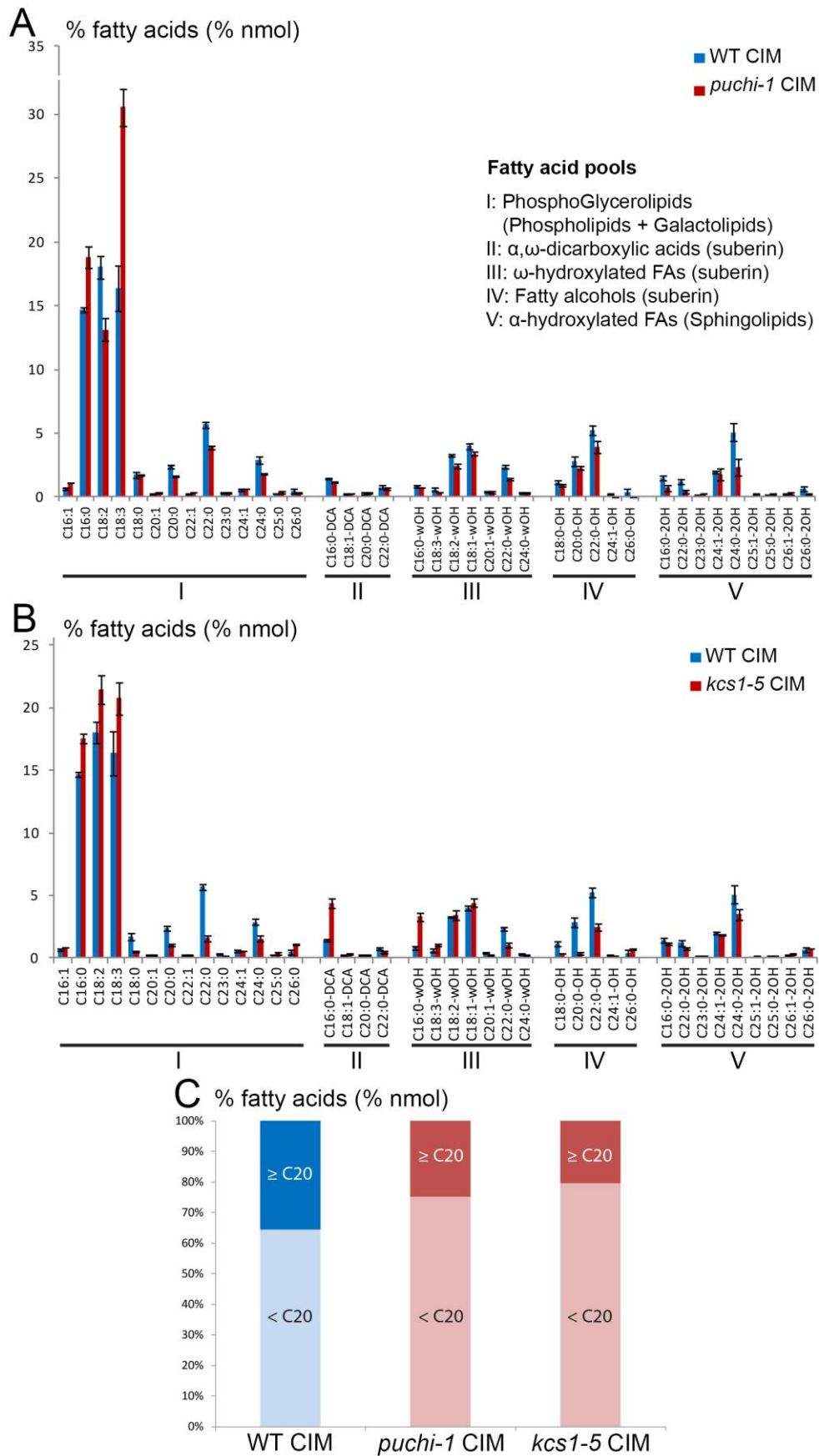


**Figure 3.14.** Global FA analysis revealed that mutation of PUCHI altered VLCFA composition in roots treated with CIM (to be continued).

**Figure 3.14 (cont).** Global FA analysis revealed that mutation of PUCHI altered VLCFA composition in roots treated with CIM. (A) Global FAs of WT (blue) and *puchi-1* (red) roots treated with CIM for 4 days. Compared to WT roots, *puchi-1* roots showed an increase in C16:0 and C18:0 and a decrease in C20:0, C22:0 and C24:0 in the phosphoglycerolipid pools, and a decrease in VLCFAs in other fatty acid pools including  $\omega$ -hydroxylated FAs, fatty alcohols and  $\alpha$ -hydroxylated FAs. (B) Global FAs of WT (blue) and *kcs1-5* (red) roots treated with CIM for 4 days. *kcs1-5* and *puchi-1* callus materials showed comparable alterations in many classes of VLCFAs. (C) The sum of < 20 carbon atom-containing FAs and  $\geq$  20 carbon atom-containing FAs from the above analyses. The legend for FA pools in (A) is applicable to (B). n = 3, 3 and 2 biological replicates for WT, *puchi-1* and *kcs1-5*.

## 2.8. Probing suberin content in WT and *puchi-1* roots

VLCFAs are components of suberin, so I tested if genes related to suberin synthesis and transport may also be in the PUCHI network. These genes were added to the potential target list and from that the TDCor algorithm produced an inference network as shown in Figure S3.5. It suggests that PUCHI might also regulates directly or indirectly suberin-related genes, and in so doing alters suberin biosynthesis/deposition in roots. In roots, suberin deposition occurs in the endodermis as well as in the outermost layer of a developing LRP (Andersen et al., 2015; Li et al., 2017), and *PUCHI* expression was detected in these two contexts (Chapter II). Previous paragraph showed that there may be differences in suberin-specific VLCFAs between *puchi-1* and WT roots grown on CIM.

To test whether there are any differences in global suberin content between WT and *puchi-1*, I used a simple staining procedure. Fluorol yellow 088 is a fluorochrome interacting with lipids (Brundrett et al., 1991; Ranathunge et al., 2011) and is widely used to visualize suberin disposition or even to compare suberin contents between different genotypes (Baxter et al., 2009; Yadav et al., 2014). Fluorol yellow staining was performed on roots of WT and *puchi-1*, as well as of *esb1-1*, a mutant line known to have higher content of suberin (Baxter et al., 2009), and *pCASPI:CDEF* in *esb1-1*, a line deficient in suberin accumulation (Naseer et al., 2012). As expected, stained roots of *esb1-1* and *pCASPI:CDEF* in *esb1-1* seedlings (not shown) gave stronger and weaker fluorescence intensity, respectively. The relative fluorescence intensity between *esb1-1* and WT roots was  $\sim 2$  (Figure 3.15A, B), which is comparable to the ratio revealed by gas chromatography-mass spectrometry (GC-MS; Ranathunge & Schreiber, 2011). Strikingly the intensity of fluorol yellow signal was significantly lower in *puchi-1* roots compared to WT roots ( $\sim 20\%$ ; Figure 3.15D, E) suggesting a lower amount of fluorol yellow substrates, possibly suberin, in this background.

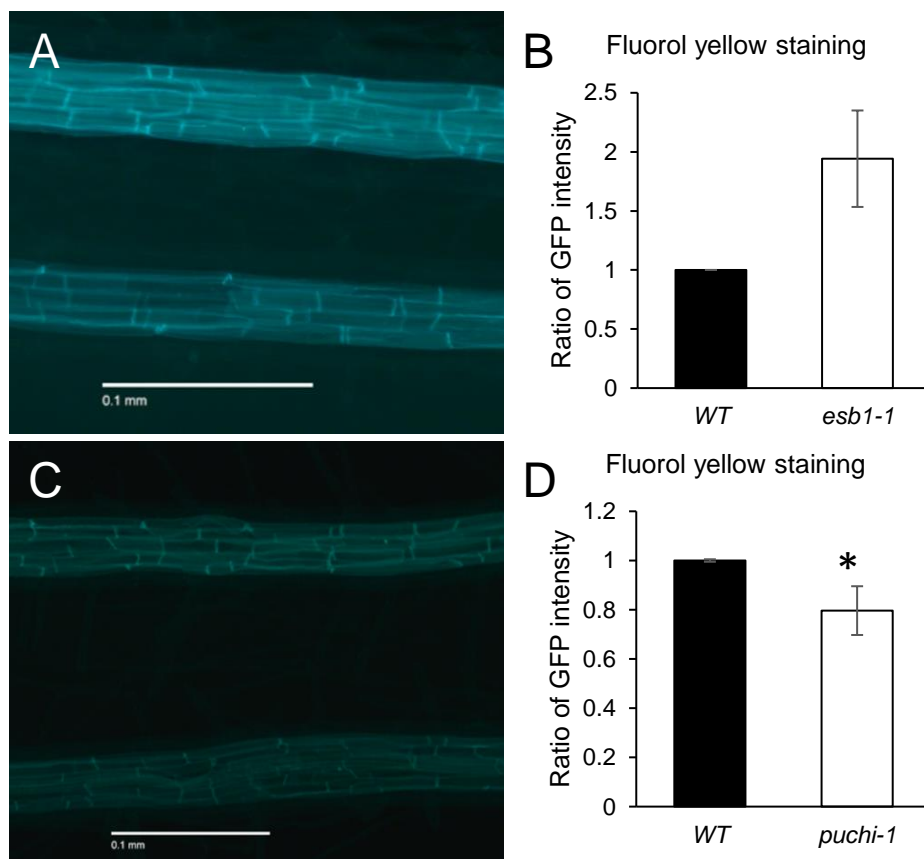


**Figure 3.15.** Suberin staining of roots with Fluorol yellow. (A) A segment of WT and *esb-1* roots, and (B) the relative GFP intensity between the two genotypes. (D) A segment of WT and *puchi-1* roots, and (E) the relative intensity between the two genotypes. 3 replicates,  $n = 40$  for WT and *puchi-1*. Data are represented as Mean  $\pm$  SEM. Significance was determined by Student's t test; \*  $p < 0.05$ .

However, the quantification of VLCFA species that are components of suberin by GC-MS on roots growing on normal MS medium provided above (Figure S3.4) convincingly demonstrates that there is no significant difference in suberin composition between WT and *puchi-1* roots. Nevertheless, one major difference in root materials between two experiments should be noted. In the fluorol yellow staining, for each pair-wise comparison the seedling of WT and *puchi-1* of the same age and comparable lengths were selected, while the materials for fatty acid analyses also came from roots of seedlings of the same age but much less homogenous. In addition, although this assay is useful for suberin visualization, the actual substrates of this staining and its specificity for suberin are less certain. The difference in fluorescence intensity therefore may reflect something else. Lastly, the possibility of an artefact during the staining experiment cannot be excluded even though the staining has been done with care in parallel and in the same condition.

### III. DISCUSSION AND PERSPECTIVES

#### 3.1. VLCFA biosynthesis genes are expressed in LRPs and the endodermis

Following the work of Dr Julien Lavenus, I tested the hypothesis that PUCHI is a regulator of VLCFA biosynthesis genes during LRP development, and that regulation can explain at least in part for the complex LR phenotype of *puchi-1* mutant. VLCFA biosynthesis genes have been studied extensively in different contexts of plant development, such as cuticular wax and suberin biosynthesis (Bach and Faure, 2010; Li-Beisson et al., 2013). However, their expression pattern during LRP development and their roles in that process are not well described. Here, I investigated the expression pattern of key, non-redundant genes in the VLCFA elongase complex, including *KCRI*, *PAS2*, *ECR* and *PAS1*, and of several *KCS* genes (*KCS1*, *KCS2* and *KCS20*) in the context of LRP development. The involvement of several *KCS* genes in LRP development was also examined.

The LR transcriptomic dataset itself provides an excellent source of information regarding gene expression dynamics throughout LRP development. Most of VLCFA biosynthesis genes displayed differential expression during this kinetic. However, since the materials used for the transcriptomic analyses were the whole root segment that contains a developing LRP (as opposed to the LRP alone), there is no warranty that these dynamics actually reflect their expression in the developing LRP. For example, some VLCFA elongation enzymes are involved in suberin biosynthesis at the endodermis (Lee et al., 2009b), and *PAS2* and *PTPLA* are expressed in the endodermis and the stele, respectively (Morineau et al., 2016). Therefore, a systematic look at VLCFA gene expression during LRP development is necessary. By using transcriptional and translational reporter lines, we have learned several key features of VLCFA biosynthesis gene expression in the context of LRP development. First, all VLCFA reporter lines analyzed were expressed in LRPs and newly emerged LRs, consistent with previous report for *PAS* and *KCS1* (Roudier et al., 2010; Shang et al., 2016). Second, while key, non-redundant genes (*KCRI*, *PAS2*, *PAS1*) seem to be expressed similarly in the whole developing LRP, several *KCS* genes seem to be expressed more specifically in the outer cell layers. This suggests that some *KCS* enzymes may be involved in producing VLCFAs of specific chain lengths in certain cell types of the developing LRP. Recently (Li et al., 2017) showed that there is a layer of suberin on top of a developing LRP, which was confirmed in our condition (not shown). Rather specific expression of *KCS1* and *KCS20* in the outermost cell layer of the developing LRPs may contribute to suberin deposition there. Third, VLCFA gene onset of expression near the root tip occurs rather concomitantly with LRP initiation. This is consistent with the observation of suberin deposition in endodermal cells surrounding developing LRPs from stage I onwards (Li et al., 2017; our observation).

All 7 GUS lines collected from different sources were transcriptional reporters (Joubès et al., 2008; Lee et al., 2009b; Morineau et al., 2016). However, we have good reasons to think that *pECR::GUS* and *pKCS1::GUS* from (Joubès et al., 2008) do not faithfully reflect the expression of *ECR* and *KCS1* in Arabidopsis. In WT plants, *pECR::GUS* showed two distinct expression patterns (strongly expressed in the primary basal meristem and tip, while the other was not) within a seedling population, and it is difficult to be sure which one reflects the true expression pattern of the gene. *pECR::GUS* expression was not detected in developing LRPs, which is strange because key, non-redundant VLCFA genes should have overlapping expression patterns to produce all the necessary components for the elongase complex. However, this argument would not stand if ECR protein or *ECR* mRNA is mobile (mRNA of *KCRI1*, *KCS8* and *KCS20* were found to be cell-to-cell mobile (Thieme et al., 2015)), or there is another ECR-like gene expressed in LRPs. The existence of another enzyme with ECR activity is possible because the loss-of-function mutation of *ECR* does not result in embryo lethality (Zheng, 2005) like other non-redundant VLCFA genes (Bach et al., 2008; Beaudoin et al., 2009; Roudier et al., 2010). The problems with *pKCS1::GUS* was that the GUS signal was not tissue-specific like other VLCFA reporter lines, while *pKCS1:KCS1-GFP*, which rescues the *kcs1* mutant, shows endodermis- and LRP-specific expression (Shang et al., 2016). The other reporter lines for *KCRI1*, *PAS2*, *PAS1*, *KCS6* and *KCS20* showed clear and similar tissue-specific expression patterns, especially in the endodermis where VLCFAs are needed for suberin biosynthesis, suggesting that they reflect well the native expression of these genes.

Altogether, our analyses demonstrated that VLCFA biosynthesis genes are expressed in developing LRPs and newly emerged LR. They are also expressed in the endodermis which play important roles in regulating LRP emergence (Vermeer et al., 2014; Stoeckle et al., 2018).

### **3.2. VLCFA biosynthesis genes are involved in LRP development and callus formation and are regulated by PUCHI**

VLCFA biosynthesis genes were identified by TDCor as potential targets of PUCHI because in the LR dataset they have similar expression profiles but shifted in time by 3 hours to that of *PUCHI*. Our expression levels (qRT-PCR) and expression pattern (reporter lines) analyses demonstrated that the regulation of PUCHI on VLCFAs does indeed happen during LRP formation. The qRT-PCR analysis on roots growing on the lateral root inducing medium (high NAA concentration) showed that in the WT VLCFA genes exhibited an induction in expression levels, but this induction was lost in *puchi-1* background. The loss of gene expression induction was observed for key VLCFA genes including *KCRI1*, *PAS2*, *ECR* and three *KCS* genes namely *KCS1*, *KCS2* and *KCS20*. In chapter II we have seen that LRP development in *puchi-1* was delayed

compared to in the WT, and one may argue that the differences in VLCFA gene expression were merely due to the differences in that LRP development. However, the roots used for qRT-PCR were growing for 24 hours on NAA-containing medium and in that condition WT and *puchi-1* roots produced LRPs of similar stages (mostly at stage II), suggesting that the changes in VLCFA gene expression levels were not due to differences in LRP development between the two genotypes but rather reflect genuine regulation of PUCHI on VLCFA gene expression. Even though, whether this regulation happens inside the developing LRP was not certain because *PUCHI* is also expressed in other tissues such as the endodermis and the stele.

By introducing VLCFA reporter lines into the *puchi-1* background, we examined in detail the effects of PUCHI absence on VLCFA gene expression patterns. VLCFA genes are expressed in developing LRPs; however, in *puchi-1* we observed a clear and consistent loss of VLCFA reporter expression. Key, non-redundant VLCFA genes namely *KCR1*, *PAS2* and *PAS1* (Bach and Faure, 2010; Haslam and Kunst, 2013) were regulated by PUCHI throughout LRP development in a similar manner. The clear loss of GUS staining in *puchi-1* background was observed in developing LRPs as well as in newly emerged LR. Curiously, the GUS staining was observed in some cells at the base and flanks of *puchi-1* LRPs and LR where PUCHI is normally supposed to be transcribed (Figure 3.7). In the wild type, loss of reporter gene expression was prominent at the tip of LRPs and LR where GFP-PUCHI proteins are not clearly detected. This could reflect a delayed modification in VLCFA biosynthesis gene regulation across LRP development or a non-cell autonomous action of PUCHI in WT LRPs. On the other hand, partially redundant *KCS* genes displayed more diverse expression patterns and regulation by PUCHI. While the loss of GUS expression in *puchi-1* LRPs was observed for *KCS1* and *KCS6* (a lesser extent for *KCS20*), both *KCS6* and *KCS20* showed a stronger GUS staining in newly emerged LR in *puchi-1* compared to in the WT (Figure 3.8). Thus PUCHI may participate to a complex spatiotemporal regulation of *KCS* gene expression, which might control the synthesis of VLCFAs of various chain lengths (Kim et al., 2013; Kosma et al., 2014; Haslam and Kunst, 2013) in distinct stages and tissues of developing LRPs.

From the data summarized above, the regulation of PUCHI on VLCFA biosynthesis genes has been well established. It is possible that the regulation is direct at least for some, because (i) VLCFA genes have similar expression profiles to that of *PUCHI* and they reach a peak just one time point (3 hours) after *PUCHI* does, and (ii) PUCHI binding motif is found on promoter sequences of several VLCFA genes.

The link between PUCHI and VLCFA biosynthesis genes was further strengthened by the similarities in root phenotype of *puchi-1* and VLCFA mutants. Both *puchi-1* and *kcs1-5* produce

more LRPs, delayed in LRP emergence and produce more calli in the callus-induction medium (CIM). The mutation of *ECR* also results in increased LRP production but at a lesser extent.

Callus formation is the first step of organ regeneration, and our regeneration assays showed that *puchi-1* calli failed to produce adventitious roots in the root-inducing medium (RIM), which further emphasizes the relevance of PUCHI in root formation in general. One question may arise, that is why *puchi-1* roots produced more LRPs but *puchi-1* callus failed to produce adventitious roots? First, PUCHI probably positively regulated key gene(s) in adventitious root regeneration from callus, and that genes(s) were not activated anymore in *puchi-1* callus. Second, on CIM, WT roots produced well-separated calli, and when being transferred to RIM, each callus would probably develop into an adventitious root. There were, however, no clear separation in *puchi-1* calli, meaning that possibly there was no clear peak of developmental cues (for example, auxin) available to direct callus cells to another developmental pathway.

However, attempt to provide evidence for a functional regulation of PUCHI on VLCFA biosynthesis genes, *e.g.* through fatty acid composition analyses, in roots growing on normal MS/2 medium as well as in LRIS for 36 hours was not successful. From the reporter line analyses in WT, we have learned that the expression of *KCS* genes, which are responsible for the production of VLCFAs of specific chain lengths, could be limited to just outermost cell layers of the primordium (*e.g.* *KCS1*). This, plus the fact the LRPs even in the lateral root induction condition constitute a small percentage of total root mass, suggest that the amount of VLCFA synthesized in developing LRPs may be too low compared to that in other root tissues such as the endodermis. Thus, it is difficult to detect any differences in fatty acids content/composition in WT and *puchi-1* roots.

Nevertheless, a similar alteration in VLCFA content was observed in *puchi-1* and *kcs1-5* roots incubated in CIM for 4 days. In this condition, the whole primary root produces calli along the pericycle, making calli a major tissue in the root, thus any differences in VLCFAs in callus between genotypes were amplified. A callus in WT has a similar structures to a LRP (Sugimoto et al., 2010) and the expression of *KCS1* was observed in the outermost layer in both cases. *KCS1* expression was lost in *puchi-1* LRP and calli (Figure 3.8 and Figure 3.12). Both *puchi-1* and *kcs1-5* produced continuous layer of calli on CIM. Coincidentally, in both *puchi-1* and *kcs1-5* calli, similar increases and decreases in VLCFAs of certain fatty acids species were observed, and overall *puchi-1* and *kcs1-5* calli accumulate more FAs < 20 and less FAs  $\geq$  20 atoms of carbon compared to those of WT (Figure 3.14). All the data suggest that the regulation of *PUCHI* on *KCS1* expression is necessary for a proper VLCFAs production that in turn ensures a correct CIM-induced callus formation.

Some differences in VLCFAs composition were detected in roots treated with CIM but not in those treated with LRIS for 36 hours or non-treated. It was likely because in CIM pericycle cells massively divide to form calli that make up a major part of the roots, while 36 hours on LRIS were not enough to amplify the proportion of LRPs in primary roots. Incubating roots on LRIS for 48 hours or more would possibly be more effective in generating more LRPs for VLCFAs analysis.

Although several experiments have been done using free VLCFAs to rescue development phenotype of mutants in VLCFA biosynthesis pathway or to induce the expression of its target genes (Qin et al., 2007; Roudier et al., 2010; Yamauchi et al., 2015; Shang et al., 2016), but so far, we have not been successful with rescuing *puchi-1* LR and callus phenotype on CIM with free VLCFAs. Alternatively, expression of *KCS1* in LRPs under the drive of *PUCHI* promoter is being done to see if *pPUCHI:KCS1* can rescue at least in part *puchi-1* LR and callus phenotype.

In summary, here we demonstrated that PUCHI regulates expression levels as well as expression pattern of key VLCFA genes, and that the regulation may be important for LRP development and CIM-induced callus formation.

### 3.3. How do VLCFAs contribute to LRP development?

The *puchi-1* loss-of-function mutant has been reported to exhibit LRPs with abnormal cell division pattern and a higher cell proliferation rate compared to WT especially at the organ flanks (Hirota et al., 2007). In chapter II, I showed that the mutant also displays a delay in LRP development and emergence, as well as higher initiation density along the primary root, with frequent clustering of primordia under normal condition and the formation of continuous callus in CIM. VLCFA mutants, notably *kcs1-5*, displayed similar phenotypes including higher initiation density, delay in LRP emergence and continuous callus in CIM. The question now is, how are VLCFAs involved in LRP development, and could the regulation of PUCHI on VLCFA biosynthesis genes explain for *puchi-1* phenotype?

First, VLCFAs are required for correct polar distribution of a key auxin transporter for LRP formation. For example, the *pas1-4* mutant which is defective in VLCFA composition produces few LR and these LR are morphologically abnormal and lack a clear auxin gradient as revealed by *DR5::GFP* (Roudier et al., 2010). This LR phenotype could be explained by the weak polar membrane distribution and cytosol aggregation of the auxin transporter PIN1 in the developing LRP. Supplement of *pas1-3* roots with exogenous VLCFAs rescued the auxin gradient defect. PAS1 seems to regulate PIN1 rather specifically because the influx carrier AUX1 was targeted correctly to the plasma membrane in the *pas1-3* mutant. Moreover, it has been demonstrated that changes in the fatty acids  $\geq 24$ /fatty acid  $\leq 24$  ratio within the pool of SLs resulted in a loss of PIN2

polarity (Wattelet-Boyer et al., 2016). However, *kcs1-5*, the mutant show similar phenotype to *puchi-1*, displayed a normal DR5::GFP pattern and PIN1:GFP distribution in the primary root tip (Shang et al., 2016). Similarly, in *puchi-1* background we could still see a clear auxin gradient in developing LRPs, implying that PIN polarity was not significantly affected (if any) at least in those that can eventually emerge. Nevertheless, delayed LRPs in *puchi-1* did not show a clear auxin gradient and changes in PIN polarity may occur in these LRPs, although it is unknown whether lack of auxin gradient was a cause or a consequence of delayed LRP development.

Second, VLCFAs are important for proper hormonal balance, which can influence cell proliferation. Mutation in *PAS1*, *PAS2*, *PAS3* and other VLCFA-related genes as well as in seedlings treated with KCS inhibitor leads to cell over-proliferation in the shoot (Nobusawa et al., 2013; Bellec et al., 2002). In the shoot, *PAS2* expression was confined specifically to the epidermis. Intriguingly, disruption of *PAS2* expression in the shoot epidermis phenocopied the *pas2-1* leaky phenotype, while expression of *PAS2* specifically in the shoot epidermis rescued the *pas2-1* phenotype, suggesting that *PAS2* activity, hence VLCFA biosynthesis, in the epidermis is necessary and sufficient for proper cell proliferation and organ development. In *pas1-3*, *pas2-1* and *pas3-1* mutants, expression of cytokinin biosynthesis genes such as *IPT3* in the vasculature was enhanced, resulting in higher levels of cytokinins and subsequently cell over-proliferation. The level of auxin (indole-3-acetic acid (IAA)) and gibberellins in these mutants was not changed. The data implies that VLCFAs synthesized in the epidermis can regulate non-cell autonomously cytokinin biosynthesis in the vasculature (Nobusawa et al., 2013). In addition, in *pas* mutants (*pas1-2*, *pas2-1* and *pas3-1*), cytokinin primary response genes including *ARR5* and *ARR6* was upregulated, while auxin primary response genes including *IAA1* and *IAA4* was down-regulated (Harrar et al., 2003). Although hormonal balance in the root of VLCFA mutants has not yet been studied, could the increase in cytokinin biosynthesis in the root (if it happens) explain for the phenotype of *puchi-1* and VLCFA mutants? It probably could not explain for the increase in LRP density in *puchi-1*, *kcs1-5* and *cer10-2* because cytokinin is known as a negative regulator of LRP initiation (Laplaze et al., 2007; Chang et al., 2015). The involvement of cytokinin homeostasis in CIM-induced callus formation in the VLCFA mutant *kcs1* has been excluded (Shang et al., 2016). In our conditions, varying cytokinin concentration in CIM did not change the callus formation capacity of *puchi-1* roots (not shown). However, since cytokinin treatment could result in additional cell divisions in WT LRPs (Laplaze et al., 2007), it could not be excluded that cell over-proliferation in the *puchi-1* and *pas1-3* LRPs was due to the hypothetical increase in cytokinin biosynthesis caused by deficient VLCFAs. Strikingly, ectopic cytokinin signaling was observed in *puchi-1* LRPs (Chapter II, Figure 2.12). Cytokinin signaling was observed earlier in *puchi-1*

LRPs and also in *puchi-1* flanks (Chapter II, Figure 2.12), where cell proliferation of the mutant occurs (Hirota et al., 2007). Therefore, it is possible that changes in VLCFAs biosynthesis lead to the alteration in cytokinin signaling in *puchi-1* LRPs, which subsequently leads to enhanced LRP cell divisions especially in the flanks.

Third, VLCFAs participate in controlling cell division and cell expansion. Bach et al. (2011) reported that the formation of the cell plate, a cell membrane and cell wall structure synthesized *de novo* to separate two daughter cells during cell division, was delayed and its ultrastructure was altered in *pas2-1* mutant. The defects were mostly due to the reduction of VLCFAs in phospholipids and sphingolipids, key membrane lipids necessary for materials transport and delivery via lipid vesicles. Root cells in *pas2-1* were also smaller than in the WT (Bach et al., 2011). Smaller sizes were also reported for leaf epidermal cells in the *ecr* (*cer10-2*) mutant which was probably caused by a reduction in VLCFAs of sphingolipids which in turn may affect membrane microdomains and endocytic membrane trafficking (Zheng, 2005). Since smaller cell size was observed in both *pas2-1* and *ecr*, it may be a common feature in mutants significantly defective in VLCFA contents. VLCFAs can also activate the biosynthesis of the gaseous hormone ethylene, and consequently promote cotton fiber and Arabidopsis cell elongation (Qin et al., 2007). Cell expansion plays an important role during LRP development, most clearly when the primordium crosses the overlaying tissues. For example, LRP height increases suddenly when it crosses the endodermis thank to the quick axial elongation of basal cells (Goh et al., 2016). *puchi-1* LRPs showed a delay in LRP progression which could be due to different reasons such as basal cell expansion and coordination between LRP development and cell wall remodeling in overlaying tissues. Given that key VLCFA biosynthesis genes were expressed in the whole developing LRP, it is possible that loss of function of these genes would lead to reduced VLCFA contents and consequently a lower cell expansion. This may explain in part for the slow progression of *puchi-1* LRPs.

Fourth, VLCFA biosynthesis genes are expressed in the endodermis which is involved in LRP development in several ways. Loss of endodermal cell volume is required for LRP initiation and subsequent development (Vermeer et al., 2014). In addition, suberin and Casparian strips surrounding endodermal cells create biophysical constraints to LRP emergence, and mutants having increased suberin deposition experience a delay in LRP emergence (Lucas et al., 2013). VLCFAs synthesized in the endodermis probably serve as starting materials for suberin biosynthesis. VLCFA composition in suberin was changed in *kcs9* roots with a decrease in C24 but an increase in C22 fatty acids (Kim et al., 2013). The double mutant *kcs2,20* displayed a decrease in C22 and C24 but an increase in C20 VLCFAs in root suberin, which was coincident

with the formation of abnormal suberin lamella (Lee et al., 2009b). These changes seem to have negligible effects on LRP development since *kcs9* and *kcs2,20* did not display any LR phenotype. Because *PUCHI* is also expressed in endodermal cells directly overlaying a developing LRP, it is possible that in the *puchi-1* mutant VLCFA biosynthesis in these cells is affected. This may lead to localized changes in suberin content/composition and consequently changes in biophysical constraints, or the response of the endodermal cells to the developing primordia. Endodermal volume loss may not be as effective as in the WT, leading to more difficulty for a LRP to cross the endodermis.

In animals, some lipids, including those derived from VLCFAs such as sphingolipids, are termed “morphogenetic lipids” because of their ability to induce stem cell differentiation and to regulate embryo development and morphogenesis. In particular, VLCFA-containing membrane lipids are thought to participate to the organization and the regulation of membrane microdomains, that are critical for membrane-bound signaling pathways, cell polarity and for the trafficking of cellular vesicles which carries proteins, lipids and RNAs (Wang and Bieberich, 2017). Moreover, sphingosine-1-phosphate, a derivative of ceramide and another morphogenetic sphingolipid, could be exported to extracellular space. There, it acts as ligand for different membrane-bound receptors which also bind to other proteins to regulate cell proliferation, migration and morphogenesis (Wang and Bieberich, 2017).

Given the essential roles of VLCFAs during plant development, it is intriguing that *puchi-1* LRPs lacking the expression of key VLCFA biosynthesis genes such as *KCRI*, *PAS2* and *PAS1* were still be able to develop and emerge. This could be explained by partial redundancy or by non-cell-autonomous action of VLCFAs synthesized in other tissues or at earlier stages of development and in a PUCHI-independent way. Such non-cell-autonomous activity of VLCFAs has already been suggested in different contexts (Faure et al., 1998; Bellec et al., 2002; Haberer et al., 2002; Nobusawa et al., 2013).

### **3.4. The PUCHI network regulating LRP development and callus formation**

To summarize our present data in relation with the current knowledge on PUCHI, VLCFAs and LR development, a schematic representation is shown in Figure 3.16. The transcription factor LBD16 (Goh et al., 2012a) can regulates PUCHI directly (Tatsuaki Goh, personal communication) or through the *TOLS2-RLK7* signaling cascade (Toyokura et al., 2018). The *TOLS2-RLK7-PUCHI* signaling pathway inhibits LR founder cell specification from pericycle cells (Toyokura et al., 2018). Our work demonstrates that *PUCHI* positively regulates the expression of VLCFA biosynthesis genes, and in parallel VLCFAs was suggested to inhibit the expression of *ALF4* and in doing so restrict pericycle cell division to form callus in callus-inducing medium (Shang et al.,

2016). In developing LRPs, the regulation of PUCHI on VLCFA biosynthesis may be needed to ensure cytokinin signaling and auxin transport/signaling which in turn is important for proper cell division and tissue organization (this work). However, PUCHI may regulate pericycle cell division and LRP formation and development through other players other than VLCFAs (dashed lines).

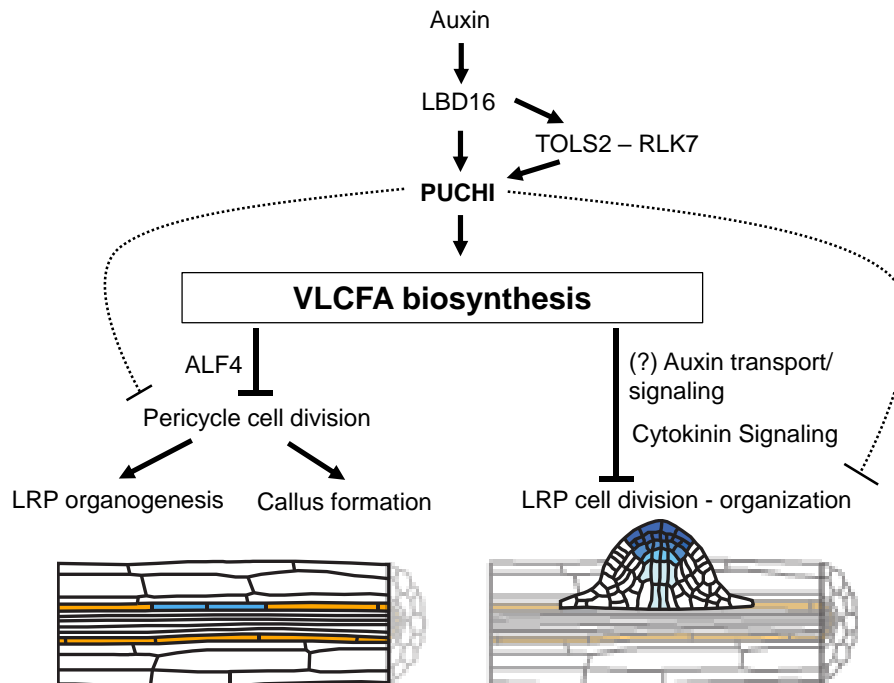


**Figure 3.16.** Possible PUCHI network regulating pericycle cell division and LRP formation and development. *LBD16* regulates *PUCHI* directly or through *TOLS2-RLK7* module. Current work shows that *PUCHI* positively regulates VLCFA biosynthesis, possibly through hormone signaling, to regulate pericycle cell division (for founder cell specification or callus formation) as well as LRP development. VLCFAs have been suggested to control pericycle cell division via inhibiting *ALF4* expression. Dashed lines suggest that *PUCHI* may regulate other factors than VLCFAs. On the left: orange: the pericycle; blue: LR founder cells. On the right: blue gradient represents the auxin gradient in developing LRPs.

#### IV. CONCLUSIONS

In conclusion, using a systems biology approach we found that the expression of multiple important enzymes catalyzing each of the four steps of the VLCFA elongation cycle are upregulated during LRP development and this is dependent on the AP2/EREPB transcription factor *PUCHI*. The regulation by *PUCHI* of an important VLCFA biosynthesis gene (*KCS1*) during callus formation was also demonstrated. In addition, the *puchi-1* loss-of-function mutant shares similar LRP, callus phenotypes and fatty acid profiles with mutants impaired in VLCFA biosynthesis. Hence, during root branching and root-derived callus formation the *PUCHI* transcription factor stimulates the expression of key VLCFAs biosynthesis genes in pericycle cells and their derivatives to regulate cell proliferation, organogenesis and organ spacing.

## SUPPLEMENTAL FIGURES

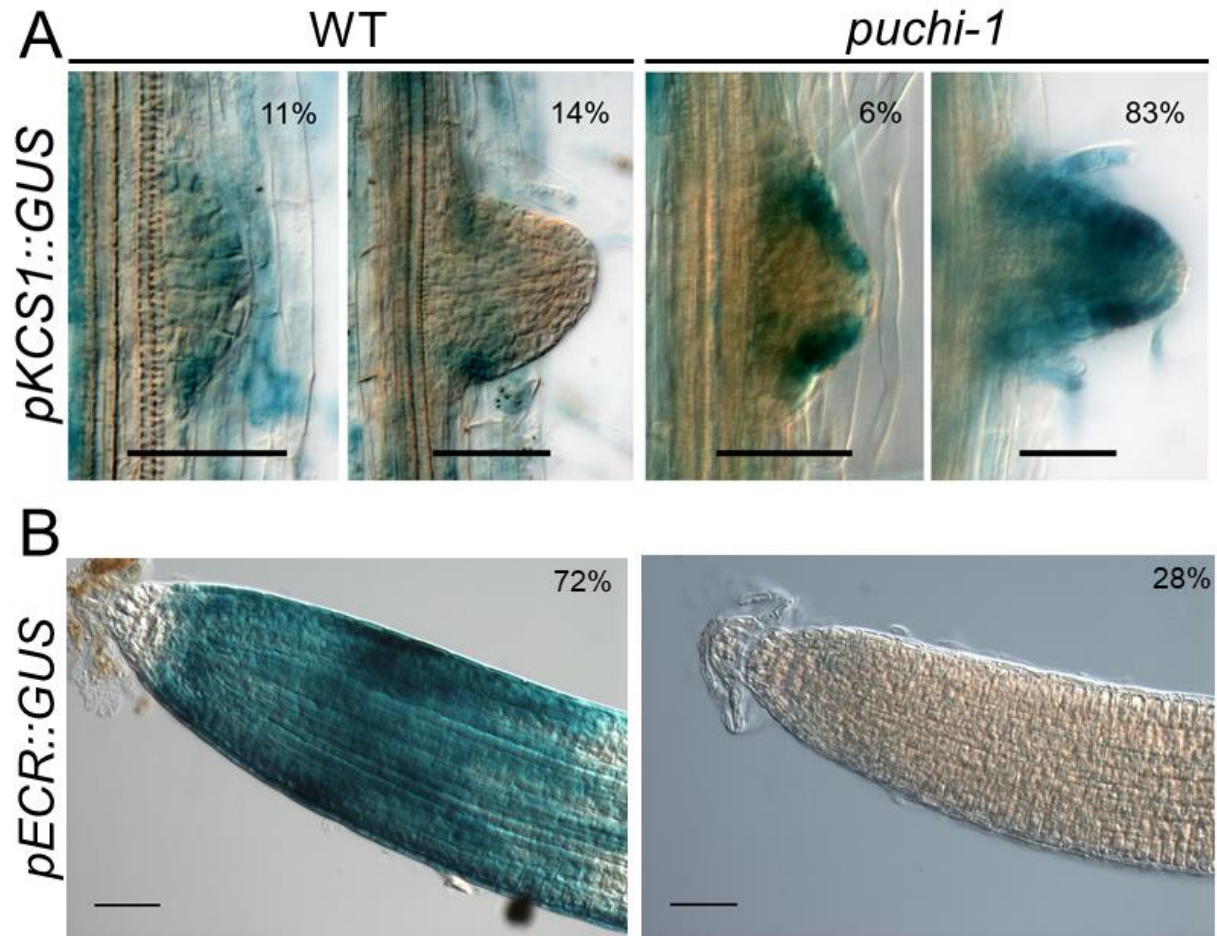


**Figure S3.1.** Expression pattern of *pKCS1::GUS* and *pECR::GUS* in the root. (A) *pKCS1::GUS* did not show a clear and consistent expression pattern, and was not expressed in a majority of developing LRPs and emerging LRs in WT. (B) *pECR::GUS* showed two different expression patterns within a population. A majority showed expression in the root tip (left) while the minority did not (right). Scale bars = 50 μm; n = 40 seedlings each genotype.

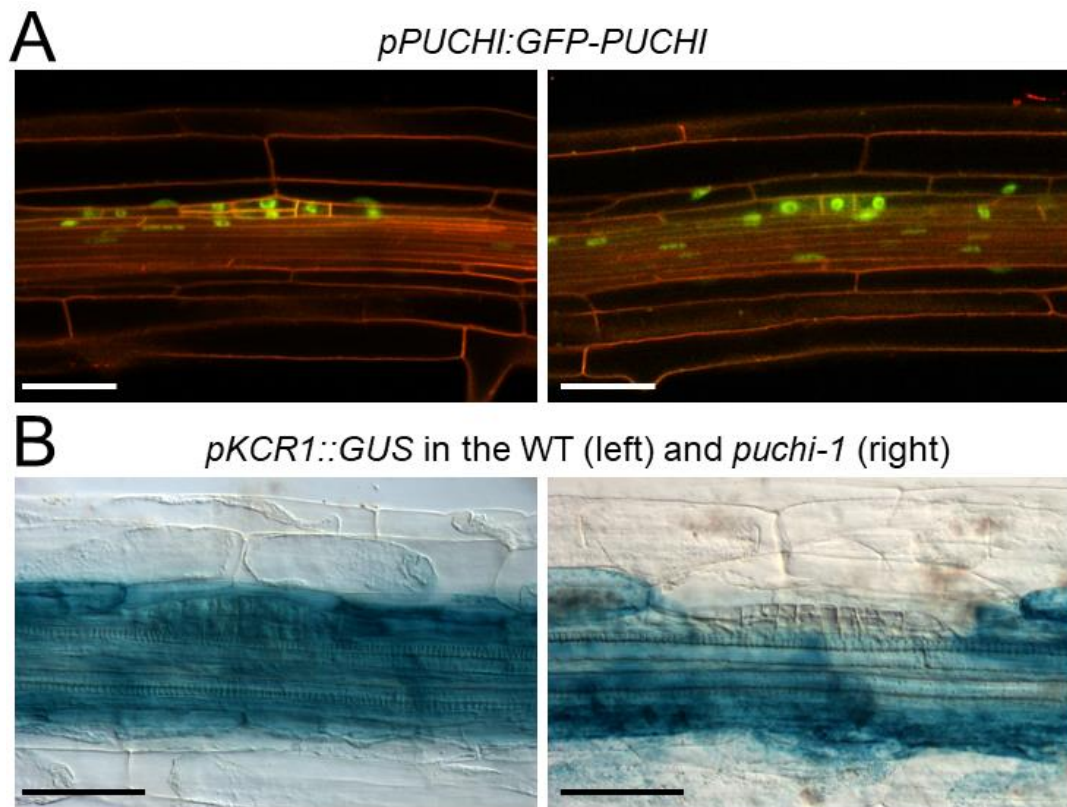


**Figure S3.2.** Expression of *pKCR1::GUS* in endodermal cells overlaying developing LRP is altered in *puchi-1*. (A) *pPUCHI:GFP-PUCHI* is expressed in the developing LRP and also in nearby endodermal cells. Cell membrane is visualized using WAVE131Y (presented as orange). (B) In WT, almost 100% endodermal cells overlaying a young LRP are positive with GUS, making a continuous expression in the endodermis, while in *puchi-1* a majority of LRP-overlaying endodermal cells lack GUS staining. Scale bar = 50  $\mu\text{m}$ . Small sample size.

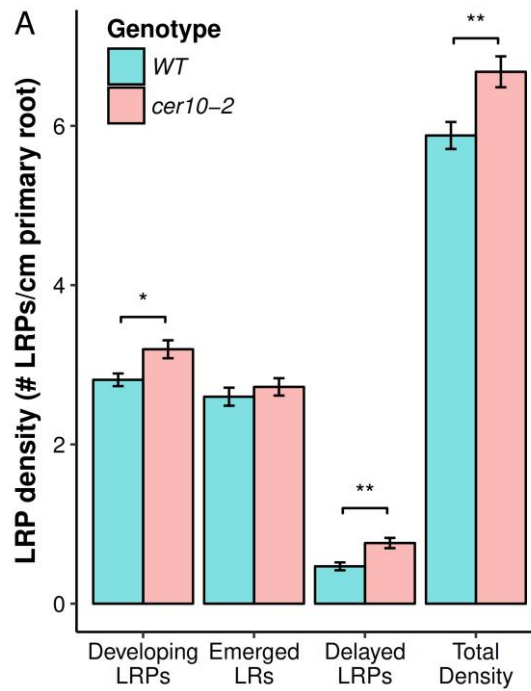


**Figure S3.3.** *cer10-2* roots produced more lateral organs than did WT roots. Density of developing LRPs, emerged LR, delayed LRPs, and total LR initiations (LRPs + LR) in 9-day old WT and *cer10-2* seedlings. 3 biological repeats.  $n \geq 20$  for each genotype each repeat. Significance was determined by Student's t test. \*  $p < 0.05$ , \*\*  $p < 0.01$ .

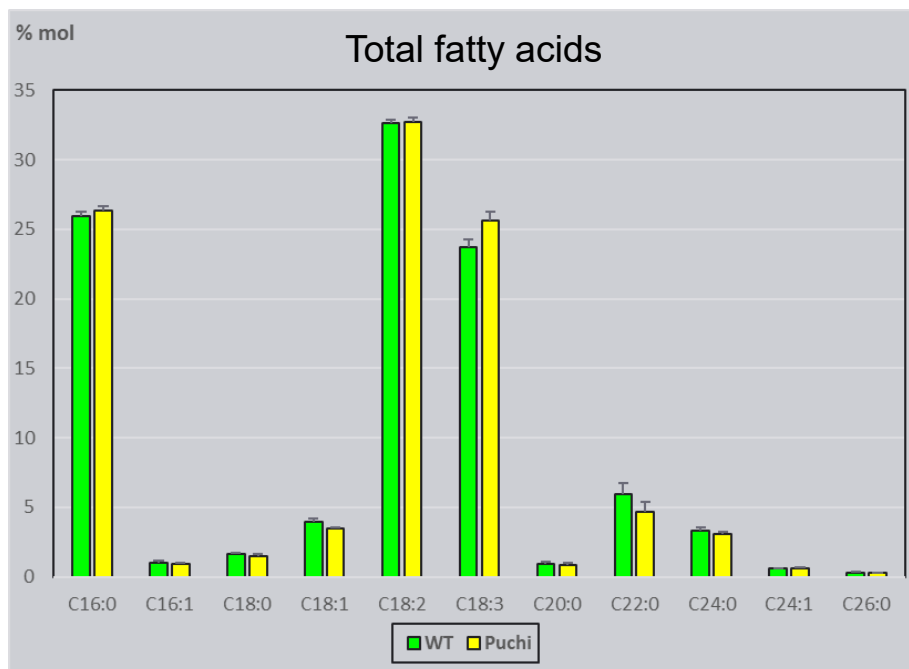


**Figure S3.4.** Total fatty acid profile from *Arabidopsis thaliana* roots. Total FAMES analysis was done on root materials of 9 days-old WT and *puchi-1* seedlings grown on normal MS/2.

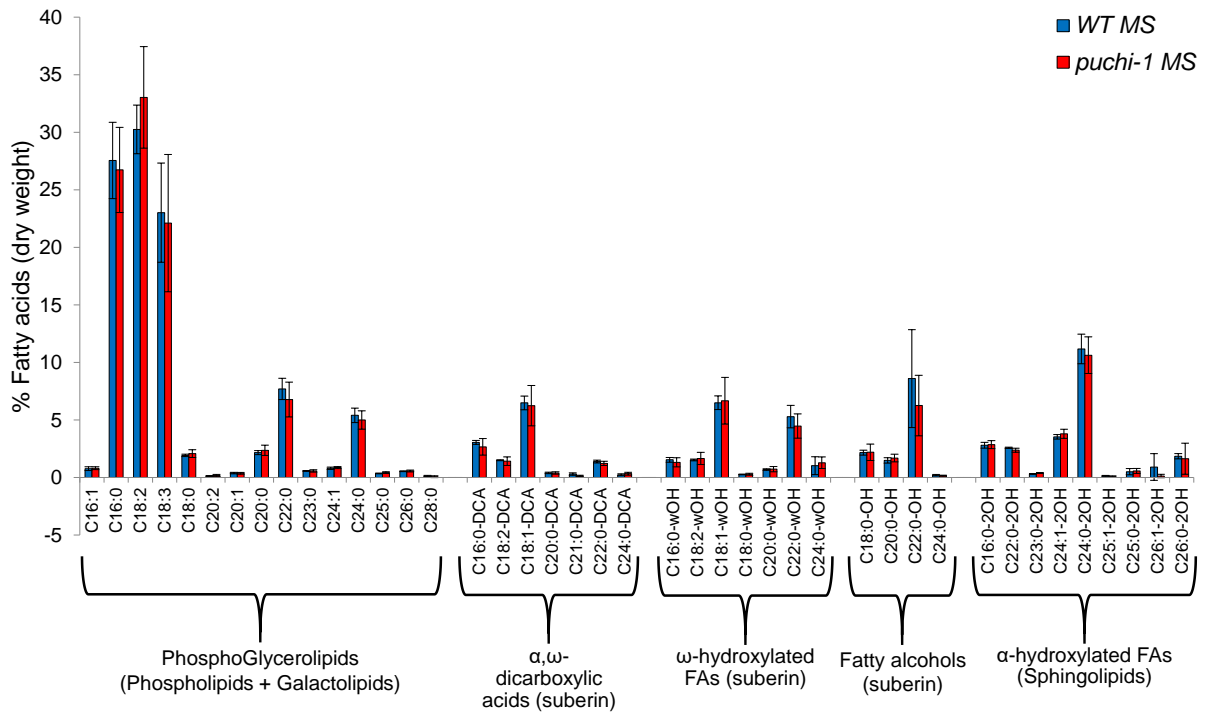


**Figure S3.5.** An analysis of VLCFA classes (in % dry weight = nmol of FA/dry weight of analysed material) of root materials of 9 days-old WT and *puchi-1* seedlings grown on normal MS/2. Quantity of VLCFAs in different lipid classes are given.

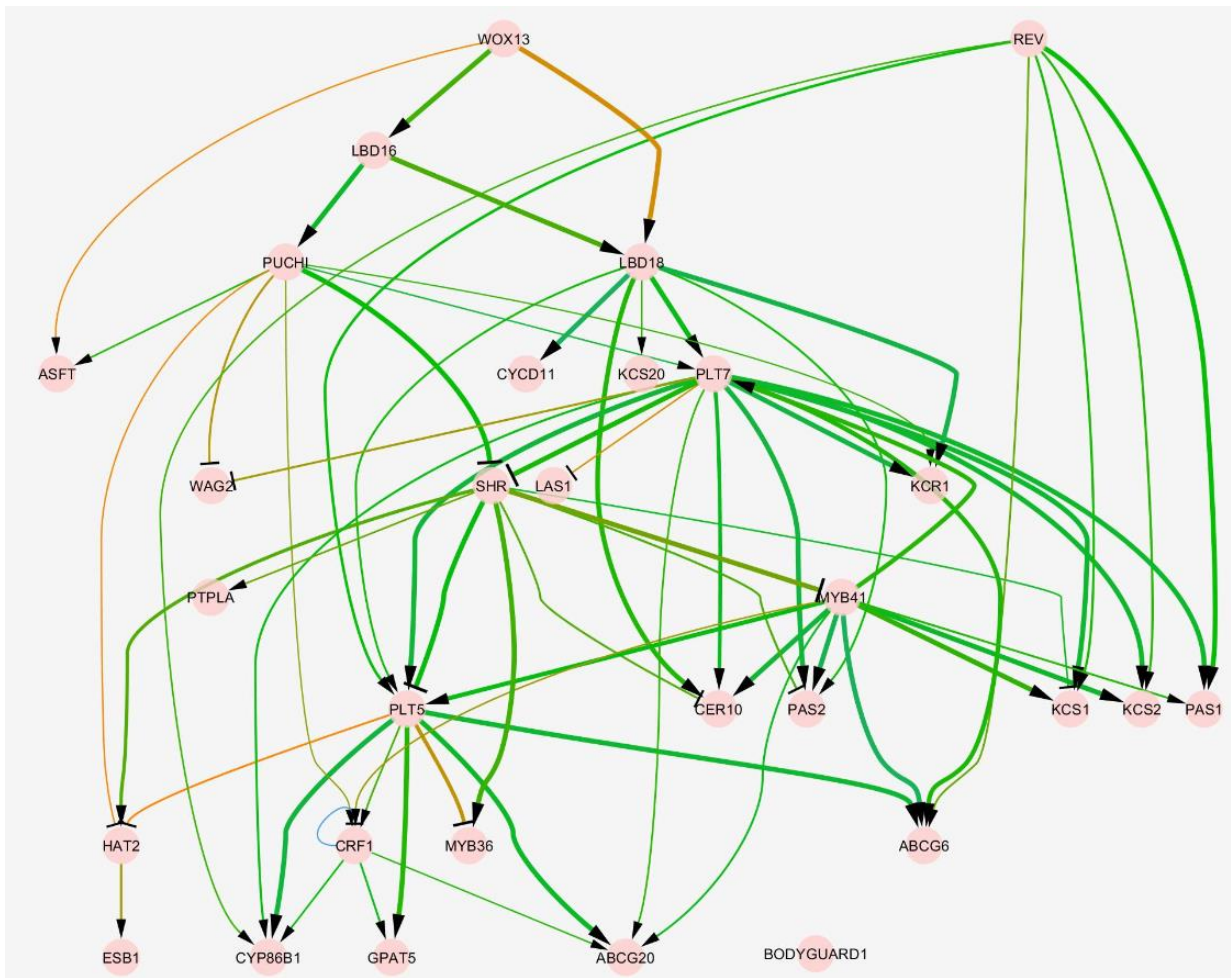


**Figure S3.6.** A subnetwork predicted by TDCor as in Figure 3.3 but with the addition of suberin-related genes (*ASTF*, *ESB1*, *CYP86B1*, *GPAT5*, *ABCG20*, *ABCG6*, *BODYGUARD1*). Legend as in Figure 3.3.

# **CHAPTER IV**

## **Potential genes regulating stem cell niche formation**

## I. INTRODUCTION

Many genes involved in apical meristem formation and/or maintenance also play critical roles in LRP meristem formation, such as *PLETHORAs* (*PLTs*), *SHORT ROOT* (*SHR*) and *SCARECROW* (*SCR*; Chapter I). When a functional meristem is defined during LRP development remains a difficult question (Trinh et al., 2018; general introduction of this PhD manuscript). While anatomical analyses as well as ablation experiments suggested that a root meristem-like organization is set at the center of a LRP at its mid-development (Malamy and Benfey, 1997; Laskowski et al., 1995; Ljung, 2005) it remains to be understood how and exactly when different functional identities are set up. Marker genes can be used to track identity acquisition in developing LRPs (Tian et al., 2014a; Goh et al., 2016; Du and Scheres, 2017b). Especially the expression of some marker genes for quiescent center (QC) is an important feature because these central cells are known to regulate stem cell identity and organize root meristem maintenance in *Arabidopsis* (Xu et al., 2006). By analyzing the expression of *WOX5::GFP* and *QC25::CFP*, (Goh et al., 2016) proposed that the quiescent center in LRPs is initiated at the transition from stage IV to V, coincident with the crossing of the LRPs through the endodermis. However, this meristem is only functionally activated only after LRP emergence (Celenza et al., 1995).

To identify potential regulators of root meristem or stem cell niche establishment during LRP formation, I relied on the LR transcriptomic dataset (Voß et al., 2015) and the TDCor algorithm (Lavenus et al., 2015). The dataset has 18 time points covering all stages of LRP formation, from initiation to emergence. More than 8000 genes are differentially expressed during the process (Voß et al., 2015). Using the LR dataset, TDCor has successfully reconstructed the sub-network constituting of ARF7 and its targets (Lavenus et al., 2015), and also correctly proposed very long chain fatty acid biosynthesis genes as targets of PUCHI (Chapter III). Here I continued exploiting the inference power of TDCor from the LR dataset with a focus on genes potentially involved in stem cell niche establishment during LRP development.

TDCor produces an inferred network by comparing the similarity and the shift in time in expression profiles of genes (Lavenus et al., 2015). To do that, it compares the profile of one gene to those of all other genes. Because of the extensive computing and the potential complexity of the output, the inference is not done on all the genes showing differential expression but on a limited number of genes of interest. The overall network is sufficiently large. For example, from a list of 128 genes known to possibly involved in LRP development, TDCor produced a network consisting of 358 edges corresponding to 206 positive interactions and 152 negative interactions (Lavenus et al., 2015). The gene list can be expanded if new genes of interest are added.

To identify potential regulators of stem cell establishment during LRP development, I used two approaches: (i) by looking for genes that are predicted to regulate a marker of stem cell establishment, or (ii) by whole network analysis to look for genes underlying transition in LRP development states. Potential genes were suggested and the roles of several genes during LRP development have been preliminarily explored.

## II. RESULTS

### 2.1. Identify potential regulators of root stem cell niche establishment in developing LRPs based on a proxy

#### 2.1.1. *PISTILLATA* as a marker for stem cell niche establishment

From an inferred network produced by TDCor, one can look for genes potentially involved in a LRP developmental event by looking at predicted regulators and/or targets of a gene important for that event. For example, given that *LBD16* is required for LRP initiation (Goh et al., 2012a), one can use it as a proxy for LRP initiation process. By looking at neighbor genes of

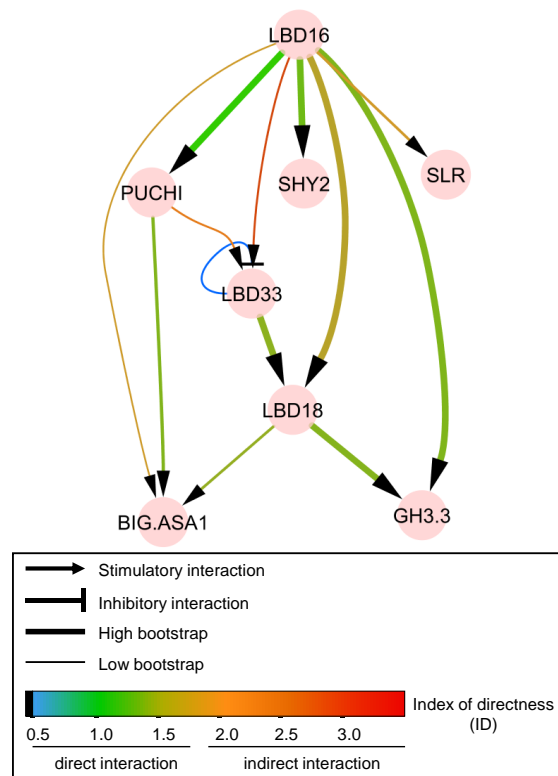


**Figure 4.1.** First downstream neighbors of *LBD16*, an important transcription factor regulating LRP initiation. Its predicted targets are also involved in LRP initiation, including *PUCHI*, *SHY2*, *SLR*, *LBD33* and *LBD18*. The legend is reproduced from (Lavenus et al., 2015).

*LBD16* in the network, potential genes involved in LRP initiation can be proposed. In the network from the 128 genes (Lavenus et al., 2015), the first neighbors of *LBD16* include *LBD33*, *LBD18*, *SHY2*, *PUCHI*, *BIG ASA1* and *GH3.3* (Figure 4.1) and these genes are involved in LRP initiation (Goh et al., 2012; Kang et al., 2013; Vermeer et al., 2014; Chapter II).

Using the same principle, to identify genes potentially involved in stem cell niche establishment during LRP formation using the LR dataset and TDCor, one would need a marker for that process. Several markers of QC identity have been described in the apical meristem of the *Arabidopsis* primary root (Sarkar et al., 2007; ten Hove et al., 2010) and some of them were reported to be expressed in LRPs, including *QC25* and *WOX5* (Goh et al., 2016). These genes or transgenes could be considered a good proxy for detecting QC identity and thus, presumably, root meristem establishment. Unfortunately we could not use them in our LR transcriptomic-based inference approach because *QC25::CFP* is a promoter trap and the associated gene is unknown (Sabatini et al., 2003), and *WOX5* is not present in the ATH1 chip used for generating the LR transcriptomic dataset. For this reason, I looked for another marker gene that could be used to track QC cell identity establishment in the LR dataset. Based on tissue specific transcriptomic studies performed in the primary root meristem performed by the lab of Prof. Philip Benfey (the U.S.A), we identified *PISTILLATA* (*PI*) as a potentially good marker for LRP QC because it is expressed specifically in the QC of the primary root (Nawy et al., 2005).

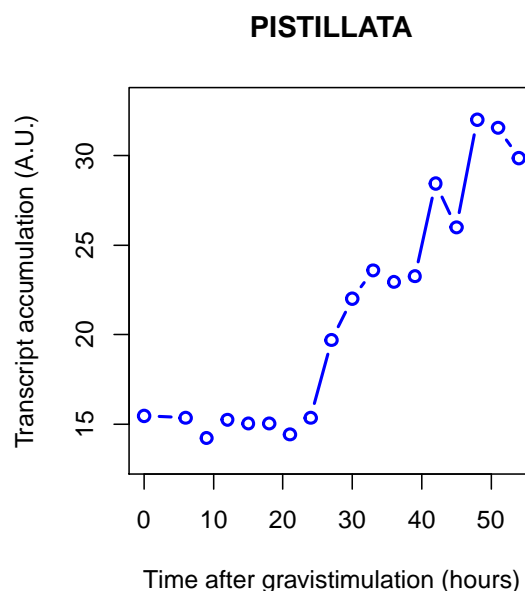


**Figure 4.2.** Expression profile of *PISTILLATA* during LRP development in the LR transcriptomic dataset.

Interestingly, *PI* is differentially expressed during LRP development (Voss et al., 2015). In the LR dataset, *PI* expression starts to increase at around 24 hours post gravistimulation (hpg) and reaches the first peak at around 33 hpg (Figure 4.2). In these experimental conditions, at around 30 hpg a majority of LRPs are at stage IV to V (Voß et al., 2015) when the onset of QC markers *QC25* and *WOX5* were observed (Goh et al., 2016). Thus, in association with its specific expression in the QC of the primary root (Nawy et al., 2005), the expression profile of *PI* during LRP development suggests that it may also be a marker for the onset of QC in LRPs.

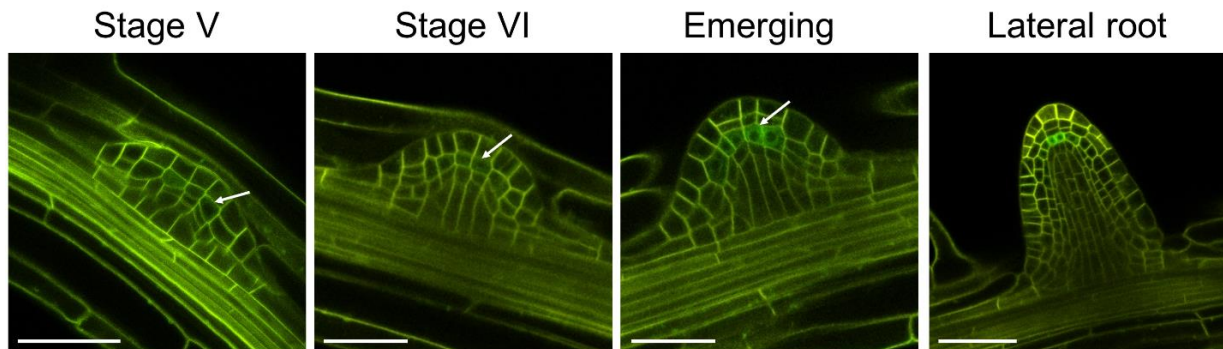


**Figure 4.3.** Expression of *PI::GFP* in the WT background. *PI* expression could only be detected from stage V onwards although at these stages the signal was generally weak, and was confined to several central cells. The expression domain seems to be more expanded than that of the QC-specific marker *QC25::CFP* described in (Goh et al., 2016). Cell membrane was visualized using WAVE131Y. Scale bar = 50  $\mu$ m.

To test if *PI* is a good marker for QC establishment, I observed and compared the expression of the transcriptional reporter *PI::GFP* described in (Nawy et al., 2005) to that of *QC25::CFP* which has been described in (Goh et al., 2016). This transgenic line was kindly provided by Philip Benfey's lab (Duke University) and was crossed into the WAVE131Y background in order to visualize better the anatomy of root tissues. In our conditions the transgene was expressed in the QC of the primary root as reported (Nawy et al., 2005). Importantly, its expression was also observed in the central cells of developing LRPs including the putative QC (Figure 4.3). The expression of *PI::GFP* was detected the earliest in stage V LRPs but the signal was generally faint (n = 5/5 LRPs) and was not visible in stage IV LRPs (n = 13/13 LRPs). This is consistent with the low expression levels detected in the LR transcriptomic dataset from 0-30 hpg (Figure 4.2). The signal was more readily observed from stage VI onwards. *PI::GFP* expression was stronger in the central cells and much weaker in the neighboring cells, similar to what described in the primary root (Nawy et al., 2005). In meristematic cells of LRPs *PI::GFP* expression was clearly visible and comparable to the expression pattern in the primary root apex. The central cells

positive with *PI::GFP* anatomically correspond to those expressing *QC25::CFP* in the QC25 reporter line. The expression dynamics of *PI::GFP* and *QC25::CFP* during LRP development were also similar, *i.e.* the onset of expression happened at stage V LRPs (Goh et al., 2016; see also Chapter II). Further experiments using the combination of *WAVE131-Red* and *PI::GFP* will be performed in order to robustly characterize the spatiotemporal expression dynamics of the *PI::GFP* reporter.

In summary, here we established *PISTILLATA* as another marker for the onset of QC identity (hence presumably, of stem cell niche formation) during LRP development. Although it has not been demonstrated that PI is indeed necessary, nor sufficient, for those cells to induce stem cell identity of their neighbors, the robust QC-specific expression pattern observed in primary roots, LRs and developing LRPs prompted us to use *PI* expression as a marker for QC-like gene expression onset in the developing LRP. Because specific probes for PI expression are present on the ATH1 microarray and because *PI* is differentially expressed during LRP development, we can use it as a proxy to look for potential regulators of stem cell niche formation using TDCor.

### **2.1.2. Selecting potential regulators of stem cell niche based on PI**

To generate the inferred network using TDCor and the LR dataset, a list of genes including 128 genes in (Lavenus et al., 2015) plus *PISTILLATA*, and an updated list consisting of 302 genes, were used. In both inferences, *PISTILLATA* was predicted to be an important node having 5 direct incoming and multiple direct outgoing edges (Figure 4.4). To look for potential regulators of *PI*, incoming nodes located one or two levels upstream of *PI* in the inferred topology were selected. In both inferences, important regulators were present such as the PLETHORA (*PLT*) gene family and *KAN4*. Because the second gene list contains many more genes than the one in (Lavenus et al., 2015), the PI subnetwork was also expanded. Expression profiles of selected genes upstream and downstream of *PI* in Figure 4.4.B is provided in Figure S4.1 and Figure S4.2, respectively. Basically, all predicted regulators of *PI* displayed a similar expression profiles to that of *PI*, *i.e.*, their expression levels were very low before 20hpg then raised quickly after that (Figure S4.1). Properties of predicted regulators of *PI* in the second network will be described in more details.



*PI* (meaning that they have similar, but shifted in time, expression profile compared to that of *PI*). There are four members of the KANADI family (*KANI-4*) and their expression patterns based on reporter line analyses during LRP development have been described (Bowman, 2004). All the four genes are expressed predominantly in the periphery of developing LRPs, except that expression of *KAN4* (the predicted regulator of *PI* in our work) is also clearly observed in the tip (possibly covering the QC) of emerging LRPs and not that clearly in the tip of younger LRPs (Bowman, 2004). In the shoot, *KAN* genes are expressed in a complementary manner to Class III HD-Zip genes. Class III HD-Zip genes (*PHB*, *PHV*, *REV*) are expressed in the center of shoot meristem and are required for meristem establishment (McConnell et al., 2001; Otsuga et al., 2001; Emery et al., 2003), while *KANI* is expressed in the periphery of the shoot meristem (Kerstetter et al., 2001; Caggiano et al., 2017). Compared to the data of (Bowman, 2004), it seems like *KAN* and Class III HD-Zip genes display complementary expression domains in both shoot meristem and lateral root contexts. The triple mutant *kan1-2 kan2-1 kan3-1* had shorter primary root and lower LR density, while the *KANI* overexpressing line (*35S::KANI:VP16:GR* on DEX) did not produce any LR (Bowman, 2004). The expression patterns and roles of Class III HD-Zip genes in LR have also been examined. *PHB*, *REV* and other member of the family *ATHB8* are expressed throughout developing LRPs. Compared to the WT, the triple mutant *phb-6 phv-5 rev-9* had similar primary root length but ~69% lower LR density while the gain-of-function mutant of *REV* produced ~30% shorter primary roots but ~48% higher LR density (Bowman, 2004). LRP morphology of these mutants were not reported, so it is not clear whether their lower LR density was due to reduced LRP initiation or defective LRP development.

*LONESOME HIGHWAY (LHW)* was predicted to be a major regulator in the *PI* network. It is critical for stele formation since a prominent feature of the mutant is to have only one single xylem and phloem poles (Ohashi-Ito and Bergmann, 2007). The mutant is able to produce LR along that single xylem pole (Parizot et al., 2007). However, using *pPIN1:PIN1-GFP* and *DR5::GFP* reporter lines, (Ohashi-Ito et al., 2013b) showed that *lhw* LR displayed a broader PIN1 expression domain and did not have a clear auxin maximum as did the WT LR. In the primary roots, *lhw* QC cells failed to express SCR and expressed *QC25::GUS* with asymmetrical intensity (Ohashi-Ito and Bergmann, 2007). The apical meristem of *lhw* roots deteriorates over time and the roots stopped growing after 19 days (Ohashi-Ito and Bergmann, 2007). *LHW* may play similar roles in auxin transport and response, and meristem maintenance in LR. Among three homologs of *LHW (LHL1-3)*, roles and expression patterns of *LHL1* and *LHL3* have been explored (Ohashi-Ito et al., 2013a). *LHL1* and *LHL3* were shown to be expressed in the stele and stele initials of the primary roots as well as in the developing LR. Although *lhl3* single mutant

and *LHL3*-overexpressing plants do not show any visible root phenotype, *lhw lhl3* double mutant shows more severe defects in the vasculature than the single mutant *lhw*. This suggested that redundantly with *LHW*, *LHL3* plays a positive role in promoting root vasculature formation (Ohashi-Ito et al., 2013a).

*ROOT MERISTEM GROWTH FACTOR 8 (RGF8, or GOLVEN 6 [GLV6], CLE-LIKE 2)*, which is also predicted to control *PI* via *PLT2*, is also interesting because it is a member of a gene family encoding for secreted peptides that maintains primary root stem cell niche by regulating expression levels of *PLTs* (*PLT1* and *PLT2*; Matsuzaki et al., 2010), which is consistent with the TDCor inference. *RGF8* is expressed throughout LRPs of early stages and then confined to the central cells (including the putative QC) at later stages (Fernandez et al., 2015). *RGF8*-silenced lines had lower LRP density but did not display any visible defects in LRP morphology. Ectopic expression of *RGF8* in the pericycle resulted in massive division of pericycle cells, however, morphology of developing LRPs, especially at later stages, were not described (Fernandez et al., 2015). The *GOLVEN* family has 11 members, and *GLV6*, *GLV10*, *GLV11*, *GLV3* and *GLV9* are expressed in the primary QC and stem cell initials (Matsuzaki et al., 2010; Fernandez et al., 2013). Among these genes, beside *GLV6*, only *GLV3* is differentially expressed in the LR dataset but the onset happens quite late (~ 40h hpg).

*LATERAL ROOT PRIMORDIUM 1 (LRP1)* is expressed specifically in LRPs from early stages and then confined to the base at later stages (Smith and Fedoroff, 1995). Loss-of-function of *LRP1* did not result in any visible phenotype, while plants overexpressing *LRP1* had longer primary roots (Krichevsky et al., 2009), suggesting that *LRP1* plays a positive role in root meristem activity. *PESCADILLO (PES)* is more strongly expressed in primary root tip and developing LRPs, and the *PES RNAi* knock-down mutants displayed severe defects in primary root meristem structure which led to a significant reduction in primary root lengths (Zografidis et al., 2014).

In summary, TDCor inference predicted several important genes with known or implied functions in regulating meristem activity as direct or close regulators of the QC-specific marker *PI*. Among them, *KAN*, Class III HD-Zip genes, *RGF*, *PES*, *LHW* and its related genes are expressed in developing LRPs and are known experimentally to be involved in LRP formation. However, it is unknown whether they also regulate meristem formation of the developing LRP. Therefore, some of them were selected as candidate genes of LRP meristem formation for further study.

### 2.1.3. Lateral root development in selected mutants

Several mutants of *KAN* and Class III HD-Zip genes, as well as of *LHW* and *LHL3* have been collected for lateral root phenotyping. *kan1-12* and *phb* are in Ler background while *kan1-11*, *phb phv cna er*, *lhw* and *lhl3* are in Col-0 background. Preliminary lateral root phenotyping analysis was performed using (i) 9-day old seedlings growing vertically on MS medium, and (ii) 5-day old seedlings growing vertically on MS medium and subjected to gravistimulation for 48 hours.

At 9 day, *kan*, *phb* and the quadruple mutant *phb phv cna er* have a similar root system to the WT (Figure 4.5A). There is no significant difference in total LRP density between WT and *kan1-11*, *kan1-12*, *phb*, and the quadruple mutant *phb phv cna er*. Mutation of *lhw* resulted in ~42% reduction in total LRP density which is consistent with the fact the mutant has only one xylem, hence one xylem pole-associated pericycle where LRP initiation happens (Parizot et al., 2007). *lhl3*, in contrast, produced ~18% increase in total LRP density (Figure 4.5A).

A preliminary gravistimulation assay for 48 hours was done to quickly assess LRP developmental progression in these mutants. Overall, LRPs in these mutants develop as well as those in the WT. Under DIC microscopy, no defects in morphology of emerging LRPs in these mutants were noted (Figure 4.5B). The anatomy of emerging LRPs in the quadruple mutant *phb phv cna er* was analyzed under confocal microscopy with the help of membrane staining using propidium iodide, and no clearly defective or aberrant features were detected, consistent with their normal developmental progression (Figure 4.5C).

Overall, the preliminary results showed that the single mutant of *KAN1*, *PHB*, and *LHL3* and the quadruple *PHB PHV CNA ER* mutation has little or no effects on LRP development.

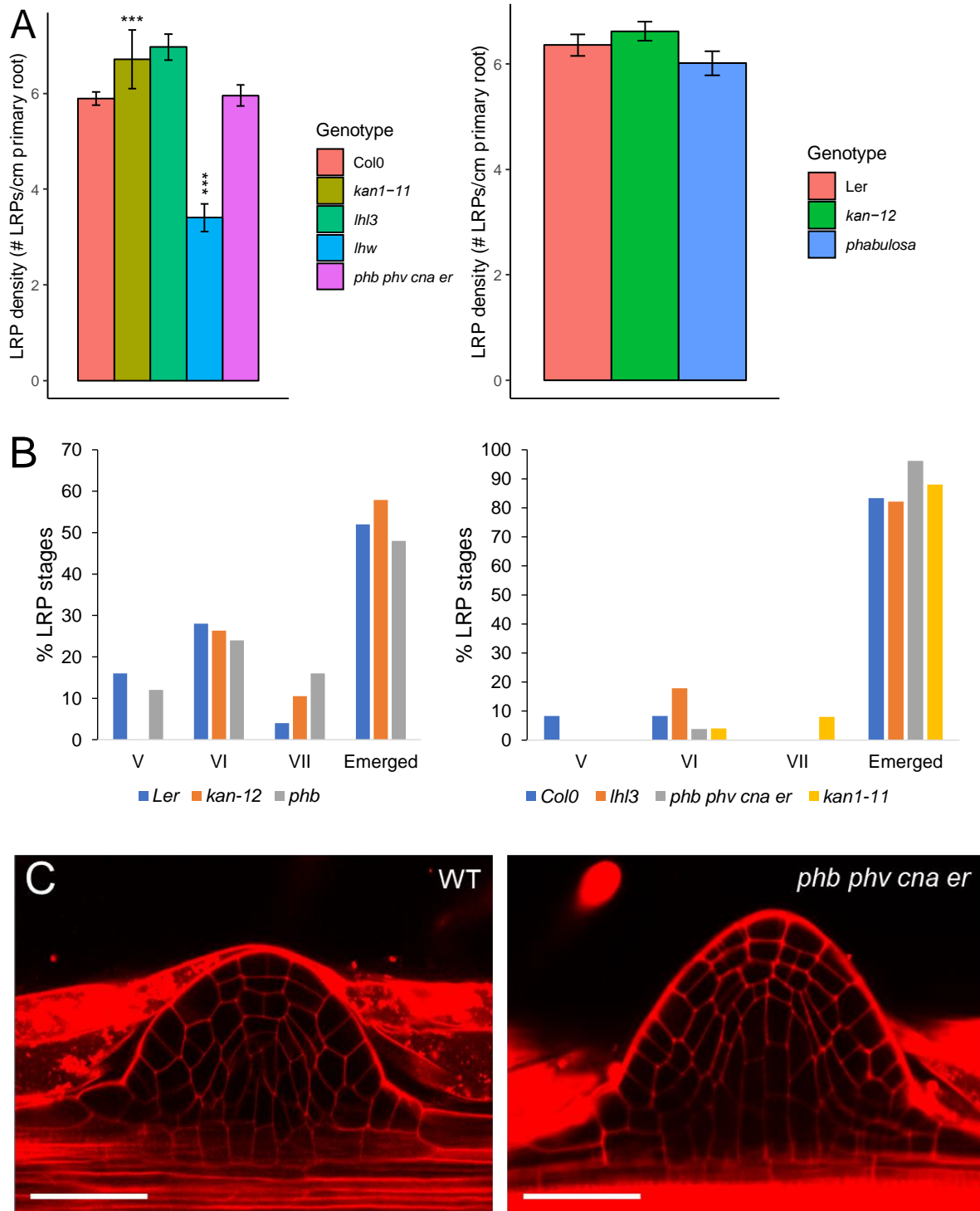


**Figure 4.5.** Lateral root phenotype of mutants of genes predicted to be upstream regulators of *PISTILLATA*. (A) Total LRP density of 9-day seedlings.  $n = 15$  for Col-0 and 8 seedlings for the others. (B) Developmental stages of LRPs of seedlings gravistimulated for 48 hours.  $n = 12$  for Col-0 and 20-28 seedlings for the others. (C) Morphology of emerging LRPs in WT and the quadruple mutant *phb phv cna er*.  $n = 6$  for the WT and = 20 seedlings for the mutant. Scale bars = 50  $\mu\text{m}$ . Data are represented as Mean  $\pm$  SEM of three biological replicates. Significance was determined by Student's  $t$  test (\*\*\*)  $p < 0.001$ .

## 2.2. Identify potential regulators of LRP stem cell niche by whole network analysis

### 2.2.1. Approach

The analyses made by (Lavenus et al., 2015) using a core list of 128 genes suggested that there exist two regulatory modules featuring different sets of the auxin-responsive factors (ARFs). One module contains the genes downstream of ARF7 and ARF19 (53 genes in total) while in the other the genes are associated with MP/ARF5, ARF6, and ARF8 (68 genes in total; Figure 4.6A).

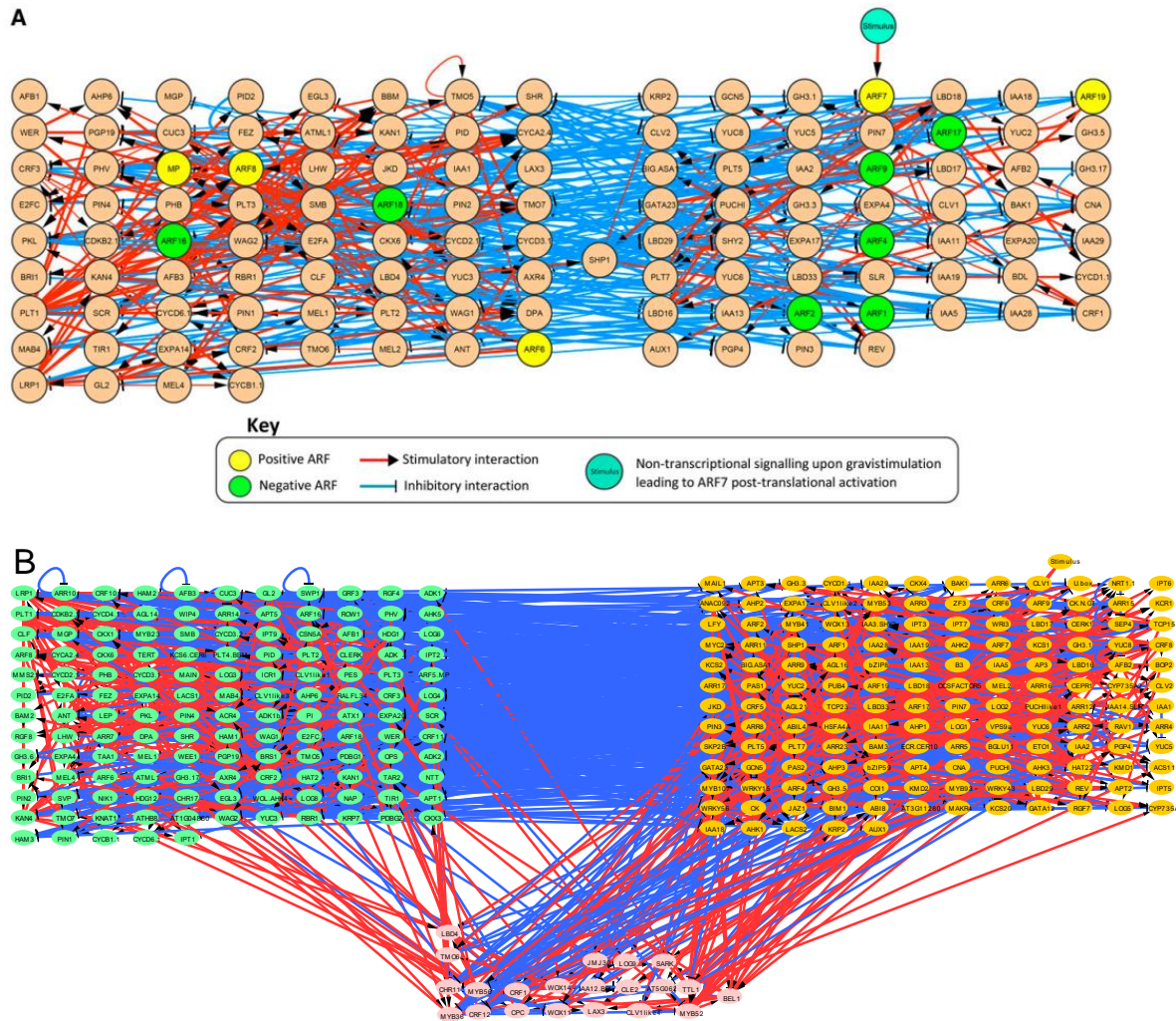


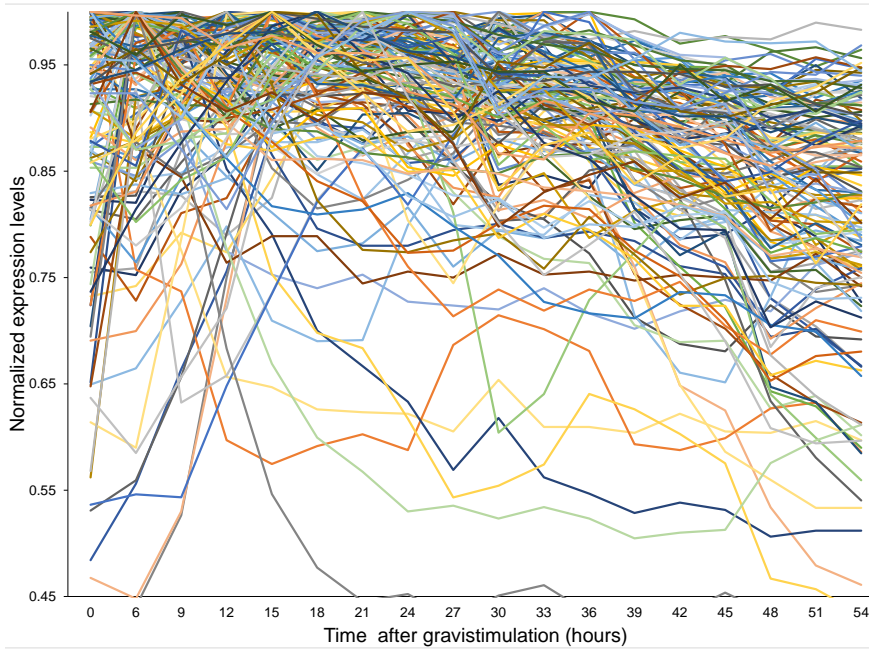
**Figure 4.6.** Whole network analyses reveal modules in gene network controlling LRP development. (A) Two modules described in (Lavenus et al., 2015) obtained from a list of 128 genes. (C) Three modules obtained from a list of 307 genes. In both network, blue edges represent inhibitory interaction, and red edges stimulatory interaction.

Genes in the first module can repress meristematic genes and patterning genes in the second module. Therefore, it is postulated that the two modules mutually inhibit each other to define two spatial domains of the developing LRP: the ARF7-ARF19 module for the flank, and the ARF5 module for the center (Lavenus et al., 2015).

The gene list used for TDCor inference grows gradually as new genes are added to see their predicted position in the network. To see if the two-module topology of the whole network

is still the case for the new gene list, we used TDCor output on the list of 307 genes and performed the same modular analysis on the inferred topology. Genes were considered one by one and from the sign of their predicted interactions, were grouped into three distinct submodules. Most of the genes clearly belonged to one of the two first sub-modules defined by intra-group positive gene-to-gene interactions, and negative interactions with genes of the other module (Lavenus et al., 2015). A small subset of genes did not display such clear organization of their interactions and were grouped in a third group. In general, the modularity of the whole-network topology still exists with one module having ARF7 and ARF19, and another having MP/ARF5, ARF6, and ARF8 and their downstream genes (Figure 4.6B). The prominent difference compared to the network from the 128-gene list is the growth in size of the third module that interacts both positively and negatively with the other two modules.

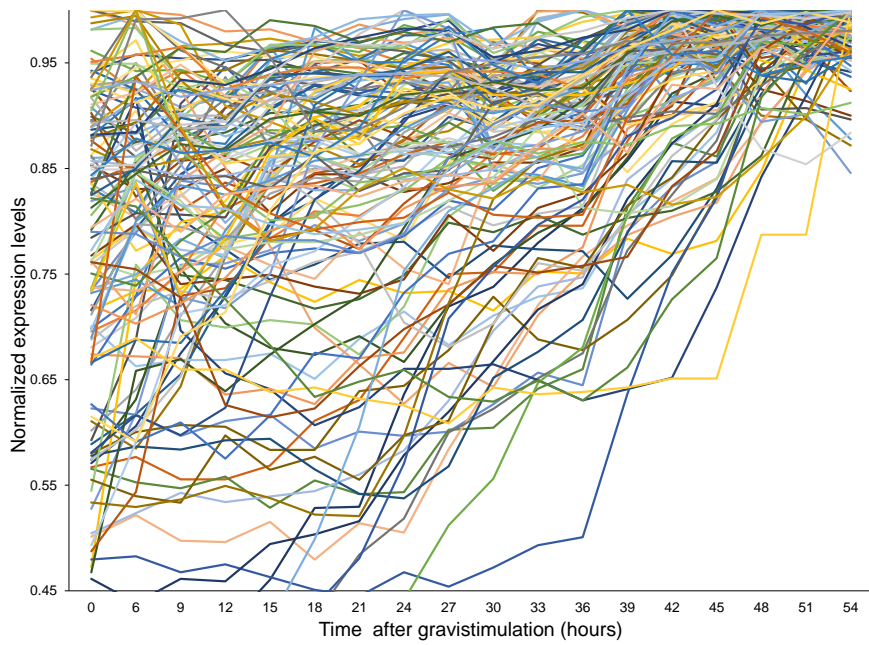
To understand better the kinetics of the genes in the 3 modules, their expression profiles during LRP formation were plotted. Genes in the ARF7 module (149 genes) were expressed early during LRP formation with 142 genes whose expression reached a peak between 0–30 hours post gravistimulation. On the contrary 135 genes in ARF5 module generally displayed contrasting behaviors since most of them (125 genes) reached a peak in expression at 30 hpg. Genes in the third module reach a peak both before and after the point of 30 hpg (Figure 4.7). The big picture of the whole network controlling LRP formation is now expanded. Lavenus et al., (2015) proposed that the ARF7 and ARF5 modules control LRP boundary and LRP meristem formation, respectively. This current network analysis rather suggests that the ARF7 and ARF5 modules constitute two big waves or series of gene expression with the point of transition around 30 hpg. ARF7 module would be responsible for LRP initiation and early development, and this is supported by experimental data showing the roles of ARF7, ARF19, and LBD targets genes in early steps of LRP development (Okushima et al., 2007; Goh et al., 2012a). On the other hand the ARF5 module would be responsible for meristem formation and LRP emergence, and this is also supported by the LRP developmental defects displayed by PLT mutants (Hofhuis et al., 2013; Du and Scheres, 2017b). If we considered that peaks in gene expression could be related to the functional importance of the corresponding gene product at that stage, and considering that genes in the third group can mediate indirect positive interactions from genes of the “early” ARF7-containing group to the “late” ARF5-containing group, the transition between the two big waves of gene expression could be mediated by genes in the third group.



ARF7 module

Number of genes: 149

No. of genes that reach a peak:	
within 30h	142
after 30h	7



ARF5 module

Number of genes: 145

No. of genes that reach a peak:	
within 30h	10
after 30h	135

**Figure 4.7.** Expression profiles extracted from the LR dataset of the genes in the three modules based on the TDCor inference for the new gene list consisting of 307 genes.

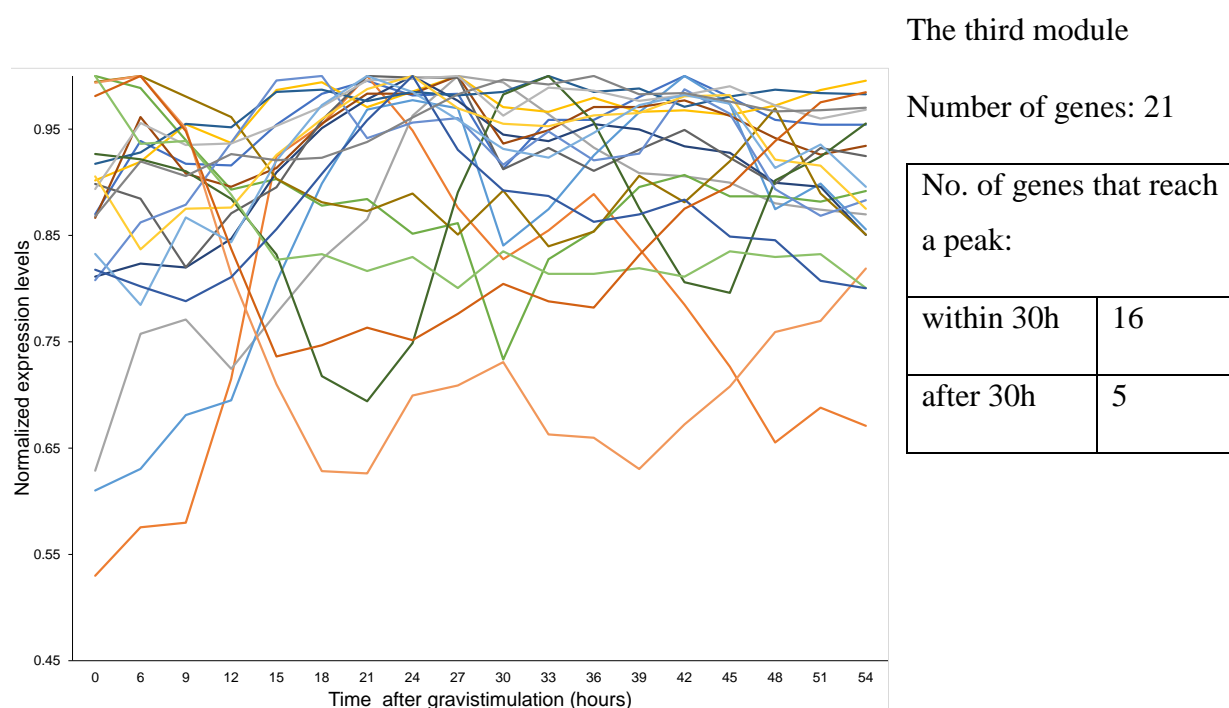


**Figure 4.7 (cont.).** Expression profiles extracted from the LR dataset of the genes in the three modules based on the TDCor inference for the new gene list consisting of 307 genes.

At 30 hpg LRPs experience a critical developmental event when they move from stage IV to stage V and concomitantly cross the endodermis (Voß et al., 2015; Goh et al., 2016). It is known that LRPs of these stages display a profound change in tissue organization and function. For example, a simple layered tissue organization is replaced by a more complex patterning at stage V (Malamy and Benfey, 1997), stage III-V or older LRPs can grow autonomously in auxin-free media while younger LRPs cannot (Laskowski et al., 1995), and expression of markers of LRP quiescent center is detected at the transition from stage IV to V (Goh et al., 2016). Last, we observed that WT roots occasionally produce delayed LRPs which seem to be unable to emerge, and most of these LRPs are at stages younger than V, supporting the essential of progressing to stage V in LRP development (Chapter III, this manuscript).

A closer look at the expression profiles of these 21 genes in the third module (Figure S4.3) showed that many of them display expression kinetics featuring two close peaks with a lower point at or around 30hpg. These 11 genes are *AT5G06270*, *BEL1*, *CLV1-like 4*, *CPC*, *CRF1*, *CRF12*, *IAA12/BDL*, *LAX3*, *LBD4*, *MYB52*, *MYB56*, *SARK*, *TTL1* and *WOX11* (less clear). The other genes displayed one major peak in expression that appeared close to around 30hpg (*JMJ30*, *TMO6* and *WOX14*) or displayed an increase in expression levels after 30hpg (*CLE2*, *CRF2*, *CRF3*, *MYB36* and *WOX11*).

The whole-network topology analysis described above reveals the possible roles of the third module in mediating the transition from the ARF7 wave to the ARF5 wave. Investigating the roles of these genes in LRP formation may reveal new factors involved in LRP development, and moreover, identify key genes regulating the formation of the meristematic domain of the developing LRP. Literature mining was performed for each of the 21 genes belonging to the third group in order to assess their relevance as putative regulators of the meristematic transition during LRP development.

The TF MYB36 was found to regulate some genes involved in reactive oxygen species (ROS) balance during LRP development (Fernández-Marcos et al., 2017). The translational fusion *MYB36-GFP* that rescues *myb36* phenotype is expressed specifically at the boundary (flanks) of the developing LRP from stage V onwards while no expression was detected in LRPs of earlier stages (Fernández-Marcos et al., 2017). The mutants display more cell division in the boundary of stage V LRPs resulting to wider and flatter LRPs. However, intriguingly, the effects were already seen in stage IV LRPs, and the mutant roots accumulate a higher percentage of stage IV LRPs suggesting that *myb36* LRPs have troubles transitioning from flat- to domed-shaped organization (Fernández-Marcos et al., 2017). It is therefore possible that *MYB36* is expressed earlier (from stage IV for example) but at an undetectable level (using the reporter line) during LRP development. In the LR dataset, *MYB36* expression reduced sharply in the first hours to a stable but low level then increased again (Figure S4.3). *MYB36* is a good example suggesting that tightly regulating cell divisions in the LRP boundary may greatly impact overall LRP development. It would be interesting to investigate in detail the kinetics of *myb36* LRP development as well as the organization of the LRP central domain and its function to see to what extent the defect in the boundary leads to disturbance in the central domain and trouble in overall LRP development.

*MYB56 (BRAVO)* has not been described in LR development, but it plays important roles in regulating primary root stem cells. In primary root apical meristem, its expression is confined to the QC cells and vascular initials. In this context, MYB56 negatively regulates QC divisions possibly by repressing cell cycle regulators (Vilarrasa-Blasi et al., 2014).

Roles of *CRF1* and *CRF12* in LR development are currently unknown, but other members of the Arabidopsis CRF gene family are involved in the root branching process. In particular, *CRF2* and *CRF3* are expressed throughout LRP formation, and loss-of-function or gain-of-function of these genes reduces or increase LR density, respectively (Jeon et al., 2016). Interestingly, gravistimulation assay indicated that LRPs of *crf2* and *crf3* are defective in LRP progression; at 54 hours after gravistimulation, while 30% of WT LRPs emerge, less than 5% of *crf3* and *crf2 crf3* LRPs reach the same stage, and a majority of un-emerged LRPs stay at stage V

(Jeon et al., 2016). Unfortunately, the authors did not report the morphology of the mutant LRPs. In the LR dataset, *CRF3* and *MYB36* display similar expression profiles (Figure S4.3), therefore possibly *CRF3* is also involved in LRP morphology. Nevertheless, given that CRF genes regulate many aspects of plant growth and development, and that both *CRF1* and *CRF12* are highly expressed in LRPs (eFP browser), it is likely that these genes are also involved in LRP development.

The *CLAVATA3 (CLV3)/EMBRYO SURROUNDING REGION (ESR)-RELATED (CLE)* gene family encodes for small peptides that have various functions in plant development, including root apical meristem maintenance and LR development (Kucukoglu and Nilsson, 2015; Yamaguchi et al., 2016). For example, *cle1* mutants have increased rate of LRP emergence in nitrate-supplemented medium (Araya et al., 2014). *CLE-LIKE* peptides also regulate LRP development as described for RGF8/CLEL2 above (Fernandez et al., 2015).

However, it should be noted that the LR dataset is not absolutely specific for LRP development because the materials used for transcriptomics contained developing LRPs and their surrounding tissues. Therefore, dynamics of genes in the third module may reflect other events than LRP organogenesis. For example, *LAX3* is not expressed in developing LRPs and in the LR dataset it reached a peak just before 30hpg and around 40hpg, most likely to assist with the emergence of LRPs through overlying tissues (Swarup et al., 2008; Porco et al., 2016). Similarly, *AT5G06270* and *CPC* are known for regulating root hair formation (Wu and Citovsky, 2017; Wada et al., 2002), and they may have no functions in LRP development. Functions in the root development and/or meristem formation/maintenance of the remaining genes in the module 3 are given in the table S4.1. The table also presents LRP-specific expression of these genes obtained from the cell-type specific transcriptomic dataset generated by (Brady et al., 2007) and visualized in the eFP browser (Waese et al., 2017). However, from the description of the materials used to generate this cell-type specific transcriptomic dataset (see Chapter V Materials and methods), it is very likely that this dataset only reflects the transcriptomic landscape of young LRPs (probably before the onset of a stem cell niche). Nevertheless, *JMJ30* was suggested to be involved in LR and callus formation (Lee et al., 2018b), and *SARK/CIK3* negatively regulates shoot apical meristem formation (Hu et al., 2018) and also functions in apical root meristem maintenance (Xiaoping Gou, personal communication).

In summary, whole network analysis suggests that there exist two major waves of gene expression during LRP development; one regulating LRP initiation and early development, and the other meristem formation and emergence. The transition between these two sequences could be mediated by a smaller gene module. This third gene module may play important roles in

initiating meristem formation or stem cell niche establishment during LRP development. Several genes in the module 3 were selected to explore further their roles in LRP development, including *MYB56* and *CRF* genes.

### 2.2.2. Lateral root phenotype of some selected mutants

Several mutants of genes in the third module have been collected. Preliminary gravistimulation assay for 48 hours was performed to the mutants of *MYB56* and *CRFs* to assess their LRP developmental progression.

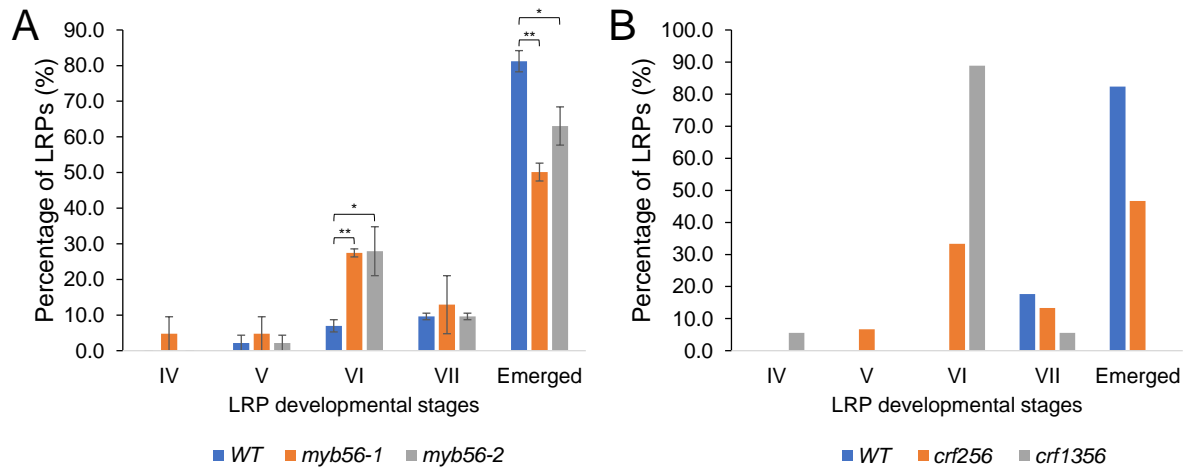


**Figure 4.8.** Lateral root phenotype of some mutants of genes in the 3<sup>rd</sup> module. (A) Developmental stages of LRPs of WT and *myb56* seedlings gravistimulated for 48 hours. 2 biological replicates; n = 20-26 seedlings for each genotype each repeat. Data are represented as Mean  $\pm$  SEM of two biological replicates. Significance was determined by Student's t test. \*  $p < 0.05$ , \*\*  $p < 0.01$ . (B) The same assay for *crf* mutants. 1 replicate; n = 15-18 seedlings.

The assays showed that *myb56* mutants was moderately defective in LRP emergence, with *myb56-1* seemed to have a stronger phenotype (Figure 4.8). At 48hpg, while ~ 80% of WT LRPs had emerged, only ~ 50% of *myb56* LRPs did so. The triple mutant *crf2,5,6* showed a similar phenotype to *myb56* mutant. The quadruple mutant *crf1,3,5,6* displayed the strongest phenotype when none of LRPs emerged at 48hpg.

The anatomy of LRPs in these mutants needs to be further studied, probably under a confocal microscope with the help of a membrane staining to see whether an anatomical defect is visible. Tracking the expression pattern of QC-specific markers like *WOX5* and *QC25* will be also necessary to understand their possible roles in regulating stem cell niche establishment.

In short, the preliminary results showed that *MYB56* and *CRF* genes may positively regulate LRP development, and are interesting candidates for the transition from the early, morphogenetic phase to the late meristem organization phase.

### III. DISCUSSION AND PERSPECTIVES

Here, I attempted to identify potential regulators of meristem formation during LRP development. It has been shown that the onset of QC, which is the organizer of the root meristem, is detected, as reported by QC-specific markers *QC25* and *WOX5*, when the developing LRP transitions from stage IV to V and crosses the endodermis (Goh et al., 2016). We therefore know that a marker of QC formation is available, and the developmental stage where QC formation happens. We used this information, coupled with the network inference from the LR dataset by TDCor, to look for the potential regulators.

In the first approach, I used *PI* as a marker of QC formation and identified several genes potentially regulating *PI* expression during LRP development. *PLTs* were placed as direct regulators of *PI*, which is consistent with their critical roles during LRP formation and meristem establishment (Du and Scheres, 2017b). *KANADI* and Class III HD-Zip genes were also predicted to control *PI* expression dynamics. Their expression and functions in LR formation as well as in primary root growth has been described (Bowman, 2004). Reduced primary root length (possibly due to lower apical meristem activity) was observed in both *KAN1* and *PHB* gain-of-function mutants. The triple mutants *phb-6 phv-5 rev-9* and *kan1-2 kan2-1 kan3-1* have shorter primary roots and a lower LR density (Bowman, 2004). However, the morphology and developmental progression of LRPs in these mutants were not reported. I collected some mutants of *KAN* and Class III HD-Zip genes for a preliminary LR phenotyping and observed that the overall root system as well as LRP emergence rate of these mutants were not affected. No defects in emerging LRP morphology were noted neither. Either these genes may not actually control LRP development, or alternatively, functional redundancy may preclude the detection of phenotypical alterations in loss of function mutants. Here I have not provided the LR development phenotype of the loss-of-function mutant of *KAN4* which is predicted as direct regulator of *PI*. The mutant has been collected and will be studied.

In the second approach, the whole network analysis revealed that there are two big “waves” of gene expression during LRP formation. Some genes of the early wave (*ARF7* module) display experimentally supported roles in LRP formation and early development, and while some members of the second wave are known to regulate meristem formation and LRP emergence. The transition between the two waves happens at around 30hpg, corresponding to stage IV-V LRPs,

and could be mediated by some genes belonging to a third module. Literature review agrees with this idea since several genes in the module play important roles in LRP morphogenesis, developmental progression and meristem maintenance such as *MYB56*, *MYB36*, *CRF* family and *SARK (CIK)* family. Our preliminary data showed that mutants of *MYB56* and *CRFs* displayed a delayed LRP emergence (Figure 4.8). Their precise roles during LRP development and especially meristem formation are worth exploring.

To explore the role of the genes mentioned above in LRP meristem establishment, several experiments can be done. First, gravistimulation assays on mutant roots should be able to tell if a gene or a group of genes is important for LRP developmental progression. Since meristem formation is initiated at around stage V, one would expect that for example in mutants of genes positively regulating meristem formation, LRPs have some difficulty passing that stage, which eventually leads to delayed LRP emergence. For example, mutants in *CRF* genes were delayed in LRP emergence (Figure 4.8) which is consistent with previous data (Jeon et al., 2016). Second, LRP morphology and expression pattern analysis of QC-specific markers such as *QC25::CFP* and *PI::GFP* in the mutant(s) should demonstrate whether the corresponding genes(s) is involved in activating and/or maintaining meristem formation/activity. Other markers of LRP meristem such as *PLTs* can also be used. Expression levels and patterns of meristematic genes like *WOX5::GFP* and *PLTs* on these mutants can also be tested to provide more support. Last, the role of these corresponding genes in establishing LR meristem can be further supported by the analysis of their spatiotemporal expression patterns which can possibly show that their expression precedes in time and space *PI* expression.

When a suitable mutant is identified, a rescue experiment may be needed to concretely demonstrate that the corresponding genes, or precisely the lack thereof, are responsible for the phenotype. The rescue experiment can be done using the concerned genes, or using key genes in LRP meristem formation such as *PLTs* if there is evidence for the link between *PLTs* and those genes. Since *PLTs* are major nodes in the subnetwork of *PI*, it is very likely that they would interact with other regulators.

To demonstrate the power or the influence of these potential regulators, an ectopic expression experiment can be done. For example, these genes can be expressed in the LRP boundary instead of in their native position that is probably in the central cells/meristematic domain. Several genes showing LRP boundary-specific expression domain have been identified such as *MYB36* (Fernández-Marcos et al., 2017). A similar experiment has been done with *PLT2* when its ectopic expression converts the shoot apex into roots (Galinha et al., 2007). Similarly, using a boundary-specific promoter to drive the expression of identified regulator(s) may result in

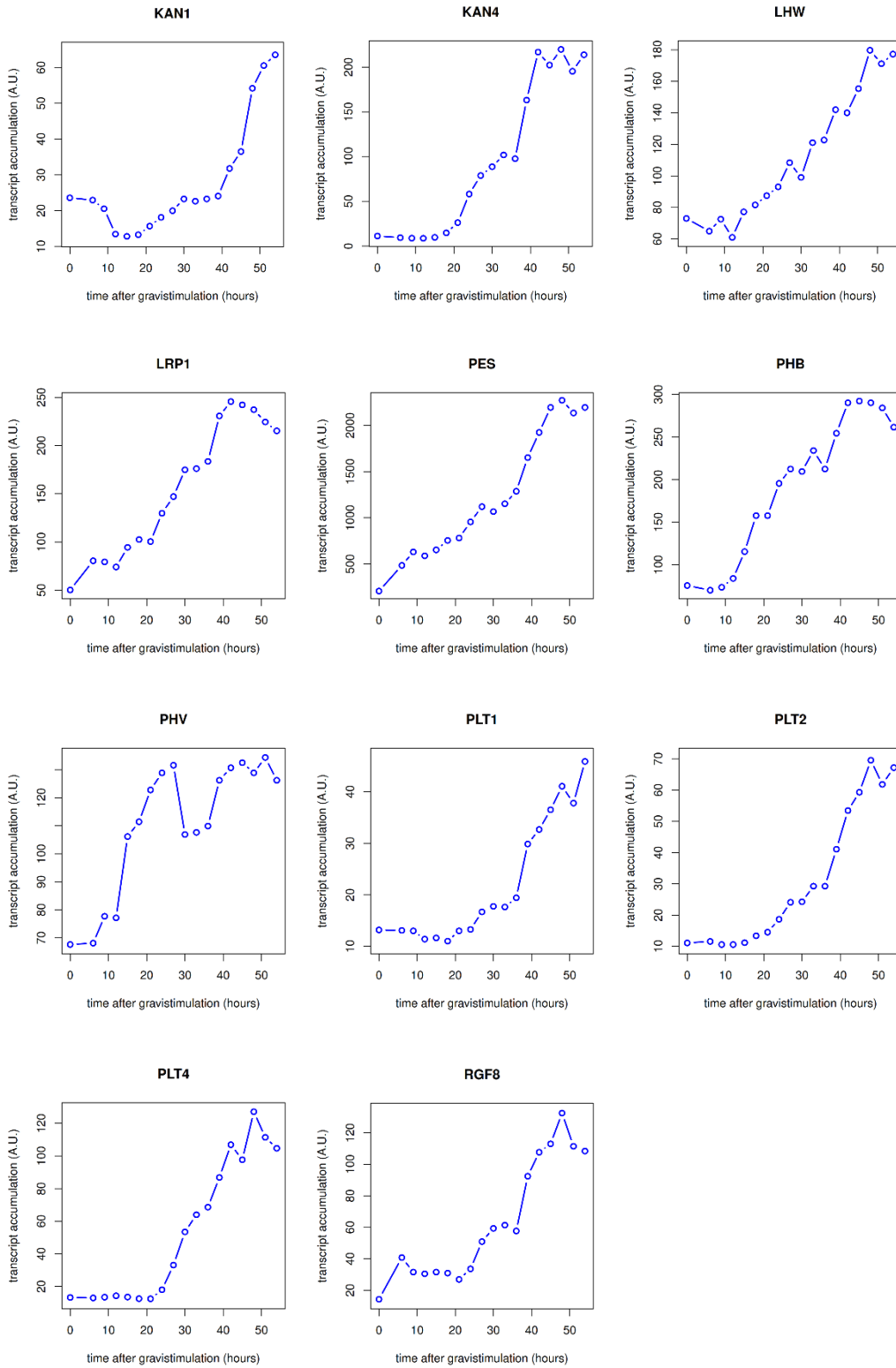
the onset of meristem formation in the boundary (visualized through QC-specific marker, for example).

One major difficulty in the project is a redundancy in function of closely related genes which we may have experienced with single mutants of *KAN*, *PHB* and *LHL* genes. Other interesting genes also have many sisters such as *CRF* and *SARK*. Higher order mutants are therefore essential for further experiments.

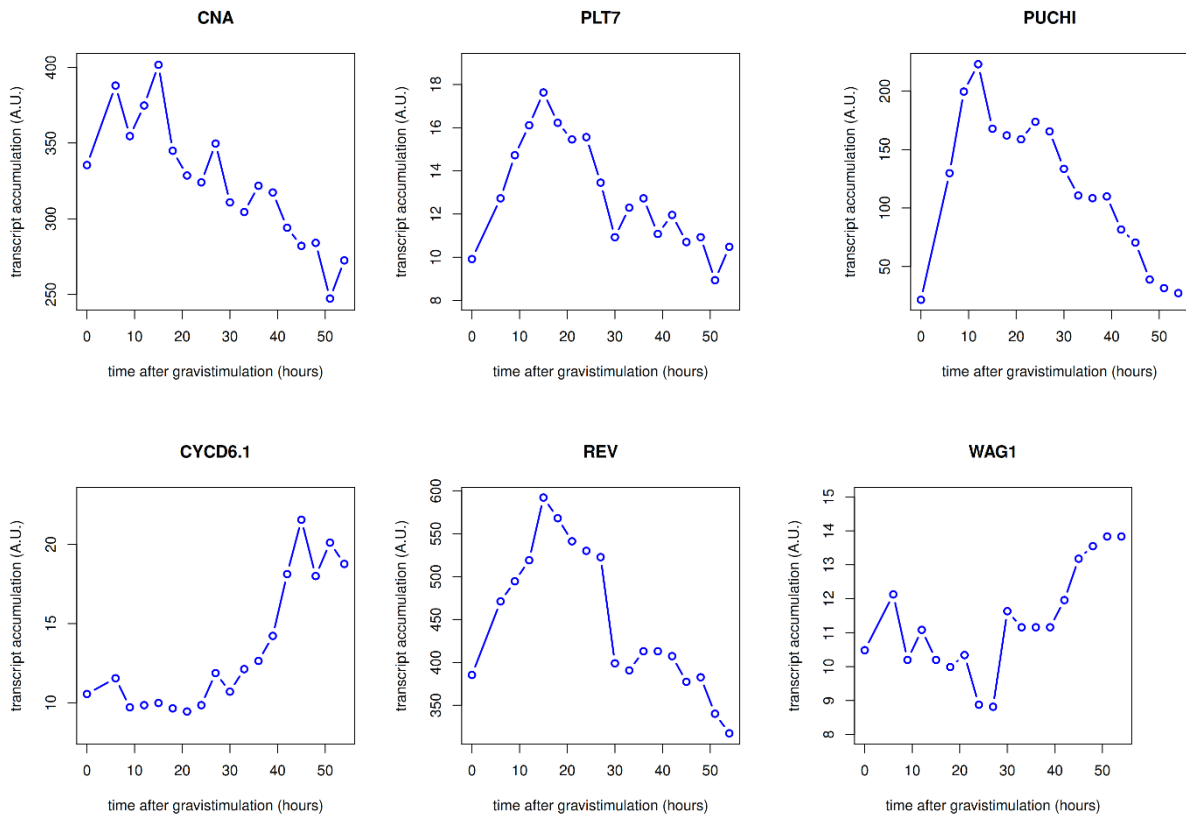
Functions of *PI* and its predicted regulation on its targets during LRP development (Figure 4.4B) are also worth investigating. A detailed LR phenotyping of *pistillata* mutants should be done to reveal its potential role in LR development. The heterozygous mutant *pistillata-1* has been collected for this purpose (Lamb and Irish, 2003). The predicted regulation of *PI* on its targets can then be tested using expression levels (qRT-PCR) and expression pattern analysis (GUS or fluorescence reporter lines).

In conclusion, gene network analysis proposed many interesting potential regulators of meristem formation/stem cell niche during LRP development, such as *KAN* and Class III HD-Zip genes, *MYB56* and *CRF* gene family. Preliminary phenotyping will be needed to narrow down the choices and higher order mutants would likely need to be produced. Functions of the regulators of interest in stem cell niche establishment would be explored through expression of QC- and other markers in the corresponding mutants and ectopic expression of these regulators.

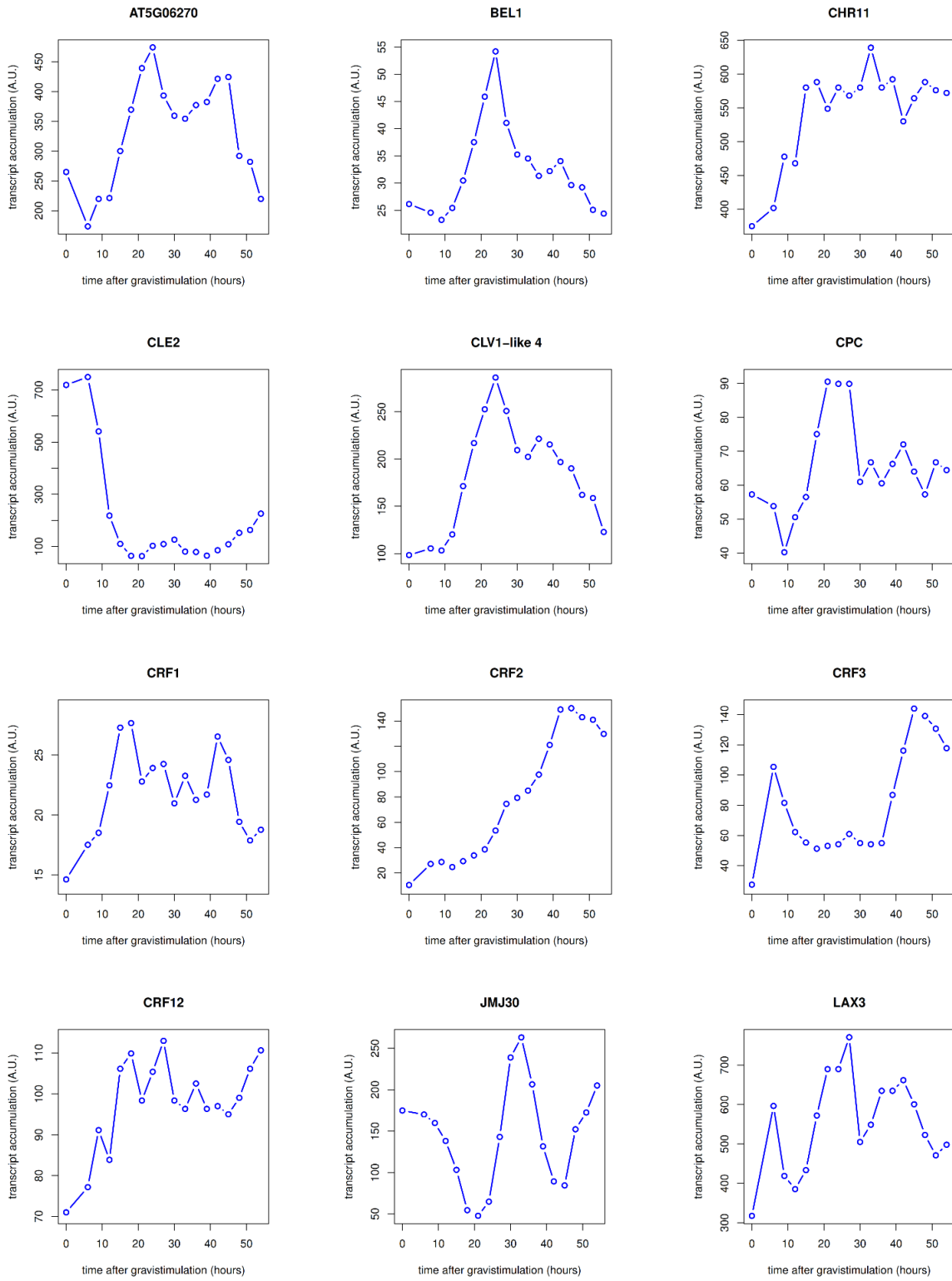
## SUPPLEMENTAL FIGURES



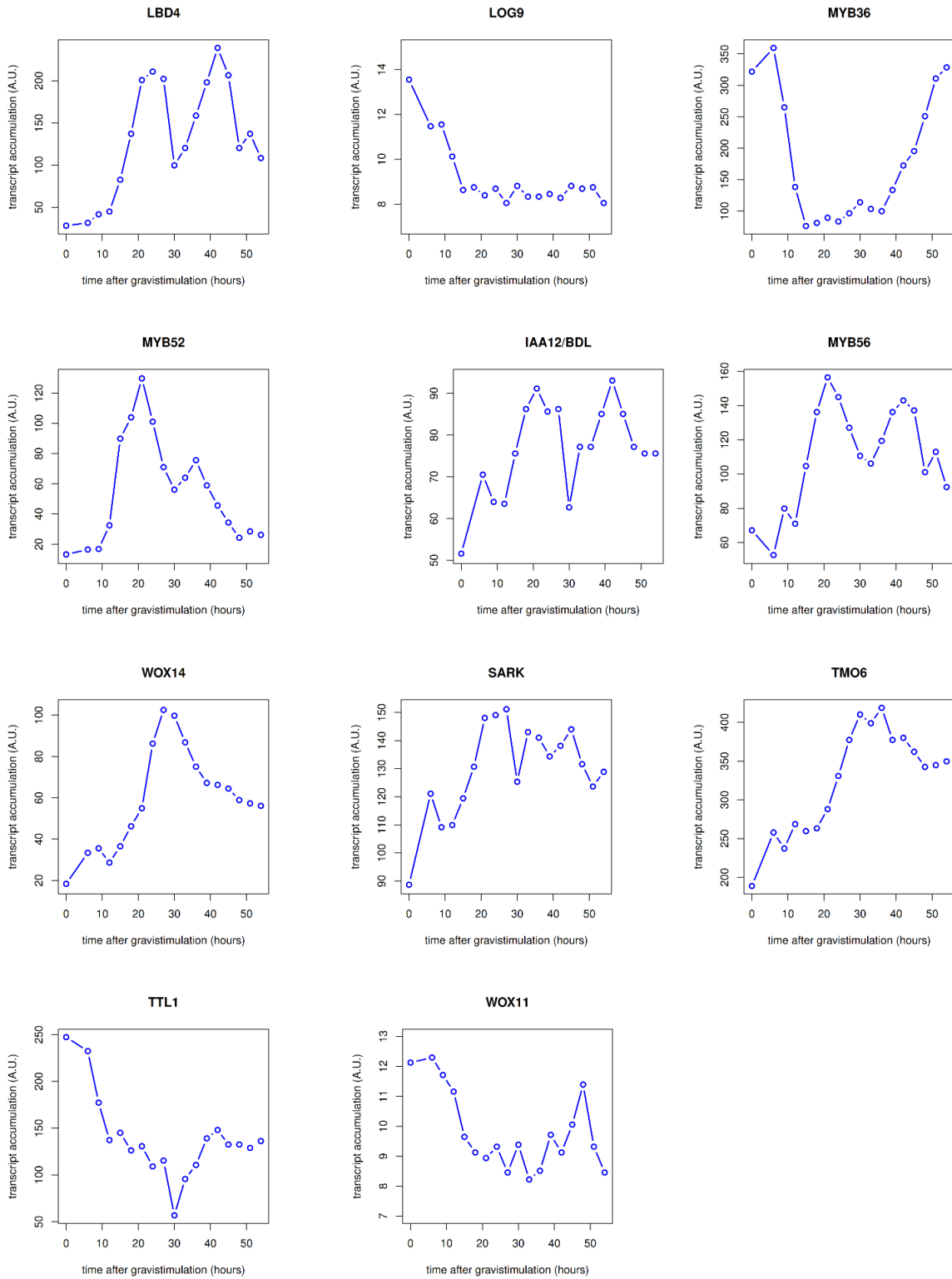
**Figure S4.1.** Expression profiles in the LR dataset of some predicted regulators of *PISTILLATA* selected from Figure 4.4B.



**Figure S4.2.** Expression profiles in the LR dataset of some predicted targets of *PISTILLATA* selected from Figure 4.4B.

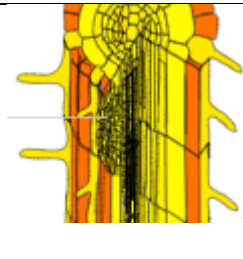
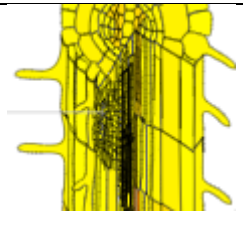
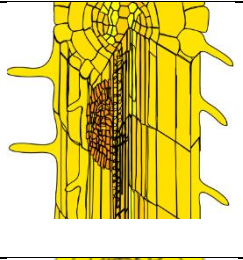
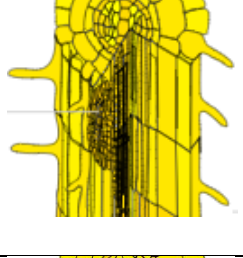
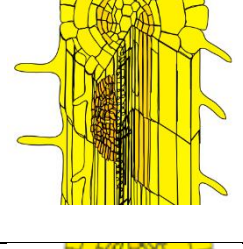
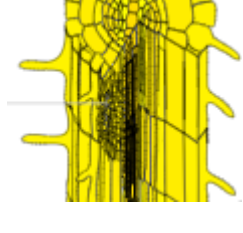


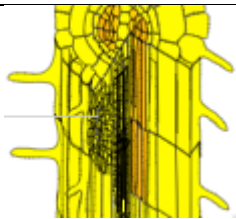
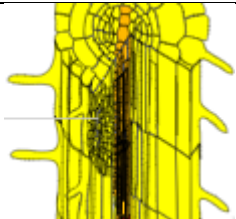
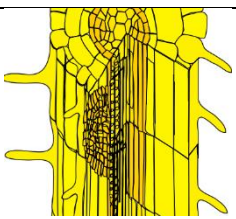
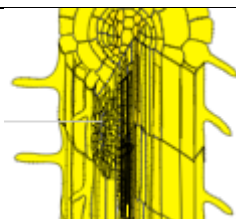
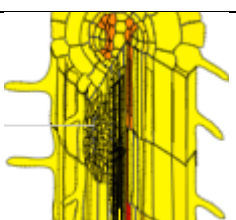
**Figure S4.3.** Expression profiles of genes in the third module in the LR dataset. (to be continued)



**Figure S4.3 (cont.).** Expression profiles of genes in the third module in the LR dataset.

**Table S1.** Functions and expression in eFP browser of several genes in the third module

Gene	Functions in LR development and/or meristem formation	Expression in the eFP browser (Waese et al., 2017)
AT5G06270	Unknown; negatively regulates root hair formation (Wu and Citovsky, 2017)	
BEL1	Required for the correct polarity of PIN1 in ovule development (Bencivenga et al., 2012)	
<i>CHR11</i>	Unknown	
<i>CPC</i>	Unknown; positively regulates root hair formation (Wada et al., 2002)	
<i>JMJ30</i>	Binds to the promoters of <i>LBD16</i> and <i>LBD29</i> to activates their expression; <i>jmj30</i> has reduced callus formation; Double mutant <i>jmj30 atxr2</i> displays a slightly reduced number of LRs (Lee et al., 2018b)	
LBD4	Unknown	

LOG9	Unknown; however, other LOG genes are known to be required for cytokinin production to maintain primary root meristem (Tokunaga et al., 2012).	
MYB52	Unknown; Repressor of the lignin biosynthesis in the cell wall (Cassan-Wang et al., 2013)	
TMO6	Partially rescued the rootless seedlings of <i>arf5/mp</i> mutant; Expressed specifically in vascular tissues (Schlereth et al., 2010)	
SARK/ CIK3	Regulates shoot meristem homeostasis as the mutants have significantly enlarged shoot apical meristem; required for CLAVATA (Hu et al., 2018) and CLE sensing in the root (Anne et al., 2018). Also involved in meristem function in the primary root (Xiaoping Gou, personal communication)	
WOX11	Upregulates <i>LBD16</i> and <i>LBD29</i> expression to stimulate adventitious root and callus formation (Liu et al., 2014, 2018; Sheng et al., 2017b)	
WOX14	Unknown; However, it promotes vascular cell division in the stem.	



# **CHAPTER V**

## **General discussions and perspectives**

The overall objective of the thesis was to understand genetic network(s) regulating LRP formation in *Arabidopsis thaliana*. Most of the work was focused on the transcription factor *PUCHI* and its predicted targets. We have first showed that *PUCHI* regulates multiple aspects of LRP formation and development. Very long chain fatty acid biosynthesis pathway was proposed as targets of *PUCHI* during the process and we have gathered a strong body of evidence to support the hypothesis. Last, the genetic network that may regulates quiescent center establishment/meristem formation during LRP development has been preliminarily explored.

In each chapter, we have discussed in detail the relevance of our findings and their pertinent relation with current knowledge on the corresponding subject. Here we make a summary of key findings and provide some broad discussions and perspectives.

### **I. *PUCHI* controls multiple aspects of plant development partially via regulating VLCFA biosynthesis**

*PUCHI* function as a negative regulator of cell division in LRPs has been described more than 10 years ago (Hirota et al., 2007). Since then, little progress has been made to understand its mechanism of action and regulation. (Kang et al., 2013) showed that *puchi-1* mutant has increased LRP density. (Toyokura et al., 2018) recently identified a genetic cascade *LBD16 - TOLS2-RLK7 - PUCHI* that is involved in LR founder cell specification and LR spacing. *PUCHI* is also directly regulated by *LBD16* (Tatsuaki Goh, personal communication).

In the above ground parts, *PUCHI* negatively regulates the conversion of secondary inflorescences into flowers as the *puchi* mutants have more secondary inflorescences (Karim et al., 2009). *puchi* flowers also have rudimentary bracts at the base of their pedicels. *PUCHI* may act together with other transcription factors (TFs) like *BLADE-ON-PETIOLE1 (BOP1)*, *BOP2*, *DORNRÖSCHEN (DRN)* and *DORNRÖSCHEN-LIKE (DRNL)* to establish floral meristem identity, possibly through regulation of the master regulator of floral meristem identity *LEAFY* (Karim et al., 2009; Chandler and Werr, 2017).

In the LRP development context, I showed that *PUCHI* regulates important aspects including (i) LRP initiation and spacing, (ii) LRP developmental progression, (iii) QC establishment and (iv) LRP cell division pattern (Chapter II).

*puchi-1* mutant had increased LRP density and produced more LRP clusters, probably through regulating founder cell specification as described in Toyokura et al. (2018). Our gravistimulation assays showed that *puchi-1* LRPs needed more time to cross the epidermis, and many LRPs in *puchi-1* roots were arrested. This possibly because their LRPs are wider and flatter (Hirota et al., 2007), making it more difficult to go through overlaying tissues, especially the

endodermis which is more rigid due to the presence of the suberin and Casparian strip (Geldner, 2013b). The coordination between LRP growth and cell wall remodeling in overlaying tissues may also contribute to the delay in *puchi-1* LRP progression.

*puchi-1* LRPs are misshaped and delayed in development, so we were curious about stem cell niche/quiescence center (QC) establishment in the mutant LRPs. QC-specific markers such as *WOX5::GFP* and *QC25::CFP* has been used to track the formation of putative QC in LRPs. Goh et al. (2016) showed that the onset of *WOX5::GFP* and *QC25::CFP* expression was observed in four central cells when LRPs transition from stage IV to V, coincident with their cross through the endodermis and the change from bilateral symmetry to radial symmetry in LRP tissue organization. In *puchi-1* background, however, we observed the expression of *QC25::CFP* in LRPs of early stages (stage II for example) and in much broader domain. The data suggests that QC onset is mis-regulated in *puchi-1* LRPs. The significance of this observation in relation to other defects in *puchi-1* LRPs is worth investigating further. From the work of (Lavenus et al., 2015) and network analyses in Chapter IV, PUCHI was proposed to be a key player in regulating early LRP development and boundary formation, and it may negatively regulates other genes that are involved in meristem formation. It can be imagined that in the mutant, PUCHI is not there anymore to repress the expression of these meristematic genes spatial-temporally. The meristem/QC is therefore initiated earlier and in a broader domain.

Hirota et al. (2007) working on LRPs of early stages showed that *puchi-1* LRPs had additional anticlinal cell division, resulting in wider LRPs compared to the WT ones. Here using *pSHR:SHR-GFP* as a marker of tissue organization, we observed that SHR-GFP signal was displaced by one cell layer, suggesting that PUCHI also regulates periclinal cell division (hence cell division in general). The rudimentary bracts at the base of *puchi-1* flowers are the result of cell proliferation (Karim et al., 2009), which is similar to the ectopic cell division in LRPs (Hirota et al., 2007), suggesting that in both shoot and root, *PUCHI* acts as a negative regulator of cell division. This role of PUCHI is clearer in the callus inducing assay when *puchi-1* roots were treated with a medium consisting of a high level of auxin and lower level of cytokinin, and they produced a continuous line a callus along the primary roots instead of calli with intervals seen in the WT roots. Cytokinin is a known hormone that stimulates cell division in LRPs (Laplaze et al., 2007), and induces a delay in LRP developmental progression (Bielach et al., 2012). Strikingly we observed an earlier and broader cytokinin signaling in young LRPs and in flanks of advanced LRPs, two features not observed in the WT. It is possible that this ectopic cytokinin signaling is responsible at least in part for the *puchi-1* LRP cell proliferation and delayed emergence.

Using the LR dataset and TDCor (Voß et al., 2015; Lavenus et al., 2015), Dr. Julien Lavenus identified VLCFA biosynthesis genes are targets of PUCHI, and he confirmed that in the context of early LRP development, VLCFA expression levels are dependent on PUCHI. In this work, we further demonstrated that PUCHI regulates expression patterns of key VLCFA genes such as *KCR1*, *PAS2*, *PAS1*, *KCS1* and *KCS6* during LRP development. VLCFA mutants displayed similar phenotype to that of PUCHI, including increased LRP density, delayed LRP developmental progression and enhanced callus formation on callus-inducing medium (CIM). *KCS1* (and probably other genes) was also regulated by PUCHI during callus formation. Callus of *puchi-1* and *kcs1-5* also shared a similar VLCFA profile. Altogether, our data strongly support that PUCHI regulates VLCFA biosynthesis genes during LRP and callus formation, and that regulation is functionally relevant and explains at least for a part of *puchi-1* phenotype. A similar regulation of *PUCHI* on VLCFA biosynthesis genes in the two contexts further stresses the observation that callus formation from multiple tissues follows a LR development pathway (Sugimoto et al., 2010), which is also reviewed in the last part of Chapter I.

To more concretely demonstrate that the regulation of PUCHI on VLCFA biosynthesis genes is relevant in LRP and callus formation, complementation experiments are being performed. I am generating transgenic plants (in both WT and *puchi-1* background) that expressing *KCS1* under the drive of *PUCHI* promoter. We chose *KCS1* because *puchi-1* and *kcs1-5* roots have similar root development and callus formation phenotype, and their roots on CIM have similar VLCFA profiles. The transgenic plants will be soon available for study.

Possible modes of action of VLCFAs during LRP development have been discussed in Chapter III. Here I would like to emphasize a link between the positive regulation of PUCHI on VLCFA biosynthesis and cytokinin signaling. Mutants that have reduced VLCFAs biosynthesis usually have elevated cytokinin signaling (Harrar et al., 2003; Nobusawa et al., 2013), and we observed ectopic and enhanced cytokinin signaling in *puchi-1* LRPs where a reduction in VLCFAs biosynthesis is supposed to happen. Theoretically, a cascade linking PUCHI to VLCFAs biosynthesis which in turn inhibits cytokinin signaling during LRP development is possible.

The regulation of PUCHI on VLCFA biosynthesis genes has been well demonstrated, but they probably may not be the only targets of PUCHI. As suggested by the transcriptomic analysis (beginning of chapter III) and as depicted in Figure 3.3, PUCHI may regulates other important genes such as *PTL7*.

## II. TDCor as a hypothesis-generating tool to identify potential genes regulating stem cell niche establishment

Generating a hypothesis is the first important step in doing research. The purpose of building the TDCor algorithm was to infer possible genetic interaction based on the LR dataset and then to construct the global gene network, and from that unknown genetic interactions can be suggested (Lavenus et al., 2015). TDCor was the tool that led to the hypothesis that PUCHI regulates VLCFA biosynthesis genes during LRP development. Although in sciences (except Mathematics and Logic) a hypothesis can never be proved, in Chapter III we have provided a strong body of evidence to support the regulation of PUCHI on VLCFA biosynthesis genes in both LRP and callus formation. This story is inspiring, and it further strengthens our confidence over the TDCor approach and performance.

In term of LR development, the LR dataset and the TDCor program can be used to explore the gene regulatory network of any developmental process given that it is governed by linear gene to gene transcriptional relationships (Lavenus et al., 2015). One just needs to include genes that may be involved in that process into the gene list for TDCor inference.

Likewise, the principle of TDCor (time-delay correlation in gene expression profiles) can be applied to infer gene networks regulating or mediating any biological process such as response of plants to biotic and abiotic stresses. However, to do that a time-series transcriptomic dataset with sufficient resolution (time points) would be needed, and this can be problematic. For example, the dataset may not be able to capture fast transcriptomic responses. Of course, the actual role of these candidate genes would need to be experimentally explored to confirm their hypothetical implication based on correlation between transcriptomic profiles. Setting the correct correlation threshold for maximum efficiency in identifying relevant candidate partner genes may be difficult. In addition, in some situations, complex feedbacks and post-transcriptional regulation may obscure the relationship between two genes.

We are continuing to exploit the TDCor program to have more insight about potential regulators of stem cell niche establishment during LRP development. For that, we used *PISTILLATA (PI)* as a marker of quiescent center onset (which may be a sign of stem cell niche/meristem establishment) because well-known markers such as *WOX5* and *QC25* are not in the LR dataset. We have demonstrated that *PI* has similar expression pattern as *QC25*, hence it is a suitable marker for the QC.

TDCor inference was run on a list of 302 genes that are potentially involved in root development or meristem formation/maintenance, and a network surrounding PI has been

constructed. One key feature of the inferred network was that PLETHORA genes (*PLT1-3*) were predicted to be important positive regulator of the QC, which is consistent with the experimental data (Du and Scheres, 2017b). Other predicted regulators are also known in meristem formation and/or maintenance in other developmental contexts (apical shoots and roots) such as the KANADI genes, Class III HD-Zip genes, *LHW*, *RGF8* and *PES*. The inferred network is therefore likely to contain some relevant biological meanings. Our LR phenotyping of some mutants of these genes have not brought about any peculiar phenotype, probably because these genes act redundantly. Further network inference and target screening is underway which hopefully will provide some new and relevant genes.

We also took another approach to look for potential regulators of QC establishment. Analyzing the whole network inference produced by TDCor, we realized that there may exist two sub-network modules: the first ARF7 module seems to be responsible for LRP initiation and early development, while the second ARF5 module responsible for stem cell niche establishment and further LRP growth. Importantly, the transition from ARF7 module to the ARF5 module may be assisted by the third, smaller module of ~ 20 genes. Literature mining showed that several genes of this module play roles in LRP development and apical meristem maintenance such as *MYB36*, *MYB56*, *CRF1*, *CRF12*, *CLE*, *JMJ30* and *SARK/CIK3*. Our preliminary data showed that *MYB56* and *CRFs* may be involved in LRP developmental progression. Further work on these genes and their mutants will shed light on their potential roles on LRP development and QC establishment.

### **III. Final conclusion**

In conclusion, my Ph.D. work has explored some genetic networks controlling LRP development in *A. thaliana*. I have first described in detail the roles of PUCHI during LRP development through the mutant phenotyping. The predicted network consisting of PUCHI and its targets VLCFA biosynthesis genes has been demonstrated to be true and relevant in both LRP and callus formation contexts. My work has expanded the current knowledge on the roles of VLCFAs in LRP development, and extended the network cascade consisting of ARF7 – LBD16 – TOLS2-RLK7 – PUCHI – VLCFAs that regulates LRP initiation and development. Finally, network analyses have proposed some interesting regulators of LRP stem cell niche establishment/QC onset and they are being experimentally explored. Our work in the future hopefully will reveal new players in that process.

# **CHAPTER VI**

## **Materials and methods**

## 5.1. Plant materials and growth conditions

*Arabidopsis thaliana* seeds were surface-sterilized using sodium dichloroisocyanurate (Sigma Aldrich) solution (0.88% w/v). The sterilizing solution was added to the tube containing *Arabidopsis* seeds, and the tube was regularly inverted for 5-6 minutes. The seeds were then rinsed twice using absolute ethanol and left for drying. Surface-sterilized seeds were placed on squared Petri dishes (~ 0.7 cm between seeds) containing ½ Murashige and Skoog solid medium (0.7% w/v plant agar) supplemented with B5 vitamins (Duchefa). Plates were kept at 4°C for 2 days and then placed in long-day conditions (16-h light/8-h dark cycle) in vertical position. Unless specified, all transgenic lines are in Columbia-0 background.

The *puchi-1* and *pPUCHI::PUCHI:GFP* lines were previously described (Hirota et al., 2007), the *DR5::GFP* synthetic auxin response reporter in (Friml et al., 2003), *pSHR:SHR-GFP* in (Nakajima et al., 2001), *TCSn::GFP* in (Zurcher et al., 2013), and *QC25::CFP* in (ten Hove et al., 2010).

The GUS reporter lines *pKCS1::GUS*, *pKCS6::GUS*, *pKCRI::GUS* and *pECR::GUS* were described in (Joubès et al., 2008), *pKCS20::GUS* in (Lee et al., 2009b), and *pPAS2::GUS* and *pPAS1::GUS* in (Morineau et al., 2016). The *kcs1-5* mutant was described in (Shang et al., 2016), *kcs9* in (Kim et al., 2013) and *kcs2 kcs20* double mutant in (Lee et al., 2009b).

The following transgenic lines were used in Chapter IV: *lhw* (SALK\_079402) (Ohashi-Ito and Bergmann, 2007), *lhw3* (SALK\_126132) (Ohashi-Ito et al., 2013a), *kan-11* (Wu et al., 2008), *kan-12* in Landsberg erecta (Ler) (Kerstetter et al., 2001), *phb-11* in Ler (Prigge et al., 2005), *phb-13 phv-11 cna-2 er-2* (Prigge et al., 2005), *myb56-1* (SALK\_060289), and *myb56-2* (SALK\_062413) (Vilarrasa-Blasi et al., 2014).

PUCHI-GR plants were obtained from Fr. Tatsuaki Goh, Japan. To generate the PUCHI-GR plants, a genomic fragment of PUCHI, including the 3.9 kb promoter region and coding region, was amplified from genomic DNA using primers gPUCHI (5'-CACCCACGAGTGCAATCACACAGA-3') and gPUCHIrev-stop (5'-AAAGACTGAGTAGAAGCCTGTAGTGT-3') and subcloned into pENTR D-TOPO using Gateway technology. The genomic fragment was then transferred to pGWB-GR(C) that contains the Gateway cassette in front of the hormone-binding domain of rat glucocorticoid receptor (GR). The PUCHI-GR construct was transformed into the *puchi-1* mutant by floral dipping (Clough and Bent, 1998).

## 5.2. Bioinformatic analyses

To identify *PUCHI* potential targets based on correlation in expression profiles, an R script was used in combination with the TDCor package (Lavenus et al., 2015) in R using the LR Dataset (Voß et al., 2015).

```
## To search for genes having correlated profiles
load("Path/TDCOREG 5.3.Rdata")
# correlation with time delay
k= as.vector(cor.data(rd[,2:18],rd["AT5G18560",1:17])) # AT5G18560:
PUCHI
names(k)=rownames(rd)
k[k>0.8] # this threshold can be set as desired
write.table(names(k)[k>0.8],"AT5G18560 _cor_80_delay.txt") # found
217 genes in the table
```

GO enrichment analysis for biological processes was done using BiNGO plugin in Cytoscape software (Maere et al., 2005; Shannon, 2003). Parameter of the analysis:

```
Selected statistical test: Hypergeometric test
Selected correction: Benjamini & Hochberg False Discovery Rate (FDR) correction
Selected significance level: 0.05
Testing option: Use whole annotation as reference set
No annotations were retrieved for the following entities: AT1G65820; AT3G56730; AT3G01690;
AT5G39090; AT1G14340; AT1G04040; AT3G01930; AT1G33100 (among 217 genes identified).
```

Expression patterns of interested genes in the root and LRPs were retrieved from the ePlant services (<http://bar.utoronto.ca/eplant/>) which is a tool to display different transcriptomic datasets, particularly the cell type-specific transcriptomic dataset from (Brady et al., 2007). To generate data for all 15 cell types in the primary roots, microarray expression profiles of 19 fluorescently-sorted GFP-marked lines were analyzed (Brady et al., 2007). RM1000 enhancer line was used as a marker for LRPs. Approximately 3/4th of the roots (from the tip upwards) of 5 to 6-day old seedlings were used for generating the data (Brady et al., 2007). Because seedlings of this age

usually have one emerging LRPs, and because only the younger part of the roots were used, then the dataset probably reflects gene expression of young LRPs (probably < stage VI).

### 5.3. Gene expression analyses

RT-PCR analysis was performed on WT and *puchi-1* root materials prepared as previously described (Himanen et al., 2004). Briefly, WT and *puchi-1* seeds were grown on ½ MS supplemented with 5µM naphthylphthalamic acid (NPA; Duchefa) for 14 days to inhibit lateral formation, then the seedlings were transferred to ½ MS supplemented with 5µM NPA to maintain LR formation inhibition in control plants, or alternatively with 10 µM naphthaleneacetic acid (NAA) to synchronously induce lateral root formation. Root materials were harvested after 24 hours and total RNA was extracted for qRT-PCR analysis as instructions of the manufacturer (RNeasy Plant, Qiagen). The normalizing gene used in this analysis was *CYCLIN-DEPENDENT KINASE A;1 (CDKA;1)* (Iwakawa et al., 2006). The calibrator condition corresponds to NPA-treated WT roots. All of the RT-PCR were performed with three biological replicates. Significance was determined by Student's t-test. Primers used are listed in *SI Appendix*, Table S3.

For GUS staining assay, 9-day old seedlings were incubated overnight at 37°C in a phosphate buffer (pH 7) containing 5 mM potassium ferricyanide, 5 mM potassium ferrocyanide and 0.5 mg/mL 5-bromo-4-chloro-3-indolyl-beta-D-glucuronic acid (X-Gluc; Duchefa) dissolved in a small volume of dimethyl sulfoxide (DMSO). Samples were then washed by 70% ethanol, mounted on slides in a chloral hydrate:glycerol:water clearing solution (4:2:1 g/mL/mL) and visualized using DIC microscopy.

To visualize the expression of GFP lines including *pPUCHI::PUCHI:GFP*, *pKCSI:KCSI-GFP*, seedlings were treated (or not) with 15µM propidium iodide (PI) supplemented with 0.004% Triton X-100 for 15-20 min as described in (Du and Scheres, 2017b), and roots were observed under Leica TCS SP8 confocal microscope.

### 5.4. Root phenotyping

For lateral root density phenotyping, 9-day old, vertically grown seedlings were first imaged using a digital camera for root length measurement. Seedlings were then mounted in the clearing solution described above, and the number of developing LRPs, delayed LRPs and emerged LR was counted. Primary root length was measured in the Fiji using the SmartRoot plugin (Schindelin et al., 2012; Lobet et al., 2011).

For the gravistimulation assay, seedlings were first grown in squared petri dishes at near-vertical position for 5 days, then dishes were turned by 90° (Figure 5.1). After 18 or 48 hours,

seedlings were mounted in the clearing solution; LRPs present in the primary root bend were visualized under DIC microscopy and imaged. LRPs were categorized into developmental stages as described in (Malamy and Benfey, 1997).

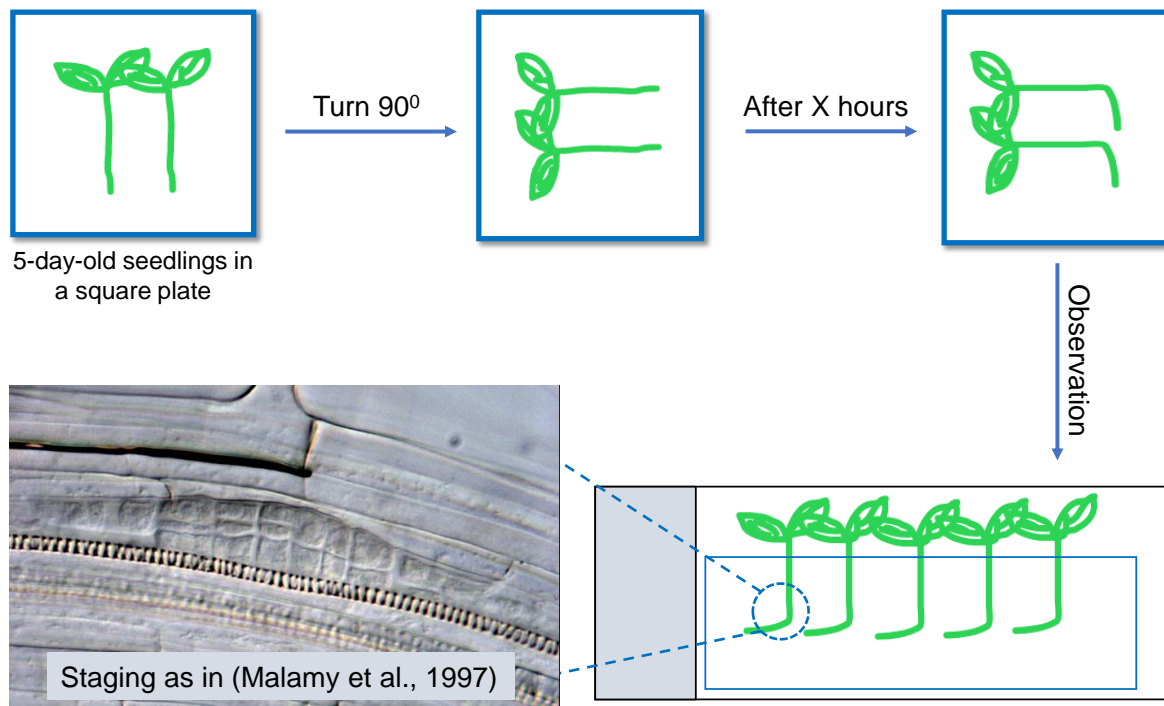


**Figure 5.1.** Illustration of the gravistimulation assay.

For measurement of LR organ spacing distances, roots of 9-day old seedlings were progressively imaged from the collar to the tip under Zeiss AX10 DIC microscope at the magnification of 20x or 40x. These photos were then stitched manually in Microsoft PowerPoint to form a large and coherent image of the corresponding root. The distances between LR organs (including emerged LRs and non-emerged LRPs) were measured on this stitched image using Fiji (Schindelin et al., 2012).

### 5.5. Fluorol yellow staining

Fluorol yellow staining with Arabidopsis seedlings was done according to the protocol obtained from <http://wp.unil.ch/geldnerlab/files/2013/07/Fluorol-Yellow-staining.pdf> which in turn is adapted from (Lux et al., 2005). After staining, WT and *puchi-1* seedlings of comparable lengths were placed side by side and their GFP images were taken progressively from the collar to the suberin onset position. Position of WT and *puchi-1* seedlings on the slide was swapped regularly to prevent any positional effects. GFP intensity of the WT and *puchi-1* roots in each image were then measured using Fiji and the ratio of GFP intensity was calculated as described in <https://theolb.readthedocs.io/en/latest/imaging/measuring-cell-fluorescence-using-imagej.html>

(McCloy et al., 2014). Signal from the background was taken into account when measuring the GFP intensity.

## 5.6. Callus formation phenotyping

Callus formation assay was performed using the callus inducing medium (CIM) as described in (Shang et al., 2016). Seedlings were first grown vertically on 1/2 MS medium for 7 days and then transferred to CIM containing MS medium supplemented with 2.2  $\mu\text{M}$  2,4-D (Sigma Aldrich) and 0.2  $\mu\text{M}$  kinetin (Duchefa) for 4 days. For *pPUCHI::PUCHI-GR/puchi-1* line, seedlings were cultured in 1/2 MS or CIM supplemented with 1  $\mu\text{M}$  dexamethasone.

For measuring callus area, ~ 1 cm of roots incubated for 4 days on CIM were progressively imaged from the collar under a microscope at the magnification of 10x. These photos were then stitched manually in Microsoft PowerPoint to form a large and coherent image of the corresponding root. Callus area of each root was then measured using Fiji (Schindelin et al., 2012). To normalize the data, callus area in a root segment was divided to its corresponding length ( $\mu\text{m}^2/\mu\text{m}$ ).

## 5.7. Organ regeneration assay

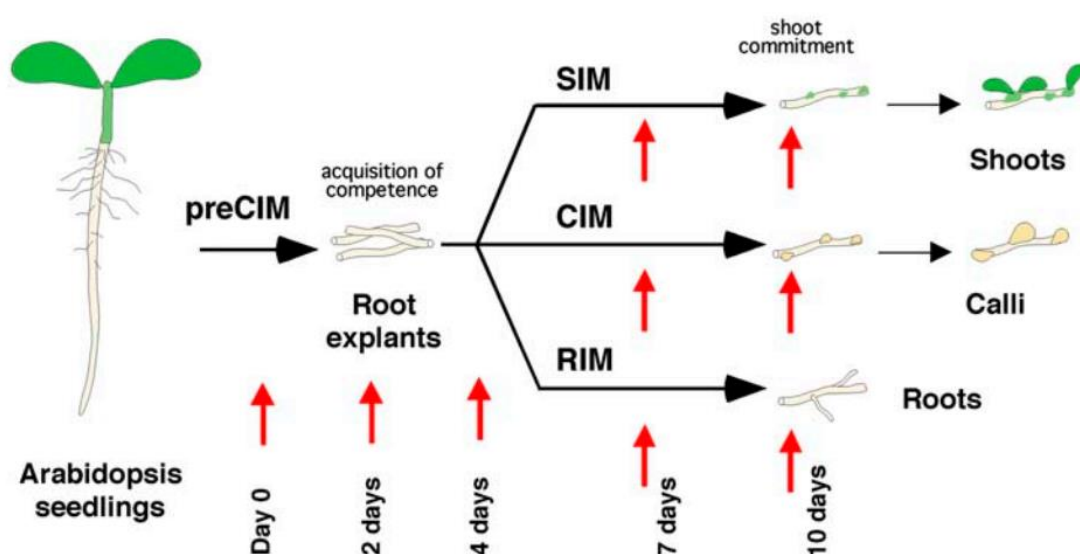


**Figure 5.2.** Outline of organ regeneration assays from callus using root- and shoot-inducing medium provided in (Che et al., 2006). The SIM: MS/2 + 0.9  $\mu\text{M}$  mg/L IAA + 5.0  $\mu\text{M}$  2-ip N<sup>6</sup>-(2-isopentenyl)adenine. The RIM: MS/2 + 0.9  $\mu\text{M}$  mg/L IAA.

Plant regeneration assays were based on the outline in (Che et al., 2006). Seven-day old seedlings on normal MS/2 medium were transferred to the CIM for 4 days. Root segments of these seedlings were then excised and transferred to freshly prepared root- or shoot-inducing medium (RIM and SIM, respectively). The SIM: MS/2 + 0.9  $\mu\text{M}$  mg/L IAA + 5.0  $\mu\text{M}$  2-ip N<sup>6</sup>-(2-

isopentenyl)adenine (Duchefa). The RIM: MS/2 + 0.9  $\mu$ M mg/L IAA (Che et al., 2006). Images of these root segments were taken after several days of incubation (0, 4, 6, 9, 12 days for RIM, for example). Number of adventitious roots produced from each segment were counted and the density of adventitious roots was calculated by dividing the number to the segment length.

### 5.8. Statistical Analysis

All the statistical analyses used in this study were performed by Microsoft Excel and R on two or three biological replicates. Significance was determined by Student's *t*-test, and the star sign was used to denote the *p*-value of the analysis. \*  $P < 0.05$ , \*\*  $P < 0.01$ , \*\*\*  $P < 0.001$ .

### 5.8. Primers

Primers used for genotyping, qRT-PCR and cloning are listed in tables below.

**Table 5.1. Primer for genotyping**

No.	Primer name	Primer sequence (5' – 3')	Usage	Notes
1	GENO- PUCHI-F	CCAAAAAAAAAAGCTTACTCATCATAAGA	PUCHI-F+R1: no band for <i>puchi-1</i> , a band ~ 1085bp for WT  PUCHI-F+R2: a band ~500bp for <i>puchi-1</i> and WT	SALK_0463 93
2	GENO- PUCHI-R1	AGCAGCGATAGAAGAAGAAGATAAA		
3	GENO- PUCHI-R2	TTGGTTGTTATTGTAAGGAGAGACAA		
4	KCS20F1	CGC GGT TCT TGA GAA GAC CGG TGT GA	For WT: R1 + F1  For <i>kcs20</i> : LBaI + F1	(Lee et al., 2009b)
5	KCS20R1	TAA AGA CTA CAA AGC CTG TCA CTG TC		
6	KCS2F1	GGA ACC TTC GAG GAT GAC TTT GAA CC	For WT: R1 + F1  For <i>kcs2</i> : LBaI + R1	
7	KCS2R1	CCC CTT CGA GAT TCC GTT ATC TTT TG		
8	<i>kcs1-5</i> LP	TGCTCTGACAATGGAAGAACC	For WT: LP + RP  For <i>kcs1-5</i> : RP + LBb1.3	SALK_2008 39
9	<i>kcs1-5</i> RP	TTCATCATCGGCCGTTATAAG		
10	<i>pas1-4</i> LP	GCAATCAGGTCACACCAGATC	For WT: LP + RP  For <i>pas1-4</i> : RP + LBb1.3	<i>pas1-4</i>  SALK_0513 24
11	<i>pas1-4</i> LP	CGACCATTTCCTCTTCCTTTC		

Chapter VI: Materials and methods

12	ECR-5'	CATGAAGGTCACCGTCGTCTCCC	5' + 3': no band for <i>cer10-2</i> ; band ~ 1800bp for WT  5'+ LB4-R: band ~ 700bp for <i>cer10-2</i> , no band for WT	Salk_088645  ( <i>cer10-2</i> )
13	ECR-3'	CTAAAGGAATGGAGGAAGTATCAC		
14	LG79-PTPLA-F	CCGTGAAGCTTCTTCGATTT	LG79 + LG103: A band for WT, no band for <i>ptpla</i>	(Morineau et al., 2016)
15	LG103-PTPLA-R	GCTTGGTGTATCGGTGAGGT		
16	CM14-ptpla-F	GCCGTGGCTGTCTATAACACTTG	CM14 + Lbb1.3: a band for <i>ptpla</i> , no band for WT	
17	8474-T-DNA	ATAATAACGCTGCGGACATCTACATTT T	8474 + KU11: a band for T-DNA  KU11 + <i>kcs6_geno_R</i> : a band for WT	KABI line: 804G08
18	KU11 - <i>cer6</i>	AACGCCTAATTACTATCAAGGCAA		
19	<i>kcs6_geno_R</i>	TCCACACGGCAGAGTTACAC		
20	LB4-R	GCGTGGACCGCTTGCTGCAACT	To verify T-DNA insertion lines	
21	LBb1.3	ATTTTGCCGATTCGGAAC		
22	kan-12- <i>geno-F</i>	ACCCTTTCTCAACTATCG  TTTTCC	A band ~ 750bp for WT; no band for <i>kan-12</i>	
23	kan-12- <i>geno_R</i>	GTTGGACGATCGGTTGT  TGTT		
24	lhw- <i>geno-LP</i>	GGGCTAAACAAAGACAA  AACG	LP + RP: a band for WT, no band for <i>lhw</i>  RP + LBb1.3: no band for WT, a band for <i>lhw</i>	SALK_0794 02
25	lhw- <i>geno-RP</i>	TTATTCGTCTAGCACCAT  CGG		
26	lh13- <i>geno-LP</i>	TCTCCATTGGTCAGATCT  TGG	LP + RP: a band for WT, no band for <i>lhw</i>	SALK_1261 32

27	lh3-geno-RP	GGTCTTATGCTGTGTTTT GGC	RP + LBb1.3: no band for WT, a band for <i>lhw</i>	
28	mGFP5-FP	CCCAATTCTTGTTGAATTAGATGG	PCR product = 639 pb	
29	mGFP5-RP	GTTACAAACTCAAGAAGGACC		
30	YFP-FP	CTGGTCGAGCTGGACGGCGACG	PCR product = 630 pb	
31	YFP-RP	CACGAACTCCAGCAGGACCATG		

**Table 5.2. Primers for qPCR used in the thesis of Dr. Julien Lavenus (2013).**

No.	Primer name	Primer sequence (5' – 3')
1	CDKA F	ATTGCGTATTGCCACTCTCATAGG
	CDKA R	TCCTGACAGGGATACCGAATGC
2	ECR F	CCTTGACCTCCCCGATTC
	ECR R	CCAGGAGTCACGGGAAGA
3	KCS1 F	CTTGCAACGTGACCACCAT
	KCS1 R	AGCACGGTCCGGTTAAAG
4	KCS2 F	CCATTGATCTCGCTAAACAGC
	KCS2 R	TCGGTCGTTGCCTAAATACC
5	KCS20 F	GCTTAGAGGCAACATTTTGAGC
	KCS20 R	GCGTATGAGTTTGTTGCAC
6	KCR1 F	GCTTAAGAGGAAGAAAGGTGCTATT
	KCR R	CACTTTGTGAACTGATCCACGTA
7	PAS2 F	TCTATGACGCCATTGAGAAGC
	PAS2 R	CAGGAGATCTGACCAAACCTACTAA

# **FRENCH SUMMARY**

## **Le résumé de la thèse en français (page 11 – 34)**

This summary is required by the doctoral school and is written by co-supervisor Dr. Soazig GUYOMARC'H.

**Propriétés du réseau de gènes contrôlant l'organisation  
du primordium de racines latérale chez *Arabidopsis thaliana***

Thèse présentée par **Mr TRINH Duy Chi**, Université de Montpellier,

ED n°584 GAIA, UMR DIADE

**SOMMAIRE**

<b>Chapitre I : Introduction</b> .....	<b>160</b>
<b>Chapitre II : Le facteur de transcription puchi régule l'initiation, le positionnement, l'organisation et l'émergence des racines latérales</b> .....	<b>164</b>
Profil d'expression de PUCHI dans les racines.....	164
PUCHI est requis pour le développement des primordia de racines latérales mais inhibe leur initiation .....	164
PUCHI est requis pour l'organisation anatomique et fonctionnelle normale du primordium de racine latérale .....	166
Conclusion du chapitre II .....	166
<b>Chapitre III : Le facteur de transcription puchi régule la voie de biosynthèse des VLCFA durant la formation des racines latérales et l'induction de la production de cals par le péri-cycle</b> .....	<b>167</b>
L'expression de multiples gènes de biosynthèse des VLCFA semble régulée par PUCHI au cours du développement des racines latérales .....	167
Plusieurs gènes de biosynthèse des VLCFA sont exprimés dans les primordia en développement de façon dépendante de PUCHI.....	168
Des plantes mutantes pour certains gènes de biosynthèse de VLCFA présentent des phénotypes racinaires similaires à puchi-1.....	170
PUCHI et la biosynthèse des VLCFA restreignent la compétence du péri-cycle à former des cals en réponse à des traitements inducteurs exogènes .....	171
La perte de fonction de PUCHI modifie la composition en VLCFA des tissus de cals produits par des racines sur milieu inducteur .....	173
Conclusion du chapitre III.....	175
<b>Chapitre IV : Utilisation de l'inférence de réseau de gènes pour rechercher les régulateurs potentiels de l'établissement de la niche de cellules souches dans le primordium de racine latérale</b> .....	<b>176</b>
Caractérisation du transgène PI::GFP comme rapporteur de l'identité centre quiescent dans le primordium de racine latérale.....	176
Identification de régulateurs potentiels de PI au cours du développement de la racine latérale et caractérisation préliminaire du phénotype racinaire.....	177
Analyse du réseau de gènes impliqué dans le développement de la racine latérale .....	178
Identification de régulateurs potentiels de la transition vers la phase méristématique et caractérisation préliminaire de leur phénotype racinaire .....	179
Conclusion du chapitre IV .....	180
<b>Chapitre V : Discussion générale</b> .....	<b>180</b>

## Chapitre I: Introduction

La croissance des végétaux dépend étroitement de l'activité de leur système racinaire, réseau ramifié de racines explorant le sol et assurant, en particulier, la nutrition hydrominérale de la plante. L'architecture de ce système racinaire se développe progressivement grâce à la capacité de tissus spécialisés, les méristèmes, à assurer la croissance en longueur des racines, et surtout grâce à la propriété des plantes de former de nouveaux méristèmes racinaires au sein même des racines existantes (Figure 1). Cette **néoformation répétée et régulée de racines latérales est cruciale pour le développement d'un système racinaire complexe** et adapté aux besoins de la plante et aux contraintes du milieu.

Du fait de leur importance pour le développement et la multiplication des plantes, et parce que la formation des racines latérales est un excellent modèle pour explorer les mécanismes d'organogénèse (Lavenus et al., 2013), les processus de ramification racinaire sont depuis longtemps intensément étudiés. La formation d'une nouvelle racine latérale débute par des divisions anticlines de cellules préalablement sélectionnées du péri-cycle (Malamy and Benfey, 1997; Wangenheim et al., 2016) (Figure 1B). Une séquence de divisions cellulaires produit alors progressivement un **primordium de racine latérale** (PRL), bordé par des cellules flanquantes et dont le centre s'organise progressivement en un nouveau méristème apical racinaire, dont dépendra la croissance de la racine latérale (RL) après émergence. L'organisation fonctionnelle du méristème apical racinaire de la racine primaire est très étudiée, et de nombreux gènes marqueurs de certaines identités cellulaires y ont été décrits (Sozzani and Iyer-Pascuzzi, 2014; Lee et al., 2013). En particulier, l'auto-maintien du méristème racinaire, dont dépend la croissance indéfinie de la racine, repose sur un petit groupe de cellules souches au centre du méristème et dont le centre organisateur, aussi appelé **centre quiescent**, exprime des gènes ou transgènes particuliers tels que *WOX5* et *QC25*. Dans le contexte du développement du primordium de racine latérale, il a été décrit que l'expression de ces gènes marqueurs apparaît au centre du primordium à un stade intermédiaire de son développement, de façon concomitante avec une transition majeure marquée par une complexification de l'organisation tissulaire, un changement de symétrie de l'organe, et le franchissement de couches cellulaires importantes dans les tissus de la racine parente (Goh et al., 2016). Ainsi, l'acquisition de l'organisation fonctionnelle du PRL est complexe, non linéaire, et probablement influencée par des signaux tissulaires ou environnementaux.

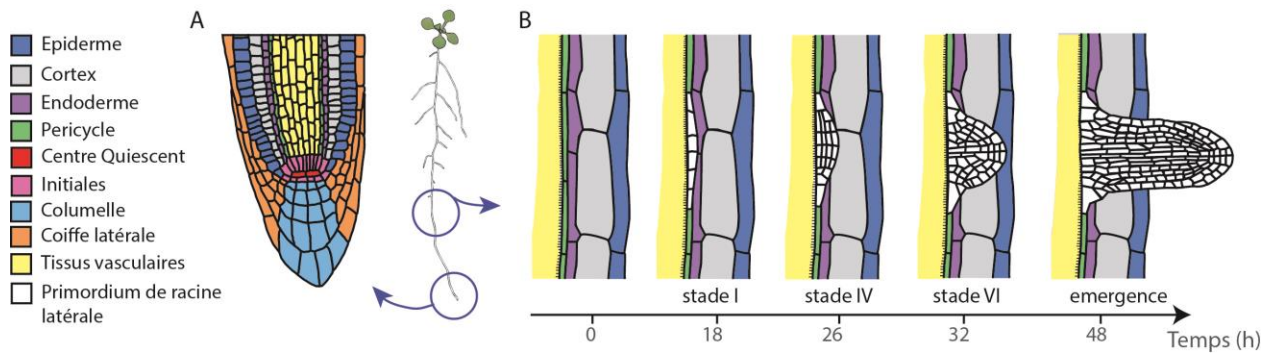


**Figure 1.** (A) Organisation du méristème apical racinaire assurant la croissance indéterminée de la racine primaire chez *Arabidopsis thaliana*. (B) Formation d'une racine latérale, à partir de cellules du péricycle, chez *A. thaliana*. En vue longitudinale, la première phase de développement (stades I à IV) est caractérisée par des divisions anticlines et péricleines construisant un organe simple délimité par des cellules flanquantes. Au contraire dès le stade V des patrons de divisions plus complexes génèrent une forme en dôme et l'anatomie caractéristique du centre du méristème racinaire, dans lequel des transgènes marqueurs du centre quiescent sont exprimés (Goh et al., 2016).

Les progrès méthodologiques, en particulier en génie génétique et en imagerie, ont permis de commencer à explorer à l'échelle moléculaire et cellulaire les mécanismes régulant la néoformation des racines latérales, en particulier chez la plante modèle *A. thaliana*. La description du phénotype racinaire altéré de mutants a permis l'identification et la description de nombreux facteurs génétiques impliqués dans la formation des racines latérales. Par ailleurs, la distribution non uniforme, et étroitement régulée, de signaux hormonaux tels que l'auxine est étroitement associée à l'organogenèse racinaire (Trinh et al., 2018). Cependant, notre compréhension du processus d'organogenèse des racines latérales reste aujourd'hui encore très limitée. En particulier, notre connaissance actuelle de ces acteurs moléculaires ne suffit pas à expliquer **l'organisation fonctionnelle du primordium de racine latérale** en un dôme bien délimité, au centre duquel les différentes identités cellulaires caractéristiques du méristème racinaire se mettent progressivement en place (Goh et al., 2016; Du and Scheres, 2017), et dont les flancs expriment des gènes particuliers.

Parmi ces derniers, le facteur de transcription PUCHI, appartenant à la famille des AP2/EREBP, est exprimé précocement dans le primordium de racine latérale puis son expression est confinée aux flancs et la base du primordium (Figure 2C) (Hirota et al., 2007). Les premières descriptions du phénotype racinaire du mutant *puchi-1* rapportent que la perte de fonction du gène altère de façon importante le processus de ramification racinaire. Les mutants *puchi-1* initient davantage de PRL en comparaison aux plantes sauvages, mais le développement de ces organes est fréquemment retardé, aboutissant à un densité de racines latérales émergées plus faible chez le

mutant que chez le sauvage (Figure 2A) (Kang et al., 2013). D'autre part, une observation plus précise montre que la séquence des divisions cellulaires et possiblement des différenciations au sein du PRL est altérée, produisant des organes élargis, aux flancs déformés (Figure 2B) (Hirota et al., 2007). Ces résultats montrent que **PUCHI est un régulateur important du développement des racines latérales** chez *A. thaliana*. Néanmoins, les gènes et les voies de signalisation ciblés par ce facteur de transcription ne sont pas identifiés, et son mode d'action au sein du PRL demeure donc inconnu.

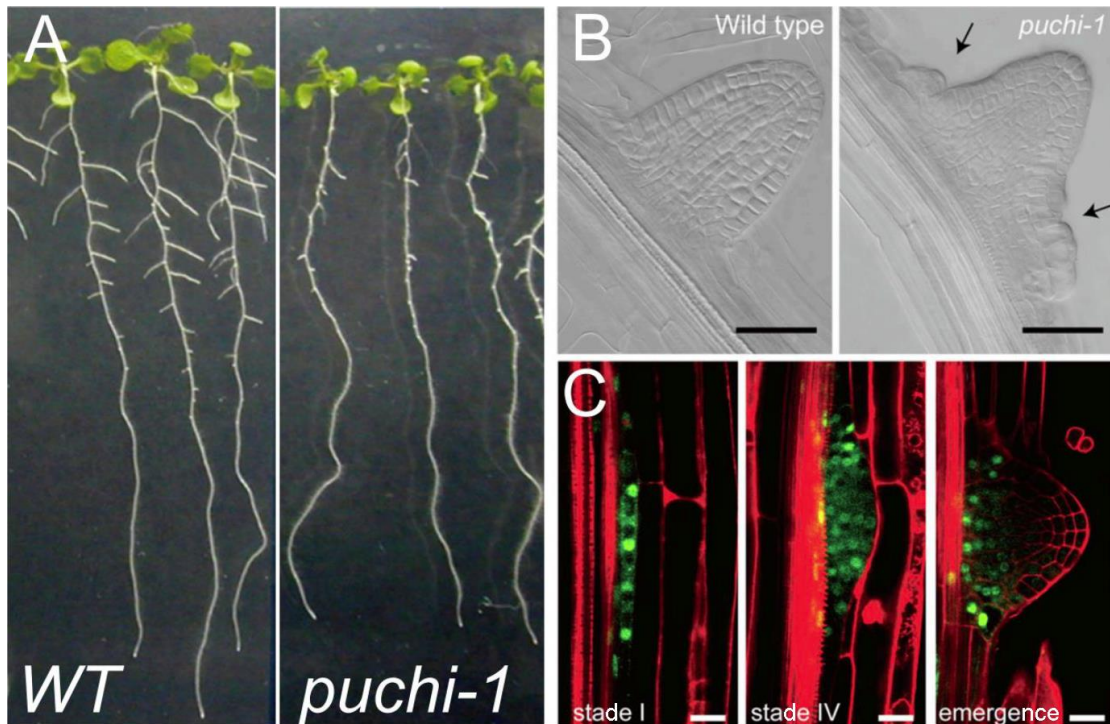


**Figure 2.** (A) Comparaison du phénotype racinaire *in vitro* de plantules de 9 jours de génotype sauvage (WT) et perte de fonction *puchi-1*. (B) Morphologie des primordia de racines latérales au microscope en contraste interférentiel. Barre d'échelle : 50  $\mu\text{m}$ . (C) Expression de la construction rapporteur *pPUCHI:PUCHI-GFP* (fluorescence verte) dans les tissus du PRL (marqué au iodure de propidium, fluorescence rouge). Barre d'échelle : 20  $\mu\text{m}$ . Adapté de (Hirota et al., 2007).

Récemment, l'obtention de larges bases de données, en particulier transcriptomiques, a permis d'étudier les propriétés plus globales des mécanismes de régulation mis en jeu lors de la ramification racinaire. En s'appuyant sur un protocole d'induction des racines latérales par gravistimulation (Lucas et al., 2013), l'équipe d'accueil a participé à la production d'une base de données documentant la dynamique d'expression des gènes au cours du développement des racines latérales, de l'induction à l'émergence (Voß et al., 2015). Par la suite, Julien Lavenus a développé au cours de son doctorat dans l'équipe (Lavenus, 2013) un algorithme permettant, à partir de cette

base de données et du calcul de la corrélation avec retard entre profils d'expression, de prédire la topologie probable des interactions génétiques sous-jacentes. La validité de ces prédictions a été mesurée concernant les cibles du facteur de transcription ARF7 (Lavenus et al., 2015). Cette **base de données**, appelée **LR transcriptomic dataset** (Voß et al., 2015), ainsi que **l'algorithme d'inférence de réseau de gènes TDCor** (Lavenus et al., 2015), sont des outils originaux et particulièrement puissants pour explorer les propriétés du réseau de gènes régulant le développement des racines latérales. Ils peuvent être utilisés pour rechercher les cibles directes ou indirectes dont l'expression est contrôlée par un gène d'intérêt. Cette approche a notamment permis d'identifier une liste de cibles potentielles de PUCHI, parmi lesquelles les gènes impliqués dans la biosynthèse des **acides gras à très longues chaînes (VLCFA)** étaient statistiquement surreprésentés. Inversement ces outils peuvent être également employés pour rechercher les **régulateurs amont de gènes d'intérêt**, par exemple, méristématiques. Enfin, la topologie prédite du réseau peut-être analysée globalement, par une stratégie de biologie des systèmes.

Ce travail de thèse a débuté en mai 2016 dans ce contexte, avec l'objectif de poursuivre l'exploitation de ces approches pour progresser dans notre compréhension des mécanismes génétiques contrôlant le développement, et particulièrement l'organisation des primordia de racine latérale. Il s'est organisé selon deux axes :

### ***1-La caractérisation du rôle de PUCHI au cours du développement des racines latérales***

En complément d'une analyse détaillée de génétique classique permettant d'affiner la caractérisation du rôle de PUCHI sur l'initiation, le développement anatomique et fonctionnel des primordia, et l'émergence des racines latérales (Chapitre II), les travaux de Trinh Duy Chi ont permis de développer puis d'étayer l'hypothèse selon laquelle PUCHI régulerait la voie de biosynthèse des VLCFA au cours de la ramification racinaire (chapitre III).

### ***2-L'identification des régulateurs clés dans la mise en place des identités méristématiques dans le primordium, en particulier le centre quiescent.***

Trinh Duy Chi a mis en place cette approche en caractérisant l'expression d'un gène marqueur du centre quiescent dans le primordium puis en débutant l'identification de régulateurs potentiels via TDCor et l'étude de leur impact sur le développement racinaire (chapitre IV).

## **Chapitre II: Le facteur de transcription PUCHI régule l'initiation, le positionnement, l'organisation et l'émergence des racines latérales**

### ***2.1. Profil d'expression de PUCHI dans les racines***

Le profil d'expression de la construction *pPUCHI ::PUCHI-GFP* a été analysé en détail dans les plantules d'*A. thaliana* cultivées au laboratoire. Dans l'ensemble, cette étude a confirmé l'expression préférentielle du rapporteur dans l'ensemble du primordium de racine latérale dès les stades précoces, puis de façon restreinte à sa base. Une expression dans les cellules du péri-cycle avoisinant le primordium, ainsi que dans l'endoderme le recouvrant est également notée. Par ailleurs, une expression faible dans les tissus vasculaires est observée. L'expression du rapporteur n'est pas détectée dans le méristème apical de la racine primaire, bien que d'autres études suggèrent une expression faible de gène endogène dans ces tissus (Brady et al., 2007).

### ***2.2. PUCHI est requis pour le développement des primordia de racines latérales mais inhibe leur initiation***

Pour identifier quels mécanismes de développement racinaire le facteur de transcription PUCHI peut réguler, le phénotype racinaire du mutant perte de fonction *puchi-1* a été analysé en détail (Figure 3). Le dénombrement des organes latéraux (primordia + racines latérales émergées) dans des racines de 9 jours cultivées verticalement sur milieu ½ MS montrent que la perte de fonction de *puchi-1* entraîne une augmentation significative de la densité d'initiation des primordia de racines latérales (nombre/cm de racine primaire) bien que la densité des racines latérales effectivement émergées soit équivalente (Figure 3A). De plus, le nombre de PRL non émergés dans la zone ramifiée de la racine primaire est très supérieur chez *puchi-1* par rapport au sauvage. Ces PRL pourraient correspondre à des primordia dont le développement est retardé, voire arrêté. De façon cohérente la distance moyenne entre deux primordia consécutifs est plus faible chez le mutant *puchi-1* (750 µm) que chez le sauvage (1850 µm) et de nombreux clusters de PRL (distants de moins de 300 µm) sont observés (Figure 3C). Pour analyser la dynamique de développement des primordia de racines latérales chez le mutant, les plantes sont soumises à un protocole de gravistimulation (Lucas et al., 2008) et le stade de développement atteint par le PRL dont la formation est induite au coude de la racine primaire est évalué 18h ou 48h après sur l'échelle définie par Malamy et Benfey, 1997 (Malamy and Benfey, 1997) (Figure 3B). Cette analyse montre que la progression du développement des PRL est ralentie dans le contexte *puchi-1* par rapport au sauvage et suggère donc que PUCHI inhibe l'initiation des racines latérales dans le péri-cycle mais stimule le développement des primordia de racines latérales une fois initiés.

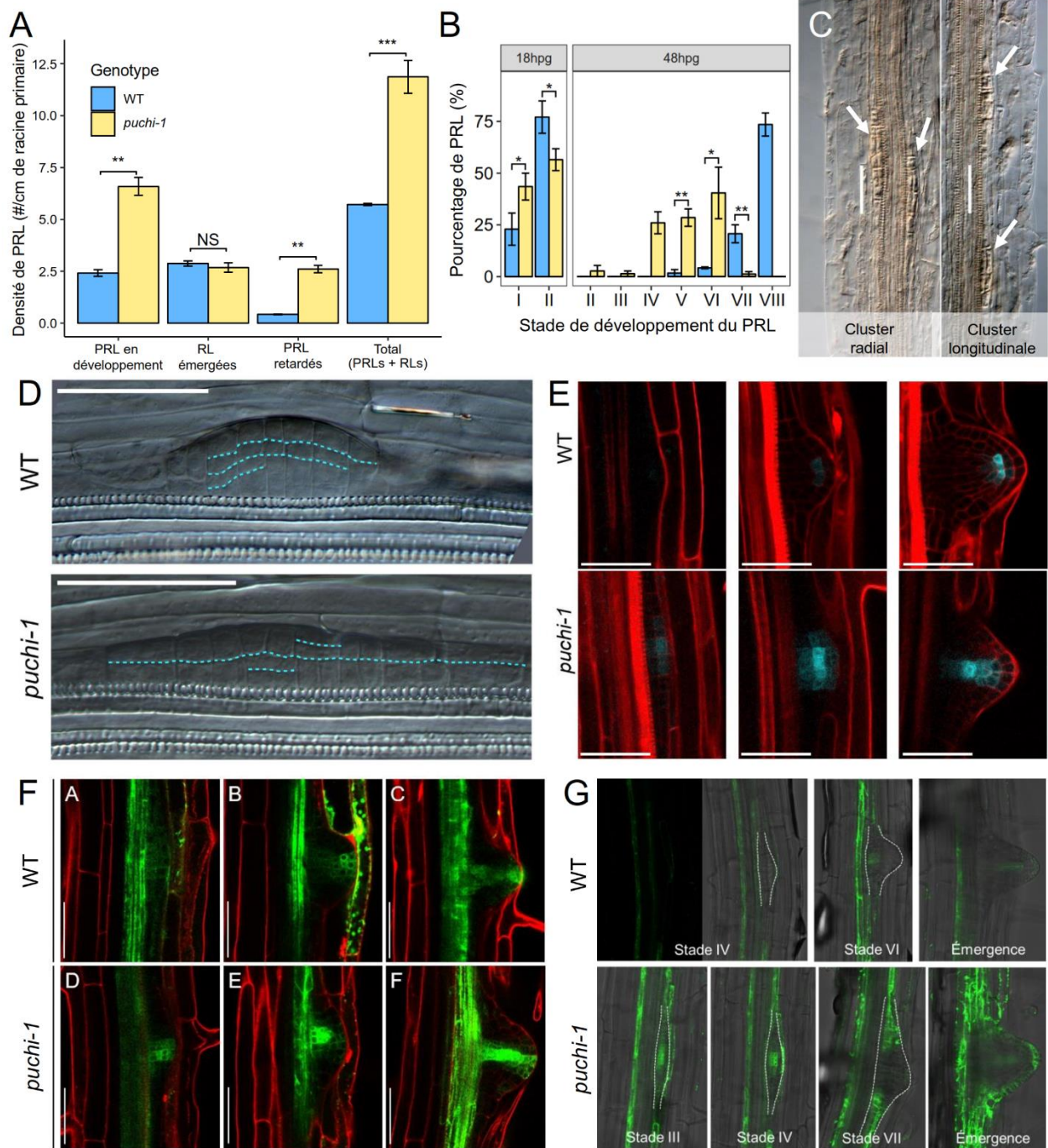


**Figure 3.** (A) Caractérisation du profil de ramification racinaire de plantules sauvages (WT) ou mutantes *puchi-1* cultivées 9 jours *in vitro* sur milieu ½ MS. Les PRL notés retardés sont ceux détectés dans les tissus plus matures que ceux dont émerge la racine latérale la plus jeune. Moyennes ± erreur standard, n= 20-30 plantes, x 3 répétitions. Les étoiles indiquent des différences significatives (test de Student) à  $p < 0,01$  (\*\*) et  $p < 0,001$  (\*\*\*). (B) Profil des stades de développement atteints par les PRL induits par gravistimulation dans des plantules sauvages (WT) ou *puchi-1*, 18h ou 48h après gravistimulation (hpg). Moyennes ± erreur standard, n= 20-30 plantes, x 3 répétitions. Les étoiles indiquent des différences significatives (test de Student) à  $p < 0,05$  (\*) et  $p < 0,01$  (\*\*). (C) Exemple de clusters de PRL chez *puchi-1*, les PRL sont indiqués par les flèches. (D) Perturbation de l'anatomie cellulaire d'un PRL *puchi-1* par rapport au sauvage (WT). (E) Visualisation du profil d'expression du transgène *QC25::CFP*, dont l'expression est caractéristique du

centre quiescent dans la racine primaire, dans les PRL sauvages (WT) et *puchi-1*. n= 15/15 plantes observées. (F) Visualisation du profil d'expression du transgène *DR5::GFP*, activé par l'auxine, dans certains PRL *puchi-1*, comparé au sauvage (WT). (G) Visualisation du profil d'expression du transgène *TCSn::GFP*, activé par les cytokinines, dans les PRL sauvages (WT) et *puchi-1*. n= 5/5 plantes observées. Barres d'échelle = 50 µm.

### ***2.3 PUCHI est requis pour l'organisation anatomique et fonctionnelle normale du primordium de racine latérale***

L'observation attentive des PRL du mutant *puchi-1* a permis de mettre en évidence qu'en plus de l'élargissement de la base des primordia (Hirota et al., 2007) (Figure 1B), la séquence - mais pas de façon visible l'orientation - des divisions cellulaires au centre du primordium était altérée, résultant en une organisation des primordia moins stéréotypée que chez les plantes sauvages (Figure 3D).

Cette observation nous a poussé à étudier le profil d'expression de marqueurs fonctionnels dans les PRL de *puchi-1*, en particulier *DR5::GFP* rapporteur du patron de signalisation auxinique dont il a été montré qu'il contrôlait le développement des PRL (Benková et al., 2003). Le distribution du signal *DR5::GFP* n'a pas révélé de différence qualitative évidente distinguant les PRL *puchi-1* des sauvages, cependant, une quantification plus poussée du signal serait nécessaire (Figure 3F). En revanche, les niveaux d'expression de *TCSn::GFP*, activé par la voie de signalisation des cytokinines, et *QC25::CFP*, marqueur de l'identité centre quiescent semblent visiblement augmentés dans le contexte mutant dans ou autour des PRL, et leur distribution tissulaire est modifiée (Figure 3E, Figure 3G). Ces données montrent donc que le facteur de transcription PUCHI est nécessaire pour observer le développement anatomique et fonctionnel correct des PRL.

### ***Conclusion du chapitre II***

Cette caractérisation détaillée du phénotype du mutant *puchi-1* a permis de confirmer les modifications phénotypiques, anatomiques et fonctionnelles rapportées précédemment dans la littérature (Hirota et al., 2007; Kang et al., 2013) et d'en éclairer de nouveaux aspects, en particulier concernant le profil de signalisation cytokininique et l'expression de *QC25::CFP*. Globalement, la fonction de PUCHI est donc nécessaire pour inhiber l'initiation des racines latérales avec une densité trop importante dans le péri-cycle, permettre la progression du développement du PRL jusqu'à l'émergence, et contrôler son organisation anatomique et fonctionnelle. Parce que ces différents aspects sont liés par des régulations complexes faisant intervenir des rétro-contrôles et des actions non cellule-autonomes, il est difficile de comprendre lesquels de ces processus sont des cibles directes de PUCHI et lesquels pourraient être au contraire des conséquences indirectes des premières altérations phénotypiques chez le mutant. Pour identifier les voies de régulation

ciblées par PUCHI dans le primordium de racine latérale, Trinh Duy Chi a donc poursuivi les analyses de la base de données LR transcriptomic dataset par l'algorithme TDCor, initiées précédemment, et a contribué à vérifier expérimentalement les prédictions selon lesquelles PUCHI régulerait de façon coordonnée la biosynthèse des acides gras à très longues chaînes au cours du développement des racines latérales.

### **Chapitre III: Le facteur de transcription PUCHI régule la voie de biosynthèse des VLCFA durant la formation des racines latérales et l'induction de la production de cals par le péricycle**

#### ***3.1. L'expression de multiples gènes de biosynthèse des VLCFA semble régulée par PUCHI au cours du développement des racines latérales***

Afin d'identifier les gènes dont l'expression pouvait être contrôlée par celle de *PUCHI* au cours du développement des racines latérales, Julien Lavenus a extrait du LR transcriptomic dataset tous les gènes dont le profil d'expression était corrélé ( $R > 0,8$ ) avec celui de *PUCHI*, avec un retard de 3h. Parmi les 217 gènes identifiés, la catégorie fonctionnelle GO de « biosynthèse des acides gras » était statistiquement surreprésentée ( $p < 0,01$  ; analyse par le logiciel BiNGO (Maere et al., 2005)). En effet, l'algorithme TDCor propose de nombreux gènes de biosynthèse des VLCFA comme cibles directes ou indirectes de PUCHI.

Les acides gras à très longue chaîne (VLCFA,  $C \geq 20$  carbones) sont essentiels au développement des animaux, des végétaux et de la levure et sont synthétisés par un complexe de 4 enzymes localisé dans le réticulum endoplasmique (Bach and Faure, 2010; Haslam and Kunst, 2013) (Figure 4A). Ces acides gras peuvent ensuite être modifiés, par exemple hydroxylés, et incorporés dans différentes classes de lipides pouvant participer aux membranes cellulaires (sphingolipides et galactolipides), au stockage d'énergie (triacylglycérols) ou à certains matériaux extracellulaires comme les cires (cutine) ou la subérine (Li-Beisson et al., 2013). Malgré son importance, leur fonction dans le développement demeure mal connue. Chez la plante modèle *A. thaliana*, ils ont été montrés comme essentiels au développement de certains organes, en particulier le primordia de racine latérale, *via* un effet possible sur la dynamique membranaire et/ou sur la signalisation hormonale (Wattelet-Boyer et al., 2016; Nobusawa et al., 2013; Roudier et al., 2010). Les profils d'expression de certains gènes de biosynthèse des VLCFA corrélés – avec retard – à l'expression de *PUCHI* au cours du développement des racines latérales sont représentés dans la Figure 4B. Le gène *KCS6* (non montré) présente une forte induction de son expression à partir de 24 hpg et jusqu'à l'émergence de la racine.

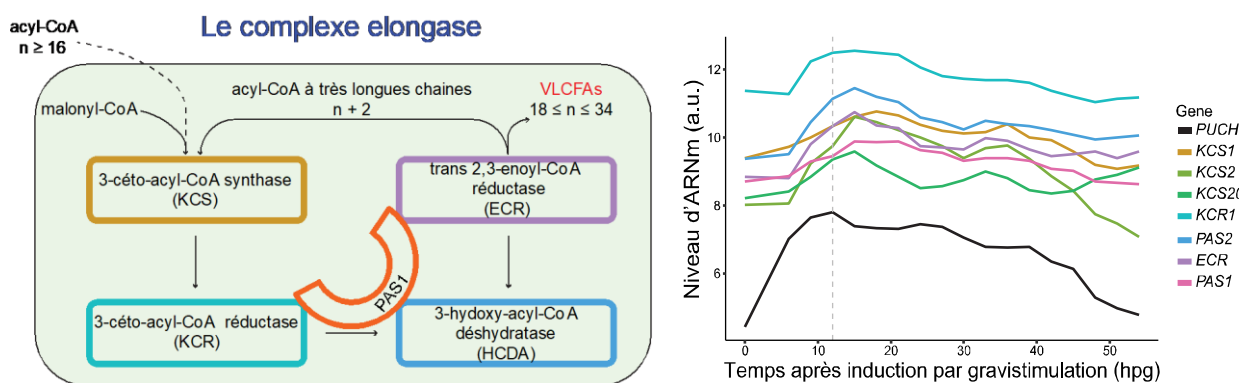


**Figure 4.** (A) Schéma de la voie de biosynthèse des acides gras à très longues chaînes. L'élargissement de la chaîne des acides gras par cycle d'ajout de 2 carbones est catalysée par un complexe enzymatique localisé dans la membrane du réticulum endoplasmique et rassemblant, dans l'ordre chronologique d'intervention : une 3-céto-acyl-coA synthase (KCS), une 3-céto-acyl-coA réductase (KCR), une 3-hydroxyacyl-coA-déshydratase (HCDA) et une trans-2,3-enoyl-coA-réductase (ECR). *PAS1* code pour une protéine chaperone du complexe. Si de multiples gènes de la famille *KCS* ont été identifiés (Joubès et al., 2008), un ou deux gènes fonctionnels ont été décrit chez *A. thaliana* dans les catégories *KCR* (Beaudoin et al., 2009), *HCDA* (Morineau et al., 2016) (gène *PAS2* et *PTPLA*), *ECR* (Zheng et al., 2005) et *PAS1* (Roudier et al., 2010b). (B) Profils d'expression des gènes *PUCHI*, de trois gènes *KCS* (*KCS1*, *KCS2*, *KCS20*), du gène *KCR1*, du gène *PAS2*, du gène *ECR* et du gène *PAS1* au cours du développement des racines latérales induites par gravistimulation dans le LR transcriptomic dataset.

### 3.2. Plusieurs gènes de biosynthèse des VLCFA sont exprimés dans les primordia en développement de façon dépendante de *PUCHI*

Pour vérifier cette prédiction, l'expression de gènes de biosynthèse des VLCFA a été mesurée par RT-qPCR dans des racines de plantules d'*A. thaliana* de 13 jours soumises à un traitement hormonal pour induire de façon massive la formation des racines latérales, et cette réponse a été comparée entre plantes de génotypes sauvage et mutante *puchi-1* (Figure 5). Les résultats indiquent que l'expression de *KCS1*, *KCS20*, *KCR1*, *PAS2* et *ECR* est bien stimulée au cours de l'induction de la formation des racines latérales et que cette stimulation est dépendante de *PUCHI*.

Pour vérifier le domaine d'expression de ces gènes en relation avec le primordium de racine latérale, les profils d'expression des constructions promoteur::rapporteur *pKCS1::KCS1-GFP* (Shang et al., 2016), *pKCS6::GUS* (Joubès et al., 2008), *pKCS20::GUS* (Joubès et al., 2008), *pKCR1::GUS* (Joubès et al., 2008), *pPAS2::GUS* (Morineau et al., 2016), et *pPAS1::GUS* (Roudier et al., 2010b) ont été analysés dans les racines de génotype sauvage et les racines mutantes *puchi-1* (Figure 6). L'ensemble de ces transgènes est exprimé dans tout ou partie des PRL en développement chez le génotype sauvage, et la perte de fonction de *PUCHI* modifie ce

patron d'expression de façon plus ou moins complexe. En particulier, *KCS1*, *KCS6*, *KCR1*, *PAS2* et *PAS1* sont fortement exprimés dans le PRL et cette expression est dépendante de PUCHI.

Malheureusement, les données concernant *pECR::GUS* (Joubès et al., 2008) se sont révélées inexploitable dans nos conditions. Cependant, les données publiées par (Brady et al., 2007) indiquent qu'*ECR* serait exprimé dans le PRL de type sauvage. Ainsi, au moins une isoforme de chacune des 4 enzymes du complexe enzymatique de biosynthèse des VLCFA, ainsi que la chaperone *PAS1*, serait bien présente dans le primordium en développement, et l'expression de certaines au moins y est positivement influencée par PUCHI.

De façon intéressante, certains de ces transgènes rapporteurs indiquent une expression forte dans l'endoderme de la racine primaire, en relation avec le développement de PRL sous-jacent.

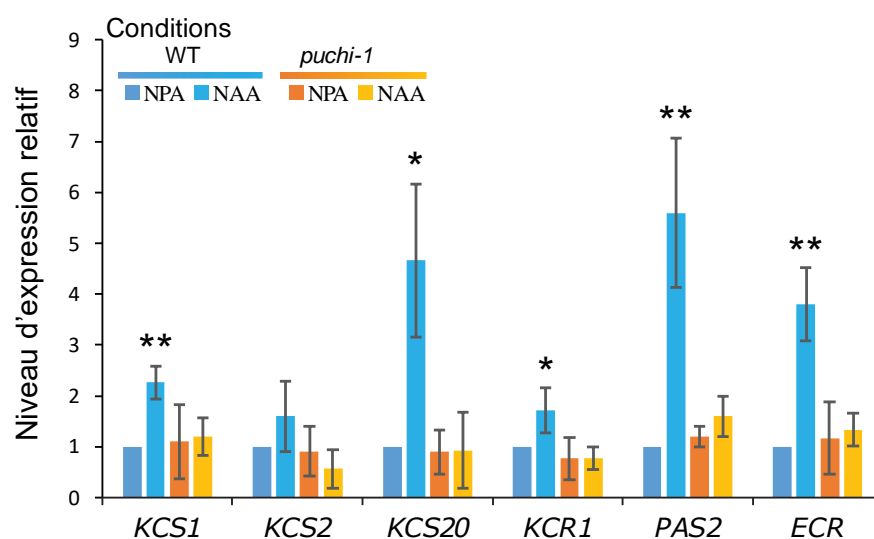


**Figure 5.** Niveau d'expression relatif, mesuré par RT-qPCR, des gènes de biosynthèse des acides gras à très longue chaîne dans les racines de plantules de 13 jours de génotype sauvage (WT) ou mutantes *puchi-1* après induction de la formation des racines latérales par traitement hormonal (adapté de (Himanen et al., 2002)). Les plantules sont d'abord cultivées pendant 12 jours sur un milieu supplémenté en 5  $\mu$ M d'acide naphthylphthalamique (NPA), un inhibiteur des transports polarisés d'auxine qui bloque la formation des racines latérales. Puis les plantules sont transférées sur milieu supplémenté en 10  $\mu$ M d'acide naphthalène-acétique (NAA), un analogue de l'auxine déclenchant de façon synchrone la formation des racines latérales sur l'ensemble du péricycle. Le traitement contrôle correspond à des plantules transférées sur NPA 5  $\mu$ M. Les racines sont prélevées et la quantification des ARNm est réalisée par RT-qPCR 24h après transfert. Le gène *CDKA* est utilisé pour comme référence interne pour la RT-qPCR. Les quantifications sont relatives au niveau d'expression mesuré pour le gène d'intérêt chez le sauvage, sur NPA. Moyennes  $\pm$  erreur standard, 3 répétitions. Les étoiles indiquent des différences significatives (test de Student) à  $p < 0,05$  (\*) et  $p < 0,01$  (\*\*). Expérience réalisée par J. Lavenus.

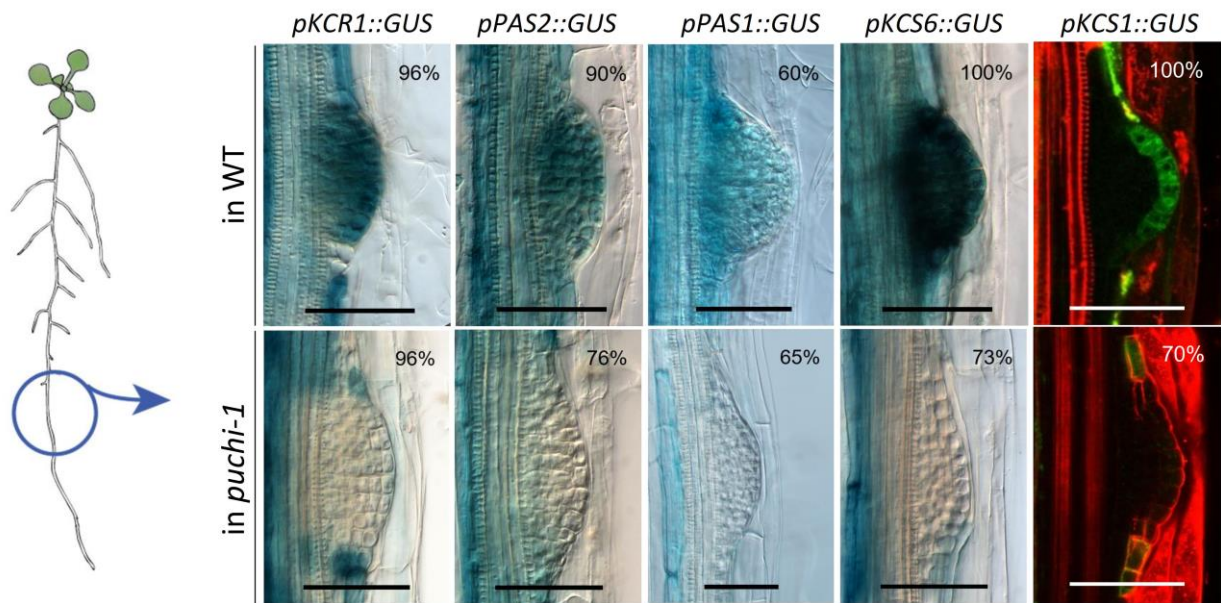


**Figure 6.** Analyse des profils d'expression de transgènes promoteur::rapporteur relatifs à des enzymes de biosynthèse des acides gras à très longues chaînes (*KCS1*, *KCS6*, *KCR1*, *PAS2*, *PAS1*) dans les primordia de racine latérale en développement de plantules sauvages (WT) et mutantes *puchi-1* de 9 jours, *in vitro*, sans traitement inducteur de la formation des racines latérales. Les pourcentages indiquent la proportion de primordia présentant le profil d'expression représenté. Barre d'échelle : 50  $\mu$ m. n=30-40 plantules pour chaque conditions.

### 3.3. Des plantes mutantes pour certains gènes de biosynthèse de VLCFA présentent des phénotypes racinaires similaires à *puchi-1*

Afin d'identifier le rôle potentiel de ces gènes de biosynthèse des VLCFA lors du développement des racines latérales, le phénotype de ramification racinaire de mutants perte de fonction dans certains de ces gènes a été caractérisé et comparé au phénotype sauvage, d'une part, et d'autre part au phénotype *puchi-1*. Le double mutant *kcs2 kcs20* n'a pas montré de différence phénotypique significative comparé au sauvage. En revanche, l'analyse détaillée des racines *kcs1-5* a révélé que comme chez *puchi-1*, mais de façon moins marquée, la densité des organes latéraux était supérieure au sauvage, et la progression du développement des PRL était ralentie (Figure 7). Les racines du mutant *cer10-2 (ecr)* présentaient également un phénotype similaire, quoique plus léger encore que *kcs1-5*. Ainsi, la perte d'expression de certaines isoformes des enzymes de biosynthèse des VLCFA affecte l'initiation et le développement des racines latérales de façon similaire, mais plus légère, que *puchi-1*. Ces résultats montrent que la régulation de ces gènes par PUCHI pourrait expliquer au moins en partie le phénotype racinaire du mutant. Le fait que PUCHI régule l'expression de plusieurs de ces isoformes, la redondance fonctionnelle complexe des enzymes KCS en fonction des tissus et des stades de développement, et l'existence possible d'isoforme(s) d'ECR non décrite(s) pourraient expliquer le phénotype sensiblement plus sévère

de *puchi-1* par rapport aux mutants de biosynthèse des VLCFA testés, et la pertinence de cette régulation coordonnée exercée par PUCHI au cours du développement des racines latérales.

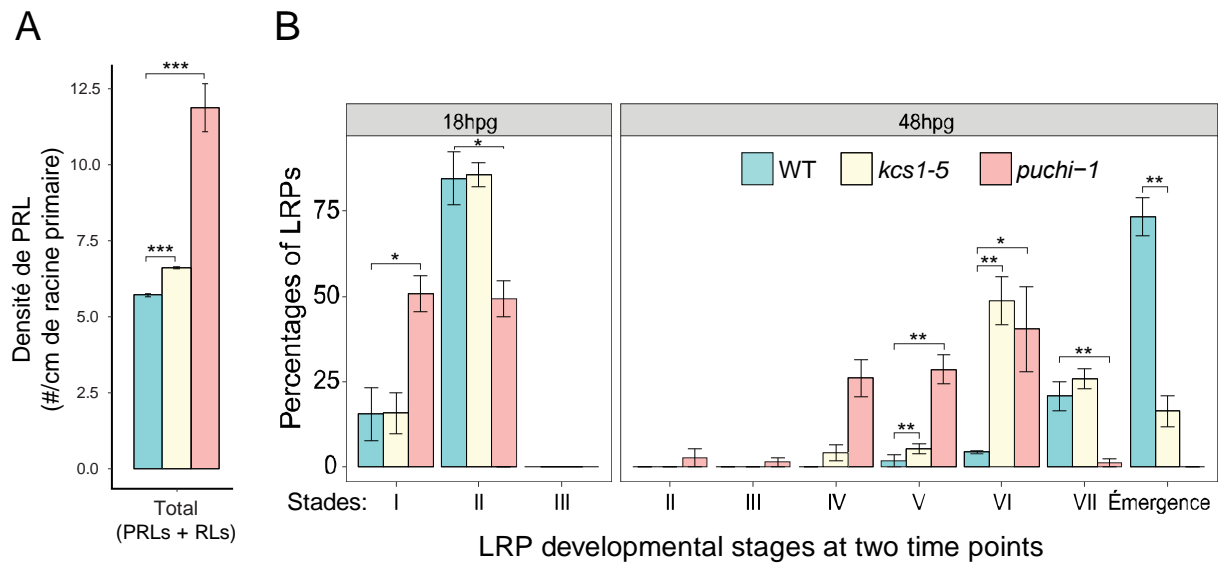


**Figure 7.** (A) Densité d’organes racinaires (primordia de racines latérales et racines latérales émergées) mesurée sur les racines primaires de plantules sauvage (wild type), mutante *kcs1-5*, et mutante *puchi-1* de 9 jours *in vitro*, sans traitement inducteur du développement des racines latérales. (B) Profil de distribution des stades de développement (Malamy and Benfey, 1997) atteints par les primordia de racines latérales dans ces racines. Moyennes  $\pm$  erreur standard, n= 20-30 plantes, x 3 répétitions. Les étoiles indiquent des différences significatives (test de Student) à  $p < 0,05$  (\*),  $p < 0,01$  (\*\*) et  $p < 0,001$  (\*\*\*).

### 3.4. PUCHI et la biosynthèse des VLCFA restreignent la compétence du péri-cycle à former des cals en réponse à des traitements inducteurs exogènes

Shang et al., (2016) ont récemment montré que la régulation de la biosynthèse des VLCFA par KCS1 influençait fortement la compétence des cellules du péri-cycle à répondre à un traitement hormonal inducteur de la callogenèse : au lieu de former des cals bien délimités comme la racine sauvage, les racines *kcs1-5* forment des cals fusionnés, moins développés. De façon intéressante, Trinh Duy Chi a montré que le mutant *puchi-1* présentait les mêmes altérations phénotypiques sur milieu inducteur de cals, et de façon encore plus sévère que *kcs1-5* (Figure 8). Ces résultats sont cohérents avec les résultats précédemment montrés car

- (i) la compétence du péri-cycle à initier la formation des cals en réponse au traitement auxine+cytokinine pourrait être comparée à la compétence du péri-cycle à initier le développement de racines latérales. Des résultats préliminaires suggèrent que le péri-cycle *puchi-1* est effectivement hypersensible aux traitements auxiniques exogènes (NAA ; 0,01  $\mu$ M à 0,1  $\mu$ M) et forme plus de LRP que le sauvage à traitement équivalent.

- (ii) plusieurs études ont montré que les premières étapes de callogénèse et de formation des racines latérales étaient anatomiquement et fonctionnellement comparables (Sugimoto et al., 2010; Perianez-Rodriguez et al., 2014).

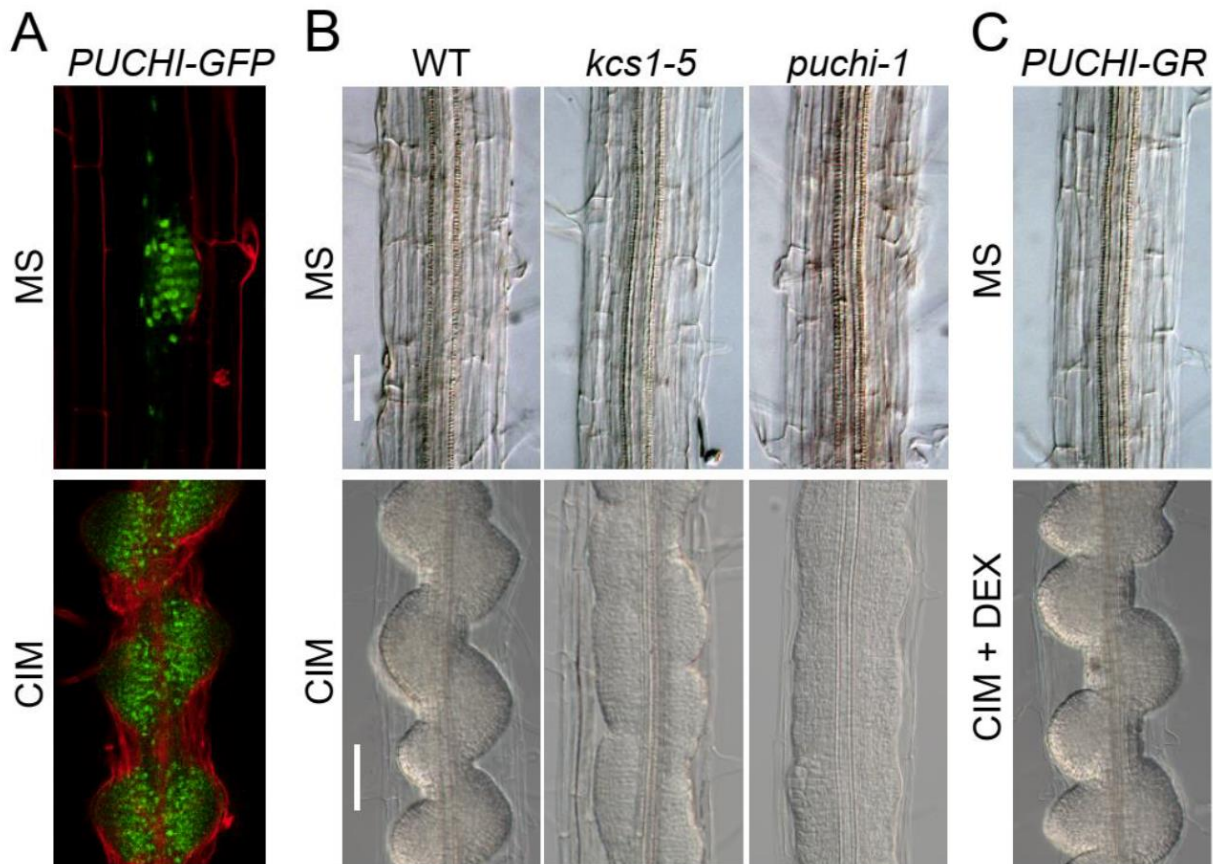


**Figure 8.** (A) Profil d'expression, par microscopie confocale, de la construction rapporteur *pPUCHI::PUCHI-GFP* (qui complète le phénotype *puchi-1* en conditions normales) dans les racines de plantules de génotype sauvage cultivées 7 jours sur milieu  $\frac{1}{2}$  MS normal (MS) puis 4 jours sur milieu inducteur de la callogénèse (CIM). Le signal vert correspond à la fluorescence de PUCHI-GFP ; le signal rouge correspond à la fluorescence du iodure de propidium, utilisé pour visualiser les contours cellulaires. (B) Visualisation, par microscopie à contraste interférentiel, de l'anatomie des racines de plantules de génotype sauvage cultivées 7 jours sur milieu normal (MS) puis 4 jours sur milieu inducteur de la callogénèse (CIM). Sur CIM les racines sauvages produisent de multiples cals distincts, tandis que les deux mutants *kcs1* et *puchi-1* produisent une couche continue de cellules en prolifération.  $n = 20$  plantes pour chaque génotype. (C) Ce phénotype du mutant *puchi-1* est complété par l'introduction d'un transgène *pPUCHI::PUCHI-GR* et l'induction de l'activité de la protéine PUCHI-GR par la dexaméthasone. Barre d'échelle : 100  $\mu\text{m}$ .  $n = 10$  plants x 2 lignées x 2 répétitions.

### ***3.5. La perte de fonction de PUCHI modifie la composition en VLCFA des tissus de cals produits par des racines sur milieu inducteur***

Pour tester si cette régulation de l'expression des gènes de biosynthèse des VLCFA se traduit par un contrôle des VLCFA effectivement produits dans les tissus racinaires, nous avons cherché à caractériser le profil lipidomique du mutant *puchi-1* afin de la comparer au sauvage. Ces caractérisations ont été réalisées en collaboration avec différentes équipes spécialisées en biochimie des lipides à l'IRD de Montpellier, à l'INRA de Versailles puis au Laboratoire de Biogénèse Membranaire de Bordeaux, et grâce à des protocoles d'analyse lipidomique par chromatographie en phase gazeuse et spectrométrie de masse très sensibles. Les analyses des racines cultivées sans traitement inducteur des racines latérales, ou dans lesquels la formation des racines latérales avait été induites par traitement hormonal, n'ont finalement pas révélé de différence significative entre le mutant *puchi-1* et le sauvage. Considérant que la proportion des tissus racinaires dans lesquels s'opérait cette régulation de l'expression des enzymes de biosynthèse des VLCFA par PUCHI pouvait être faible même sur milieu auxinique, l'analyse lipidomique a été réalisée sur des racines cultivées sur milieu inducteur de la callogenèse, dans lesquelles cette proportion de tissus est importante (Figure 8A). Dans ces conditions, une réduction significative de la proportion d'acides gras à très longues chaînes a été détectée chez *puchi-1*, par rapport au sauvage et de façon comparable à *kcs1-5* (Figure 9).

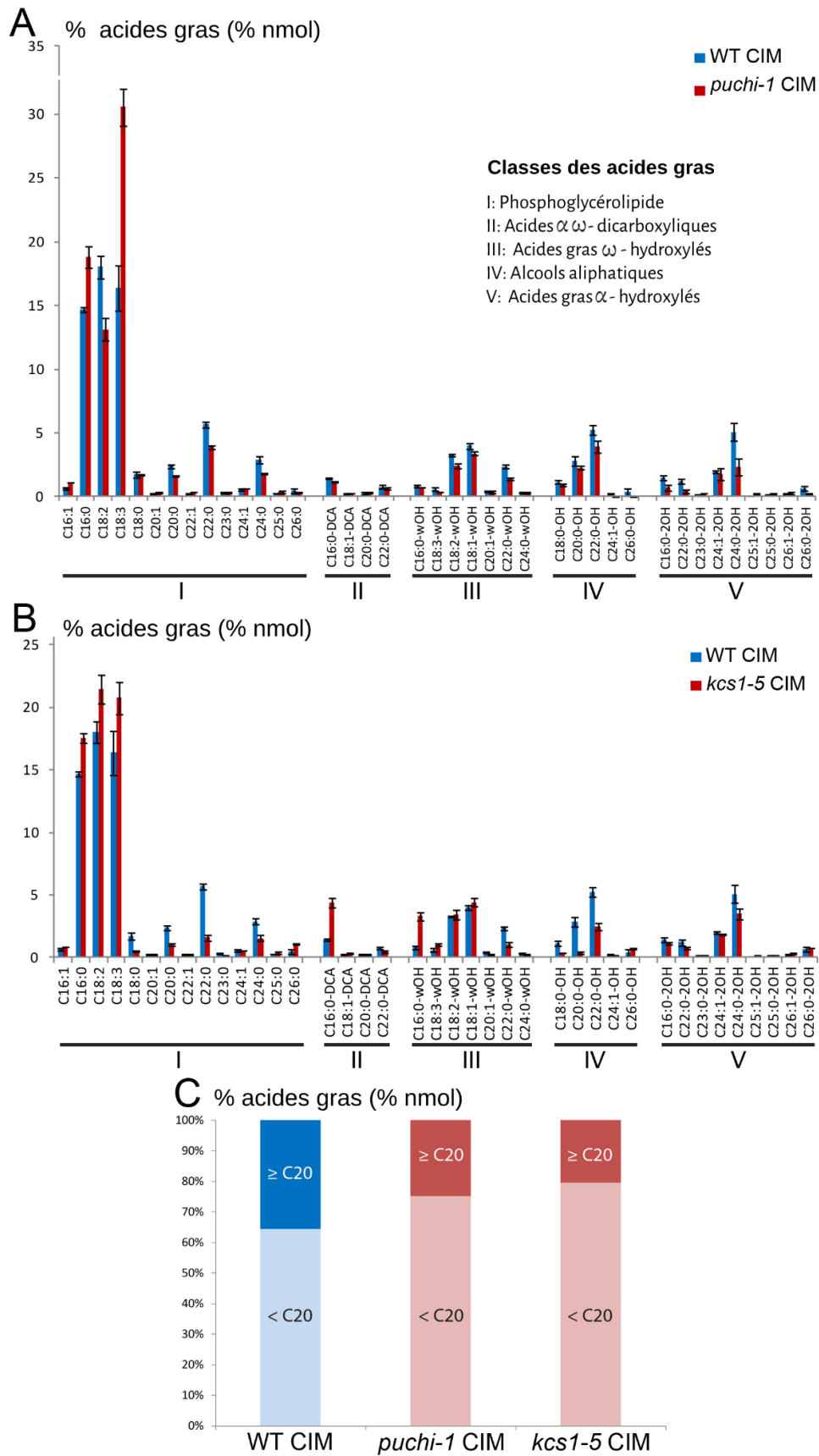


**Figure 9.** A : Profil des acides gras à longues et très longues chaînes extraits de racines de plantules sauvages (WT) et *puchi-1* de 11 jours cultivées sur milieu inducteur de la callogenèse depuis 4 jours. B : Profil des acides gras à longues et très longues chaînes extraits de racines de plantules sauvages (WT) et

*kcs1-5* de 11 jours cultivées sur milieu inducteur de la callogenèse depuis 4 jours. C : proportion des acides gras à très longues chaînes (VLCFA,  $C \geq 20$ ) dans les acides gras extraits des plantules précédentes.

### 3.6. Conclusion du chapitre III

Ainsi, l'approche sans *a priori*, via l'exploration des cibles prédites par TDCor, a permis de mettre en évidence que PUCHI contrôle, de façon directe ou indirecte, l'induction de l'expression de plusieurs gènes de biosynthèse des acides gras à très longues chaînes, en particulier *KCS1*, dans le primordium de racine latérale. Le phénotype de ramification racinaire en conditions normales, la réponse au milieu inducteur de la callogenèse, et le profil biochimique des VLCFA (sur milieu inducteur de la callogenèse) des deux mutants *kcs1-5* et *puchi-1* sont proches, confirmant que la perturbation de l'expression des gènes de biosynthèse des VLCFA pourrait expliquer au moins en partie le phénotype du mutant *puchi*. Des essais de complémentation de *puchi-1* par l'expression d'un transgène *pPUCHI::KCS1-GFP* sont actuellement en cours pour tester cette hypothèse.

*KCS1* a été montrée comme particulièrement importante pour la synthèse des acides gras de chaîne C26, tandis que *KCS20* et *KCS6*, deux autres enzymes dont l'expression est influencée par PUCHI au cours du développement des racines latérales (ces travaux), catalyseraient principalement la synthèse des C22 et C28, respectivement (Kim et al., 2013). La proportion des VLCFA de multiples classes est effectivement plus faible dans les racines *puchi-1* sur CIM comparées au sauvage, et la proportion en C16 et C18 augmente de façon cohérente.

Cette induction de la biosynthèse des VLCFA pourrait avoir de multiples rôles dans le contexte du primordium de racine latérale. Tout d'abord, elle pourrait participer à la sécrétion de subérine, formant une couche hydrophobe recouvrant le dôme du primordium (Li et al., 2017), et par là influencer les transferts d'eau ou de composés hydrosolubles comme l'auxine ou des peptides signaux, entre le primordium et les tissus sus-jacents. Les VLCFA pourraient également être incorporés dans les membranes plasmiques ou du système endomembranaire et influencer la dynamique de ces membranes, la localisation de protéines ou lipides effecteurs, la signalisation intercellulaire, la division cellulaire. Il a notamment été montré que les VLCFA interagissaient avec les voies de régulation du développement par l'auxine (Wattelet-Boyer et al., 2016; Roudier et al., 2010b), les cytokinines (Nobusawa et al., 2013), et l'éthylène (Yamauchi et al., 2015). Compte tenu du rôle clé de l'équilibre entre signalisation auxinique et signalisation cytokinine dans de multiples processus d'organogenèse, en particulier racinaire, les résultats obtenus dans ces travaux sur la distribution du signal cytokinine dans les PRL *puchi-1* sont particulièrement intéressants. Ils montrent notamment que PUCHI est également un régulateur de l'organisation fonctionnelle du PRL, ce qui est l'objet de la seconde partie de ce travail de thèse.

## **Chapitre IV: Utilisation de l'inférence de réseau de gènes pour rechercher les régulateurs potentiels de l'établissement de la niche de cellules souches dans le primordium de racine latérale**

L'organisation d'un méristème racinaire fonctionnel au sein du PRL est un processus clé dont dépend la croissance de la racine latérale après émergence. De façon intéressante, les résultats actuels suggèrent que c'est un phénomène progressif, débutant visiblement à la transition entre le stade IV et le stade V du développement du PRL avec l'induction de l'expression marquée de *QC25::CFP* et de *WOX5::nls::GFP*, marqueurs du centre quiescent dans le contexte de la racine primaire, au centre du primordium, au moment où ce PLR franchit l'endoderme et entame une séquence plus complexe de divisions cellulaires (Goh et al., 2016). De façon intéressante, c'est un phénomène étonnamment robuste, influencé par de nombreux régulateurs connus du méristème apical racinaire, en particulier les facteurs de transcription PLETHORA, SCARECROW et SHORT-ROOT, mais parvenant à être mis en place dans la plupart des mutants concernés. Trinh Duy Chi a donc exploité la base de données LR transcriptomic dataset et l'algorithme TDCor pour rechercher des facteurs pouvant contrôler la mise en place du centre quiescent dans le PRL. Pour ce faire, ni *QC25* ni *WOX5* n'étant présents sur la puce Affymetrix servant de base au LR transcriptomic dataset, la première étape a consisté à identifier un nouveau gène marqueur de l'identité centre quiescent et exprimé dans le LR transcriptomic dataset.

### ***4.1. Caractérisation du transgène *PI::GFP* comme rapporteur de l'identité centre quiescent dans le primordium de racine latérale***

Des études préalablement publiées ont cherché à identifier les facteurs de transcription exprimés préférentiellement dans le centre quiescent de la racine primaire (Nawy et al., 2005). Parmi ceux-ci, le facteur de transcription PISTILLATA, de la famille des MADS-box, était particulièrement intéressant car

- (i) des mesures d'expression tissu-spécifique, et une construction *PI::GFP* montrent une expression enrichie dans le centre quiescent de la racine primaire (Brady et al., 2007; Nawy et al., 2005),
- (ii) *PI* est un régulateur bien décrit de l'identité cellulaire dans le contexte du méristème floral
- (iii) *PI* est présent dans le LR transcriptomic dataset, donc différentiellement exprimé dans les tissus racinaires formant une racine latérale en réponse à la gravistimulation. Plus particulièrement, l'expression de *PI*, faible au départ, augmente nettement à partir de 24 hpg, quand la majorité des PRL sont à des stades IV et V.



transcriptomic dataset. Le rapidité de calcul et la précision de ces prédictions diminuant avec le nombre de gènes considérés, différentes listes ont été testées, la plus grande incluant plus de 300 gènes connus pour être impliqués fonctionnellement, ou spécifiquement exprimés, dans les méristèmes apicaux, racinaires ou caulinaires, et au cours du développement des racines latérales. Les réseaux prédits sont alors explorés afin d'identifier les régulateurs potentiels de *PI* (Figure 10B).

Les résultats préliminaires suggèrent que les régulateurs transcriptionnels prédits de *PI* le sont de façon relativement robuste. Parmi ceux-ci, les facteurs de transcription PLT1, 2, 3 et 4 sont intéressants car ce sont des régulateurs bien connus de l'auto-maintien du méristème apical racinaire de la racine primaire (Aida et al., 2004; Santuari et al., 2016), et des données récentes ont révélé leur importance dans l'organisation fonctionnelle du PRL (Du and Scheres, 2017; Hofhuis et al., 2013).

D'autres facteurs prédits comme régulateurs de *PI* dans le LR transcriptomic dataset retiennent l'attention car leur rôle dans l'organisation fonctionnelle de tissus en croissance est également connu : notamment *LHW* (Ohashi-Ito et al., 2014) et les facteurs de transcription de la famille KANADI (*KAN4*) et HD-ZipIII (*PHB*) (Hawker and Bowman, 2004; Lee and Clark, 2015).

Ces analyses se poursuivent afin de consolider la sélection de gènes candidats régulateurs potentiels de *PI*, et dont la redondance fonctionnelle pourrait être limitée. Des allèles mutants perte de fonction de ces gènes seront alors recherchés et la dépendance de l'expression de *PI* vis à vis de ces régulateurs devra alors être confirmée de la même façon que pour les gènes cibles de *PUCHI*. L'analyse du promoteur de *PI* pourrait éventuellement révéler la présence de motifs de liaison pour certains de ces facteurs de transcription, pour lesquels l'hypothèse d'une régulation directe de *PI* pourra alors être proposée.

#### **4.3. Analyse du réseau de gènes impliqué dans le développement de la racine latérale**

L'inférence par TDCor de réseaux de gènes impliqués dans le développement des racines latérales à partir du LR transcriptomic dataset produit de façon robuste une structure en 3 ensembles : deux sous-réseaux assez étendus, à l'intérieur desquels de nombreuses régulations positives connectent les différents gènes, et qui sont liés l'un à l'autre au contraire par des relations mutuellement exclusives, et un troisième groupe de gènes, moins nombreux, dont les interactions ne permettent pas de les classer dans l'un ou l'autre des deux premiers groupes (Lavenus et al., 2015). Cette structure de réseau suggère un mécanisme de bifurcation entre l'activité des deux premiers grands groupes de gènes. Le premier comprend *ARF7*, *PUCHI*, et d'autres facteurs dont l'expression, élevée dans les phases précoces du développement du PRL, décline rapidement et est pour certains spatialement réduite à la base du primordium. L'autre groupe comprend *ARF5* et

d'autres facteurs de transcription caractéristiques de l'organisation fonctionnelle du méristème apical racinaire, tels que *SCR*, *SHR*, *PLT1-4*. De façon intéressante TDCor prédit que *PI* appartient à ce second groupe de gènes, en aval, particulièrement, de *PLT1*, *PLT2* et *PLT3*. L'expression des gènes de ce second groupe est faible en début de développement et augmente significativement dans la seconde moitié de la séquence de développement du PRL. Leur domaine d'expression est souvent central dans le PRL, dans la zone où le méristème racinaire est mis en place (Du and Scheres, 2017; Lavenus et al., 2015).

La structure globale du réseau génétique pourrait donc expliquer la transition dans le temps et la disjonction dans l'espace des deux domaines d'expression correspondant à ces deux sous-réseaux. Les gènes du troisième groupe seraient susceptible de médier la transition, dans la zone centrale du méristème et/ou à partir d'un stade de développement intermédiaire, entre l'activité des gènes du groupe *ARF7* vers celle des gènes du groupe *ARF5*. Ces gènes constituent donc des candidats pour le déclenchement de la transition vers la mise en place du méristème, et en particulier, le centre quiescent. Parmi ces gènes, des facteurs de transcription de la famille WOX (*WOX11*, *WOX14*), MYB (*MYB56*), et CRF sont particulièrement intéressants.

#### ***4.4. Identification de régulateurs potentiels de la transition vers la phase méristématique et caractérisation préliminaire de leur phénotype racinaire***

Les gènes candidats identifiés sur la base de leur profil d'expression dans le LR transcriptomic dataset et des données fonctionnelles publiées dans la littérature seront analysés de façon à tester expérimentalement leur rôle dans le développement du PRL et particulièrement, la mise en place du méristème.

La caractérisation du phénotype racinaire a déjà été initiée chez certains des mutants de ces gènes candidats disponibles dans les collections. Des résultats préliminaires suggèrent que le mutant *myb56* et les mutants multiples *crf* sont affectés dans la progression du développement de racine latérale (Figure 11). Ces analyses seront poursuivies et enrichies par des analyses détaillées de l'anatomie des PRL mutants et de leur organisation fonctionnelle, en particulier concernant l'expression du marqueur *PI::GFP*.

Le profil d'expression de ces gènes régulateurs dans les PRL sera également étudié. Si les données suggèrent que ces régulateurs contrôlent bien l'induction de l'expression de *PI* de façon cellule-autonome, cette hypothèse sera vérifiée en induisant l'expression de ces gènes dans d'autres régions du primordium et en analysant l'impact sur l'expression de *PI::GFP*.

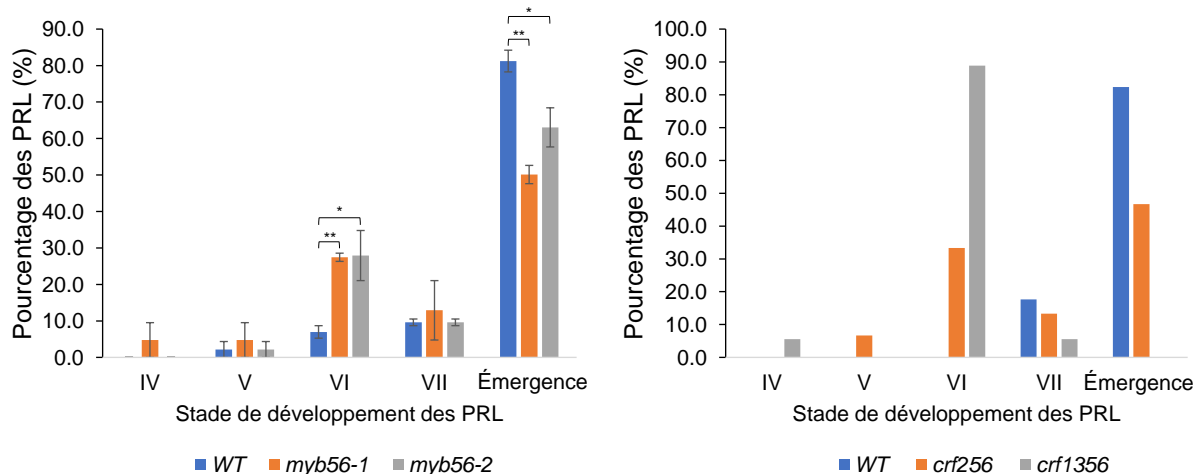


**Figure 11.** Profil de distribution des stades de développement atteints par les primordia de racine latérale induits par gravistimulation, et observés au microscope à contraste interférentiel 48h après gravistimulation, dans le contexte sauvage (WT) et dans des génotypes mutants *myb56* (A) et *crf256* et *crf1356* (B). n = 20-26 plantules, 1 répétition.

#### 4.5. Conclusion du chapitre IV

La caractérisation du profil d'expression de la construction *PI::GFP* a permis de confirmer que le gène *PISTILLATA* constituait un bon marqueur de la mise en place du centre quiescent dans le primordium de racine latérale. La recherche de gènes candidats par des approches d'inférence de réseaux de gènes a permis d'identifier un nombre important de régulateurs potentiels, parmi lesquels les plus intéressants sont actuellement sélectionnés en fonction des données connues sur ces gènes et des outils disponibles. De façon intéressante, les protocoles d'induction de racines latérales permettent d'explorer relativement rapidement et de façon précise le phénotype de ramification racinaire d'un nombre conséquent de génotypes (Lavenus et al., 2013). Toutefois, il est possible que des propriétés de redondance fonctionnelle masquent la contribution d'un gène pris isolément (*e.g.* *PLT*; (Du and Scheres, 2017)). Des mutants multiples pourront alors être générés.

#### Chapitre V: Discussion générale

Cette thèse a porté sur l'exploration des propriétés du réseau de gènes régulant le développement des racines latérales et a ciblé particulièrement deux questions :

- (i) Quels sont les processus cellulaires contrôlés par le facteur de transcription PUCHI lors du développement des racines latérales ?

(ii) Quels sont les facteurs génétiques contrôlant la mise en place du méristème dans le primordium de racines latérales et particulièrement, l'établissement *de novo* du centre quiescent ?

Ces objectifs ont été abordés en utilisant une stratégie originale combinant l'exploration de base de données transcriptomiques, l'inférence de réseau de gènes et la caractérisation fonctionnelle classique des gènes candidats identifiés, en aval de *PUCHI* ou en amont de *PI*.

Cette approche s'est révélée efficace pour mettre en évidence que *PUCHI* exerce, de façon inattendue, un rôle de master régulateur de la voie de biosynthèse des VLCFA en contrôlant la dynamique d'expression de plusieurs gènes de biosynthèse lors du développement des PRL. Compte tenu du phénotype racinaire de certains des mutants pour ces gènes, la perte de cette régulation chez le mutant *puchi-1* pourrait expliquer le retard de développement des PRL et leur densité plus importante le long de la racine primaire. Toutefois le rôle précis des VLCFA dans ces processus demeure inconnu. Par ailleurs, la complexité des patrons d'expression des gènes de biosynthèse des VLCFA dans et autour du PRL suggère que *PUCHI* n'est pas le seul régulateur à intervenir.

Les recherches futures pourront s'attacher à caractériser le rôle des VLCFA dans le développement des PRL et l'importance de cette régulation coordonnée par *PUCHI*. Des analyses en microscopie électronique sont en cours afin de comparer l'ultrastructure cellulaire dans les PRL *puchi-1* et sauvages. La cartographie plus fine et quantitative de la signalisation auxine et cytokinine dans les primordia (Figure 3), ainsi que la caractérisation des profils de localisation des transporteurs d'auxine (Wattelet-Boyer et al., 2016; Roudier et al., 2010b) pourraient contribuer à éclaircir les mécanismes d'organisation fonctionnelle affectés par la modification du profil lipidomique.

La recherche des régulateurs contrôlant la mise en place du centre quiescent est à un stade moins avancé mais de nombreux candidats ont d'ores et déjà été identifiés. Les données de la littérature, et des expériences préliminaires de phénotypage racinaire ont attiré l'attention sur un petit nombre de gènes dont la caractérisation va être poursuivie. De façon intéressante, la stratégie de recherche, basée sur la corrélation entre profils d'expression dans des bases de données transcriptomiques permet d'identifier des candidats sans *a priori* trop étroit sur leur fonction. Dans ce contexte, il est particulièrement notable d'identifier des régulateurs connus de l'organisation fonctionnelle d'autres territoires, comme contrôlant potentiellement la mise en place des identités méristématiques dans le primordium.



# **REFERENCES**

**For both the French summary and the English thesis**

- Aida, M., Beis, D., Heidstra, R., Willemsen, V., Blilou, I., Galinha, C., Nussaume, L., Noh, Y., Amasino, R., and Scheres, B.** (2004). The PLETHORA Genes Mediate Patterning of the Arabidopsis Root Stem Cell Niche. *Cell* **119**: 109–120.
- De Almeida Engler, J. et al.** (2009). Systematic analysis of cell-cycle gene expression during Arabidopsis development. *Plant J.* **59**: 645–660.
- Alon, U.** (2007). Network motifs: Theory and experimental approaches. *Nat. Rev. Genet.* **8**: 450–461.
- Andersen, T.G., Barberon, M., and Geldner, N.** (2015). Suberization-the second life of an endodermal cell. *Curr. Opin. Plant Biol.* **28**: 9–15.
- Anne, P., Amiguet-Vercher, A., Brandt, B., Kalmbach, L., Geldner, N., Hothorn, M., and Hardtke, C.S.** (2018). CLERK is a novel receptor kinase required for sensing of root-active CLE peptides in *Arabidopsis*. *Development* **145**: dev162354.
- Aoyama, T. and Chua, N.H.** (1997). A glucocorticoid-mediated transcriptional induction system in transgenic plants. *Plant J.* **11**: 605–612.
- Araya, T., Miyamoto, M., Wibowo, J., Suzuki, A., Kojima, S., Tsuchiya, Y.N., Sawa, S., Fukuda, H., von Wirén, N., and Takahashi, H.** (2014). CLE-CLAVATA1 peptide-receptor signaling module regulates the expansion of plant root systems in a nitrogen-dependent manner. *Proc. Natl. Acad. Sci.* **111**: 2029–2034.
- Atta, R., Laurens, L., Boucheron-Dubuisson, E., Guivarc’h, A., Carnero, E., Giraudat-Pautot, V., Rech, P., and Chriqui, D.** (2009). Pluripotency of Arabidopsis xylem pericycle underlies shoot regeneration from root and hypocotyl explants grown in vitro. *Plant J.* **57**: 626–644.
- Bach, L. et al.** (2008). The very-long-chain hydroxy fatty acyl-CoA dehydratase PASTICCINO2 is essential and limiting for plant development. *Proc. Natl. Acad. Sci.* **105**: 14727–14731.
- Bach, L. and Faure, J.D.** (2010). Role of very-long-chain fatty acids in plant development, when chain length does matter. *Comptes Rendus - Biol.* **333**: 361–370.
- Bach, L., Gissot, L., Marion, J., Tellier, F., Moreau, P., Satiat-Jeunemaitre, B., Palauqui, J.-C., Napier, J.A., and Faure, J.-D.** (2011). Very-long-chain fatty acids are required for cell plate formation during cytokinesis in *Arabidopsis thaliana*. *J. Cell Sci.* **124**: 3223–3234.
- Bagchi, R., Melnyk, C.W., Christ, G., Winkler, M., Kirchsteiner, K., Salehin, M., Mergner, J., Niemeyer, M., Schwechheimer, C., Calderón Villalobos, L.I.A., and Estelle, M.** (2018). The *Arabidopsis* ALF4 protein is a regulator of SCF E3 ligases. *EMBO J.* **37**: 255–268.
- Band, L.R. et al.** (2012). Root gravitropism is regulated by a transient lateral auxin gradient controlled by a tipping-point mechanism. *Proc. Natl. Acad. Sci.* **109**: 4668–4673.
- Bao, Y. et al.** (2014). Plant roots use a patterning mechanism to position lateral root branches toward available water. *Proc. Natl. Acad. Sci.* **111**: 9319–9324.
- Baxter, I., Hosmani, P.S., Rus, A., Lahner, B., Borevitz, J.O., Muthukumar, B., Mickelbart, M. V., Schreiber, L., Franke, R.B., and Salt, D.E.** (2009). Root suberin forms an extracellular barrier that affects water relations and mineral nutrition in *Arabidopsis*. *PLoS Genet.* **5**.
- Beaudoin, F., Wu, X., Li, F., Haslam, R.P., Markham, J.E., Zheng, H., Napier, J.A., and Kunst, L.** (2009). Functional Characterization of the Arabidopsis  $\beta$ -Ketoacyl-Coenzyme A

- Reductase Candidates of the Fatty Acid Elongase. *Plant Physiol.* **150**: 1174–1191.
- Beeckman, T.** (2009). *Annual Plant Reviews, Root Development* (John Wiley & Sons).
- Beeckman, T., Burssens, S., and Inze, D.** (2001). The peri-cell-cycle in *Arabidopsis*. *J. Exp. Bot.* **52**: 403–411.
- Beeckman, T. and De Smet, I.** (2014). Pericycle. *Curr. Biol.* **24**: 378–379.
- Bellec, Y., Harrar, Y., Butaeye, C., Darnet, S., Bellini, C., and Faure, J.D.** (2002). Pasticcino2 is a protein tyrosine phosphatase-like involved in cell proliferation and differentiation in *Arabidopsis*. *Plant J.* **32**: 713–722.
- Bellini, C., Pacurar, D.I., and Perrone, I.** (2014). Adventitious Roots and Lateral Roots: Similarities and Differences. *Annu. Rev. Plant Biol.* **65**: 639–666.
- Bencivenga, S., Simonini, S., Benkova, E., and Colombo, L.** (2012). The Transcription Factors BEL1 and SPL Are Required for Cytokinin and Auxin Signaling During Ovule Development in *Arabidopsis*. *Plant Cell* **24**: 2886–2897.
- Benitez-Alfonso, Y.** (2014). Symplastic intercellular transport from a developmental perspective. *J. Exp. Bot.* **65**: 1857–1863.
- Benitez-Alfonso, Y., Faulkner, C., Pendle, A., Miyashima, S., Helariutta, Y., and Maule, A.** (2013). Symplastic Intercellular Connectivity Regulates Lateral Root Patterning. *Dev. Cell* **26**: 136–147.
- Benková, E., Michniewicz, M., Sauer, M., Teichmann, T., Seifertová, D., Jürgens, G., and Friml, J.** (2003). Local, Efflux-Dependent Auxin Gradients as a Common Module for Plant Organ Formation. *Cell* **115**: 591–602.
- Berckmans, B. et al.** (2011). Auxin-Dependent Cell Cycle Reactivation through Transcriptional Regulation of *Arabidopsis* E2Fa by Lateral Organ Boundary Proteins. *Plant Cell* **23**: 3671–3683.
- Bielach, A., Podlešáková, K., Marhavý, P., Duclercq, J., Cuesta, C., Müller, B., Grunewald, W., Tarkowski, P., and Benková, E.** (2012). Spatiotemporal Regulation of Lateral Root Organogenesis in *Arabidopsis* by Cytokinin. *Plant Cell* **24**: 3967–3981.
- Birnbaum, K.D.** (2016). How many ways are there to make a root? *Curr. Opin. Plant Biol.* **34**: 61–67.
- Bishopp, A., Help, H., El-Showk, S., Weijers, D., Scheres, B., Friml, J., Benková, E., Mähönen, A.P., and Helariutta, Y.** (2011a). A mutually inhibitory interaction between auxin and cytokinin specifies vascular pattern in roots. *Curr. Biol.* **21**: 917–926.
- Bishopp, A., Lehesranta, S., Vatén, A., Help, H., El-Showk, S., Scheres, B., Helariutta, K., Mähönen, A.P., Sakakibara, H., and Helariutta, Y.** (2011b). Phloem-transported cytokinin regulates polar auxin transport and maintains vascular pattern in the root meristem. *Curr. Biol.* **21**: 927–932.
- Blacklock, B.J. and Jaworski, J.G.** (2006). Substrate specificity of *Arabidopsis* 3-ketoacyl-CoA synthases. *Biochem. Biophys. Res. Commun.* **346**: 583–590.
- Blilou, I., Xu, J., Wildwater, M., Willemsen, V., Paponov, I., Friml, J., Heidstra, R., Aida, M., Palme, K., and Scheres, B.** (2005). The PIN auxin efflux facilitator network controls growth and patterning in *Arabidopsis* roots. *Nature* **433**: 39–44.
- Bouyer, D., Roudier, F., Heese, M., Andersen, E.D., Gey, D., Nowack, M.K., Goodrich, J.,**

- Renou, J.P., Grini, P.E., Colot, V., and Schnittger, A.** (2011). Polycomb repressive complex 2 controls the embryo-to-seedling phase transition. *PLoS Genet.* **7**.
- Bowman, N.P.H.A.J.L.** (2004). Roles for Class III HD-Zip and KANADI Genes in Arabidopsis Root Development. *Plant Physiol.* **135**: 2261–2270.
- Brady, S.M., Orlando, D.A., Lee, J.-Y., Wang, J.Y., Koch, J., Dinneny, J.R., Mace, D., Ohler, U., and Benfey, P.N.** (2007). A High-Resolution Root Spatiotemporal Map Reveals Dominant Expression Patterns. *Science* (80-. ). **318**: 801–806.
- Breuer, C., Braidwood, L., and Sugimoto, K.** (2014). Endocycling in the path of plant development. *Curr. Opin. Plant Biol.* **17**: 78–85.
- Brundrett, M.C., Kendrick, B., and Peterson, C.A.** (1991). Efficient lipid staining in plant material with sudan red 7B or fluorol [correction of fluoral] yellow 088 in polyethylene glycol-glycerol. *Biotech. Histochem.* **66**: 111–116.
- Bustillo-Avedaño, E., Ibáñez, S., Sanz, O., Barross, J.A.S., Gude, I., Perianez-Rodriguez, J., Micol, J.L., del Pozo, J.C., Moreno-Risueno, M.A., and Perez-Perez, J.M.** (2017). Regulation of Hormonal Control, Cell Reprogramming and Patterning during De Novo Root Organogenesis. *Plant Physiol.* **176**: pp.00980.2017.
- Caggiano, M.P., Yu, X., Bhatia, N., Larsson, A., Ram, H., Ohno, C.K., Sappl, P., Meyerowitz, E.M., Jönsson, H., and Heisler, M.G.** (2017). Cell type boundaries organize plant development. *Elife* **6**: 1–32.
- De Caluwé, J., Xiao, Q., Hermans, C., Verbruggen, N., Leloup, J.-C., and Gonze, D.** (2016). A Compact Model for the Complex Plant Circadian Clock. *Front. Plant Sci.* **7**: 1–15.
- Casimiro, I., Beeckman, T., Graham, N., Bhalerao, R., Zhang, H., Casero, P., Sandberg, G., and Bennett, M.J.** (2003). Dissecting Arabidopsis lateral root development. *Trends Plant Sci.* **8**: 165–171.
- Casimiro, I., Marchant, A., Bhalerao, R.P., Beeckman, T., Dhooge, S., Swarup, R., Graham, N., Inze, D., Sandberg, G., Casero, P.J., and Bennett, M.** (2001). Auxin Transport Promotes Arabidopsis Lateral Root Initiation. *Plant Cell* **13**: 843.
- Cassan-Wang, H., Goué, N., Saidi, M.N., Legay, S., Sivadon, P., Goffner, D., and Grima-Pettenati, J.** (2013). Identification of novel transcription factors regulating secondary cell wall formation in Arabidopsis. *Front. Plant Sci.* **4**: 1–14.
- Cazzonelli, C.I. et al.** (2013). Role of the Arabidopsis PIN6 Auxin Transporter in Auxin Homeostasis and Auxin-Mediated Development. *PLoS One* **8**.
- Celenza, J.L., Grisafi, P.L., and Fink, G.R.** (1995). A pathway for lateral root formation in Arabidopsis thaliana. *Genes Dev.* **9**: 2131–42.
- Chandler, J.W. and Werr, W.** (2017). DORNRÖSCHEN, DORNRÖSCHEN-LIKE, and PUCHI redundantly control floral meristem identity and organ initiation in Arabidopsis. *J. Exp. Bot.* **68**: 3457–3472.
- Chang, L., Ramireddy, E., and Schmülling, T.** (2015). Cytokinin as a positional cue regulating lateral root spacing in Arabidopsis. *J. Exp. Bot.* **66**: 4759–4768.
- Chanvivattana, Y.** (2004). Interaction of Polycomb-group proteins controlling flowering in Arabidopsis. *Development* **131**: 5263–5276.
- Che, P., Lall, S., and Howell, S.H.** (2007). Developmental steps in acquiring competence for shoot development in Arabidopsis tissue culture. *Planta* **226**: 1183–1194.

- Che, P., Lall, S., Nettleton, D., and Howell, S.H.** (2006). Gene expression programs during shoot, root, and callus development in *Arabidopsis* tissue culture. *Plant Physiol.* **141**: 620–37.
- Chiatante, D., Rost, T., Bryant, J., and Scippa, G.S.** (2018). Regulatory networks controlling the development of the root system and the formation of lateral roots: a comparative analysis of the roles of pericycle and vascular cambium. *Ann. Bot.*: 1–14.
- Choe, G. and Lee, J.Y.** (2017). Push–pull strategy in the regulation of postembryonic root development. *Curr. Opin. Plant Biol.* **35**: 158–164.
- Clough, S.J. and Bent, A.F.** (1998). Floral dip: A simplified method for *Agrobacterium*-mediated transformation of *Arabidopsis thaliana*. *Plant J.* **16**: 735–743.
- Cui, H., Levesque, M.P., Vernoux, T., Jung, J.W., Paquette, A.J., Gallagher, K.L., Wang, J.Y., Blilou, I., Scheres, B., and Benfey, P.N.** (2007). An evolutionarily conserved mechanism delimiting SHR movement defines a single layer of endodermis in plants. *Science* (80-. ). **316**: 421–425.
- Van Damme, D., De Rybel, B., Gudesblat, G., Demidov, D., Grunewald, W., De Smet, I., Houben, A., Beeckman, T., and Russinova, E.** (2011). *Arabidopsis*  $\alpha$  Aurora Kinases Function in Formative Cell Division Plane Orientation. *Plant Cell* **23**: 4013–4024.
- Dembinsky, D. et al.** (2007). Transcriptomic and Proteomic Analyses of Pericycle Cells of the Maize Primary Root. *Plant Physiol.* **145**: 575–588.
- Deng, Q., Wang, X., Zhang, D., Wang, X., Feng, C., and Xu, S.** (2017). BRS1 function in facilitating lateral root emergence in *Arabidopsis*. *Int. J. Mol. Sci.* **18**: 1–11.
- Derkacheva, M. and Hennig, L.** (2014). Variations on a theme: Polycomb group proteins in plants. *J. Exp. Bot.* **65**: 2769–2784.
- DiDonato, R.J., Arbuckle, E., Buker, S., Sheets, J., Tobar, J., Totong, R., Grisafi, P., Fink, G.R., and Celenza, J.L.** (2004). *Arabidopsis* ALF4 encodes a nuclear-localized protein required for lateral root formation. *Plant J.* **37**: 340–353.
- Ditengou, F.A., Teale, W.D., Kochersperger, P., Flittner, K.A., Kneuper, I., van der Graaff, E., Nziengui, H., Pinoso, F., Li, X., Nitschke, R., Laux, T., and Palme, K.** (2008). Mechanical induction of lateral root initiation in *Arabidopsis thaliana*. *Proc. Natl. Acad. Sci.* **105**: 18818–18823.
- Doerner, P.** (1998). Root development: quiescent center not so mute after all. *Curr. Biol.* **8**: R42–R44.
- Dolan, L., Janmaat, K., Willemsen, V., Linstead, P., Poethig, S., Roberts, K., and Scheres, B.** (1993). Cellular organisation of the *Arabidopsis thaliana* root. *Development* **119**: 71–84.
- de Dorlodot, S., Forster, B., Pagès, L., Price, A., Tuberosa, R., and Draye, X.** (2007). Root system architecture: opportunities and constraints for genetic improvement of crops. *Trends Plant Sci.* **12**: 474–481.
- Du, Y. and Scheres, B.** (2017a). Lateral root formation and the multiple roles of auxin. *J. Exp. Bot.*
- Du, Y. and Scheres, B.** (2017b). PLETHORA transcription factors orchestrate de novo organ patterning during *Arabidopsis* lateral root outgrowth. *Proc. Natl. Acad. Sci.* **114**: 201714410.
- Dubrovsky, J.G.** (2000). Pericycle Cell Proliferation and Lateral Root Initiation in *Arabidopsis*.

- Plant Physiol. **124**: 1648–1657.
- Dubrovsky, J.G. and Forde, B.G.** (2012). Quantitative Analysis of Lateral Root Development: Pitfalls and How to Avoid Them. *Plant Cell* **24**: 4–14.
- Dubrovsky, J.G., Gambetta, G.A., Hernández-Barrera, A., Shishkova, S., and González, I.** (2006). Lateral root initiation in Arabidopsis: Developmental window, spatial patterning, density and predictability. *Ann. Bot.* **97**: 903–915.
- Dubrovsky, J.G., Rost, T.L., Colón-Carmona, A., and Doerner, P.** (2001). Early primordium morphogenesis during lateral root initiation in Arabidopsis thaliana. *Planta* **214**: 30–36.
- Dubrovsky, J.G., Sauer, M., Napsucialy-Mendivil, S., Ivanchenko, M.G., Friml, J., Shishkova, S., Celenza, J., and Benkova, E.** (2008). Auxin acts as a local morphogenetic trigger to specify lateral root founder cells. *Proc. Natl. Acad. Sci.* **105**: 8790–8794.
- el-Showk, S., Help-Rinta-Rahko, H., Blomster, T., Siligato, R., Marée, A.F.M., Mähönen, A.P., and Grieneisen, V.A.** (2015). Parsimonious Model of Vascular Patterning Links Transverse Hormone Fluxes to Lateral Root Initiation: Auxin Leads the Way, while Cytokinin Levels Out. *PLoS Comput. Biol.* **11**: 1–40.
- Emery, J.F., Floyd, S.K., Alvarez, J., Eshed, Y., Hawker, N.P., Izhaki, A., Baum, S.F., and Bowman, J.L.** (2003). Radial Patterning of Arabidopsis Shoots by Class III HD-ZIP and KANADI Genes. *Curr. Biol.* **13**: 1768–1774.
- Fan, M., Xu, C., Xu, K., and Hu, Y.** (2012). LATERAL ORGAN BOUNDARIES DOMAIN transcription factors direct callus formation in Arabidopsis regeneration. *Cell Res.* **22**: 1169–1180.
- Faure, J.D., Vittorioso, P., Santoni, V., Fraiser, V., Prinsen, E., Barlier, I., Van Onckelen, H., Caboche, M., and Bellini, C.** (1998). The PASTICCINO genes of Arabidopsis thaliana are involved in the control of cell division and differentiation. *Development* **125**: 909–918.
- Feng, Z., Sun, X., Wang, G., Liu, H., and Zhu, J.** (2012). LBD29 regulates the cell cycle progression in response to auxin during lateral root formation in Arabidopsis thaliana. *Ann. Bot.* **110**: 1–10.
- Fernández-Marcos, M., Desvoyes, B., Manzano, C., Liberman, L.M., Benfey, P.N., del Pozo, J.C., and Gutierrez, C.** (2017). Control of Arabidopsis lateral root primordium boundaries by MYB36. *New Phytol.* **213**: 105–112.
- Fernandez, A., Drozdzecki, A., Hoogewijs, K., Nguyen, A., Beekman, T., Madder, A., and Hilson, P.** (2013). Transcriptional and Functional Classification of the GOLVEN/ROOT GROWTH FACTOR/CLE-Like Signaling Peptides Reveals Their Role in Lateral Root and Hair Formation. *Plant Physiol.* **161**: 954–970.
- Fernandez, A., Drozdzecki, A., Hoogewijs, K., Vassileva, V., Madder, A., Beekman, T., and Hilson, P.** (2015). The GLV6/RGF8/CLEL2 peptide regulates early pericycle divisions during lateral root initiation. *J. Exp. Bot.* **66**: 5245–5256.
- Fiebig, A., Mayfield, J.A., Miley, N.L., Chau, S., Fischer, R.L., and Preuss, D.** (2000). Alterations in CER6, a gene identical to CUT1, differentially affect long-chain lipid content on the surface of pollen and stems. *Plant Cell* **12**: 2001–8.
- Fisher, A.P. and Sozzani, R.** (2016). Uncovering the networks involved in stem cell maintenance and asymmetric cell division in the Arabidopsis root. *Curr. Opin. Plant Biol.* **29**: 38–43.

- Friml, J., Vieten, A., Sauer, M., Weijers, D., Schwarz, H., Hamann, T., Offringa, R., and Jürgens, G.** (2003). Efflux-dependent auxin gradients establish the apical–basal axis of *Arabidopsis*. *Nature* **426**: 147–153.
- Fukaki, H., Tameda, S., Masuda, H., and Tasaka, M.** (2002). Lateral root formation is blocked by a gain-of-function mutation in the solitary-root/IAA14 gene of *Arabidopsis*. *Plant J.* **29**: 153–168.
- Fukaki, H., Taniguchi, N., and Tasaka, M.** (2006). PICKLE is required for SOLITARY-ROOT/IAA14-mediated repression of ARF7 and ARF19 activity during *Arabidopsis* lateral root initiation. *Plant J.* **48**: 380–389.
- Galinha, C., Bilsborough, G., and Tsiantis, M.** (2009). Hormonal input in plant meristems: A balancing act. *Semin. Cell Dev. Biol.* **20**: 1149–1156.
- Galinha, C., Hofhuis, H., Luijten, M., Willemsen, V., Blilou, I., Heidstra, R., and Scheres, B.** (2007). PLETHORA proteins as dose-dependent master regulators of *Arabidopsis* root development. *Nature* **449**: 1053–1057.
- Geldner, N.** (2013a). Casparian strips. *Curr. Biol.* **23**: R1025–R1026.
- Geldner, N.** (2013b). The Endodermis. *Annu. Rev. Plant Biol.* **64**: 531–558.
- Geldner, N., Anders, N., Wolters, H., Keicher, J., Kornberger, W., Müller, P., Delbarre, A., Ueda, T., Nakano, A., and Jürgens, G.** (2003). The *Arabidopsis* GNOM ARF-GEF mediates endosomal recycling, auxin transport, and auxin-dependent plant growth. *Cell* **112**: 219–30.
- Genschik, P., Marrocco, K., Bach, L., Noir, S., and Criqui, M.C.** (2014). Selective protein degradation: A rheostat to modulate cell-cycle phase transitions. *J. Exp. Bot.* **65**: 2603–2615.
- Godfray, H.C.J., Beddington, J.R., Crute, I.R., Haddad, L., Lawrence, D., Muir, J.F., Pretty, J., Robinson, S., Thomas, S.M., and Toulmin, C.** (2010). Food Security: The Challenge of Feeding 9 Billion People. *Science* (80-. ). **327**: 812–818.
- Goh, T., Joi, S., Mimura, T., and Fukaki, H.** (2012a). The establishment of asymmetry in *Arabidopsis* lateral root founder cells is regulated by LBD16/ASL18 and related LBD/ASL proteins. *Development* **139**: 883–893.
- Goh, T., Kasahara, H., Mimura, T., Kamiya, Y., and Fukaki, H.** (2012b). Multiple AUX/IAA-ARF modules regulate lateral root formation: The role of *Arabidopsis* SHY2/IAA3-mediated auxin signalling. *Philos. Trans. R. Soc. B Biol. Sci.* **367**: 1461–1468.
- Goh, T., Toyokura, K., Wells, D.M., Swarup, K., Yamamoto, M., Mimura, T., Weijers, D., Fukaki, H., Laplaze, L., Bennett, M.J., and Guyomarc’h, S.** (2016). Quiescent center initiation in the *Arabidopsis* lateral root primordia is dependent on the SCARECROW transcription factor. *Development* **143**: 3363–3371.
- Gray, J.E., Holroyd, G.H., van der Lee, F.M., Bahrami, A.R., Sijmons, P.C., Woodward, F.I., Schuch, W., and Hetherington, A.M.** (2000). The HIC signalling pathway links CO<sub>2</sub> perception to stomatal development. *Nature* **408**: 713–716.
- Green, J.B.A. and Sharpe, J.** (2015). Positional information and reaction-diffusion: two big ideas in developmental biology combine. *Development* **142**: 1203–1211.
- Gu, X., Xu, T., and He, Y.** (2014). A Histone H3 Lysine-27 Methyltransferase Complex Represses Lateral Root Formation in *Arabidopsis thaliana*. *Mol. Plant* **7**: 977–988.

- Gunning, B.E.S., Hughes, J.E., and Hardham, A.R.** (1978). Formative and proliferative cell divisions, cell differentiation, and developmental changes in the meristem of *Azolla* roots. *Planta* **143**: 121–144.
- Gutierrez, L., Mongelard, G., Floková, K., Păcurar, D.I., Novák, O., Staswick, P., Kowalczyk, M., Păcurar, M., Demailly, H., Geiss, G., and Bellini, C.** (2012). Auxin Controls *Arabidopsis* Adventitious Root Initiation by Regulating Jasmonic Acid Homeostasis. *Plant Cell* **24**: 2515–2527.
- Guyomarc'h, S., Leran, S., Auzon-Cape, M., Perrine-Walker, F., Lucas, M., and Laplaze, L.** (2012). Early development and gravitropic response of lateral roots in *Arabidopsis thaliana*. *Philos. Trans. R. Soc. B Biol. Sci.* **367**: 1509–1516.
- Haberer, G., Erschadi, S., and Torres-Ruiz, R.A.** (2002). The *Arabidopsis* gene PEPINO/PASTICCINO2 is required for proliferation control of meristematic and non-meristematic cells and encodes a putative anti-phosphatase. *Dev. Genes Evol.* **212**: 542–550.
- Haecker, A., Gross-Hardt, R., Geiges, B., Sarkar, A., Breuninger, H., Herrmann, M., and Laux, T.** (2004). Expression dynamics of WOX genes mark cell fate decisions during early embryonic patterning in *Arabidopsis thaliana*. *Development* **131**: 657–68.
- Hammer, G.L., Dong, Z., McLean, G., Doherty, A., Messina, C., Schussler, J., Zinselmeier, C., Paszkiewicz, S., and Cooper, M.** (2009). Can changes in canopy and/or root system architecture explain historical maize yield trends in the U.S. corn belt? *Crop Sci.* **49**: 299–312.
- Harrar, Y., Bellec, Y., Bellini, C., and Faure, J.** (2003). Hormonal control of cell proliferation requires PASTICCINO genes. *Plant Physiol.* **132**: 1217–1227.
- Haslam, T.M. and Kunst, L.** (2013). Extending The Story Of Very-Long-Chain Fatty Acid Elongation. *Plant Sci.* **210**: 93–107.
- Hegebarth, D., Buschhaus, C., Joubès, J., Thoraval, D., Bird, D., and Jetter, R.** (2017). *Arabidopsis* ketoacyl-CoA synthase 16 (KCS16) forms C36/C38acyl precursors for leaf trichome and pavement surface wax. *Plant Cell Environ.* **40**: 1761–1776.
- Himanen, K.** (2002). Auxin-Mediated Cell Cycle Activation during Early Lateral Root Initiation. *PLANT CELL ONLINE* **14**: 2339–2351.
- Himanen, K., Vuylsteke, M., Vanneste, S., Vercruyse, S., Boucheron, E., Alard, P., Chriqui, D., Van Montagu, M., Inze, D., and Beekman, T.** (2004). Transcript profiling of early lateral root initiation. *Proc Natl Acad Sci U S A* **101**: 5146–5151.
- Hirota, A., Kato, T., Fukaki, H., Aida, M., and Tasaka, M.** (2007). The Auxin-Regulated AP2/EREBP Gene PUCHI Is Required for Morphogenesis in the Early Lateral Root Primordium of *Arabidopsis*. *Plant Cell Online* **19**: 2156–2168.
- Ho, K.K., Zhang, H., Golden, B.L., and Ogas, J.** (2013). PICKLE is a CHD subfamily II ATP-dependent chromatin remodeling factor. *Biochim. Biophys. Acta - Gene Regul. Mech.* **1829**: 199–210.
- Hofhuis, H., Laskowski, M., Du, Y., Prasad, K., Grigg, S., Pinon, V., and Scheres, B.** (2013). Phyllotaxis and rhizotaxis in *Arabidopsis* are modified by three plethora transcription factors. *Curr. Biol.* **23**: 956–962.
- ten Hove, C.A., Lu, K.-J., and Weijers, D.** (2015). Building a plant: cell fate specification in the early *Arabidopsis* embryo. *Development* **142**: 420–430.

- ten Hove, C.A., Willemsen, V., de Vries, W.J., van Dijken, A., Scheres, B., and Heidstra, R.** (2010). SCHIZORIZA Encodes a Nuclear Factor Regulating Asymmetry of Stem Cell Divisions in the Arabidopsis Root. *Curr. Biol.* **20**: 452–457.
- Hu, B., Zhang, G., Liu, W., Shi, J., Wang, H., Qi, M., Li, J., Qin, P., Ruan, Y., Huang, H., Zhang, Y., and Xu, L.** (2017). Divergent regeneration-competent cells adopt a common mechanism for callus initiation in angiosperms. *Regeneration* **4**: 132–139.
- Hu, C. et al.** (2018). A group of receptor kinases are essential for CLAVATA signalling to maintain stem cell homeostasis. *Nat. Plants* **4**: 205–211.
- Hu, X. and Xu, L.** (2016). Transcription Factors WOX11/12 Directly Activate WOX5/7 to Promote Root Primordia Initiation and Organogenesis. *Plant Physiol.* **172**: 2363–2373.
- Ivanova, N.B.** (2003). Response to Comments on “ ‘Stemness’: Transcriptional Profiling of Embryonic and Adult Stem Cells” and “A Stem Cell Molecular Signature.” *Science* (80-. ). **302**: 393d–393.
- Iwakawa, H., Shinmyo, A., and Sekine, M.** (2006). Arabidopsis CDKA;1, a cdc2 homologue, controls proliferation of generative cells in male gametogenesis. *Plant J.* **45**: 819–831.
- Jansen, L., Parizot, B., and Beeckman, T.** (2013). Inducible System for Lateral Roots in Arabidopsis thaliana and Maize. In *Plant Organogenesis: Methods and Protocols*, I. De Smet, ed (Humana Press: Totowa, NJ), pp. 149–158.
- Jansen, L., Roberts, I., de Rycke, R., and Beeckman, T.** (2012). Phloem-associated auxin response maxima determine radial positioning of lateral roots in maize. *Philos. Trans. R. Soc. B Biol. Sci.* **367**: 1525–1533.
- Jeon, J., Cho, C., Lee, M.R.R., Van Binh, N., and Kim, J.** (2016). CYTOKININ RESPONSE FACTOR2 ( CRF2 ) and CRF3 Regulate Lateral Root Development in Response to Cold Stress in Arabidopsis. *Plant Cell* **28**: 1828–1843.
- Jiang, J., Wang, T., Wu, Z., Wang, J., Zhang, C., Wang, H., Wang, Z.X., and Wang, X.** (2015). The Intrinsically Disordered Protein BKI1 Is Essential for Inhibiting BRI1 Signaling in Plants. *Mol. Plant* **8**: 1675–1678.
- Jin, J., Tian, F., Yang, D.C., Meng, Y.Q., Kong, L., Luo, J., and Gao, G.** (2017). PlantTFDB 4.0: Toward a central hub for transcription factors and regulatory interactions in plants. *Nucleic Acids Res.* **45**: D1040–D1045.
- Joubès, J., Raffaele, S., Bourdenx, B., Garcia, C., Laroche-Traineau, J., Moreau, P., Domergue, F., and Lessire, R.** (2008). The VLCFA elongase gene family in Arabidopsis thaliana: Phylogenetic analysis, 3D modelling and expression profiling. *Plant Mol. Biol.* **67**: 547–566.
- Kang, N.Y., Lee, H.W., and Kim, J.** (2013). The AP2/EREBP gene PUCHI co-acts with LBD16/ASL18 and LBD18/ASL20 downstream of ARF7 and ARF19 to regulate lateral root development in arabidopsis. *Plant Cell Physiol.* **54**: 1326–1334.
- Kang, Y.H. and Hardtke, C.S.** (2016). Arabidopsis MAKR5 is a positive effector of BAM3-dependent CLE45 signaling. *EMBO Rep.* **17**: 1145–1154.
- Kareem, A., Durgaprasad, K., Sugimoto, K., Du, Y., Pulianmackal, A.J., Trivedi, Z.B., Abhayadev, P. V., Pinon, V., Meyerowitz, E.M., Scheres, B., and Prasad, K.** (2015). PLETHORA genes control regeneration by a two-step mechanism. *Curr. Biol.* **25**: 1017–1030.

- Karim, M.R., Hirota, A., Kwiatkowska, D., Tasaka, M., and Aida, M.** (2009). A Role for Arabidopsis PUCHI in Floral Meristem Identity and Bract Suppression. *Plant Cell Online* **21**: 1360–1372.
- Kerstetter, R.A., Bollman, K., Taylor, R.A., Bomblies, K., and Poethig, R.S.** (2001). KANADI regulates organ polarity in Arabidopsis. *Nature* **411**: 706–709.
- Kim, J., Jung, J.H., Lee, S.B., Go, Y.S., Kim, H.J., Cahoon, R., Markham, J.E., Cahoon, E.B., and Suh, M.C.** (2013). Arabidopsis 3-Ketoacyl-Coenzyme A Synthase9 Is Involved in the Synthesis of Tetracosanoic Acids as Precursors of Cuticular Waxes, Suberins, Sphingolipids, and Phospholipids. *Plant Physiol.* **162**: 567–580.
- Komaki, S. and Sugimoto, K.** (2012). Control of the plant cell cycle by developmental and environmental cues. *Plant Cell Physiol.* **53**: 953–964.
- Koornneef, M. and Meinke, D.** (2010). The development of Arabidopsis as a model plant. *Plant J.* **61**: 909–921.
- Kosma, D.K., Murmu, J., Razeq, F.M., Santos, P., Bourgault, R., Molina, I., and Rowland, O.** (2014). AtMYB41 activates ectopic suberin synthesis and assembly in multiple plant species and cell types. *Plant J.* **80**: 216–229.
- Krichevsky, A., Zaltsman, A., Kozlovsky, S. V., Tian, G.W., and Citovsky, V.** (2009). Regulation of Root Elongation by Histone Acetylation in Arabidopsis. *J. Mol. Biol.* **385**: 45–50.
- Krogan, N.T., Marcos, D., Weiner, A.I., and Berleth, T.** (2016). The auxin response factor MONOPTEROS controls meristem function and organogenesis in both the shoot and root through the direct regulation of PIN genes. *New Phytol.* **212**: 42–50.
- Kucukoglu, M. and Nilsson, O.** (2015). CLE peptide signaling in plants - the power of moving around. *Physiol. Plant.* **155**: 74–87.
- Kuijken, R.C.P., Van Eeuwijk, F.A., Marcelis, L.F.M., and Bouwmeester, H.J.** (2015). Root phenotyping: From component trait in the lab to breeding. *J. Exp. Bot.* **66**: 5389–5401.
- Lamb, R.S. and Irish, V.F.** (2003). Functional divergence within the APETALA3/PISTILLATA floral homeotic gene lineages. *Proc. Natl. Acad. Sci.* **100**: 6558–6563.
- Laplaze, L. et al.** (2007). Cytokinins Act Directly on Lateral Root Founder Cells to Inhibit Root Initiation. *Plant Cell Online* **19**: 3889–3900.
- Laplaze, L., Parizot, B., Baker, A., Ricaud, L., Martinière, A., Auguy, F., Franche, C., Nussaume, L., Bogusz, D., and Haseloff, J.** (2005). GAL4-GFP enhancer trap lines for genetic manipulation of lateral root development in Arabidopsis thaliana. *J. Exp. Bot.* **56**: 2433–2442.
- Laskowski, M., Grieneisen, V.A., Hofhuis, H., Ten Hove, C.A., Hogeweg, P., Marée, A.F.M., and Scheres, B.** (2008). Root system architecture from coupling cell shape to auxin transport. *PLoS Biol.* **6**: 2721–2735.
- Laskowski, M. and ten Tusscher, K.H.** (2017). Periodic Lateral Root Priming: What Makes It Tick? *Plant Cell* **29**: 432–444.
- Laskowski, M.J., Williams, M.E., Nusbaum, H.C., and Sussex, I.M.** (1995). Formation of lateral root meristems is a two-stage process. *Development* **121**: 3303–10.
- Lau, S., Smet, I. De, Kolb, M., Meinhardt, H., and Jürgens, G.** (2011). Auxin triggers a

- genetic switch. *Nat. Cell Biol.* **13**: 611–615.
- Laux, T.** (2003). The stem cell concept in plants: A matter of debate. *Cell* **113**: 281–283.
- Lavenus, J. et al.** (2015). Inference of the Arabidopsis Lateral Root Gene Regulatory Network Suggests a Bifurcation Mechanism That Defines Primordia Flanking and Central Zones. *Plant Cell* **27**: 1368–1388.
- Lavenus, J., Goh, T., Roberts, I., Guyomarc'h, S., Lucas, M., De Smet, I., Fukaki, H., Beeckman, T., Bennett, M., and Laplaze, L.** (2013a). Lateral root development in Arabidopsis: Fifty shades of auxin. *Trends Plant Sci.* **18**: 1360–1385.
- Lavenus, J., Lucas, M., Laplaze, L., and Guyomarc'h, S.** (2013b). The Dicot Root as a Model System for Studying Organogenesis. In *Plant Organogenesis: Methods and Potocols, Methods in Molecular Biology*, pp. 235–245.
- Lavrekha, V. V., Pasternak, T., Ivanov, V.B., Palme, K., and Mironova, V. V.** (2017). 3D analysis of mitosis distribution highlights the longitudinal zonation and diarch symmetry in proliferation activity of the Arabidopsis thaliana root meristem. *Plant J.* **92**: 834–845.
- Lee, H.W. and Kim, J.** (2013). EXPANSINA17 Up-Regulated by LBD18/ASL20 promotes lateral root formation during the auxin response. *Plant Cell Physiol.* **54**: 1600–1611.
- Lee, H.W., Kim, N.Y., Lee, D.J., and Kim, J.** (2009a). LBD18/ASL20 Regulates Lateral Root Formation in Combination with LBD16/ASL18 Downstream of ARF7 and ARF19 in Arabidopsis. *Plant Physiol.* **151**: 1377–1389.
- Lee, K., Park, O.S., and Seo, P.J.** (2017). Arabidopsis ATXR2 deposits H3K36me3 at the promoters of LBD genes to facilitate cellular dedifferentiation. *Sci. Signal.* **10**: 1–11.
- Lee, K., Park, O.S., and Seo, P.J.** (2018a). ATXR2 as a core regulator of de novo root organogenesis. *Plant Signal. Behav.* **13**.
- Lee, K., Park, O.S., and Seo, P.J.** (2018b). JM30-mediated demethylation of H3K9me3 drives tissue identity changes to promote callus formation in Arabidopsis. *Plant J.* **95**: 961–975.
- Lee, M.M. and Schiefelbein, J.** (1999). WEREWOLF, a MYB-related protein in Arabidopsis, is a position-dependent regulator of epidermal cell patterning. *Cell* **99**: 473–83.
- Lee, S.B., Jung, S.J., Go, Y.S., Kim, H.U., Kim, J.K., Cho, H.J., Park, O.K., and Suh, M.C.** (2009b). Two Arabidopsis 3-ketoacyl CoA synthase genes, KCS20 and KCS2/DAISY, are functionally redundant in cuticular wax and root suberin biosynthesis, but differentially controlled by osmotic stress. *Plant J.* **60**: 462–475.
- Lee, Y., Lee, W.S., and Kim, S.-H.** (2013). Hormonal regulation of stem cell maintenance in roots. *J. Exp. Bot.* **64**: 1153–1165.
- Li-Beisson, Y. et al.** (2013). Acyl-Lipid Metabolism. *Arab. B.* **11**: e0161.
- Li, B., Kamiya, T., Kalmbach, L., Yamagami, M., Yamaguchi, K., Shigenobu, S., Sawa, S., Danku, J.M.C., Salt, D.E., Geldner, N., and Fujiwara, T.** (2017). Role of LOTR1 in Nutrient Transport through Organization of Spatial Distribution of Root Endodermal Barriers. *Curr. Biol.* **27**: 758–765.
- Li, G., Santoni, V., and Maurel, C.** (2014). Plant aquaporins: Roles in plant physiology. *Biochim. Biophys. Acta - Gen. Subj.* **1840**: 1574–1582.
- Lieberman, L.M., Sparks, E.E., Moreno-Risueno, M.A., Petricka, J.J., and Benfey, P.N.** (2015). MYB36 regulates the transition from proliferation to differentiation in the

- Arabidopsis root. Proc. Natl. Acad. Sci. U. S. A. **112**: 12099–104.
- Liu, J., Hu, X., Qin, P., Prasad, K., Hu, Y., and Xu, L.** (2018). The WOX11 - LBD16 Pathway Promotes Pluripotency Acquisition in Callus Cells during de Novo Shoot Regeneration in Tissue Culture. *Plant Cell Physiol.* **59**: 734–743.
- Liu, J., Sheng, L., Xu, Y., Li, J., Yang, Z., Huang, H., and Xu, L.** (2014). WOX11 and 12 Are Involved in the First-Step Cell Fate Transition during de Novo Root Organogenesis in Arabidopsis. *Plant Cell* **26**: 1081–1093.
- Ljung, K.** (2005). Sites and Regulation of Auxin Biosynthesis in Arabidopsis Roots. *Plant Cell Online* **17**: 1090–1104.
- Lobet, G., Pagès, L., and Draye, X.** (2011). A Novel Image-Analysis Toolbox Enabling Quantitative Analysis of Root System Architecture. *Plant Physiol.* **157**: 29–39.
- Louveaux, M., Julien, J.-D., Mirabet, V., Boudaoud, A., and Hamant, O.** (2016). Cell division plane orientation based on tensile stress in *Arabidopsis thaliana*. *Proc. Natl. Acad. Sci.* **113**: E4294–E4303.
- Lucas, M. et al.** (2013). Lateral root morphogenesis is dependent on the mechanical properties of the overlaying tissues. *Proc. Natl. Acad. Sci.* **110**: 5229–5234.
- Lucas, M. et al.** (2011). SHORT-ROOT Regulates Primary, Lateral, and Adventitious Root Development in Arabidopsis. *Plant Physiol.* **155**: 384–398.
- Lucas, M., Guédon, Y., Jay-Allemand, C., Godin, C., and Laplaze, L.** (2008). An auxin transport-based model of root branching in Arabidopsis thaliana. *PLoS One* **3**.
- de Luis Balaguer, M.A., Fisher, A.P., Clark, N.M., Fernandez-Espinosa, M.G., Möller, B.K., Weijers, D., Lohmann, J.U., Williams, C., Lorenzo, O., and Sozzani, R.** (2017). Predicting gene regulatory networks by combining spatial and temporal gene expression data in *Arabidopsis* root stem cells. *Proc. Natl. Acad. Sci.* **114**: E7632–E7640.
- Lux, A., Morita, S., Abe, J., and Ito, K.** (2005). An improved method for clearing and staining free-hand sections and whole-mount samples. *Ann. Bot.* **96**: 989–996.
- Lynch, J.** (1995). Root Architecture and Plant Productivity. *Plant Physiol.* **109**: 7–13.
- Lynch, J.P.** (2013). Steep, cheap and deep: An ideotype to optimize water and N acquisition by maize root systems. *Ann. Bot.* **112**: 347–357.
- Lynch, J.P.** (2007). TURNER REVIEW No. 14. Roots of the Second Green Revolution. *Aust. J. Bot.* **55**: 493.
- Maere, S., Heymans, K., and Kuiper, M.** (2005). BiNGO: A Cytoscape plugin to assess overrepresentation of Gene Ontology categories in Biological Networks. *Bioinformatics* **21**: 3448–3449.
- Malamy, J.E.** (2005). Intrinsic and environmental response pathways that regulate root system architecture. *Plant, Cell Environ.* **28**: 67–77.
- Malamy, J.E. and Benfey, P.N.** (1997). Organization and cell differentiation in lateral roots of *Arabidopsis thaliana*. *Development* **124**: 33–44.
- Manzano, C., Ramirez-Parra, E., Casimiro, I., Otero, S., Desvoves, B., De Rybel, B., Beeckman, T., Casero, P., Gutierrez, C., and C. del Pozo, J.** (2012). Auxin and Epigenetic Regulation of SKP2B, an F-Box That Represses Lateral Root Formation. *Plant Physiol.* **160**: 749–762.

- Marhavý, P., Montesinos, J.C., Abuzeineh, A., Van Damme, D., Vermeer, J.E.M., Duclercq, J., Rakusová, H., Nováková, P., Friml, J., Geldner, N., and Benková, E.** (2016). Targeted cell elimination reveals an auxin-guided biphasic mode of lateral root initiation. *Genes Dev.* **30**: 471–483.
- Marhavý, P., Vanstraelen, M., De Rybel, B., Zhaojun, D., Bennett, M.J., Beeckman, T., and Benková, E.** (2013). Auxin reflux between the endodermis and pericycle promotes lateral root initiation. *EMBO J.* **32**: 149–158.
- Matsuzaki, Y., Ogawa-Ohnishi, M., Mori, A., and Matsubayashi, Y.** (2010). Secreted peptide signals required for maintenance of root stem cell niche in Arabidopsis. *Science* (80-. ). **329**: 1065–1067.
- McCloy, R.A., Rogers, S., Caldon, C.E., Lorca, T., Castro, A., and Burgess, A.** (2014). Partial inhibition of Cdk1 in G2phase overrides the SAC and decouples mitotic events. *Cell Cycle* **13**: 1400–1412.
- McConnell, J.R., Emery, J., Eshed, Y., Bao, N., Bowman, J., and Barton, M.K.** (2001). Role of PHABULOSA and PHAVOLUTA in determining radial patterning in shoots. *Nature* **411**: 709–713.
- Millar, A.A.** (1999). CUT1, an Arabidopsis Gene Required for Cuticular Wax Biosynthesis and Pollen Fertility, Encodes a Very-Long-Chain Fatty Acid Condensing Enzyme. *Plant Cell Online* **11**: 825–838.
- Millar, A.A. and Kunst, L.** (1997). Very-long-chain fatty acid biosynthesis is controlled through the expression and specificity of the condensing enzyme. *Plant J.* **12**: 121–131.
- Möller, B.K., Xuan, W., and Beeckman, T.** (2017). Dynamic control of lateral root positioning. *Curr. Opin. Plant Biol.* **35**: 1–7.
- Moreno-Risueno, M.A., Van Norman, J.M., Moreno, A., Zhang, J., Ahnert, S.E., and Benfey, P.N.** (2010). Oscillating gene expression determines competence for periodic Arabidopsis root branching. *Science* (80-. ). **329**: 1306–1311.
- Morineau, C., Gissot, L., Bellec, Y., Hematy, K., Tellier, F., Renne, C., Haslam, R., Beaudoin, F., Napier, J., and Faure, J.D.** (2016). Dual fatty acid elongase complex interactions in arabidopsis. *PLoS One* **11**: 1–20.
- Moriwaki, T., Miyazawa, Y., Kobayashi, A., Uchida, M., Watanabe, C., Fujii, N., and Takahashi, H.** (2011). Hormonal Regulation of Lateral Root Development in Arabidopsis Modulated by MIZ1 and Requirement of GNOM Activity for MIZ1 Function. *Plant Physiol.* **157**: 1209–1220.
- Morris, E.C. et al.** (2017). Shaping 3D Root System Architecture. *Curr. Biol.* **27**: R919–R930.
- Murphy, E. et al.** (2016). RALFL34 regulates formative cell divisions in Arabidopsis pericycle during lateral root initiation. *J. Exp. Bot.* **67**: 4863–4875.
- Nacry, P., Canivenc, G., Muller, B., Azmi, A., Van Onckelen, H., Rossignol, M., and Dumas, P.** (2005). A role for auxin redistribution in the responses of the root system architecture to phosphate starvation in Arabidopsis. *Plant Physiol.* **138**: 2061–2074.
- Nakajima, K., Sena, G., Nawy, T., and Benfey, P.N.** (2001). Intercellular movement of the putative transcription factor SHR in root patterning. *Nature* **413**: 307–311.
- Napsucialy-Mendivil, S., Alvarez-Venegas, R., Shishkova, S., and Dubrovsky, J.G.** (2014). Arabidopsis homolog of trithorax1 (ATX1) is required for cell production, patterning, and

- morphogenesis in root development. *J. Exp. Bot.* **65**: 6373–6384.
- Naseer, S., Lee, Y., Lapierre, C., Franke, R., Nawrath, C., and Geldner, N.** (2012). Casparian strip diffusion barrier in *Arabidopsis* is made of a lignin polymer without suberin. *Proc. Natl. Acad. Sci.* **109**: 10101–10106.
- Nawy, T., Lee, J.-Y., Colinas, J., Wang, J.Y., Thongrod, S.C., Malamy, J.E., Birnbaum, K., and Benfey, P.N.** (2005). Transcriptional profile of the *Arabidopsis* root quiescent center. *Plant Cell* **17**: 1908–25.
- Nieuwland, J., Maughan, S., Dewitte, W., Scofield, S., Sanz, L., and Murray, J.A.** (2009). The D-type cyclin CYCD4;1 modulates lateral root density in *Arabidopsis* by affecting the basal meristem region. *Proc. Natl. Acad. Sci. U. S. A.* **106**: 22528–22533.
- Nobusawa, T., Okushima, Y., Nagata, N., Kojima, M., Sakakibara, H., and Umeda, M.** (2013). Synthesis of Very-Long-Chain Fatty Acids in the Epidermis Controls Plant Organ Growth by Restricting Cell Proliferation. *PLoS Biol.* **11**: e1001531.
- Van Norman, J.M., Breakfield, N.W., and Benfey, P.N.** (2011). Intercellular Communication during Plant Development. *Plant Cell* **23**: 855–864.
- Van Norman, J.M., Xuan, W., Beeckman, T., and Benfey, P.N.** (2013). To branch or not to branch: the role of pre-patterning in lateral root formation. *Development* **140**: 4301–4310.
- Ohashi-Ito, K. and Bergmann, D.C.** (2007). Regulation of the *Arabidopsis* root vascular initial population by LONESOME HIGHWAY. *Development* **134**: 2959–2968.
- Ohashi-Ito, K., Matsukawa, M., and Fukuda, H.** (2013a). An atypical bHLH transcription factor regulates early xylem development downstream of auxin. *Plant Cell Physiol.* **54**: 398–405.
- Ohashi-Ito, K., Oguchi, M., Kojima, M., Sakakibara, H., and Fukuda, H.** (2013b). Auxin-associated initiation of vascular cell differentiation by LONESOME HIGHWAY. *Development* **140**: 765–9.
- Okushima, Y., Fukaki, H., Onoda, M., Theologis, A., and Tasaka, M.** (2007). ARF7 and ARF19 Regulate Lateral Root Formation via Direct Activation of LBD/ASL Genes in *Arabidopsis*. *PLANT CELL ONLINE* **19**: 118–130.
- Olmo, R., Cabrera, J., Moreno-Risueno, M.A., Fukaki, H., Fenoll, C., and Escobar, C.** (2017). Molecular Transducers from Roots Are Triggered in *Arabidopsis* Leaves by Root-Knot Nematodes for Successful Feeding Site Formation: A Conserved Post-Embryogenic De novo Organogenesis Program? *Front. Plant Sci.* **8**: 1–14.
- Oparka, K.J., Prior, D.A.M., and Wright, K.M.** (1995). Symplastic communication between primary and developing lateral roots of *Arabidopsis thaliana*. *J. Exp. Bot.* **46**: 187–197.
- Osmont, K.S., Sibout, R., and Hardtke, C.S.** (2007). Hidden branches: developments in root system architecture. *Annu. Rev. Plant Biol.* **58**: 93–113.
- Otsuga, D., DeGuzman, B., Prigge, M.J., Drews, G.N., and Clark, S.E.** (2001). REVOLUTA regulates meristem initiation at lateral positions. *Plant J.* **25**: 223–236.
- Palovaara, J., de Zeeuw, T., and Weijers, D.** (2016). Tissue and Organ Initiation in the Plant Embryo: A First Time for Everything. *Annu. Rev. Cell Dev. Biol.* **32**: 47–75.
- Parizot, B. et al.** (2007). Diarch Symmetry of the Vascular Bundle in *Arabidopsis* Root Encompasses the Pericycle and Is Reflected in Distich Lateral Root Initiation. *Plant Physiol.* **146**: 140–148.

- Péret, B. et al.** (2012). Auxin regulates aquaporin function to facilitate lateral root emergence. *Nat. Cell Biol.* **14**: 991–998.
- Péret, B. et al.** (2013). Sequential induction of auxin efflux and influx carriers regulates lateral root emergence. *Mol. Syst. Biol.* **9**: 1–15.
- Perianez-Rodriguez, J., Manzano, C., and Moreno-Risueno, M.A.** (2014). Post-embryonic organogenesis and plant regeneration from tissues: two sides of the same coin? *Front. Plant Sci.* **5**: 1–11.
- Perilli, S., Di Mambro, R., and Sabatini, S.** (2012). Growth and development of the root apical meristem. *Curr. Opin. Plant Biol.* **15**: 17–23.
- Petrasek, J. and Friml, J.** (2009). Auxin transport routes in plant development. *Development* **136**: 2675–2688.
- Petricka, J.J., Winter, C.M., and Benfey, P.N.** (2012). Control of Arabidopsis Root Development. *Annu. Rev. Plant Biol.* Vol 63 **63**: 563–590.
- Pi, L., Aichinger, E., van der Graaff, E., Llavata-Peris, C.I., Weijers, D., Hennig, L., Groot, E., and Laux, T.** (2015). Organizer-Derived WOX5 Signal Maintains Root Columella Stem Cells through Chromatin-Mediated Repression of CDF4 Expression. *Dev. Cell* **33**: 576–588.
- Porco, S. et al.** (2016). Lateral root emergence in *Arabidopsis* is dependent on transcription factor LBD29 regulation of auxin influx carrier *LAX3*. *Development* **143**: 3340–3349.
- Prigge, M.J., Otsuga, D., Alonso, J.M., Ecker, J.R., Drews, G.N., and Clark, S.E.** (2005). Class III homeodomain-leucine zipper gene family members have overlapping, antagonistic, and distinct roles in Arabidopsis development. *Plant Cell* **17**: 61–76.
- Pruitt, R.E., Vielle-Calzada, J.-P., Ploense, S.E., Grossniklaus, U., and Lolle, S.J.** (2000). FIDDLEHEAD, a gene required to suppress epidermal cell interactions in Arabidopsis, encodes a putative lipid biosynthetic enzyme. *Proc. Natl. Acad. Sci.* **97**: 1311–1316.
- Qin, Y.-M., Hu, C.-Y., Pang, Y., Kastaniotis, A.J., Hiltunen, J.K., and Zhu, Y.-X.** (2007). Saturated Very-Long-Chain Fatty Acids Promote Cotton Fiber and Arabidopsis Cell Elongation by Activating Ethylene Biosynthesis. *Plant Cell Online* **19**: 3692–3704.
- Ranathunge, K. and Schreiber, L.** (2011). Water and solute permeabilities of Arabidopsis roots in relation to the amount and composition of aliphatic suberin. *J. Exp. Bot.* **62**: 1961–1974.
- Ranathunge, K., Schreiber, L., and Franke, R.** (2011). Suberin research in the genomics era—New interest for an old polymer. *Plant Sci.* **180**: 339–413.
- Rashotte, A.M., Brady, S.R., Reed, R.C., Ante, S.J., and Muday, G.K.** (2000). Basipetal Auxin Transport Is Required for Gravitropism in Roots of Arabidopsis. *Plant Physiol.* **122**: 481–490.
- Reinhardt, H., Hachez, C., Bienert, M.D., Beebo, A., Swarup, K., Voss, U., Bouhidel, K., Frigerio, L., Schjoerring, J.K., Bennett, M.J., and Chaumont, F.** (2016). Tonoplast aquaporins facilitate lateral root emergence. *Plant Physiol.*: pp.01635.2015.
- Riou-Khamlichi, C., Huntley, R., Jacqumard, A., and Murray, J.A.H.** (1999). Cytokinin activation of Arabidopsis cell division through a D-type cyclin. *Science* (80-. ). **283**: 1541–1544.
- Roberts, I. et al.** (2016). CEP5 and XIP1/CEPR1 regulate lateral root initiation in Arabidopsis.

- J. Exp. Bot. **67**: 4889–4899.
- Rogers, E.D. and Benfey, P.N.** (2015). Regulation of plant root system architecture: Implications for crop advancement. *Curr. Opin. Biotechnol.* **32**: 93–98.
- Rosspopoff, O., Chelysheva, L., Saffar, J., Lecorgne, L., Gey, D., Caillieux, E., Colot, V., Roudier, F., Hilson, P., Berthomé, R., Da Costa, M., and Rech, P.** (2017). Direct conversion of root primordium into shoot meristem relies on timing of stem cell niche development. *Development* **144**: 1187–1200.
- Roudier, F. et al.** (2010). Very-Long-Chain Fatty Acids Are Involved in Polar Auxin Transport and Developmental Patterning in Arabidopsis. *Plant Cell* **22**: 364–375.
- De Rybel, B. et al.** (2010). A novel Aux/IAA28 signaling cascade activates GATA23-dependent specification of lateral root founder cell identity. *Curr. Biol.* **20**: 1697–1706.
- Sabatini, S., Heidstra, R., Wildwater, M., and Scheres, B.** (2003). SCARECROW is involved in positioning the stem cell niche in the Arabidopsis root meristem. *Genes Dev.* **17**: 354–8.
- Sablowski, R.** (2007). The dynamic plant stem cell niches. *Curr. Opin. Plant Biol.* **10**: 639–644.
- Sanz, L. et al.** (2011). The *Arabidopsis* D-Type Cyclin CYCD2;1 and the Inhibitor ICK2/KRP2 Modulate Auxin-Induced Lateral Root Formation. *Plant Cell* **23**: 641–660.
- Sarkar, A.K., Luijten, M., Miyashima, S., Lenhard, M., Hashimoto, T., Nakajima, K., Scheres, B., Heidstra, R., and Laux, T.** (2007). Conserved factors regulate signalling in *Arabidopsis thaliana* shoot and root stem cell organizers. *Nature* **446**: 811–814.
- Sassi, M. and Traas, J.** (2015). When biochemistry meets mechanics: A systems view of growth control in plants. *Curr. Opin. Plant Biol.* **28**: 137–143.
- Schena, M., Lloyd, a M., and Davis, R.W.** (1991). A steroid-inducible gene expression system for plant cells. *Proc. Natl. Acad. Sci. U. S. A.* **88**: 10421–10425.
- Scheres, B.** (2007). Stem-cell niches: Nursery rhymes across kingdoms. *Nat. Rev. Mol. Cell Biol.* **8**: 345–354.
- Scheres, B. and Krizek, B.A.** (2018). Coordination of growth in root and shoot apices by AIL/PLT transcription factors. *Curr. Opin. Plant Biol.* **41**: 95–101.
- Scheres, B. and Laskowski, M.** (2016). Root patterning: It takes two to tangle. *J. Exp. Bot.* **67**: 1201–1203.
- Schindelin, J. et al.** (2012). Fiji: An open-source platform for biological-image analysis. *Nat. Methods* **9**: 676–682.
- Schlereth, A., Möller, B., Liu, W., Kientz, M., Flipse, J., Rademacher, E.H., Schmid, M., Jürgens, G., and Weijers, D.** (2010). MONOPTEROS controls embryonic root initiation by regulating a mobile transcription factor. *Nature* **464**: 913–916.
- Schuettengruber, B., Bourbon, H.M., Di Croce, L., and Cavalli, G.** (2017). Genome Regulation by Polycomb and Trithorax: 70 Years and Counting. *Cell* **171**: 34–57.
- Shang, B., Xu, C., Zhang, X., Cao, H., Xin, W., and Hu, Y.** (2016). Very-long-chain fatty acids restrict regeneration capacity by confining pericycle competence for callus formation in *Arabidopsis*. *Proc. Natl. Acad. Sci.* **113**: 5101–5106.
- Shannon, P.** (2003). Cytoscape: A Software Environment for Integrated Models of Biomolecular Interaction Networks. *Genome Res.* **13**: 2498–2504.

- Sheng, L., Hu, X., Du, Y., Zhang, G., Huang, H., Scheres, B., and Xu, L.** (2017a). Non-canonical *WOX11* -mediated root branching contributes to plasticity in *Arabidopsis* root system architecture. *Development* **144**: 3126–3133.
- Sheng, L., Hu, X., Du, Y., Zhang, G., Huang, H., Scheres, B., and Xu, L.** (2017b). Non-canonical *WOX11* -mediated root branching contributes to plasticity in *Arabidopsis* root system architecture. *Development*: dev.152132.
- Singh, S., Singh, A., Roy, S., and Sarkar, A.K.** (2012). SWP1 negatively regulates lateral root initiation and elongation in *Arabidopsis*. *Plant Signal. Behav.* **7**.
- de Smet, I.** (2012). Lateral root initiation: One step at a time. *New Phytol.* **193**: 867–873.
- De Smet, I. et al.** (2007). Auxin-dependent regulation of lateral root positioning in the basal meristem of *Arabidopsis*. *Development* **134**: 681–690.
- De Smet, I. et al.** (2010). Bimodular auxin response controls organogenesis in *Arabidopsis*. *Proc. Natl. Acad. Sci.* **107**: 2705–2710.
- De Smet, I. et al.** (2008). Receptor-Like Kinase ACR4 Restricts Formative Cell Divisions in the *Arabidopsis* Root. *Science* (80-. ). **322**: 594–597.
- De Smet, I. and Beeckman, T.** (2011). Asymmetric cell division in land plants and algae: The driving force for differentiation. *Nat. Rev. Mol. Cell Biol.* **12**: 177–188.
- De Smet, I., Vanneste, S., Inzé, D., and Beeckman, T.** (2006). Lateral root initiation or the birth of a new meristem. *Plant Mol. Biol.* **60**: 871–887.
- Smith, D.L. and Fedoroff, N. V** (1995). LRP1, a gene expressed in lateral and adventitious root primordia of *Arabidopsis*. *Plant Cell* **7**: 735–745.
- Smith, S. and De Smet, I.** (2012). Root system architecture: insights from *Arabidopsis* and cereal crops. *Philos. Trans. R. Soc. B Biol. Sci.* **367**: 1441–1452.
- Smolarkiewicz, M. and Dhonukshe, P.** (2013). Formative cell divisions: Principal determinants of plant morphogenesis. *Plant Cell Physiol.* **54**: 333–342.
- Sozzani, R. and Iyer-Pascuzzi, A.** (2014). Postembryonic control of root meristem growth and development. *Curr. Opin. Plant Biol.* **17**: 7–12.
- Spradling, A., Drummond-Barbosa, D., and Kai, T.** (2001). Stem cells find their niche. *Nature* **414**: 98–104.
- Stahl, Y. et al.** (2013). Moderation of *Arabidopsis* root stemness by CLAVATA1 and ARABIDOPSIS CRINKLY4 receptor kinase complexes. *Curr. Biol.* **23**: 362–371.
- Stahl, Y. and Simon, R.** (2005). Plant stem cell niches. *Int. J. Dev. Biol.* **49**: 479–489.
- Stoeckle, D., Thellmann, M., and Vermeer, J.E.** (2018). Breakout — lateral root emergence in *Arabidopsis thaliana*. *Curr. Opin. Plant Biol.* **41**: 67–72.
- Sugimoto, K., Jiao, Y., and Meyerowitz, E.M.** (2010). *Arabidopsis* Regeneration from Multiple Tissues Occurs via a Root Development Pathway. *Dev. Cell* **18**: 463–471.
- Swarup, K. et al.** (2008). The auxin influx carrier LAX3 promotes lateral root emergence. *Nat Cell Biol* **10**: 946–954.
- Tai, A.P.K., Martin, M.V., and Heald, C.L.** (2014). Threat to future global food security from climate change and ozone air pollution. *Nat. Clim. Chang.* **4**: 817–821.

- Tang, L.P., Zhou, C., Wang, S.S., Yuan, J., Zhang, X.S., and Su, Y.H.** (2017). FUSCA3 interacting with LEAFY COTYLEDON2 controls lateral root formation through regulating YUCCA4 gene expression in *Arabidopsis thaliana*. *New Phytol.* **213**: 1740–1754.
- Thieme, C.J., Rojas-Triana, M., Stecyk, E., Schudoma, C., Zhang, W., Yang, L., Minãmbres, M., Walther, D., Schulze, W.X., Paz-Ares, J., Scheible, W.R., and Kragler, F.** (2015). Endogenous *Arabidopsis* messenger RNAs transported to distant tissues. *Nat. Plants* **1**: 1–8.
- Tian, H., Jia, Y., Niu, T., Yu, Q., and Ding, Z.** (2014a). The key players of the primary root growth and development also function in lateral roots in *Arabidopsis*. *Plant Cell Rep.* **33**: 745–753.
- Tian, H., De Smet, I., and Ding, Z.** (2014b). Shaping a root system: Regulating lateral versus primary root growth. *Trends Plant Sci.* **19**: 426–431.
- Todd, J., Post-Beittenmiller, D., and Jaworski, J.G.** (1999). KCS1 encodes a fatty acid elongase 3-ketoacyl-CoA synthase affecting wax biosynthesis in *Arabidopsis thaliana*. *Plant J.* **17**: 119–130.
- Tokunaga, H., Kojima, M., Kuroha, T., Ishida, T., Sugimoto, K., Kiba, T., and Sakakibara, H.** (2012). *Arabidopsis* lonely guy (LOG) multiple mutants reveal a central role of the LOG-dependent pathway in cytokinin activation. *Plant J.* **69**: 355–365.
- Toyokura, K. et al.** (2018). Lateral Inhibition by a Peptide Hormone-Receptor Cascade during *Arabidopsis* Lateral Root Founder Cell Formation. *Dev. Cell*: 1–12.
- Trenkamp, S., Martin, W., and Tietjen, K.** (2004). Specific and differential inhibition of very-long-chain fatty acid elongases from *Arabidopsis thaliana* by different herbicides. *Proc. Natl. Acad. Sci.* **101**: 11903–11908.
- Tresch, S., Heilmann, M., Christiansen, N., Looser, R., and Grossmann, K.** (2012). Inhibition of saturated very-long-chain fatty acid biosynthesis by mefluidide and perfluidone, selective inhibitors of 3-ketoacyl-CoA synthases. *Phytochemistry* **76**: 162–171.
- Trinh, C.D., Laplaze, L., and Guyomarc'h, S.** (2018). Lateral Root Formation: Building a Meristem de novo. In *Annual Plant Reviews online* (John Wiley & Sons, Ltd: Chichester, UK), pp. 1–44.
- Ulmasov, T., Murfett, J., Hagen, G., and Guilfoyle, T.J.** (1997). Aux/IAA proteins repress expression of reporter genes containing natural and highly active synthetic auxin response elements. *Plant Cell* **9**: 1963–71.
- Vanneste, S. et al.** (2005). Cell cycle progression in the pericycle is not sufficient for SOLITARY ROOT/IAA14-mediated lateral root initiation in *Arabidopsis thaliana*. *Plant Cell* **17**: 3035–50.
- Vanstraelen, M. and Benková, E.** (2012). Hormonal Interactions in the Regulation of Plant Development. *Annu. Rev. Cell Dev. Biol.* **28**: 463–487.
- Vaughan-Hirsch, J., Goodall, B., and Bishopp, A.** (2018). North, East, South, West: mapping vascular tissues onto the *Arabidopsis* root. *Curr. Opin. Plant Biol.* **41**: 16–22.
- Vermeer, J.E.M., Von Wangenheim, D., Barberon, M., Lee, Y., Stelzer, E.H.K., Maizel, A., and Geldner, N.** (2014). A spatial accommodation by neighboring cells is required for organ initiation in *Arabidopsis*. *Science* (80-. ). **343**: 178–183.
- Vernoux, T. et al.** (2011). The auxin signalling network translates dynamic input into robust

patterning at the shoot apex. *Mol. Syst. Biol.* **7**.

- Vilarrasa-Blasi, J., González-García, M.P., Frigola, D., Fàbregas, N., Alexiou, K.G., López-Bigas, N., Rivas, S., Jauneau, A., Lohmann, J.U., Benfey, P.N., Ibañes, M., and Caño-Delgado, A.I.** (2014). Regulation of plant stem cell quiescence by a brassinosteroid signaling module. *Dev. Cell* **30**: 36–47.
- Vishwanath, S.J., Delude, C., Domergue, F., and Rowland, O.** (2015). Suberin: biosynthesis, regulation, and polymer assembly of a protective extracellular barrier. *Plant Cell Rep.* **34**: 573–586.
- Voß, U. et al.** (2015). The circadian clock rephases during lateral root organ initiation in *Arabidopsis thaliana*. *Nat. Commun.* **6**.
- Wada, T., Kurata, T., Tominaga, R., Koshino-Kimura, Y., Tachibana, T., Goto, K., Marks, M.D., Shimura, Y., and Okada, K.** (2002). Role of a positive regulator of root hair development, CAPRICE, in *Arabidopsis* root epidermal cell differentiation. *Development* **129**: 5409–19.
- Waese, J. et al.** (2017). ePlant: Visualizing and Exploring Multiple Levels of Data for Hypothesis Generation in Plant Biology. *Plant Cell* **29**: tpc.00073.2017.
- Wang, G. and Bieberich, E.** (2017). Morphogenetic Sphingolipids in Stem Cell Differentiation and Embryo Development. In *Lipidomics of Stem Cells*, A. Pébay and R.C.B. Wong, eds (Springer International Publishing: Cham), pp. 11–40.
- Wang, J., Tian, C., Zhang, C., shi, bihai, Cao, X., Zhang, T.-Q., zhao, zhong, Wang, J.-W., and Jiao, Y.** (2017). Cytokinin Signaling Activates WUSCHEL Expression during Axillary Meristem Initiation. *Plant Cell* **29**: tpc.00579.2016.
- Wang, X. and Chory, J.** (2006). Brassinosteroids Regulate Dissociation of BKK1, a Negative Regulator of BRI1 Signaling, from the Plasma Membrane. *Science* (80-. ). **313**: 1118–1122.
- Von Wangenheim, D., Fangerau, J., Schmitz, A., Smith, R.S., Leitte, H., Stelzer, E.H.K., and Maizel, A.** (2016). Rules and self-organizing properties of post-embryonic plant organ cell division patterns. *Curr. Biol.* **26**: 439–449.
- von Wangenheim, D., Goh, T., Dietrich, D., and Bennett, M.J.** (2017). *Plant Biology: Building Barriers... in Roots.* *Curr. Biol.* **27**: R172–R174.
- Wattelet-Boyer, V., Brocard, L., Jonsson, K., Esnay, N., Joubès, J., Domergue, F., Mongrand, S., Raikhel, N., Bhalerao, R.P., Moreau, P., and Boutté, Y.** (2016). Enrichment of hydroxylated C24- and C26-acyl-chain sphingolipids mediates PIN2 apical sorting at trans-Golgi network subdomains. *Nat. Commun.* **7**.
- Weijers, D., Schlereth, A., Ehrismann, J.S., Schwank, G., Kientz, M., and Jürgens, G.** (2006). Auxin triggers transient local signaling for cell specification in *Arabidopsis* embryogenesis. *Dev. Cell* **10**: 265–270.
- Weijers, D. and Wagner, D.** (2016). Transcriptional Responses to the Auxin Hormone. *Annu. Rev. Plant Biol.* **67**: 539–574.
- Willemsen, V., Bauch, M., Bennett, T., Campilho, A., Wolkenfelt, H., Xu, J., Haseloff, J., and Scheres, B.** (2008). The NAC Domain Transcription Factors FEZ and SOMBRERO Control the Orientation of Cell Division Plane in *Arabidopsis* Root Stem Cells. *Dev. Cell* **15**: 913–922.
- Winter, D., Vinegar, B., Nahal, H., Ammar, R., Wilson, G. V., and Provart, N.J.** (2007). An

“Electronic Fluorescent Pictograph” Browser for Exploring and Analyzing Large-Scale Biological Data Sets. *PLoS One* **2**: e718.

- Wisniewska, J., Xu, J., Seifertová, D., Brewer, P.B., Ruzicka, K., Blilou, I., Rouquié, D., Benková, E., Scheres, B., and Friml, J.** (2006). Polar PIN localization directs auxin flow in plants. *Science* **312**: 883.
- Wu, G., Lin, W. -c., Huang, T., Poethig, R.S., Springer, P.S., and Kerstetter, R.A.** (2008). KANADI1 regulates adaxial-abaxial polarity in Arabidopsis by directly repressing the transcription of ASYMMETRIC LEAVES2. *Proc. Natl. Acad. Sci.* **105**: 16392–16397.
- Wu, R. and Citovsky, V.** (2017). Adaptor proteins GIR1 and GIR2. I. Interaction with the repressor GLABRA2 and regulation of root hair development. *Biochem. Biophys. Res. Commun.* **488**: 547–553.
- Xu, C., Cao, H., Xu, E., Zhang, S., and Hu, Y.** (2018a). Genome-Wide Identification of Arabidopsis LBD29 Target Genes Reveals the Molecular Events behind Auxin-Induced Cell Reprogramming during Callus Formation. *Plant Cell Physiol.* **59**: 744–755.
- Xu, C., Cao, H., Zhang, Q., Wang, H., Xin, W., Xu, E., Zhang, S., Yu, R., Yu, D., and Hu, Y.** (2018b). Control of auxin-induced callus formation by bZIP59-LBD complex in Arabidopsis regeneration. *Nat. Plants* **4**: 108–115.
- Xu, J., Hofhuis, H., Heidstra, R., Sauer, M., Friml, J., and Scheres, B.** (2006). A molecular framework for plant regeneration. *Science* (80-. ). **311**: 385–388.
- Xuan, W. et al.** (2016). Cyclic programmed cell death stimulates hormone signaling and root development in Arabidopsis. *Science* (80-. ). **351**: 384–387.
- Xuan, W., Audenaert, D., Parizot, B., Möller, B.K., Njo, M.F., De Rybel, B., De Rop, G., Van Isterdael, G., Mähönen, A.P., Vanneste, S., and Beeckman, T.** (2015). Root cap-derived auxin pre-patterns the longitudinal axis of the arabidopsis root. *Curr. Biol.* **25**: 1381–1388.
- Yadav, V., Molina, I., Ranathunge, K., Castillo, I.Q., Rothstein, S.J., and Reed, J.W.** (2014). ABCG Transporters Are Required for Suberin and Pollen Wall Extracellular Barriers in Arabidopsis. *Plant Cell* **26**: 3569–3588.
- Yamauchi, T., Shiono, K., Nagano, M., Fukazawa, A., Ando, M., Takamure, I., Mori, H., Nishizawa, N.K., Kawai-Yamada, M., Tsutsumi, N., Kato, K., and Nakazono, M.** (2015). Ethylene Biosynthesis Is Promoted by Very-Long-Chain Fatty Acids during Lysigenous Aerenchyma Formation in Rice Roots. *Plant Physiol.* **169**: 180–193.
- Yamaguchi, Y.L., Ishida, T., and Sawa, S.** (2016). CLE peptides and their signaling pathways in plant development. *J. Exp. Bot.* **67**: 4813–4826.
- Yoshida, S., BarbierdeReuille, P., Lane, B., Bassel, G.W., Prusinkiewicz, P., Smith, R.S., and Weijers, D.** (2014). Genetic control of plant development by overriding a geometric division rule. *Dev. Cell* **29**: 75–87.
- Yu, J., Liu, W., Liu, J., Qin, P., and Xu, L.** (2017). Auxin Control of Root Organogenesis from Callus in Tissue Culture. *Front. Plant Sci.* **8**: 1–4.
- Yu, P., Baldauf, J., Lithio, A., Marcon, C., Nettleton, D., Li, C., and Hochholdinger, F.** (2016). Root type specific reprogramming of maize pericycle transcriptomes by local high nitrate results in disparate lateral root branching patterns. *Plant Physiol.* **170**: pp.01885.2015.

- Yu, P., Eggert, K., von Wirén, N., Li, C., and Hochholdinger, F.** (2015). Cell Type-Specific Gene Expression Analyses by RNA Sequencing Reveal Local High Nitrate-Triggered Lateral Root Initiation in Shoot-Borne Roots of Maize by Modulating Auxin-Related Cell Cycle Regulation.
- Yue, K. et al.** (2016). PP2A-3 interacts with ACR4 and regulates formative cell division in the *Arabidopsis* root. *Proc. Natl. Acad. Sci.* **113**: 1447–1452.
- Yue, K. and Beeckman, T.** (2014). Cell-to-cell communication during lateral root development. *Mol. Plant* **7**: 758–760.
- Zhan, A., Schneider, H., and Lynch, J.P.** (2015). Reduced Lateral Root Branching Density Improves Drought Tolerance in Maize. *Plant Physiol.* **168**: 1603–1615.
- Zhang, W., Swarup, R., Bennett, M., Schaller, G.E., and Kieber, J.J.** (2013). Cytokinin induces cell division in the quiescent center of the arabidopsis root apical meristem. *Curr. Biol.* **23**: 1979–1989.
- Zhao, Y.** (2010). Auxin Biosynthesis and Its Role in Plant Development. *Annu. Rev. Plant Biol.* **61**: 49–64.
- Zheng, H.** (2005). Disruptions of the Arabidopsis Enoyl-CoA Reductase Gene Reveal an Essential Role for Very-Long-Chain Fatty Acid Synthesis in Cell Expansion during Plant Morphogenesis. *Plant Cell Online* **17**: 1467–1481.
- Zipori, D.** (2004). The nature of stem cells: State rather than entity. *Nat. Rev. Genet.* **5**: 873–878.
- Zografidis, A., Kapolas, G., Podia, V., Beri, D., Papadopoulou, K., Milioni, D., and Haralampidis, K.** (2014). Transcriptional regulation and functional involvement of the Arabidopsis pescadillo ortholog AtPES in root development. *Plant Sci.* **229**: 53–65.
- Zurcher, E., Tavor-Deslex, D., Lituiev, D., Enkerli, K., Tarr, P.T., and Muller, B.** (2013). A Robust and Sensitive Synthetic Sensor to Monitor the Transcriptional Output of the Cytokinin Signaling Network in Planta. *Plant Physiol.* **161**: 1066–1075.

# APPENDIXES

## APPENDIX 1

TAIR ID and names of the 217 genes showing an expression profile similar to that of *PUCHI* as revealed by TDCor.

Gene names retrieved from TAIR: <https://www.arabidopsis.org/tools/bulk/genes/index.jsp>

ID	Gene Name	ID	Gene Name
AT1G01120	3-KETOACYL-COA SYNTHASE 1 ( <i>KCS1</i> )	AT3G23430	PHOSPHATE 1 ( <i>PHO1</i> )
AT1G01610	GLYCEROL-3-PHOSPHATE ACYLTRANSFERASE 4 ( <i>GPAT4</i> )	AT3G23600	ALPHA/BETA-HYDROLASES SUPERFAMILY PROTEIN (AT3G23600)
AT1G04040	HAD SUPERFAMILY, SUBFAMILY IIIB ACID PHOSPHATASE (AT1G04040)	AT3G25610	ATPASE E1-E2 TYPE FAMILY PROTEIN / HALOACID DEHALOGENASE-LIKE HYDROLASE FAMILY PROTEIN (AT3G25610)
AT1G04220	3-KETOACYL-COA SYNTHASE 2 ( <i>KCS2</i> )	AT3G26830	CYTOCHROME P450 SUPERFAMILY PROTEIN ( <i>PAD3</i> )
AT1G04330	HYPOTHETICAL PROTEIN (AT1G04330)	AT3G27090	DCD (DEVELOPMENT AND CELL DEATH) DOMAIN PROTEIN (AT3G27090)
AT1G06640	2-OXOGLUTARATE (2OG) AND FE (II)-DEPENDENT OXYGENASE SUPERFAMILY PROTEIN (AT1G06640)	AT3G44990	XYLOGLUCAN ENDO-TRANSGLYCOSYLASE-RELATED 8 ( <i>XTH31</i> )
AT1G06650	2-OXOGLUTARATE (2OG) AND FE (II)-DEPENDENT OXYGENASE SUPERFAMILY PROTEIN (AT1G06650)	AT3G45410	CONCANAVALIN A-LIKE LECTIN PROTEIN KINASE FAMILY PROTEIN (AT3G45410)
AT1G07240	UDP-GLUCOSYL TRANSFERASE 71C5 ( <i>UGT71C5</i> )	AT3G45640	MITOGEN-ACTIVATED PROTEIN KINASE 3 ( <i>MPK3</i> )
AT1G08310	ALPHA/BETA-HYDROLASES SUPERFAMILY PROTEIN (AT1G08310)	AT3G50350	MEMBRANE INSERTASE, PUTATIVE (DUF1685) (AT3G50350)
AT1G08480	SUCCINATE DEHYDROGENASE SUBUNIT ( <i>SDH6</i> )	AT3G51430	CALCIUM-DEPENDENT PHOSPHOTRIESTERASE SUPERFAMILY PROTEIN ( <i>YLS2</i> )
AT1G09560	GERMIN-LIKE PROTEIN 5 ( <i>GLP5</i> )	AT3G51520	DIACYLGLYCEROL ACYLTRANSFERASE FAMILY ( <i>DGAT2</i> )
AT1G10730	CLATHRIN ADAPTOR COMPLEXES MEDIUM SUBUNIT FAMILY PROTEIN (AT1G10730)	AT3G52850	VACUOLAR SORTING RECEPTOR HOMOLOG 1 ( <i>VSR1</i> )
AT1G13080	CYTOCHROME P450, FAMILY 71, SUBFAMILY B, POLYPEPTIDE 2 ( <i>CYP71B2</i> )	AT3G53820	C2H2 AND C2HC ZINC FINGERS SUPERFAMILY PROTEIN (AT3G53820)
AT1G14130	2-OXOGLUTARATE (2OG) AND FE (II)-DEPENDENT OXYGENASE SUPERFAMILY PROTEIN (AT1G14130)	AT3G54010	FKBP-TYPE PEPTIDYL-PROLYL CIS-TRANS ISOMERASE FAMILY PROTEIN ( <i>PAS1</i> )
AT1G14340	RNA-BINDING (RRM/RBD/RNP MOTIFS) FAMILY PROTEIN (AT1G14340)	AT3G54420	HOMOLOG OF CARROT EP3-3 CHITINASE ( <i>EP3</i> )
AT1G17860	KUNITZ FAMILY TRYPSIN AND PROTEASE INHIBITOR PROTEIN (AT1G17860)	AT3G55090	ABC-2 TYPE TRANSPORTER FAMILY PROTEIN ( <i>ABCG16</i> )
AT1G17980	POLY (A) POLYMERASE 1 ( <i>PAP51</i> )	AT3G56360	HYPOTHETICAL PROTEIN (AT3G56360)
AT1G18720	ER MEMBRANE PROTEIN, PUTATIVE (DUF962) (AT1G18720)	AT3G56730	PUTATIVE ENDONUCLEASE OR GLYCOSYL HYDROLASE (AT3G56730)
AT1G19250	FLAVIN-DEPENDENT MONOOXYGENASE 1 ( <i>FMO1</i> )	AT3G56980	BASIC HELIX-LOOP-HELIX (BHLH) DNA-BINDING SUPERFAMILY PROTEIN ( <i>BHLH39</i> )
AT1G23800	ALDEHYDE DEHYDROGENASE 2B7 ( <i>ALDH2B7</i> )	AT3G58170	BET1P/SFT1P-LIKE PROTEIN 14A ( <i>BS14A</i> )
AT1G23850	TRANSMEMBRANE PROTEIN (AT1G23850)	AT3G61200	THIOESTERASE SUPERFAMILY PROTEIN (AT3G61200)

AT1G26590	C2H2-LIKE ZINC FINGER PROTEIN (AT1G26590)	AT3G62560	RAS-RELATED SMALL GTP-BINDING FAMILY PROTEIN (AT3G62560)
AT1G27980	DIHYDROSPHINGOSINE PHOSPHATE LYASE ( <i>DPL1</i> )	AT3G63170	CHALCONE-FLAVANONE ISOMERASE FAMILY PROTEIN ( <i>FAP1</i> )
AT1G30370	ALPHA/BETA-HYDROLASES SUPERFAMILY PROTEIN ( <i>DLAH</i> )	AT4G00030	PLASTID-LIPID ASSOCIATED PROTEIN PAP / FIBRILLIN FAMILY PROTEIN (AT4G00030)
AT1G30400	MULTIDRUG RESISTANCE-ASSOCIATED PROTEIN 1 ( <i>ABCC1</i> )	AT4G00880	SAUR-LIKE AUXIN-RESPONSIVE PROTEIN FAMILY (AT4G00880)
AT1G30500	NUCLEAR FACTOR Y, SUBUNIT A7 ( <i>NF-YA7</i> )	AT4G01440	NODULIN MTN21 /EAMA-LIKE TRANSPORTER FAMILY PROTEIN (UMAMIT31)
AT1G31940	CYSTIC FIBROSIS TRANSMEMBRANE CONDUCTANCE REGULATOR (AT1G31940)	AT4G01610	CYSTEINE PROTEINASES SUPERFAMILY PROTEIN (AT4G01610)
AT1G33090	MATE EFFLUX FAMILY PROTEIN (AT1G33090)	AT4G03260	OUTER ARM DYNEIN LIGHT CHAIN 1 PROTEIN (AT4G03260)
AT1G33100	MATE EFFLUX FAMILY PROTEIN (AT1G33100)	AT4G03960	PHOSPHOTYROSINE PROTEIN PHOSPHATASES SUPERFAMILY PROTEIN ( <i>PFA-DSP4</i> )
AT1G33490	E3 UBIQUITIN-PROTEIN LIGASE (AT1G33490)	AT4G04470	PEROXISOMAL MEMBRANE 22 KDA (MPV17/PMP22) FAMILY PROTEIN ( <i>PMP22</i> )
AT1G34340	ALPHA/BETA-HYDROLASES SUPERFAMILY PROTEIN (AT1G34340)	AT4G04830	METHIONINE SULFOXIDE REDUCTASE B5 ( <i>MSRB5</i> )
AT1G35560	TCP FAMILY TRANSCRIPTION FACTOR (AT1G35560)	AT4G11960	PGR5-LIKE B ( <i>PGRL1B</i> )
AT1G48300	DIACYLGLYCEROL ACYLTRANSFERASE ( <i>DGAT3</i> )	AT4G12390	PECTIN METHYLESTERASE INHIBITOR 1 ( <i>PME1</i> )
AT1G48600	S-ADENOSYL-L-METHIONINE-DEPENDENT METHYLTRANSFERASES SUPERFAMILY PROTEIN ( <i>PMEAMT</i> )	AT4G14710	RMLC-LIKE CUPINS SUPERFAMILY PROTEIN ( <i>ATARD2</i> )
AT1G48750	BIFUNCTIONAL INHIBITOR/LIPID-TRANSFER PROTEIN/SEED STORAGE 2S ALBUMIN SUPERFAMILY PROTEIN (AT1G48750)	AT4G18360	ALDOLASE-TYPE TIM BARREL FAMILY PROTEIN ( <i>GOX3</i> )
AT1G52420	UDP-GLYCOSYLTRANSFERASE SUPERFAMILY PROTEIN (AT1G52420)	AT4G18880	HEAT SHOCK TRANSCRIPTION FACTOR A4A ( <i>HSF A4A</i> )
AT1G53270	ABC-2 TYPE TRANSPORTER FAMILY PROTEIN ( <i>ABCG10</i> )	AT4G20000	VQ MOTIF-CONTAINING PROTEIN (AT4G20000)
AT1G53280	CLASS I GLUTAMINE AMIDOTRANSFERASE-LIKE SUPERFAMILY PROTEIN ( <i>DJ1B</i> )	AT4G21910	MATE EFFLUX FAMILY PROTEIN (AT4G21910)
AT1G54920	HYPOTHETICAL PROTEIN (AT1G54920)	AT4G22890	PGR5-LIKE A ( <i>PGR5-LIKE A</i> )
AT1G55960	POLYKETIDE CYCLASE/DEHYDRASE AND LIPID TRANSPORT SUPERFAMILY PROTEIN (AT1G55960)	AT4G23880	HYPOTHETICAL PROTEIN (AT4G23880)
AT1G56500	HALOACID DEHALOGENASE-LIKE HYDROLASE FAMILY PROTEIN (AT1G56500)	AT4G23980	AUXIN RESPONSE FACTOR 9 ( <i>ARF9</i> )
AT1G63440	HEAVY METAL ATPASE 5 ( <i>HMA5</i> )	AT4G24130	DUF538 FAMILY PROTEIN (PROTEIN OF UNKNOWN FUNCTION, DUF538) (AT4G24130)
AT1G64780	AMMONIUM TRANSPORTER 1;2 ( <i>AMT1;2</i> )	AT4G27710	CYTOCHROME P450, FAMILY 709, SUBFAMILY B, POLYPEPTIDE 3 ( <i>CYP709B3</i> )
AT1G64860	SIGMA FACTOR A ( <i>SIGA</i> )	AT4G28110	MYB DOMAIN PROTEIN 41 ( <i>MYB41</i> )
AT1G65820	MICROSOMAL GLUTATHIONE S-TRANSFERASE (AT1G65820)	AT4G30830	MYOSIN-LIKE PROTEIN (PROTEIN OF UNKNOWN FUNCTION, DUF593) (AT4G30830)
AT1G65850	DISEASE RESISTANCE PROTEIN (TIR-NBS-LRR CLASS) FAMILY (AT1G65850)	AT4G31240	PROTEIN KINASE C-LIKE ZINC FINGER PROTEIN (AT4G31240)

AT1G66240	HOMOLOG OF ANTI-OXIDANT 1 ( <i>ATX1</i> )	AT4G31330	TRANSMEMBRANE PROTEIN, PUTATIVE (PROTEIN OF UNKNOWN FUNCTION, DUF599) (AT4G31330)
AT1G67730	BETA-KETOACYL REDUCTASE 1 ( <i>KCRI</i> )	AT4G31670	UBIQUITIN-SPECIFIC PROTEASE 18 ( <i>UBP18</i> )
AT1G68300	ADENINE NUCLEOTIDE ALPHA HYDROLASES-LIKE SUPERFAMILY PROTEIN (AT1G68300)	AT4G32650	POTASSIUM CHANNEL PROTEIN ( <i>KAT3</i> )
AT1G69850	NITRATE TRANSPORTER 1:2 ( <i>NRT1:2</i> )	AT4G33160	F-BOX FAMILY PROTEIN (AT4G33160)
AT1G70470	TRANSMEMBRANE PROTEIN (AT1G70470)	AT4G33420	PEROXIDASE SUPERFAMILY PROTEIN (AT4G33420)
AT1G72540	PROTEIN KINASE SUPERFAMILY PROTEIN (AT1G72540)	AT4G34120	CYSTATHIONINE BETA-SYNTHASE (CBS) FAMILY PROTEIN ( <i>LEJ1</i> )
AT1G72800	RNA-BINDING (RRM/RBD/RNP MOTIFS) FAMILY PROTEIN (AT1G72800)	AT4G35220	CYCLASE FAMILY PROTEIN (AT4G35220)
AT1G73500	MAP KINASE KINASE 9 ( <i>MKK9</i> )	AT4G36140	DISEASE RESISTANCE PROTEIN (TIR-NBS-LRR CLASS) (AT4G36140)
AT1G74210	PLC-LIKE PHOSPHODIESTERASES SUPERFAMILY PROTEIN (GDPD5)	AT4G36610	ALPHA/BETA-HYDROLASES SUPERFAMILY PROTEIN (AT4G36610)
AT1G74770	ZINC ION BINDING PROTEIN (AT1G74770)	AT4G37200	THIOREDOXIN SUPERFAMILY PROTEIN ( <i>HCF164</i> )
AT1G75370	SEC14P-LIKE PHOSPHATIDYLINOSITOL TRANSFER FAMILY PROTEIN (AT1G75370)	AT5G02100	OXYSTEROL-BINDING FAMILY PROTEIN ( <i>UNE18</i> )
AT1G75920	GDSL-LIKE LIPASE/ACYLHYDROLASE SUPERFAMILY PROTEIN (AT1G75920)	AT5G02560	HISTONE H2A 12 ( <i>HTA12</i> )
AT1G76150	ENOYL-COA HYDRATASE 2 ( <i>ECH2</i> )	AT5G02620	ANKYRIN-LIKE1 ( <i>ANK1</i> )
AT1G76360	PROTEIN KINASE SUPERFAMILY PROTEIN (AT1G76360)	AT5G03880	THIOREDOXIN FAMILY PROTEIN (AT5G03880)
AT1G77420	ALPHA/BETA-HYDROLASES SUPERFAMILY PROTEIN (AT1G77420)	AT5G04150	BASIC HELIX-LOOP-HELIX (BHLH) DNA-BINDING SUPERFAMILY PROTEIN (BHLH101)
AT1G77600	ARM REPEAT SUPERFAMILY PROTEIN (AT1G77600)	AT5G05250	HYPOTHETICAL PROTEIN (AT5G05250)
AT1G78320	GLUTATHIONE S-TRANSFERASE TAU 23 ( <i>GSTU23</i> )	AT5G06960	OCS-ELEMENT BINDING FACTOR 5 ( <i>OBF5</i> )
AT1G79700	INTEGRASE-TYPE DNA-BINDING SUPERFAMILY PROTEIN ( <i>WRI4</i> )	AT5G08240	TRANSMEMBRANE PROTEIN (AT5G08240)
AT2G11520	CALMODULIN-BINDING RECEPTOR-LIKE CYTOPLASMIC KINASE 3 ( <i>CRCK3</i> )	AT5G08500	TRANSMEMBRANE CLPTM1 FAMILY PROTEIN (AT5G08500)
AT2G17430	SEVEN TRANSMEMBRANE MLO FAMILY PROTEIN ( <i>MLO7</i> )	AT5G10230	ANNEXIN 7 ( <i>ANNAT7</i> )
AT2G17500	AUXIN EFFLUX CARRIER FAMILY PROTEIN (AT2G17500)	AT5G10480	PROTEIN-TYROSINE PHOSPHATASE-LIKE, PTPLA ( <i>PAS2</i> )
AT2G17640	TRIMERIC LPXA-LIKE ENZYMES SUPERFAMILY PROTEIN ( <i>ATSERAT3;1</i> )	AT5G11650	ALPHA/BETA-HYDROLASES SUPERFAMILY PROTEIN (AT5G11650)
AT2G17650	AMP-DEPENDENT SYNTHETASE AND LIGASE FAMILY PROTEIN (AT2G17650)	AT5G11770	NADH-UBIQUINONE OXIDOREDUCTASE 20 KDA SUBUNIT (AT5G11770)
AT2G18490	C2H2-LIKE ZINC FINGER PROTEIN (AT2G18490)	AT5G12420	O-ACYLTRANSFERASE (WSD1-LIKE) FAMILY PROTEIN (AT5G12420)
AT2G22660	DNA-BINDING PROTEIN, PUTATIVE (DUPLICATED DUF1399) (AT2G22660)	AT5G15240	TRANSMEMBRANE AMINO ACID TRANSPORTER FAMILY PROTEIN (AT5G15240)

AT2G23320	WRKY DNA-BINDING PROTEIN 15 ( <i>WRKY15</i> )	AT5G17000	ZINC-BINDING DEHYDROGENASE FAMILY PROTEIN (AT5G17000)
AT2G27550	CENTRORADIALI (ATC)	AT5G20270	HEPTAHELICAL TRANSMEMBRANE PROTEIN1 ( <i>HHP1</i> )
AT2G32560	F-BOX FAMILY PROTEIN (AT2G32560)	AT5G23840	MD-2-RELATED LIPID RECOGNITION DOMAIN-CONTAINING PROTEIN (AT5G23840)
AT2G33330	PLASMODESMATA-LOCATED PROTEIN 3 ( <i>PDLP3</i> )	AT5G25830	GATA TRANSCRIPTION FACTOR 12 ( <i>GATA12</i> )
AT2G35060	K <sup>+</sup> UPTAKE PERMEASE 11 ( <i>KUP11</i> )	AT5G27350	MAJOR FACILITATOR SUPERFAMILY PROTEIN ( <i>SFP1</i> )
AT2G35780	SERINE CARBOXYPEPTIDASE-LIKE 26 ( <i>SCPL26</i> )	AT5G38280	PR5-LIKE RECEPTOR KINASE ( <i>PR5K</i> )
AT2G37460	NODULIN MTN21 /EAMA-LIKE TRANSPORTER FAMILY PROTEIN ( <i>UMAMIT12</i> )	AT5G39090	HXXXD-TYPE ACYL-TRANSFERASE FAMILY PROTEIN (AT5G39090)
AT2G37760	NAD (P)-LINKED OXIDOREDUCTASE SUPERFAMILY PROTEIN ( <i>AKR4C8</i> )	AT5G39610	NAC DOMAIN CONTAINING PROTEIN 6 ( <i>NAC6</i> )
AT2G38460	IRON REGULATED 1 ( <i>IREG1</i> )	AT5G39730	AIG2-LIKE (AVIRULENCE INDUCED GENE) FAMILY PROTEIN (AT5G39730)
AT2G41120	DUF309 DOMAIN PROTEIN (AT2G41120)	AT5G39950	THIOREDOXIN 2 ( <i>TRX2</i> )
AT2G41480	PEROXIDASE SUPERFAMILY PROTEIN (AT2G41480)	AT5G42440	PROTEIN KINASE SUPERFAMILY PROTEIN (AT5G42440)
AT2G42600	PHOSPHOENOLPYRUVATE CARBOXYLASE 2 ( <i>PPC2</i> )	AT5G42890	STEROL CARRIER PROTEIN 2 ( <i>SCP2</i> )
AT2G42790	CITRATE SYNTHASE 3 ( <i>CSY3</i> )	AT5G42980	THIOREDOXIN 3 ( <i>TRX3</i> )
AT2G43320	S-ADENOSYL-L-METHIONINE-DEPENDENT METHYLTRANSFERASES SUPERFAMILY PROTEIN (AT2G43320)	AT5G45060	DISEASE RESISTANCE PROTEIN (TIR-NBS-LRR CLASS) FAMILY (AT5G45060)
AT2G43420	3-BETA HYDROXYSTEROID DEHYDROGENASE/ISOMERASE FAMILY PROTEIN (AT2G43420)	AT5G46780	VQ MOTIF-CONTAINING PROTEIN (AT5G46780)
AT2G43680	IQ-DOMAIN 14 ( <i>IQD14</i> )	AT5G46790	PYR1-LIKE 1 ( <i>PYL1</i> )
AT2G44230	HYPOTHETICAL PROTEIN ( <i>DUF946</i> ) (AT2G44230)	AT5G49170	HYPOTHETICAL PROTEIN (AT5G49170)
AT2G46100	NUCLEAR TRANSPORT FACTOR 2 ( <i>NTF2</i> ) FAMILY PROTEIN (AT2G46100)	AT5G50200	NITRATE TRANSMEMBRANE TRANSPORTER ( <i>WR3</i> )
AT2G47630	ALPHA/BETA-HYDROLASES SUPERFAMILY PROTEIN (AT2G47630)	AT5G50820	NAC DOMAIN CONTAINING PROTEIN 97 ( <i>NAC097</i> )
AT2G48130	BIFUNCTIONAL INHIBITOR/LIPID-TRANSFER PROTEIN/SEED STORAGE 2S ALBUMIN SUPERFAMILY PROTEIN (AT2G48130)	AT5G51550	EXORDIUM LIKE 3 ( <i>EXL3</i> )
AT2G48140	BIFUNCTIONAL INHIBITOR/LIPID-TRANSFER PROTEIN/SEED STORAGE 2S ALBUMIN SUPERFAMILY PROTEIN ( <i>EDA4</i> )	AT5G52240	MEMBRANE STEROID BINDING PROTEIN 1 ( <i>MSBP1</i> )
AT3G01210	RNA-BINDING (RRM/RBD/RNP MOTIFS) FAMILY PROTEIN (AT3G01210)	AT5G53110	RING/U-BOX SUPERFAMILY PROTEIN (AT5G53110)
AT3G01690	ALPHA/BETA-HYDROLASES SUPERFAMILY PROTEIN (AT3G01690)	AT5G53850	HALOACID DEHALOGENASE-LIKE HYDROLASE FAMILY PROTEIN (AT5G53850)
AT3G01930	MAJOR FACILITATOR SUPERFAMILY PROTEIN (AT3G01930)	AT5G55970	RING/U-BOX SUPERFAMILY PROTEIN (AT5G55970)
AT3G02730	THIOREDOXIN F-TYPE 1 ( <i>TRXF1</i> )	AT5G56150	UBIQUITIN-CONJUGATING ENZYME 30 ( <i>UBC30</i> )

AT3G03490	PEROXIN 19-1 ( <i>PEX19-1</i> )	AT5G56460	PROTEIN KINASE SUPERFAMILY PROTEIN (AT5G56460)
AT3G06510	GLYCOSYL HYDROLASE SUPERFAMILY PROTEIN ( <i>SFR2</i> )	AT5G57390	AINTEGUMENTA-LIKE 5 ( <i>AIL5</i> )
AT3G07130	PURPLE ACID PHOSPHATASE 15 ( <i>PAP15</i> )	AT5G58330	LACTATE/MALATE DEHYDROGENASE FAMILY PROTEIN (AT5G58330)
AT3G07720	GALACTOSE OXIDASE/KELCH REPEAT SUPERFAMILY PROTEIN (AT3G07720)	AT5G59250	MAJOR FACILITATOR SUPERFAMILY PROTEIN (AT5G59250)
AT3G08510	PHOSPHOLIPASE C 2 ( <i>PLC2</i> )	AT5G59590	UDP-GLUCOSYL TRANSFERASE 76E2 ( <i>UGT76E2</i> )
AT3G11080	RECEPTOR LIKE PROTEIN 35 ( <i>RLP35</i> )	AT5G60360	ALEURAIN-LIKE PROTEASE ( <i>ALP</i> )
AT3G13090	MULTIDRUG RESISTANCE-ASSOCIATED PROTEIN 8 ( <i>ABCC6</i> )	AT5G60900	RECEPTOR-LIKE PROTEIN KINASE 1 ( <i>RLK1</i> )
AT3G13790	GLYCOSYL HYDROLASES FAMILY 32 PROTEIN ( <i>ATBFRUCT1</i> )	AT5G62480	GLUTATHIONE S-TRANSFERASE TAU 9 ( <i>GSTU9</i> )
AT3G14570	GLUCAN SYNTHASE-LIKE 4 ( <i>GSL04</i> )	AT5G64120	PEROXIDASE SUPERFAMILY PROTEIN (AT5G64120)
AT3G15760	CYTOCHROME P450 FAMILY PROTEIN (AT3G15760)	AT5G64280	DICARBOXYLATE TRANSPORTER 2.2 ( <i>DIT2.2</i> )
AT3G20120	CYTOCHROME P450, FAMILY 705, SUBFAMILY A, POLYPEPTIDE 21 ( <i>CYP705A21</i> )	AT5G65970	SEVEN TRANSMEMBRANE MLO FAMILY PROTEIN ( <i>MLO10</i> )
AT3G21260	GLYCOLIPID TRANSFER PROTEIN (GLTP) FAMILY PROTEIN ( <i>GLTP3</i> )	ATCG00490	RIBULOSE BISPHOSPHATE CARBOXYLASE LARGE CHAIN ( <i>RBCL</i> )
AT3G22160	VQ MOTIF-CONTAINING PROTEIN (AT3G22160)		

## APPENDIX 2

ID, common name, availability in the LR dataset and function of VLCFA biosynthesis genes.

Gene ID	Common name	In the LR dataset?	Biochemical function, from (Trenkamp et al., 2004; Blacklock and Jaworski, 2006; Tresch et al., 2012)	<i>In planta</i> function/Mutant phenotype
AT1G01120	<i>KCS1</i>	Yes	Substrate specificity: C20:0; C20:1; C16:1; C18:0, C18:1, C20:1. Produces: C20:0; C20:1; C22:0; C24:0; C26:0.	Cuticular wax production (Todd et al., 1999). Mutant: thinner stems and more sensitive to dry air (Todd et al., 1999), enhanced callus formation on callus-induction medium (Shang et al., 2016).
AT1G04220	<i>KCS2/DAISY</i>	Yes	Produces: C20:0, C22:0, C24:0.	Cuticular wax and root suberin biosynthesis; act redundantly with <i>KCS20</i> (Lee et al., 2009b). Mutant: slight reduction in primary root growth (Lee et al., 2009b).
AT1G07720	<i>KCS3</i>	Yes	In yeast, expressed but no activity detected.	
AT1G19440	<i>KCS4</i>	Yes	In yeast, expressed but no activity detected.	
AT1G25450	<i>KCS5/CER60</i>	Yes	Produces: C24:0, C26:0, C28:0.	
AT1G68530	<i>KCS6/CER6</i>	Yes	Produces: C24:0, C26:0, C28:0..	Cuticular wax biosynthesis. Mutant: waxless stems and siliques, conditional male sterility (Millar, 1999; Fiebig et al., 2000)
AT1G71160	<i>KCS7</i>	No	In yeast, expressed but no activity detected.	
AT2G15090	<i>KCS8</i>	Yes	In yeast, expressed but no activity detected.	
AT2G16280	<i>KCS9</i>	Yes	Substrates: C16:1, C18:1, C18:2. Produces: C24.	Cuticular wax, suberin polyester and sphingolipid biosynthesis (Kim et al., 2013).
AT2G26250	<i>KCS10/FDH</i>	Yes	In yeast, expressed but no activity detected.	Possibly involved in cuticle biosynthesis, required for epidermal functions (Pruitt et al., 2000).
AT2G26640	<i>KCS11</i>	Yes	Substrates: C16:0, C16:1, C18:0.	

AT2G28630	<i>KCSI2</i>	Yes	In yeast, expressed but no activity detected.	
AT2G46720	<i>KCSI3/HIC</i>	No	No information.	Mutant: increased stomata density in response to elevated CO <sub>2</sub> (Gray et al., 2000).
AT3G10280	<i>KCSI4</i>	No	No information.	
AT3G52160	<i>KCSI5</i>	No	In yeast, expressed but no activity detected.	
AT4G34250	<i>KCSI6</i>	Yes	Produces: C34 to C38 (Hegebarth et al., 2017).	Wax biosynthesis in leaf trichomes (Hegebarth et al., 2017).
AT4G34510	<i>KCSI7</i>	Yes	Substrates: C16:0, C18:0, C20:0, C22:0. Produces: C20:0, C20:1, C24:0, C26:0.	
AT4G34520	<i>KCSI8/FAEI</i>	No	VLCFA synthesis for seed storage triacylglycerols. Substrates: C16:0, C18:0, C20:0, C22:0 Produces: C20:0, C20:1, C22:0, C22:1, C24:0, C24:1, C26:0.	
AT5G04530	<i>KCSI9</i>	No	In yeast, expressed but no activity detected.	
AT5G43760	<i>KCS20</i>	Yes	Produces: C22:0, C24:0, C26:0.	Cuticular wax and root suberin biosynthesis; act redundantly with KCS2 (Lee et al., 2009b). Mutant: slight reduction in primary root growth (Lee et al., 2009b).
AT5G49070	<i>KCS21</i>	No	No information.	
AT1G67730	<i>KCR1</i>	Yes	Required for VLCFA biosynthesis (Beaudoin et al., 2009).	Knock-out mutant: embryo lethal. Knock-down mutant: severely affected, fused vegetative and reproductive organs, less lateral roots and root hairs (Beaudoin et al., 2009).
AT1G24470	<i>KCR2</i>	No	In yeast, expressed but no activity detected (Beaudoin et al., 2009).	
AT5G10480	<i>PAS2</i>	Yes	Required for VLCFA biosynthesis (Bach et al., 2008).	Knock-out mutant: embryo lethal. Knock-down mutant: severely affected (Bach et al., 2008).
AT3G55360	<i>ECR/CER10</i>	Yes	Required for VLCFA biosynthesis (Zheng, 2005).	Cuticular wax biosynthesis. Mutant: glossy stem, fused organs, reduced cell sizes (Zheng, 2005).

AT3G54010	<i>PASI</i>	Yes	Interact with other VLCFA enzymes to form the elongase complex (Roudier et al., 2010).	Mutant: severely affected, reduced lateral root formation and growth (Roudier et al., 2010).
AT5G59770	<i>PTPLA</i>	Yes	PAS2-like function but in root vascular tissues. Required for VLCFA biosynthesis (Morineau et al., 2016)	No visible phenotype (Morineau et al., 2016)

### APPENDIX 3

**Binding motif of the TF PUCHI** retrieved from the Plant Transcription Factor Database v4.0 (<http://planttfdb.cbi.pku.edu.cn/>).



**List of predicted binding sites of the TF PUCHI on VCLFA promoters:**

Promoter	Start	Stop	Strand	Score	p-value	Matched sequence
<i>KCRI</i>	3135	3149	+	12.7812	8.19E-06	AAACCTCCGCCGATA
<i>KCSI</i>	662	676	-	6.64062	9.33E-05	TTTTATCCGCCACAA
<i>KCSI7</i>	1481	1495	-	22.7812	1.16E-08	CTGTCGCCGCCGTCA
	1484	1498	-	13.4375	6.04E-06	GTTCTGTCGCCGCCG
	1691	1705	-	12.0938	1.11E-05	TTGTCTCCGCCACAA
	1633	1647	+	8.95312	4.00E-05	CCAACGTCACCGCTC
	395	409	+	8.34375	5.04E-05	CCTTCTCCGCCTGAC
	392	406	+	7.29688	7.39E-05	ACTCCTTCTCCGCCT
<i>KCSI8</i>	1169	1183	+	6.90625	8.50E-05	CTTTATCCGCCATGA
<i>KCS20</i>	2482	2496	+	10.8125	1.92E-05	AAGTCATCGCCGTCT
	2485	2499	+	6.71875	9.08E-05	TCATCGCCGTCTCTT
<i>KCS5</i>	1592	1606	+	12.3281	1.00E-05	TCCAAACCGCCGCC
	77	91	-	12.2344	1.05E-05	CAACCGTCGCCATCG
	999	1013	+	9.51562	3.22E-05	TTCTCTCCGCCATCC
	80	94	-	9.3125	3.49E-05	TAGCAACCGTCGCCA
	1595	1609	+	7.45312	6.99E-05	AAACCGCCGCCCCCA
	954	968	+	6.6875	9.18E-05	ATCTCTCCGTCGTAC
<i>KCS6</i>	1594	1608	-	9.70312	3.00E-05	CAGCCTCCACCATCA
<i>KCS9</i>	3024	3038	-	7.79688	6.17E-05	ACGGATCCGCCATTA
<i>PLPLA</i>	1222	1236	-	21.0156	5.84E-08	CTCTCTCCGCCGCCG
	1219	1233	-	16.2344	1.47E-06	TCTCCGCCGCCGAAT
	1171	1185	-	15.8281	1.83E-06	CTGCCACCGCCGGGA

	360	374	+	14.875	3.00E-06	GCTCCTCCGCAGCCA
	1174	1188	-	13.1094	7.04E-06	CACCTGCCACCGCCG
	472	486	+	11.4062	1.50E-05	ATTTCTCCACCGCCT
	475	489	+	11.1875	1.64E-05	TCTCCACCGCCTTAA
	1385	1399	-	10.875	1.87E-05	TGTTACCGCCGACG
	1382	1396	-	8.14062	5.43E-05	TCACCGCCGACGAAA
	2881	2895	-	7.53125	6.79E-05	AATCTACCGCCGGAT
	437	451	-	6.5	9.80E-05	GTATCTCCTCCGTTG

# **PUBLICATIONS, COMMUNICATIONS AND TRAINING**

## LIST OF PUBLICATIONS

**Trinh, C.D., Laplaze, L., and Guyomarc'h, S.** (2018). Lateral Root Formation: Building a Meristem de novo. In Annual Plant Reviews online (John Wiley & Sons, Ltd: Chichester, UK), pp. 1–44.

Duy Chi Trinh, Julien Lavenus, Quentin Drogue, Virginie Vaissayre, Mikael Lucas, Tatsuaki Goh, Ute Voss, Frédérique Tellier, Pascal Gantet, Jean-Denis Faure, Yohann Boutté, Stéphane Dussert, Hidehiro Fukaki, Malcolm J. Bennett, Laurent Laplaze and Soazig Guyomarc'h. **PUCHI regulates Very Long Chain Fatty Acid biosynthesis during lateral root and callus formation.** (in preparation for PNAS).

## SCIENTIFIC COMMUNICATION

- 12th Congress Of The International Plant Molecular Biology (IPMB2108), Montpellier, France, 5-10 August 2018: oral presentation.
- First International Plant Systems Biology Meeting (iPSB2018), Roscoff, France, September 10-14 2018: poster presentation.
- Lateral root workshop in Nottingham, UK 2018 and in Montpellier 2017: oral presentation.

## TRAINING/FORMATION

### **Catégorie : Insertion professionnelle**

■ Doctoriales® Transfrontalières/ Cross-Border doctorials (19 mars 2017) Domaine du Mas Blanc Alénya

25 heures enregistrées par : Collège Doctoral Languedoc Roussillon.

Total du nombre d'heures pour la catégorie Insertion professionnelle : 25 h

### **Catégorie : Communication**

■ First international plant systems biology meeting CNRS - Conférences Jacques Monod - Roscoff (France)

4 heures enregistrées par : GAIA - Biodiversité, Agriculture, Alimentation, Environnement, Terre, Eau.

Total du nombre d'heures pour la catégorie Communication : 4 h

### **Catégorie : Ethique et intégrité scientifique**

■ Formation à l'éthique de la recherche et à l'intégrité scientifique (06 novembre 2017) Bat 23, salle STP 5, Campus Triolet

7 heures enregistrées par : GAIA - Biodiversité, Agriculture, Alimentation, Environnement, Terre, Eau.

Total du nombre d'heures pour la catégorie Ethique et intégrité scientifique : 7 h

### **Catégorie : Méthodes, outils, langages**

■ FLE - Français Langue Étrangère 2016 (26 septembre 2016) Université de Montpellier , Département des Langues Bâtiment 5

30 heures enregistrées par : Collège Doctoral Languedoc Roussillon.

■ Dealing with scientific literature : efficient reading and good note taking habits (05 octobre 2016)

25 heures enregistrées par : Collège Doctoral Languedoc Roussillon.

■ Start with R (01 février 2017) salle 050 - Bât.1 - Campus st Priest, 860 rue de Saint Priest, 34090 Montpellier

18 heures enregistrées par : Collège Doctoral Languedoc Roussillon.

Total du nombre d'heures pour la catégorie Méthodes, outils, langages : 73 h

**Total participation : 109 heures / 6 modules**

# PUCHI regulates Very Long Chain Fatty Acid biosynthesis during lateral root and callus formation

Duy Chi Trinh<sup>1,2</sup>, Julien Lavenus<sup>1,5</sup>, Quentin Drogue<sup>1</sup>, Tatsuaki Goh<sup>3</sup>, Mikaël Lucas<sup>1</sup>, Hidehiro Fukaki<sup>4</sup>, Malcolm Bennett<sup>5</sup>, Laurent Laplace<sup>1</sup>, Soazig Guyomarc'h<sup>1</sup>

<sup>1</sup>UMR "Diversité Adaptation et Développement des plantes" (DIADE), IRD/Université de Montpellier, Montpellier, France  
<sup>2</sup>Department of Pharmacological, Medical and Agronomical Biotechnology, University of Science and Technology of Hanoi, Hanoi, Vietnam  
<sup>3</sup>Laboratory of Plant Developmental Signaling, Nara Institute of Science and Technology, Nara, Japan  
<sup>4</sup>Department of Biology, Graduate School of Science, Kobe University, Kobe, Japan  
<sup>5</sup>Centre for Plant Integrative Biology, School of Biosciences, University of Nottingham, Nottingham, United Kingdom

## Lateral root primordia formation and the roles of PUCHI

Root system architecture, *i.e.* the configuration of a whole root system in the soil, is considered a major determinant of plant performance and crop yield (1). In many plant species such as *A. thaliana* the mature root system is largely derived from lateral roots (LRs) formed after germination (Fig. 1).

We have previously suggested an early patterning mechanism defining the central region and flanks of the LR primordia (LRP) and identified genes involved in this process (2). One such is the transcription factor PUCHI which was previously showed to control cell division and proliferation during LRP formation (Fig. 2) (2, 3). No targets of PUCHI have been reported.

Here, by using a systems biology approach combining a transcriptomic dataset and a gene regulatory network inference algorithm we identified very long chain fatty acids (VLCFA) biosynthesis genes as potential targets of PUCHI. Experimental evidences support our hypothesis.

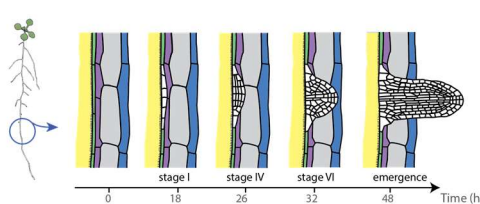


Figure 1: Root system architecture in *Arabidopsis* is largely determined by the formation of LRs. LRPs (white) are initiated from a specific tissue of the primary root (green) and its formation is usually categorized into different stages (4).

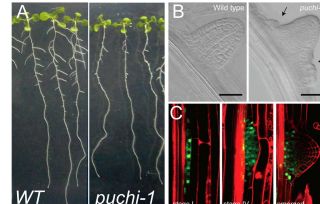


Figure 2: Primary root and LRP phenotypes (A and B) of PUCHI loss-of-function mutant (*puchi-1*). (C) Expression pattern of PUCHI::GFP (green) from ref (3).

## Identify VLCFA biosynthesis genes as targets of PUCHI using a systems biology approach

We used an inhouse algorithm called TDCor (2) in combination with a previously generated time course transcriptomic dataset covering the whole process of LR organogenesis (5) to search for genes having correlated but delayed expression profiles with that of PUCHI. 217 genes were found. GO analysis on these 217 genes revealed that VLCFA biosynthesis is the most strongly overrepresented biological process. Expression profiles of PUCHI and VLCFA genes are shown in Fig. 3.

VLCFAs are components of phospholipids and sphingolipids, triacylglycerols, suberin and waxes. They are synthesized by the fatty acid elongase complex consisting of enzymes of 4 families: KCS, KCR, HCD/PAS2 and ECR (Fig. 4). While there is only one functional KCR, PAS2 and ECR, multiple KCS enzymes are responsible for the final VLCFA chain lengths (6). VLCFAs are essential for plant development, and were recently showed to control cell competence for callus formation in callus-inducing conditions (6, 7).

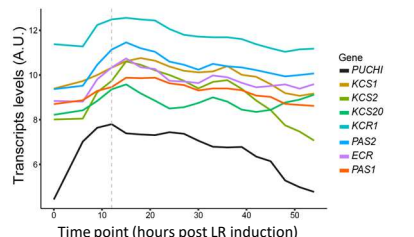


Figure 3: Expression profiles of PUCHI and selected VLCFA biosynthesis genes from the transcriptomic dataset (5). Refer to Figure 1 for LRP developmental stages at the indicated time points.

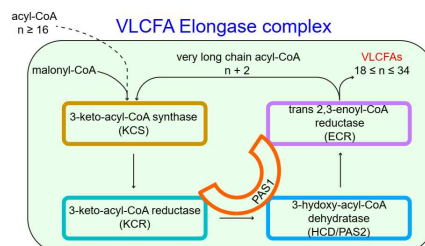


Figure 4: Schematic representation of the VLCFA elongation cycle.

## PUCHI regulates expression levels and expression patterns of VLCFA biosynthesis genes during LRP formation

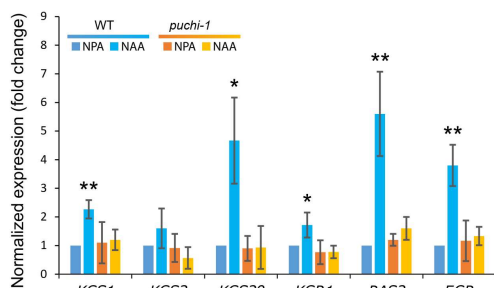


Figure 5: Expression levels of VLCFA genes as revealed by qRT-PCR during LRP formation are dependent on PUCHI. LRP formation was blocked by NPA (an auxin transport inhibitor) and then synchronously induced by NAA (an auxin) treatment. \*  $P < 0.05$ , \*\*  $P < 0.01$ .

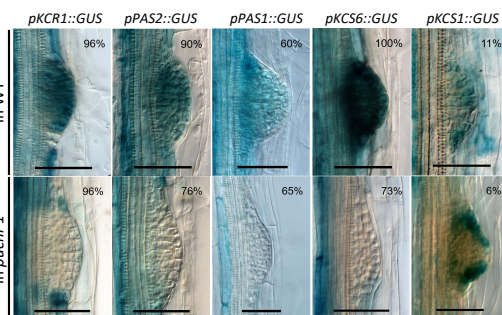


Figure 6: Promoter::GUS reporter analyses show that VLCFA biosynthesis genes are expressed in WT developing LRPs and their correct expression patterns are dependent on PUCHI (one developmental point is illustrated). Bars = 50  $\mu$ m.

## PUCHI and VLCFA mutants show similar developmental phenotypes

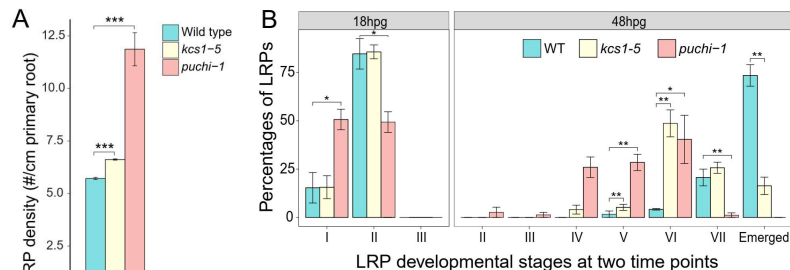


Figure 7. *puchi-1* and a key VLCFA mutant (*kcs1-5*) showed similar LR defects, including higher LRP densities (A) which translate into shorter interval LRP spacing (not showed), and delay in LRP developmental progression (B). In (B) LRP formation was synchronously induced and LRP developmental stages were scored at 18 and 48 hours after the induction. Note the clear difference in the percentages of emerged LRs in WT, *puchi-1* and *kcs1-5*. \*  $P < 0.05$ , \*\*  $P < 0.01$ , \*\*\*  $P < 0.001$ .

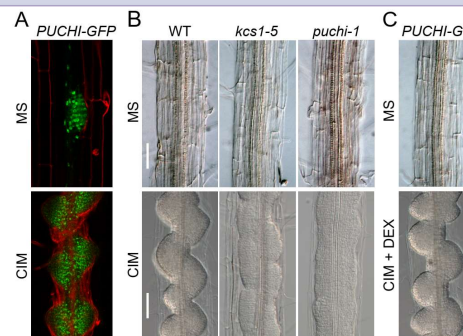


Figure 8. PUCHI and VLCFAs control callus formation in callus-inducing medium (CIM) containing high levels of auxin. (A) PUCHI::GFP is expressed during LRP and callus formation. (B) On CIM, WT roots produce calli with intervals, while *puchi-1* and *kcs1-5* roots produce a continuous layer of proliferating cells. (C) *puchi-1* phenotype on CIM is rescued by a dexamethasone-PUCHI-GR construct + dexamethasone (DEX). Bars = 100  $\mu$ m.

## Conclusions and perspectives

Using a systems biology approach, we discovered that expression of very long chain fatty acid (VLCFA) biosynthesis genes is induced downstream of PUCHI, a transcription factor controlling cell division and morphogenesis during lateral root formation. We also show that the PUCHI-mediated regulation of VLCFA biosynthesis is also involved in root derived callus formation, the first step in *in vitro* plant regeneration. More experiments are on-going to corroborate the hypothesis such as VLCFA quantification in WT and *puchi-1* roots and rescuing *puchi-1* LR phenotype by VLCFA complementation.

### References

- Smith S, De Smet I (2012). DOI: 10.1098/rstb.2011.0234
- Lavenus et al., 2015. DOI: 10.1105/tpc.114.132993
- Malamy JE, Benfey PN (1997). PubMed: 9006065
- Hirota et al., 2007. DOI: 10.1105/tpc.107.050674
- Voss et al., 2015. DOI: 10.1038/ncomms8641
- Haslam, Kunst, 2013. DOI: 10.1016/j.plantsci.2013.05.008
- Shang et al., 2016. DOI: 10.1073/pnas.1522466113